



The
University
Of
Sheffield.

Screening of Novel Synthetic Compounds and Marine Extract Libraries in In Vitro and In Vivo Models of Motor Neuron Disease (MND/ALS) for Discovering New Potentially Therapeutic Neurotrophin Mimetics.

Marco Destro

Registration number
180264205

A thesis submitted in partial fulfilment of the requirements for the degree of
Doctor of Philosophy

The University of Sheffield
Faculty of Medicine, Dentistry and Health
Department of Neuroscience

Submission Date:
March 2023

Preface

This work was conducted under EuroNeurotrophin, a European Innovative Training Network for the discovery of neurotrophins small molecule mimetics as potential therapeutic agents for neurodegeneration and neuroinflammation. This project has received funding from the European Union's Horizon 2020 research and innovation programme under the Marie Skłodowska-Curie grant agreement No 765704. The original plan of drug screening of multiple libraries, isolating and characterizing compounds, and the *in vivo* drug testing in zebrafish models has been delayed and the *in vivo* drug testing in mouse models did not occur due to the COVID-19 pandemic. Furthermore, the secondment at the Dresden University of Technology supervised by Dr Vasileia Ismini Alexaki for testing the drugs in multiple sclerosis cellular and mouse models did not happen due the COVID-19 pandemic. All the experimental work described in chapters 3, 4 and 5 was carried out by me, Marco Destro, unless otherwise stated.

Mr Paolo Giaccio contributed to the isolation and characterization through chromatography and nuclear magnet resonance of the compounds and subfractions derived from the positive hits obtained from the marine extracts screening, under the guidance and supervision of Prof Vassilios Roussis and Prof Efstathia Ioannou at the National and Kapodistrian University of Athens.

Mr Athanasios Alexandros Tsengenes and Ms Christina Athanasiou provided guidance for the *in silico* molecular docking of the isolated compounds, under the supervision of Prof Rebecca Wade at the Heidelberg Institute for Theoretical Studies. This experimental section has been carried out remotely due to the COVID-19 pandemic. Dr David J Burrows provided technical support for maintenance, screening and treatment of the employed zebrafish *in vivo* model, as well as guidance during the experimental procedures.

Chapter 1 describes the pathophysiological aspects of amyotrophic lateral sclerosis, the role of neurotrophins in the disorder and as potential therapeutic agents, and the role of neurotrophin mimetics as a potential way to overcome the neurotrophin limitations as treatment for the amyotrophic lateral sclerosis. Chapter 2 illustrates the materials and methods employed in the result chapters 3-5. Chapter 3 describes the co-culture primary and multi-donor screening assays for the identification of positive hits among the libraries

screened, with particular focus on the Marine Extract library. Chapter 4 explains the results obtained from the fractionations and characterization of the marine extract top hits and the molecular docking data of the compounds obtained as well as their putative role as neurotrophin mimetics. Chapter 5 describes the attempts for understanding the potential mechanism of action of the main top hit selected from the previous results and the *in vivo* experiments using a zebrafish model. Chapter 6 discusses the possible implications of the results listed in the previous chapters, also providing ideas and indications for future work.

Acknowledgements

As any PhD student who gets at this point realizes, it would probably need an entire new thesis just to thank everyone who has been with me during this long journey. Firstly, I would like to thank my supervisors Prof Dame Pamela Shaw, and Prof Laura Ferraiuolo for their constant support and enormous patience throughout the entire length of my PhD. I know I have been a tough one, and I am extremely sorry for all the stress and mess I created. My gratitude towards you as people, and my respect for you as scientists are immense. I would also like to thank Dr Matthew Stopford for all the academic and personal support, you have been the best I could possibly ask for. I have learnt so much from you and I have been extraordinarily lucky to have been shadowing you during my first year at SITraN. I would also love to thank all the wonderful people I met at SITraN and who became close friends of mine: Janny, Monika, Allan, Amy, Andre, Chloe, Cleide, Noemi, Paolo M, Ilaria, Matilde, Lara, Michela, Hubashia, Anushka, Aytac, Paolo G, Daniele, Alessia, and the list goes on. And of course, I want to thank my dear home friends: Pilat, Erica, Scussel, Siro, Jabbo, Jabba, Giulio, Faghe and Dema. I have surely forgot someone, sorry. You have all always been with me even when my body, my mind, and my soul (I do not believe in the soul but just in case I am wrong it is better to include it) completely derailed. Throughout all the darkest times, you have always been there cheering me up and making me feel I was worth it. You have all been more than just friends, you are part of my family.

And talking about family, of course Mom and Dad, you have supported me and allowed me to accomplish my dreams, and that is invaluable. Thanks for being what you are for me.

I do not think that there are words available in any spoken language that can really express my thoughts about what you all are and what you all have been for me in the last years of my life.

You are the best people I have ever met, and I am glad, despite all the personal troubles I had in the last years, that I have shared a slice of my life with you. For what it matters, I love you all, and I only wish the best for your future. Thank you from the deepest part of my heart.

Declaration

I, the author, confirm that the Thesis is my own work. I am aware of the University's Guidance on the Use of Unfair Means (www.sheffield.ac.uk/ssid/unfair-means). This work has not been previously presented for an award at this, or any other, university.

Abstract

Background: Neurotrophins are a class of polypeptides able to recover and improve neuronal function during neurodegenerative conditions. The challenges of developing neurotrophins as clinical candidates have limited their potential therapeutic use. A solution to overcome these issues is the development of neurotrophin mimetics that mimic endogenous neurotrophins.

Aims and Objectives: 1) Screening three libraries of compounds or marine extracts to identify therapeutic molecules promoting motor neuronal survival in co-culture i-astrocytes derived from a panel of ALS patient lines. 2) Isolate and characterize the constituents of the top hit extracts and test their efficacy on the co-culture assay. 3) Perform *in silico* screening to predict which top hits can be potential small neurotrophin mimetics. 4) Understand the molecular mechanisms of the top hits. 5) Test the therapeutic efficacy of the top hits in ALS C9ORF72 zebrafish models.

Results: Three extracts (BI0394, BI0788 and BI0987) were able to significantly increase motor neuronal survival in co-culture with an array of ALS derived i-astrocytes. BI0788 has shown the most promising results and was taken forward for isolation and characterization. 7 x BI0788 constituents could act as neurotrophin mimetics. BI0788 treatment showed increased nuclear translocation of NF- κ B in the tested C9ORF72 and SOD1 lines. BI0788 and its fractions produced a toxic effect on C9ORF72 embryos at all tested concentrations.

Conclusions: The screening experiments showed that BI0788 significantly promoted motor neuronal survival in co-culture with i-astrocytes derived from SOD1, C9ORF72 and sporadic ALS patients, indicating that marine extracts could contain molecules able to have therapeutic effects in ALS. Some molecules isolated from the extract were shown to be potential neurotrophin mimetics through *in silico* screening. Mechanistic effects and the precise molecule or mixture of molecules within BI0788 which have this capability remain to be elucidated with further studies, and the effect on *in vivo* models will require future research to be confirmed.

Table of Contents

Preface	2
Acknowledgements.....	4
Declaration.....	5
Abstract.....	5
List of Tables	13
List of Figures	14
Chapter 1: Introduction	16
1.1 Clinical Presentation of Amyotrophic Lateral Sclerosis	16
1.2 Aetiology of ALS	18
1.3 Genetics	19
1.3.1 Superoxide Dismutase 1	20
1.3.2 C9orf72.....	22
1.3.3 Fused in Sarcoma and TAR DNA-Binding Protein 43	23
1.4 Pathophysiological Mechanisms.....	25
1.4.1 Impaired Protein Homeostasis.....	26
1.4.2 Oxidative Stress.....	26
1.4.3 Aberrant RNA metabolism.....	27
1.4.4 Excitotoxicity.....	28
1.4.5 Mitochondrial Dysfunction	28
1.5 Neuronal Vulnerability in ALS	29
1.6 Glial Involvement in ALS.....	30
1.7 Neurotrophins.....	32
1.7.1 Trk Signalling	34
1.7.2 p75NTR Signalling	35
1.8 Alteration of Neurotrophin levels in the ALS Neuropathology.....	36
1.8.1 Direct infusion of Neurotrophic Factors and Neurotrophins as treatment for neurodegenerative disorders	36
1.8.2 Gene therapy approaches employing Neurotrophic Factors and Neurotrophins	38
1.9 Small neurotrophin mimetics	41
1.10 iNPCs in vitro models for ALS studies	42
1.11 Marine Extracts.....	43
1.12 Overall Hypothesis, Aims and Objectives	45
Chapter 2: Materials and Methods.....	46
2.1 Cell lines	46
2.2 i-Astrocyte differentiation	47

2.3 Mouse embryonic stem cell (mESC) maintenance	48
2.4 mESC split.....	48
2.5 Differentiation of motor neurons	49
2.6 Dissociation of EBs with papain	50
2.7 High-throughput drug screening on human iastrocyte – murine Hb9-GFP+ motor neuron co-cultures	52
2.8 Small-scale extracts of bacterial and fungal strains forming the Marine Extracts library utilized for the co-culture screening.....	53
2.9 Isolation and characterization of bacterial strain secondary metabolites	55
2.10 In silico screening of UNICAEN 18000-membered compound library for candidate selection for co-culture screening.....	55
2.11 Generation of DHEA derivatives substituted by five, six or three membered-17-spiro substituents for co-culture screening.....	57
2.12 SDS-polyacrylamide gel preparation.....	57
2.13 Cell lysis for immunoblotting	58
2.14 Bradford assay	58
2.15 SDS-polyacrylamide gel electrophoresis.....	59
2.16 Immunoblotting	59
2.17 Paraformaldehyde fixation	60
2.18 Immunocytochemistry	60
2.19 Zebrafish C9ORF72 screening assay.....	61
2.20 Molecular docking.....	62
2.21 Statistical Analysis.....	63
Chapter 3: Screening of a library of marine extracts in a panel of ALS-derived iAstrocytes and motor neurons co-cultures	64
3.1 Introduction	64
3.2 Screening marine extracts for neuroprotective effects in a motor neuron-astrocyte co-culture system.....	66
3.3 Multi-donor Screening in iAstrocyte co-cultures derived from ALS patients carrying different ALS-related genetic mutations.....	74
3.4 Screening of Dehydroepiandrosterone (DHEA) derivatives for neuroprotective effects in a motor neuron -astrocyte co-culture system.....	83
3.5 Discussion.....	86
Chapter 4: Isolation and characterization of BI788 constituents and <i>in silico</i> analysis for potential neurotrophin receptor binding.....	90
4.1 Introduction	90
4.2 Isolation and Characterization of Secondary Metabolites from BI0987.....	92

4.3 Screening 2,5-diketopiperazines Isolated from BI0987 for neuroprotective effects in a motor neuron and C9ORF72 iastrocyte co-culture assay	97
4.4 Screening 2,5-diketopiperazines Isolated from BI0987 for neuroprotective effects in a motor neuron -SOD1 astrocyte co-culture assay.....	99
4.5 BIO788 fractions multi-donor screening.....	101
4.6 Loading, Preparing and Styling Ligands for Molecular Docking of Neurotrophin Receptors ...	105
4.7 Loading, Preparing and Styling Ligands for Molecular Docking of Neurotrophin Receptors ...	111
4.8 Protein Preparation and Site Map analysis.....	114
4.9 Molecular Docking	117
4.10 Discussion:	122
Chapter 5: Molecular Analysis of BI788 and In Vivo Testing on Zebrafish ALS models.....	125
5.1 Introduction	125
5.2 P75 receptor expression in a panel of i-astrocytes and motor neuron lines.....	127
5.3 NF-kB screening in BIO788 treated and untreated cells.	129
5.4 C9orf72 Zebrafish lines treatment with BIO788.....	131
5.5 Discussion.....	133
Chapter 6: Final Discussion	137
Chapter 7: Appendix	143
7.1 Patient #17 Screening of BIO788 sub-fractions (ENT-M217-M225).....	143
7.2 Patient #102 Screening of BIO788 sub-fractions (ENT-M217-M225).....	144
7.3 Patient #201 Screening of BIO788 sub-fractions (ENT-M217-M225).....	145
Bibliography	146

Abbreviations

7,8-DHF	7 8-Hydroxyflavone
AD	Alzheimer's disease
ADME	Absorption, Distribution, Metabolism, and Excretion
ALS	Amyotrophic Lateral Sclerosis
ASPA	Animals Scientific Procedures Act
BBB	Blood Brain Barrier
BDNF	Brain-Derived Neurotrophic Factor
CNS	Central Nervous System
CNTF	Ciliary Neurotrophic Factor
CREB	cAMP Response Element-Binding Protein
DENN	Differentially Expressed in Normal and Neoplastic Cells
DHEA	Dehydroepiandrosterone
DMSO	Dimethyl Sulfoxide
dpf	Days post fertilization
DPR	Dipeptide Repeat Protein
EBs	Embryoid Bodies
EC50	Effective Concentration 50
ECM	Extracellular Matrix
ERK	Extracellular Signal-Regulated Kinase
ESC	Embryonic Stem Cells
fALS	Familial ALS
FBS	Fetal Bovine Serum
FISH	Fluorescence In Situ Hybridization
FTD	Frontotemporal Dementia
FTLD	Frontotemporal Lobar Degeneration
FUS	Fused in Sarcoma

G4C2	GGGGCC hexanucleotide
GDNF	Glial Cell-Derived Neurotrophic Factor
GFP	Green Fluorescent Protein
GFR α	GDNF family receptor subunits
HITS	Heidelberg Institute for Theoretical Studies
hnRNPA1	Heterogeneous Nuclear Ribonucleoprotein A1
HPLC	High Performance Liquid Chromatography
HRP	Heathshock Response Protein
HSP	Heathshock Protein
HSR	Heathshock Response
HTS	High-Throughput Screening
HTDS	High-Throughput Drug Screening
IC50	Inhibitory Concentration 50
IGF	Insulin-like Growth Factor
INF γ	Interferon γ
iNPC	Induced Neural progenitor Cell
JNK	c-Jun N-Terminal Kinase
LC-MS	Liquid Chromatography Coupled Mass Spectrometry
LIF	Leukaemia Inhibiting Factor
LMN	Lower Motor Neurons
LTD	Long Term Depression
LTP	Long Term Potentiation
MCM	Molecular and Cellular Modelling Group
MCT4	Monocarboxylate Transporter 4
MEF	Mitotically Inactive Primary Mouse Embryonic Fibroblast
mESCs	Mouse Embryonic Stem Cells
MN	Motor Neurons

MND	Motor Neuron Disease
MPCs	Muscle Progenitor Cells
MPLC	Medium Pressure Liquid Chromatography
mTORC1	Mammalian Target of Rapamycin 1
NF-κB	Nuclear Factor Kappa-Light-Chain-Enhancer of Activated B Cells
NGF	Nerve Growth Factor
NHRF	National Hellenic Research Foundation
NKUA	National Kapodistrian University of Athens
NMR	Nuclear Magnetic Resonance
NRTN	Neuritin
NT3	Neurotrophin 3
NT4	Neurotrophin 4
NTFs	Neurotrophic Factors
P75NTR (p75)	75 kDa Neurotrophin Receptor
PBS	Phosphate Saline Buffer
PD	Parkinson's Disease
PDB	Protein database
PFA	Paraformaldehyde
PGD2	Prostaglandin D2
PGE2	Prostaglandin E2
PI3K	Phosphoinositide 3-Kinase
PSC	Pluripotent Stem Cell
RhoGDI	Rho Gdp-Dissociation Inhibitor
RIP2	Receptor-Interacting-Serine/Threonine-Protein Kinase 2
ROS	Reactive Oxygen Species
sALS	Sporadic ALS
Shc	Src Homologous and Collagen-Like
SITraN	Sheffield Institute for Translational Neuroscience

SOD1	Superoxide Dismutase 1
TARDBP	TAR DNA-Binding Protein
TDP43	TAR DNA-Binding Protein 43
TGF- β	Transforming Growth Factor β
TLC	Thin Layer Chromatography
TNF- α	Tumor Necrosis Factor α
TNFR	Tumor Necrosis Factor Receptor
Trk	Receptor Tyrosine Kinase
TRAF6	TNF Receptor Associated Factor 6
ULK1	Unc-51 Like Autophagy Activating Kinase 1
UMN	Upper Motor Neurons
UPDRS	Unified Parkinson's Disease Rating Scale
UPR	Unfolded-Protein Response
UPS	Ubiquitin-Proteasome System
VEGF	Vascular Endothelial Growth Factor
VLC	Vacuum Liquid Chromatography

List of Tables

Chapter 1:

Table 1.1 List of genes involved in ALS.	19
--	----

Chapter 2:

Table 2. 1 iNPC Lines Clinical Information	46
Table 2. 2 iNPC Medium	47
Table 2. 3 i-Astrocyte Medium	48
Table 2. 4 mESC Medium.....	49
Table 2. 5 EB Medium.....	49
Table 2. 6 Enzyme Buffer.....	51
Table 2. 7 MN Medium	51
Table 2. 8 A1BFe+C medium.....	53
Table 2. 9 PD-S medium.....	54
Table 2. 10 Composition of 5% stacking gel and 12% resolving gel	58
Table 2. 11 Antibodies for Immunoblotting	60
Table 2. 12 Antibodies for Immunocytochemistry	61
Table 2. 13 E3 Embryo Medium 60x.....	62

Chapter 3:

Table 3. 1 List of all extracts tested in the primary screening assay with the source and amount received.....	72
Table 3. 2 List of all lines used for the top hit marine extracts multi-donor screening.....	76

Chapter 4:

Table 4. 1 Eluents employed for the first phase of BI0987 chromatography.....	93
Table 4. 2 Eluents employed for the second phase of BI0987 chromatography	94
Table 4. 3 Main QikProp properties analysed for the NPs	112
Table 4. 4 Compounds with highest XP docking in TrkA and TrkB	118
Table 4. 5 XP docking scores and structures of the best positive hits for the p75 ^{NTR} receptor.....	121

List of Figures

Chapter 1:

Figure 1. 1 Molecular mechanisms leading to motor neuron injury in ALS.	25
Figure 1. 2 Neurotrophin Receptors	33

Chapter 2:

Figure 2. 1 Differentiation of mESCs into murine Hb9-GFP+ MNs over a 7-day differentiation period (images provided by Dr M. Stopford)	50
--	----

Chapter 3:

Figure 3. 1 384w template layout.....	69
Figure 3. 2 Top hits from the marine extracts screen in C9orf72-ALS patient iAstrocyte and Hb9-GFP+ mouse motor neuron co-culture	70
Figure 3. 3 Top hit BI0394 screen in C9orf72-ALS patient #78 and #ALS-52 iAstrocyte and Hb9-GFP+ mouse motor neuron co-culture	77
Figure 3. 4 Top hit BI0394 screen in SOD1-ALS patient #102 and #ND29505 iAstrocyte and Hb9-GFP+ mouse motor neuron co-culture	77
Figure 3. 5 Top hit BI0394 screening in sALS patient #009, #012 and #017 iAstrocyte and Hb9-GFP+ mouse motor neuron co-culture	78
Figure 3. 6 Top hit BI0788 screen in C9orf72-ALS patient #78 and #ALS-52 iAstrocyte and Hb9-GFP+ mouse motor neuron co-culture	79
Figure 3. 7 Top hit BI0788 screen in SOD1-ALS patient #102 and #ND29505 iAstrocyte and Hb9-GFP+ mouse motor neuron co-culture	79
Figure 3. 8 Top hit BI0788 screen in sALS patient #009, #012 and #017 iAstrocyte and Hb9-GFP+ mouse motor neuron co-culture	80
Figure 3. 9 Top hit BI0987 screen in C9orf72-ALS patient #78 and #ALS-52 iAstrocyte and Hb9-GFP+ mouse motor neuron co-culture	81
Figure 3. 10 Top hit BI0987 screening in SOD1-ALS patient #102 and #ND29505 iAstrocyte and Hb9-GFP+ mouse motor neuron co-culture	81
Figure 3. 11 Top hit BI0987 screening in sALS patient #009, #012 and #017 iAstrocyte and Hb9-GFP+ mouse motor neuron co-culture	82
Figure 3. 12 <i>Dose-Response curves obtained from the steroid compound screen in C9orf72-ALS patient iAstrocyte-Hb9 GFP+ mouse motor neuron co-culture</i>	85

Chapter 4:

Figure 4. 1 Isolation of secondary metabolites from BI0987.....	95
Figure 4. 2 2,5-diketopiperazines isolated from BI0987.....	96
Figure 4. 3 2,5-diketopiperazines isolated from BI0987 did not improve motor neuron survival in the C9orf72-ALS patient iAstrocyte and Hb9-GFP+ mouse motor neuron co-culture.....	98
Figure 4. 4 2,5-diketopiperazines isolated from BI0987 did not improve motor neuron survival in the SOD1-ALS patient iAstrocyte and Hb9-GFP+ mouse motor neuron co-culture.....	100

Figure 4. 5a Isolation of sub-fractions and secondary metabolites from BI0788	105
Figure 4. 5b M219 screen in sALS patient #17, C9orf72-ALS patient #201 and SOD1-ALS patient #102 iAstrocyte and Hb9-GFP+ mouse motor neuron co-culture	105
Figure 4. 6 Library of compounds from the top hit extracts after preparation for the docking process	110
Figure 4. 7 Binding sites of the external domain of TrkA.	115
Figure 4. 8 Binding sites of the external domain of TrkB.....	116
Figure 4. 9 Binding sites of the external domain of p75.....	116
Figure 4. 10 A. TrkA; B. TrkB and C. p75 ^{NTR} with the identified binding sites and their volumes.....	116
Figure 4. 11 Poses of compounds with best XP docking scores in TrkA sites 1a and 1b.....	119
Figure 4. 12 Poses of compounds with best XP docking scores in TrkB sites 1a and 1b	119
Figure 4. 13 Structures of the best positive docking score hits for TrkA and TrkB receptors	120

Chapter 5:

Figure 5. 1 P75 western-blot on a panel of iastrocytes, mns and murine lines/tissues.....	128
Figure 5. 2 NF-kB screening in ALS-iastrocyte lines having different ALS-associated mutation upon BI0788 treatment.....	130
Figure 5. 3 Schematic of transgene used to create pure repeat RAN transgenic zebrafish lines.....	132
Figure 5. 4 DsRed expression images obtained in control lines through InCell Analyzer 2000.....	133

Chapter 7:

Figure 7. 1 Patient #17 Screening of BI0788 sub-fractions (ENT-M217-M225)	128
Figure 7. 2 Patient #102 Screening of BI0788 sub-fractions (ENT-M217-M225)	130
Figure 7. 3 Patient #201 Screening of BI0788 sub-fractions (ENT-M217-M225)	132

Chapter 1: Introduction

1.1 Clinical Presentation of Amyotrophic Lateral Sclerosis

Amyotrophic lateral sclerosis (ALS) is a fatal neurodegenerative disease characterized by dysfunction and loss of upper motor neurons (UMNs) and lower motor neurons (LMNs) (Hardiman *et al.*, 2017). This manifests as muscle weakness, muscle wasting, paralysis, and eventually death due to respiratory failure. Death typically occurs 2–5 years after symptom onset (Phukan, Pender and Hardiman, 2007; Goldstein and Abrahams, 2013; Al-Chalabi, van den Berg and Veldink, 2016; Hardiman *et al.*, 2017). ALS is clinically and neuropathologically heterogeneous, and therefore disease duration is highly variable: patients can die within months to several decades after clinical onset (Phukan, Pender and Hardiman, 2007; Goldstein and Abrahams, 2013). ALS is the most common form of motor neuron disease (MND), and the term ALS also used synonymously with MND. ALS is also known as Lou Gehrig's disease or Charcot's disease. ALS patients display amyotrophy, caused by LMN-related muscle loss resulting from denervation (amyotrophy), and sclerosis, because of UMN-related degeneration of the lateral corticospinal tract that is phenotypically displayed as hardening and gliosis. Extra-motor systems (especially executive frontal, temporal and behavioural circuits) can also degenerate in ALS, which leads to extra-motor symptoms (Al-Chalabi, van den Berg and Veldink, 2016; Hardiman *et al.*, 2017).

The age of clinical onset is also highly variable. The disease onset mean age is 65 years from data obtained through population-based studies (Robberecht and Philips, 2013), but ALS can start at different ages. In this respect, incidence is generally very low before the fourth decade of life (1.5/100,000/year), then increases sharply and reaches its highest between 60 and 79 years (10–15/100,000/year). After the 80 year the incidence starts to decrease (Robberecht and Philips, 2013). Interestingly, patients with young-onset (also known as juvenile ALS) or also with an onset prior to the fourth decade of life may show atypical clinical features, such as a higher prevalence of UMN rather than LMN signs, mainly spinal onset, more prolonged survival compared to the usual 3-5 years, and male predominance (Wijesekera and Leigh, 2009).

The fact that it is possible to appreciate a peak in the age incidence curve suggests that ALS is the result of a time-dependent exposure to risk factors of both genetic and environmental

origin. An early onset of ALS could be due to a higher exposure and predisposition to those risk factors (Phukan, Pender and Hardiman, 2007; Robberecht and Philips, 2013).

The initial clinical presentation of ALS can vary between patients (Swinnen and Robberecht, 2014; Ajroud-Driss and Siddique, 2015). Approximately 75% of patients present with the limb onset form of the disease exhibiting symptoms that are associated to the focal muscle weakness and that begin either proximally or more commonly distally within the lower and upper limbs. Muscle weakness, muscle atrophy and fasciculations, are signs of LMN involvement. Hyperreflexia and hypertonia and pyramidal distribution weakness indicate UMN involvement. Interestingly, certain LMN subgroups are relatively resistant to degeneration, such as the ocular MNs (Nijssen, Comley and Hedlund, 2017) and Onuf's nucleus in the sacral spinal cord which innervates muscles of the pelvic floor.

Although ALS is mainly characterised by motor dysfunction, up to 50% of patients show also cognitive and/or behavioural impairment. Only in extremely rare instances, cognitive impairment or behavioural disturbances can be the initial manifestation of ALS (Swinnen and Robberecht, 2014; Ajroud-Driss and Siddique, 2015). Approximately 13% of ALS patients also have frontotemporal dementia (FTD) and are described as having ALS-FTD (Al-Chalabi, van den Berg and Veldink, 2016; Hardiman *et al.*, 2017). FTD represents a major subgroup within the broad spectrum of neurological disorders that constitute frontotemporal lobar degeneration (FTLD), a pathology characterized by atrophy in the frontal and temporal lobes of the brain. The high relevance of extramotor symptoms in ALS re-characterized this disorder as a multisystem neurodegenerative process rather than neuromuscular; because extra-motor areas of the brain may undergo degeneration (Neary, Snowden and Mann, 2005; Phukan, Pender and Hardiman, 2007; Lillo and Hodges, 2009; Ferrari *et al.*, 2011; Swinnen and Robberecht, 2014; Hardiman *et al.*, 2017).

1.2 Aetiology of ALS

The cause of ALS is incompletely understood. All evidence accumulated from clinical and basic research proposed ALS as a complex genetic disorder with multiple causes.

Mathematical models used to analyse population-based registers have highlighted that individuals with ALS possess a higher number of 'at risk' variants of different genes compared to healthy subjects. Those determine the individual's susceptibility, which then can act in combination other environmental and random effects to allow the disease to manifest (Kenna et al., 2013; Renton, Chiò and Traynor, 2013; Al-Chalabi et al., 2014; Boylan, 2015; Hardiman et al., 2017).

ALS has two clinically defined but indistinguishable subtypes: familial (FALS) and sporadic ALS (SALS). Patients belonging to the FALS subgroup report a family history of ALS showing usually an autosomal dominant Mendelian pattern of inheritance linked to mutations in genes involved in a wide variety of functions, and even roles in non-neuronal cells. 5% - 10% of ALS patients display a family history of ALS itself or FTD in a first degree relative, while up to the 20% possess an affected relative in more extensive family studies (Al-Chalabi et al., 2010; Boylan, 2015; Hardiman et al., 2017).

Most ALS cases are considered SALS, as they appear to occur randomly throughout the community, but is well recognized that the amount of SALS cases is over-estimated due to a lack information about family history of certain patients. Twin studies have shown heritability even in apparently sporadic ALS, suggesting that a relevant genetic contribution is present even in patients with no family history. Certain haplotypes increase the risk for the disease (Byrne et al., 2013; Renton, Chiò and Traynor, 2013; Al-Chalabi et al., 2014; Leblond et al., 2014; Swinnen and Robberecht, 2014; Boylan, 2015; Al-Chalabi, van den Berg and Veldink, 2016; Hardiman et al., 2017). Overall, the heritability of ALS is estimated at ~ 60%.

1.3 Genetics

In the last years, our knowledge of ALS genetic causes increased rapidly, as well as the relationship between different disease subtypes and the clinical outcomes. Genetic factors involved in ALS can range from highly penetrant to sequences which seems to have a very mild impact on the susceptibility to this disorder. Also, epigenetics appears to be involved in ALS. Remarkably, most causative genetic variants are generally implicated in a relatively small group of cellular functions including vesicle transport, autophagy, DNA/RNA processing, oxidative stress, and metabolism. Of the 30 known genes that have been to discover to play an important role in the development of ALS (**Table 1.1**) (Corcia et al., 2017; Chia, Chiò and Traynor, 2018), our current knowledge derives mainly from studies of ancestral European and East Asian populations. Four of these genes account for up to 70% of all FALS cases in the above-mentioned populations, namely: *SOD1*, *FUS*, *TARDBP* and *C9ORF72* (Renton, Chiò and Traynor, 2013; Leblond et al., 2014; Zufiria et al., 2016; Hardiman et al., 2017; Mead et al., 2023).

Table 1.1 List of genes involved in ALS.

Locus Number	Chromosome	Gene	Encoded Protein
ALS 1	21q22.11	<i>SOD1</i>	Cu-Zn superoxide dismutase
ALS 2	2q33.1	<i>ALS2</i>	Aslin
ALS 3	18q21	<i>Unknown</i>	N/A
ALS 4	9q34.13	<i>SETX</i>	Senataxin
ALS 5	15q21.1	<i>SPG11</i>	Spataxin
ALS 6	16p11.2	<i>FUS</i>	Fused in sarcoma RNA binding protein
ALS 7	20p13	<i>Unknown</i>	N/A
ALS 8	20q13.32	<i>VAPB</i>	Vesicle-associated membrane protein
ALS 9	14q11.2	<i>ANG</i>	Angiogenin
ALS 10	1p36.22	<i>TARDBP</i>	TDP-43
ALS 11	6q21	<i>FIG4</i>	Polyphosphoinositide phosphatase
ALS 12	10p13	<i>OPTN</i>	Optineurin
ALS 13	12q24.12	<i>ATXN2</i>	Ataxin 2
ALS 14	9p13.3	<i>VCP</i>	Valosin-containing protein / Transitional endoplasmic reticulum ATPase
ALS 15	Xp11.21	<i>UBQLN2</i>	Ubiquilin 2
ALS 16	9p13.3	<i>SIGMAR1</i>	Sigma non-opioid intracellular receptor 1
ALS 17	3p11.2	<i>CHMP2B</i>	Charged multivesicular body protein 2b
ALS 18	17p13.2	<i>PFN1</i>	Profilin-1
ALS 19	2q34	<i>ERBB4</i>	Receptor tyrosine-protein kinase erbB-4
ALS 20	12q13.13	<i>HNRNPA1</i>	Heterogeneous nuclear ribonucleoprotein A1
ALS 21	5q31.2	<i>MATR3</i>	Matrin-3
ALS 22	2q35	<i>TUBA4A</i>	Tubulin α 4A chain

ALS 23	10q22.3	ANXA11	Annexin A11
ALS 24	4q33	NEK1	Serine–threonine protein kinase Nek1
ALS 25	12q13.3	KIF5A	Kinesin heavy chain isoform 5A
FTD1-ALS	9p21.2	C9ORF72	Chromosome 9 open reading frame 72
FTD-ALS2	22q11.23	CHCHD10	Coiled-coil–helixcoiled–coil-helix domain containing protein 10
FTD-ALS3	5q35.3	SQSTM1	Sequestosome-1
FTD-ALS4	12q14.2	TBK1	Serine–threonine protein kinase
FTD-ALS5	16p13.3	CCNF	Cyclin F
ALS-new	3p21.1	GLT8D1	Glycosyltransferase 8 domain-containing protein 1
ALS-new	2p13.3	TIA1	Cytotoxic granule associated RNA-binding protein
ALS-new	21q22.3	C21orf2	Cilia and Flagella associated protein 410
ALS-new	17q21.2	DNAJC7	DnaJ heat shock protein family (Hsp40) member C7
ALS-new	2p14	LGALS1	Galectin-related protein
ALS-new	9p24.3	KANK1	KN motif and ankyrin repeat domain-containing protein 1
ALS-new	7q31.2	CAV1	Caveolin 1
ALS-new	9q22.31	SPTLC1	Serine palmitoyltransferase, long-chain base subunit 1
ALS-new	10q25.2	ACSL5	Long-chain fatty acid coenzyme A ligase 5
ALS-putative	8p21	ELP3	Elongator protein 3
ALS-putative	2p13	DCTN1	Dynactin
ALS-putative	1p36.13	PARK9	Probable cationtransporting ATPase 13A2

1.3.1 Superoxide Dismutase 1

Sequence variants in the gene encoding the Cu/Zn superoxide dismutase enzyme (*SOD1*) on chromosome 21q12.1 were the first gene variants found to be causative of ALS (Rosen et al., 1993). The native *SOD1* protein consists of 154 amino acids, and it catalyses the dismutation of the superoxide anion to hydrogen peroxide, reducing oxidative stress. The *SOD1* gene encodes the translation of an antioxidant enzyme mainly found as a 32-kilodalton homodimer in different cellular compartments, including: nucleus, cytoplasm, and mitochondrial intermembrane space (Rosen et al., 1993).

The more than 185 *SOD1* variants linked to ALS account for about the 20% of patients with FALS and 1–2% of SALS, with a degree of geographical variation. (Renton, Chiò and Traynor, 2013). The mutations are distributed in all the 5 exons of *SOD1*. The majority are missense mutations, but some C-terminal truncation mutations, small deletions or insertions have been reported as well. The pattern of inheritance is autosomal dominant except for the p.D90A mutation, the most common *SOD1* mutation worldwide, which is recessive in Scandinavia and dominant in other populations; the reasons for this are poorly understood (Giannini et al., 2010; Andersen and Al-Chalabi, 2011; Tortelli et al., 2013; Boylan, 2015; Li and Wu, 2016).

Mutated *SOD1* triggers neurotoxicity, but the molecular pathogenesis of SOD1 ALS is not yet fully understood. However, there is evidence of toxic gain-of-function mechanisms that lead to motor neuron degeneration (Ferrari et al., 2011; Al-Chalabi, van den Berg and Veldink, 2016).

Dysregulation of iron metabolism and oxidative stress are frequently found in both ALS patients and animal models carrying *SOD1* mutations (Ferrari et al., 2011). It has been hypothesized that ALS-related mutations of *SOD1* can induce a conformational change in the protein that can lead to a toxic effect detrimental for the motor neurons (Ferrari et al., 2011). In this respect, the oxidative stress observed because of mutations in *SOD1* has been associated to a gain in *SOD1* toxicity rather than a loss of enzymatic function (Redler and Dokholyan, 2012).

Even though oxidative stress seems to be relevant for the pathophysiology of SOD1- ALS, the main hypothesis underpinning *SOD1* toxicity is that most mutations induce a conformational change that leads to *SOD1* misfolding. Misfolded mutant *SOD1* proteins are targeted for degradation through ubiquitylation; however, the misfolded proteins seem to accumulate as oligomers and later as aggregates which may be resistant to ubiquitination preventing their recognition and degradation by the proteasomal. Consequently, the aberrant proteins accumulate and impair the ubiquitin-proteasome system (UPS) provoking the accumulation also of other proteins that should be normally processed by the UPS. Then, this accumulation events together with other stressors, such as ageing, triggers the unfolded-protein response (UPR) and leads to the impairment of many other cellular functions causing axonal retraction, denervation, and ultimately cellular death (Bruijn et al., 1998; Andersen and Al-Chalabi, 2011; Bendotti et al., 2012; Robberecht and Philips, 2013).

Evidence supports the involvement of a mutated *SOD1* prion-like mechanism in ALS able to promote protein aggregation and symptoms worsening pathology in ALS patients (McAlary et al., 2020).

The initial demonstration of the capacity of cellular *SOD1* to misfold or aggregate in a prion-like way within living cells involved the introduction of recombinant *SOD1* aggregates into cultured cells that were overproducing mutant *SOD1* variants linked to ALS (Münch et al., 2011). The suggestion was made that the foreign *SOD1* aggregates entered the cells by macropinocytosis and escaped the macropinosomes to instigate the aggregation of cytosolic

SOD1 (Münch et al., 2011; Holmes et al., 2013; Grad et al., 2014; Zeineddine et al., 2015). Grad et al. (2014) identified two primary processes by which propagation was occurring: the release of aggregates from dying cells, and the accumulation of misfolded protein inside exosomes. Recently, it has also been demonstrated that misfolded SOD1 is carried by extracellular vesicles that are purified from the neural tissues of SOD1-G93A mice (Silverman et al., 2019), providing additional evidence that this mechanism may play a significant role in the prion-like spread of protein aggregation in ALS.

1.3.2 C9orf72

The mutations in the *C9ORF72* gene, located on chromosome 9p21.2, that cause ALS are hexanucleotide repeat expansion mutations (DeJesus-Hernandez et al., 2011). *C9ORF72* contains a GGGGCC hexanucleotide (G4C2) sequence that is in the first intron between two transcription initiation sites. In most healthy individuals, the G4C2 sequence is repeated two-to-eight times (Babić Leko et al., 2019). It is rarely repeated more than five times and repeats of > 30 seem to have no negative effect on gene function, but the minimum repeat length associated with ALS has not been discovered yet (Rohrer et al., 2015; Iacoangeli et al., 2019). *C9ORF72* repeat expansion is the most common gene variant associated with fALS. It is found in 40% of fALS and about 6–8% of SALS patients, with variation in the incidence between different countries. Inheritance is autosomal dominant with incomplete penetrance (Majounie et al., 2012). This expansion is also found in 25% of patients with familial FTD without ALS and 6% of patients with sporadic FTD. In families with ALS-FTD, the frequency reaches 50–72%. The physiological function of *C9ORF72* is poorly understood, but it is considered to be mainly cytosolic and is structurally related to differentially expressed in normal and neoplastic cells (DENN) domain proteins, a class of highly conserved GDP–GTP exchange factors for RAB GTPases (Levine et al., 2013). A role related to the lysosomes has been proposed thanks to data showing impairment of lysosomal morphology and enhancement of mammalian target of rapamycin 1 (mTORC1) in *C9ORF72* KO animal and cellular models (Amick and Ferguson, 2017; Webster et al., 2018). *C9ORF72* seems to be able to interact with Rab1a and the Unc-51-like kinase 1 (ULK1) autophagy initiation complex. *C9ORF72* impacts the initiation of autophagy through the regulation of Rab1a-dependent trafficking of the ULK1 autophagy initiation complex towards the phagophore (Webster et al., 2016).

The molecular pathogenesis of the repeat expansions in *C9ORF72* remains to be elucidated; both gain of function and loss of function mechanisms may both be at play. ALS patients with a *C9ORF72* expansion show a reduction of up to 50% of *C9ORF72* mRNA levels, suggesting that the expansion allele decreases the production of mature *C9ORF72* mRNAs (DeJesus-Hernandez et al., 2011). Therefore, the *C9ORF72* expansion could be a loss-of-function mutation. Since ALS caused by *C9ORF72* mutations is dominantly inherited, this could indicate haplo-insufficiency as a possible pathological mechanism. Fluorescence in situ hybridization (FISH) experiments have demonstrated that the expanded G4C2 repeat RNA adopts unusual secondary structures, in particular G-quadruplexes, and these secondary structures act as a sink for nuclear RNA-binding inducing the formation of nuclear foci in neurons of *C9ORF72* ALS patients (DeJesus-Hernandez et al., 2011). The foci sequester RNA-binding proteins, compromising the correct splicing of other mRNAs and therefore promoting the expression of proteins containing or lacking certain essential sequences. Therefore, expanded *C9ORF72* pre-mRNA may exert a deleterious gain-of-function effect. These two mechanisms are not mutually exclusive and of course other mechanisms caused by the expansion of the repeated sequence can be causative of ALS (Robberecht and Philips, 2013; Boylan, 2015; Li and Wu, 2016; Zhang and Ashizawa, 2017).

Inhibition of endosomal trafficking and the perturbation of endocytosis after a reduction in the *C9ORF72* protein level is also proposed as a potential explanation of *C9ORF72* role in the development of ALS and FTD, but *C9ORF72* knockout mice did not show any sign of motor neuron degeneration (Burk and Pasterkamp, 2019). A third proposed pathophysiological mechanism relates to the non-AUG translation of G4C2 RNA repeats into toxic dipeptide repeat proteins (DPRs): polyGP, polyGA, polyGR, polyPA and polyPR (Cheng et al., 2018). Even if the phenomenon of DPR aggregation has been widely found in C9-ALS patients motor neurons, the precise pathophysiological role remains unknown. Interestingly, among the 5 different DPRs only poly-PR, poly-GR, and poly-GA are currently known to be toxic. PolyGA is thought to be the most toxic among them, and with evidence that it can activate programmed cell death and TDP-43 cleavage (Cheng et al., 2018).

1.3.3 Fused in Sarcoma and TAR DNA-Binding Protein 43

Variants in the gene fused in sarcoma (*FUS*) on chromosome 16p11.2 have emerged as the third most common cause of ALS, accounting for about 3-5 % FALS and ~1 % SALS. *FUS* is a

nuclear RNA-binding protein containing multiple RNA-binding domains and a prion-like domain. *FUS* seems to bind co-transcriptionally to very long intron sequences of pre-mRNAs from more than 5,500 genes, stabilizing and regulating their splicing. Several of these genes encode known neuronal proteins (Dormann and Haass, 2011). Variants altering these functions can contribute to neurodegeneration, but the molecular pathogenesis of FUS-ALS is not fully understood. Most FUS mutations cause a disruption of nuclear import and lead to the mislocalization of the FUS protein into the cytoplasm, where it forms toxic inclusions. The aggregation propensity of FUS is determined by its prion-like domain (Dormann and Haass, 2011; Robberecht and Philips, 2013; Boylan, 2015; Li and Wu, 2016).

Mutations in TAR DNA Binding Protein (*TARDBP*) on chromosome 1p36.22, which encodes the TAR DNA-binding protein 43 (TDP43), account for 4 % of FALS cases and ~1 % of SALS. TDP43 belongs to the family of heterogenous ribonucleoproteins and can bind both DNA and RNA. It is known to be multifunctional and shows involvement in transcription, RNA splicing and transport. TDP43 targets more than 6,000 mRNAs (Polymenidou et al., 2011). The pathogenic mechanism of disease-linked *TARDBP* variants has still not been fully elucidated, but disease-associated mutations lead to a redistribution of TDP43 location from the nucleus to cytoplasm where it forms toxic inclusions (Prasad et al., 2019).

Despite the atherogenicity of ALS aetiology, 97 % of patients show common the accumulation of TDP-43 in ALS affected tissues (Ling et al., 2013; Scotter et al., 2015). This accumulation of TDP-43 is also found in tau-negative FTD as a clinical overlap with ALS (Neumann et al., 2006). TDP-43 protein was found as major component of the ubiquitinated neuronal cytoplasmic inclusions in cortical neurons of FTD patients and in spinal motor neurons in ALS patients (Neumann et al., 2006). Neurodegenerative diseases associated with the accumulation of TDP-43 are named TDP-43 proteinopathies, the term TDP-43 proteinopathy also indicates the histopathological transformation of TDP-43 occurring during the disease progression (Kwong et al, 2007), which is highlighted by the accumulation of fragmented and full-length TDP-43 protein as ubiquitinated, hyperphosphorylated and detergent-resistant aggregates in the cytoplasm, and consequent reduction of nuclear TDP-43 (Neumann et al., 2006). The diffusion of TDP-43 proteinopathy from spinal and cortical motor neurons and glial cells to other cortical regions can also be adopted as a measure of ALS stages and progression (Ash et al., 2010).

1.4 Pathophysiological Mechanisms

The fundamental pathophysiological mechanisms underlying ALS are not fully understood, but during the past years researchers have made many important discoveries related to the identification of the genetic causes of ALS, and models have been developed to study relevant biological mechanisms for disease pathobiology and motor neuron degeneration (Renton, Chiò and Traynor, 2013). Cellular disruption in ALS, as in other neurodegenerative diseases, is likely to be caused by a complex interplay resulting from many different interacting mechanisms (**Figure 1.1**), but the contribution of these different factors to the overall human pathobiology has not been fully elucidated yet. Moreover, it cannot be assumed that all these factors are involved in all cases of ALS, as this human disease is heterogeneous. Nonetheless, the study of these mechanisms is fundamental to understand the pathophysiology of ALS and is the driver of current and future targeted drug development (Wijesekera and Leigh, 2009; Hardiman et al., 2017).

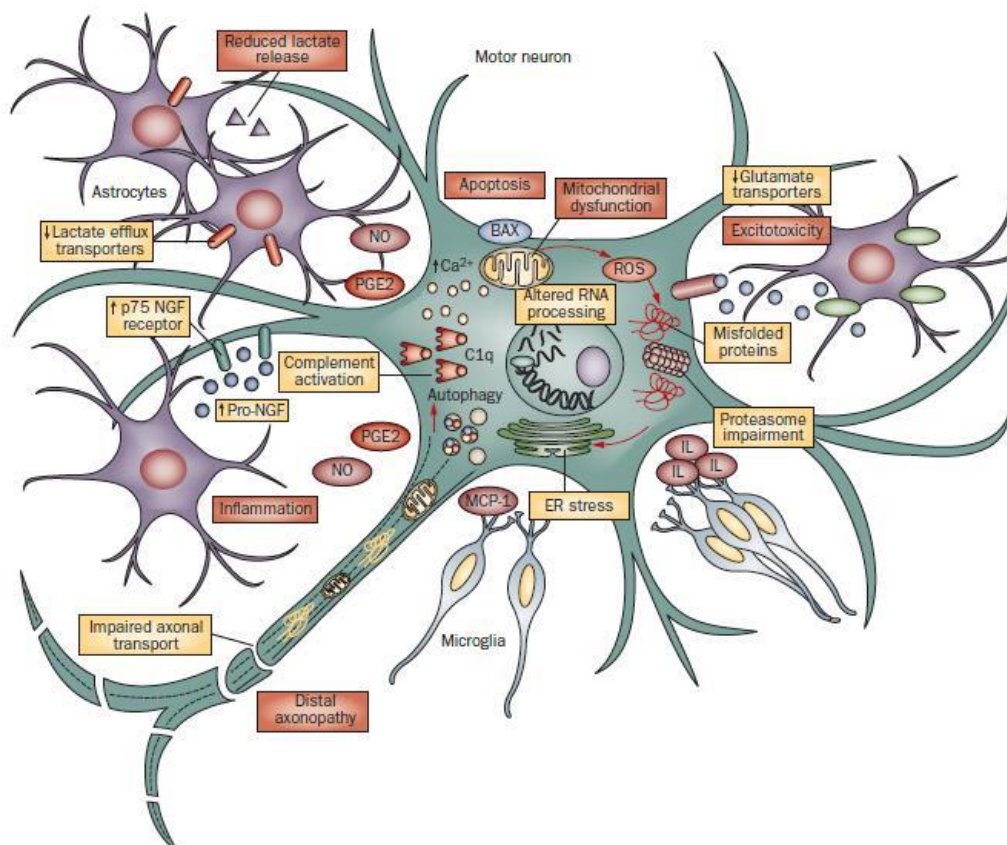


Figure 1. 1 Molecular mechanisms leading to motor neuron injury in ALS.

Mechanisms involved include glial cell activation, abnormal RNA metabolism, protein aggregation, ER stress, excitotoxicity, mitochondrial impairment, and impaired axonal transport. This image has been obtained from (Ferraiuolo, Kirby, et al., 2011).

1.4.1 Impaired Protein Homeostasis

Mutations in many ALS-related genes cause the translation of misfolded proteins with abnormal cellular localization and higher propensity to cause inclusions. These mutated proteins can directly or indirectly impair several cellular mechanisms, such as the proteasomal or autophagic system leading to impaired protein turnover. Pathological protein aggregates seem to represent a cardinal feature of ALS, as intra-cytoplasmic inclusions are a hallmark of both sporadic and familial ALS (Renton et al., 2011). However, it is still unclear and has not been completely demonstrated whether aggregate formation directly causes cellular toxicity and has a key role in pathogenesis. One possibility is that aggregates may be a leading cause of neurodegeneration, or they could even be part of a defence mechanism that aims at reducing intracellular concentrations of toxic proteins (Wijesekera and Leigh, 2009; Ferraiuolo, Kirby, et al., 2011; Hardiman et al., 2017).

1.4.2 Oxidative Stress

Oxidative stress can induce damage at the structural level of proteins, lipids, DNA and RNA and modify redox-associated signalling. This stress is due to an impairment of the balance between the formation and removal of reactive oxygen species (ROS), or eventually from an impairment of the cells related to their ability to remove or repair proteins damaged by the ROS. The role of oxidative stress in ALS has been extensively studied following the discovery of ALS-linked mutations in *SOD1*, which indeed encodes one of the most relevant human antioxidant proteins. Therefore, it has been taken into consideration as one of the putative pathogenic mechanisms involved in this disorder. This hypothesis is also reinforced by several findings that detected biochemical changes in cells obtained from ALS patients and in animal models leading to elevation of free radical damage to proteins, lipids and DNA, and abnormal free radical metabolism (Mitsumoto et al., 2008). Interestingly, a peculiar feature of *SOD1* is that the protein itself is particularly susceptible to oxidative post-translational modifications on cysteine residues, and these modifications have been recently shown to play an important role in the abnormal aggregation of mutant *SOD1*. (Furukawa and O'Halloran, 2006).

The abnormal biochemical reactions caused by ALS-linked mutations *SOD1* induce the generation of the following ROS: the superoxide anion (O_2^-), hydroxyl radical (OH), hydrogen peroxide (H_2O_2), and peroxynitrite ($ONOO^-$). For instance, an increased

production of H₂O₂ caused by mutant SOD1 has been described in in vitro systems of ALS (Ighodaro and Akinloye, 2018), even though this has not been detected consistently in spinal cord and brain biosamples obtained from mutant *SOD1* transgenic mice (Nita and Grzybowski, 2016).

1.4.3 Aberrant RNA metabolism

Alteration of RNA processing is another key theme in the pathophysiology of ALS, since most ALS cases for which we know the cause, are related to mutations in proteins involved in RNA metabolism or mutations involved in RNA sequestration, for example *TARDBP*, *FUS*, *C9ORF72*, Heterogeneous nuclear ribonucleoprotein A1 (*HNRNPA1*) (Purice and Taylor, 2018). RNA undergoes complex processing as it transits from the nucleus to the cytoplasm. This level of complexity, other than allowing a precise control of gene expression, also provides many different opportunities for interfering with its regulation leading to pathological effects. Some examples of RNA metabolism alteration mechanisms include interfering with RNA synthesis, transport, assembly with polyribosomes for translation and enhancing the degradation rate. In this respect, it is possible to observe and analyse alterations of RNA metabolism in ALS at different levels, such as: gene transcription, RNA granule formation, transport, and translational regulation (Strong, 2010; Ferraiuolo, Kirby, et al., 2011; Hardiman et al., 2017).

The modulation of RNA stability is essential for the regulation of gene expression, and its turnover is strongly influenced by the interaction with specific RNA-binding proteins. These trans-acting factors may be either stabilizing or destabilizing, and their specific RNA binding activity depends not only on their structure, but also on both post-translational modifications and the nature of the associated proteins which form the RNA binding complex. Consequently, different possible alterations concerning the interactions between trans-acting and corresponding cis-acting elements can affect mRNA stability promoting cellular degeneration in ALS patients (Bolognani and Perrone-Bizzozero, 2008; Strong, 2010).

There are also several significant consequences of impaired phase transitions by ALS-associated RNA-binding proteins, including alterations in the properties of RNA granules (Nedelsky and Taylor, 2019), generation of oligomers with toxic properties, and a partial or complete loss of the normal function of RNA-binding proteins (Lagier-Tourenne et al., 2012; Taylor, Brown Jr and Cleveland, 2016). In this respect, the relocation into the cytoplasm of

ALS-linked mutant TDP-43, FUS and hnRNPA1 (Renton et al., 2011; Johnson et al., 2014), can be associated with a cytoplasmic sink caused produced by cytoplasmic RNA granules with a low level of dynamic mobility (Hyman, Weber and Jülicher, 2014). The direct consequence of this relocation is the diminution of RNA-binding proteins from the nucleus with the potential to cause loss of key nuclear functions.

1.4.4 Excitotoxicity

Excitotoxicity describes the neuronal damage associated with an excessive activation of glutamate receptors. Glutamate, being the major excitatory neurotransmitter in the CNS, can signal through a wide category of metabotropic and ionotropic receptors. Excitotoxicity can be triggered through an increased level of glutamate at the synaptic cleft or by an increased sensitivity of the postsynaptic neurons to that neurotransmitter. In both situations, excitotoxicity leads to an impairment in neuronal homeostasis or glutamate receptor expression (van Cutsem et al., 2005). The main hypothesis for explaining the excitotoxicity pathogenic mechanism proposes that an over-stimulation of glutamate receptors induces a massive calcium influx into the neurons, which in turn causes secondary effects such as activation of proteolytic pathways, activation of ROS-generating enzyme systems, perturbation of mitochondrial function and ATP production (Wijesekera and Leigh, 2009; Ferraiuolo, Kirby, et al., 2011; Hardiman et al., 2017).

Excitotoxicity has been found to be a common mechanisms of motor neuron degeneration in all forms of ALS, but its relevance as a major causative mechanism still needs to be proved. Even if rodent models provided several lines of evidence supporting the role of excitotoxicity in ALS, and reducing excitotoxicity is nowadays one the few effective strategies for slowing the progression of the disorder. In fact, one of the mechanisms of action of the first FDA-approved treatment for ALS, named riluzole, is indeed the blockage of voltage-gated Na⁺ channels on presynaptic neurons reducing glutamate release and glutamatergic neurotransmission. However, other anti-glutamate agents have not been effective in clinical trials (Wang et al., 2011).

1.4.5 Mitochondrial Dysfunction

Abnormalities in mitochondrial morphology and biochemistry have been reported in skeletal muscle and spinal motor neurons from some ALS patients. In mutant SOD1 transgenic mice, the mutant protein aggregates in vacuoles in the mitochondrial inter-

membrane space, and it has been postulated that these protein-containing vacuoles may lead to organelle dysfunction by impeding protein import (Vande Velde et al., 2008; Ferraiuolo, Kirby, et al., 2011). For instance, electron microscopy analysis detected the presence of human *SOD1G93A* in mice showing vacuolated mitochondria. Those mice have been shown to have a drastically reduced mitochondrial activity and ATP production (Muyderman and Chen, 2014), and this deficit increased during disease progression. Indeed, data demonstrated that the infiltration of mutant SOD1 into the mitochondrial intermembrane space is itself pathogenic and sufficient to cause neuronal death (Magrané et al., 2009).

ALS patient samples harbouring mutant SOD1 highlighted the presence mitochondrial damage and defective respiratory chain function, and reinforced the hypothesis that dysregulated energy metabolism is an important pathophysiological mechanism in ALS (Parone et al., 2013; Hardiman et al., 2017). Interestingly, mitochondria purified from the CNS of mutant SOD1 transgenic mice have also a reduced capacity for buffering calcium (Ferraiuolo, Kirby, et al., 2011), which in addition to discovery of a disrupted ER–mitochondria calcium exchange in ALS mouse models, indicates that mitochondrial impairment could also increase the susceptibility of motor neurons to excitotoxicity (Grosskreutz, Van Den Bosch and Keller, 2010).

1.5 Neuronal Vulnerability in ALS

The increased vulnerability of precise neuronal groups to neurodegeneration is a key feature of ALS. Motor neurons are the main neuronal subtype involved in ALS. Neurons in the prefrontal and temporal cortex are also affected in ALS, but to varying degrees, while sensory and autonomic neurons as well as cerebellar neurons are often preserved or just mildly affected (Fu, Hardy and Duff, 2018).

The reason why motor neurons are more susceptible to mutations that indeed affect ubiquitously distributed proteins is not completely understood. These cells seem to have specific features that may predispose them to age-related degeneration. One of these important properties is thought to be the large cell size, including long axons and large terminal arbours. This feature imposes several conditions that must be satisfied to avoid cell injury: extremely efficient intracellular transport, high metabolic demand, robust

cytoskeletal support, and fine regulation of mRNA distribution for protein synthesis (Ferraiuolo, Kirby, et al., 2011; Robberecht and Philips, 2013).

1.6 Glial Involvement in ALS

Extensive neuroinflammation and gliosis occur in ALS, as well as other neurodegenerative diseases. This aspect can be seen in imaging studies in patients with ALS in vivo, as well as in human post-mortem samples and in rodent models of ALS (Corcia et al., 2013; Brites and Vaz, 2014). The evidence of this prominent reactive gliosis, in addition to several findings coming from studies carried out on ALS transgenic mice expressing the mutant hSOD1 enzyme, which have shown the presence of mSOD1 inclusions in various glial subpopulations (Bruijn et al., 1997; Stieber, Gonatas and Gonatas, 2000), brought to light the hypothesis that neuronal death in ALS may not be a cell-autonomous process. Thus, the neighbouring glial cells could have a crucial role in the disease (Yamanaka et al., 2008; Wang et al., 2009; Robberecht and Philips, 2013). The first evidence that glial cells could have a relevant role in motor neuron degeneration and disease progression in the context of ALS has been shown in chimeric mice having a mixture of mSOD1 expressing cells and wild type cells. Disease onset and progression were highly affected by the level of the mSOD1 expressing cells (Clement et al., 2003). Depletion of mSOD1 from motor neurons showed a delayed disease onset, while depletion from glial cells delayed disease progression (Boillée et al., 2006). For the scope of this thesis, I will focus on the role of astrocytes in the pathogenesis of ALS.

Astrocytes are ectodermal glial cells involved in many important functions aimed at maintaining and nourishing neurons, such as neurotransmitter recycling, ion homeostasis, and metabolic support to surrounding neurons. Among the diverse functions carried out by astrocytes, they are also involved in the neuroinflammatory response. In physiological conditions, astrocytes manage the health of motor neurons providing nutritional and trophic support, and modulating synaptic activity and plasticity through the expression and secretion of a wide variety of mediators, such as neuropeptides (Prada et al., 2011), neurotrophins (Bergami et al., 2008; Gómez-Gonzalo et al., 2010), cytokines (Bruno et al., 1998; Fujita, Tozaki-Saitoh and Inoue, 2009), cholesterol and apolipoprotein E (Mauch et al., 2001). During injury or chronic neurodegenerative diseases, astrocytes undergo a complex biochemical and morphological remodelling called reactive astrogliosis and become

reactive. Reactive astrogliosis is commonly regarded as a sign of neuroinflammatory reaction, and it is associated with a change in the expression and secretion of several astrocytic molecules, including cytokines, chemokines, eicosanoids, ROS, NO and excitatory aminoacids. These molecules exert important regulatory effects, and neuropathologies or CNS injury can alter the production and the secretion of those astrocytic molecules, resulting in an unbalance of the tuning of the neuroinflammatory reaction, that can then be translated into neurotoxic events crucial in the pathogenesis of several chronic neurodegenerative disorders, including ALS (Sofroniew, 2015).

Astrocytes have also been implicated in dysregulated metabolic support towards motor neurons in ALS. Astrocytes are well known to increase their glycolytic activity under conditions of enhanced neuronal activity and metabolic demand. Astrocytes distribute glucose and lactate, which are used as energy substrates by neurons (Fünfschilling et al., 2012; Philips and Rothstein, 2014). Mutant SOD1 astrocytes show significant alterations in their metabolic pattern and lower cellular lactate shuttling function when are put in co-culture with motor neurons (Madji Hounoum et al., 2017; Valbuena et al., 2017). Moreover, decreased expression of monocarboxylate transporter 4 (MCT4), the astrocytic lactate transporter, and decreased levels of lactate in the spinal cord have been described in mSOD1 mice (Ferraiuolo, Higginbottom, et al., 2011; Pehar, Harlan and Vargas, 2017). In ALS astrocytes release insufficient neurotrophic factors, which are essential for the maintenance of neuronal health. Brain-derived neurotrophic factor (BDNF), glial cell-derived neurotrophic factor (GDNF), ciliary neurotrophic factor (CNTF), and vascular endothelial growth factor (VEGF) can be release by astrocytes for rescuing motor neurons in case of injury (Ekestern, 2004; Van Den Bosch et al., 2004; Van Den Bosch and Robberecht, 2008). It has been shown that a haplotype causing low expression levels of VEGF in ALS patients increased the vulnerability of motor neurons to the process of degeneration. This effect has been also confirmed through the deletion of VEGF in *SOD1G93A* mice (Lambrechts et al., 2003). Astrocytes, being an important source of VEGF, can improve motor neuron survival in case of insults (Van Den Bosch et al., 2004; Evans et al., 2013). Thus, astrocytes of ALS patients may not appropriately support motor neurons with metabolic substrates and trophic factors, causing indirect damage.

In addition, activated astrocytes may also release pro-inflammatory factors contributing to neuroinflammation (Ekestern, 2004; Dewil et al., 2007; Philips and Rothstein, 2014) and directly damaging motor neurons. mSOD1 astrocytes secrete several pro-inflammatory molecules that may exacerbate neurodegeneration, such as prostaglandin D2 (PGD2) and prostaglandin E2 (PGE2) (Di Giorgio et al., 2008; Liang et al., 2008), tumor necrosis factor α (TNF- α), interferon γ (INF γ) (Aebischer et al., 2011) and transforming growth factor beta (TGF- β) (Endo et al., 2015). Also, In the CNS, glutamate clearance is mediated by glutamate uptake transporters expressed principally by astrocytes (Mahmoud et al., 2019) and mutations in the SOD1 gene have been shown to decrease glutamate uptake from astrocytes leading to excitotoxicity towards the surrounding motor neurons (Van Den Bosch et al., 2006).

A better understanding of the role of astrocytes in the neurodegenerative process of ALS could make them an interesting therapeutic target. Modulating astrocyte biology may be an interesting therapeutic approach for slowing down ALS progression (Pehar, Harlan and Vargas, 2017).

1.7 Neurotrophins

In mammals, the family of neurotrophins includes the following 4 members: nerve growth factor (NGF), BDNF, neurotrophin-3 (NT-3) and neurotrophin 4 (NT-4, also known as NT-4/5). These molecules are all polypeptides that can homodimerize to operate a wide variety of functions in both neural and non-neural tissues, regulating adult physiology and embryonic development. Alteration of neurotrophin levels is associated with neurodegenerative and psychiatric disorders. These molecules are well known to improve neuronal survival, regulate axonal and dendritic growth/guidance to form connect synapsis, regulate the release of neurotransmitters, and are involved in long-term potentiation (LTP) and synaptic plasticity (Huang and Reichardt, 2001; Bothwell, 2016).

The 4 neurotrophins can signal through three paralogous receptor tyrosine kinases (TrkA, TrkB and TrkC) and neurotrophin receptor (p75NTR). The latter receptor belongs to the TNF receptor superfamily. p75NTR signalling can be triggered by all 4 neurotrophins, while the binding to a precise Trk receptor is specific for each neurotrophin. NGF binds preferentially to TrkA; BDNF and NT4 to TrkB; and NT3 to TrkC (Skaper, 2008) (Figure 2). The interactions of neurotrophins with the Trk receptors have been always considered to be of “high

affinity”, but data have shown that binding of NGF to TrkA, and of BDNF to TrkB is of “low affinity” (Allen, Watson and Dawbarn, 2011) and becomes high affinity through regulation of receptor dimerization, structural modifications, or association with p75NTR. P75NTR, as well as being able to bind the neurotrophins, can also act as a co-receptor binding other Trk receptors (Mitre, Mariga and Chao, 2017). For instance, p75NTR binding to TrkA increases its affinity and specificity for NGF (Uren and Turnley, 2014).

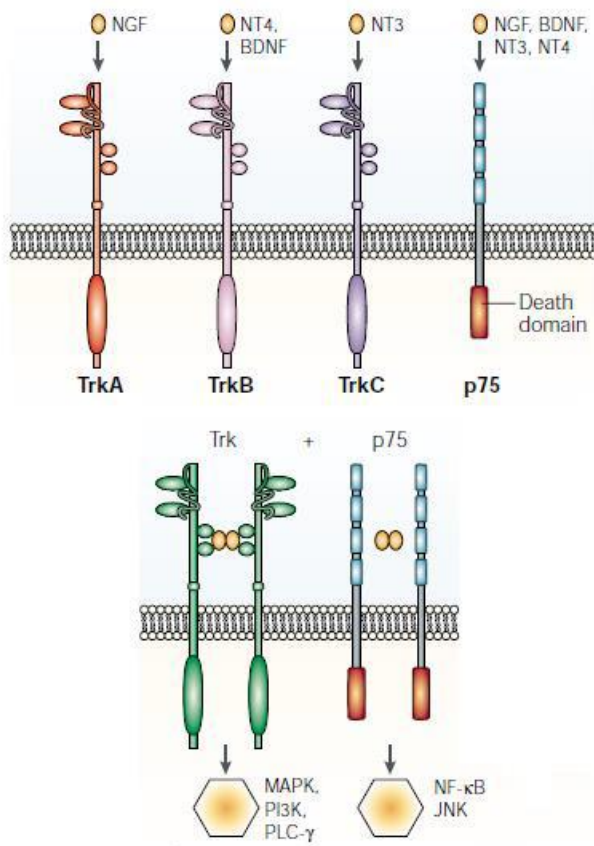


Figure 1. 2 Neurotrophin Receptors

Neurotrophins bind selectively to specific Trk receptors, while all neurotrophins bind to p75NTR. Each receptor activates several signal transduction pathways. This image has been modified from (Chao, 2003).

This ability of Trk and p75NTR receptors to interact, provides different levels of affinity and is essential to properly regulate the effects of different neurotrophins and discriminate between them.

Neurotrophins and the relevant receptors are not expressed in *Drosophila melanogaster* or *Caenorhabditis elegans*. This indicates that those molecules are not essential for the development of neuronal circuits but have a critical involvement in more complex aspects of neuronal activity, including for instance the formation of new long lasting synaptic connections (Chao, 2003).

p75NTR and Trk receptors are co-expressed in many cellular types and usually provide for opposite functions. (Bothwell, 2016). Generally, Trk signalling is involved in activities that support neurons, while p75NTR signalling is usually associated with cellular death and degeneration. For instance, in sympathetic neurons TrkA signalling promotes axon growth and neuronal survival, while p75NTR signalling promotes axon degeneration and neuronal cell death (Luther and Birren, 2009). Interactions between different neurotrophin receptors allow control of a wide variety of mechanisms and provides an extraordinary level of complexity.

Neurotrophins are synthesized as precursors (pro-neurotrophins) that are then cleaved intracellularly by FURIN or pro-convertases at the level of a highly conserved dibasic amino-acid cleavage site. The cleavage releases the N-terminal prodomain peptide, which is believed to have a role in the processes of folding and intracellular sorting of neurotrophins, and the C-terminal mature neurotrophin (on average 12 kDa) (Teng et al., 2010). The mature neurotrophin is then activated through the formation of stable non-covalent dimers. Interestingly, the cleavage can happen either during the secretory pathway or after secretion; in this way the receptors can bind both proneurotrophins and mature neurotrophins. Proneurotrophins have higher affinity than mature neurotrophins for p75NTR but cannot bind to Trk receptors (Boutillier et al., 2008; Bothwell, 2016). This higher affinity is due to the association of p75NTR with Vps10p-domain proteins that in turn can bind a conserved motif in the pro-neurotrophins (Leloup, Chataigner and Janssen, 2018). This feature adds additional combinations to finely regulate different cellular pathways and mechanisms through neurotrophin receptor signalling, and the presence or absence of specific Trk receptors on different neuronal cell types determines which specific effects can be activated. (Meeker and Williams, 2014).

1.7.1 Trk Signalling

The classical Trk signalling is analogous to other receptor tyrosine kinases. Neurotrophin binding triggers dimerization of the Trk receptor and induces transphosphorylation of

cytoplasmic domain tyrosine residues. This transphosphorylation then starts the recruitment of adapter proteins that further the signalling (Blondy et al., 2019). Neuronal survival promoted by neurotrophins binding to their Trk receptors gathers Src homologous and collagen-like (Shc), which bind as well Trk receptors and enhances phosphoinositide 3-kinase (PI3K) and Akt activities (Ahmed and Prigent, 2017). Trk receptors are also able to phosphorylate Shc after its binding, and this phenomenon leads to an increase of Ras and extracellular signal-regulated kinase (ERK) activities. All these molecules can then influence different transcriptional events including the induction of the cyclic AMP-response element binding (CREB) transcription factor which plays roles on cell cycle regulation, neurite outgrowth and synaptic plasticity (Wang et al., 2018).

Trk receptors possess a particular signalling feature compared to many other receptor tyrosine kinases. Trk receptors can achieve retrograde axonal signalling through signalling endosomes (Wang et al., 2018). Usually, receptor tyrosine kinase activation leads to its endocytosis followed either by lysosomal degradation or repositioning to the cell surface, but Trk receptors can regulate neuronal survival or differentiation through the generation of signalling endosomes following endocytosis of the neurotrophin/Trk complex. This activated complex is delivered to the somatic compartment through axonal transport and can control the nuclear transactivation of genes (Bothwell, 2016; Yamashita and Kuruvilla, 2016).

1.7.2 p75NTR Signalling

Being a death receptor, p75NTR possesses a juxta-membrane region of the cytoplasmic domain that can be bound by TNF receptor associated factor 6 (TRAF6). This binding pursues a signalling cascade that activates nuclear factor kappa-light-chain-enhancer of activated B cells (NF- κ B) and c-Jun N-terminal kinase (JNK) (Hayden and Ghosh, 2014; Walsh, Lee and Choi, 2015). Without neurotrophin binding, death domains of p75NTR dimers form a complex that binds Rho GDP-dissociation inhibitor (RhoGDI) and promotes RhoA activation. When a neurotrophin dimer binds to the extracellular domain of the p75NTR dimer, it triggers the separation of death domains revealing a receptor-interacting-serine/threonine-protein kinase 2 (RIP2) (Lin et al., 2015). RIP2 binds that site and displaces RhoGDI, initiating JNK activation and terminating RhoA activation (Dovas and Couchman, 2005; Bothwell, 2016).

However, TRAF6, RhoGDI and RIP2 are just a small part of the wide array of adaptor proteins

that mediate p75NTR signalling (Bothwell, 2016).

p75NTR, as mentioned before, is known to promote cell death (Kraemer et al., 2014). This process can be used during different developmental stages for cell depletion and to refine target innervation (Dekkers, Nikolettou and Barde, 2013), but is also often encountered during inflammatory events (Mao et al., 2017) and displays increased Rac and JNK activities, which have been shown to be associated with NGF-dependent cellular death (Kraemer et al., 2014). However, p75NTR can also signal anti-apoptotic and pro-survival responses (Huang and Reichardt, 2001), but its high affinity for proneurotrophins makes it more prone to pro-apoptotic pathways (Huang and Reichardt, 2001).

1.8 Alteration of Neurotrophin levels in the ALS Neuropathology

Many studies have examined levels of neurotrophins and their receptors in both in vitro and in vivo models of ALS. Alterations of their levels have been found at different stages of the disorder and suggest that this phenomenon might play a relevant role in disease pathogenesis (Pradhan, Noakes and Bellingham, 2019). BDNF promotes motor neuronal survival in a *SOD1G93A* mice (Deng et al., 2016; Sobuś, 2016). Injection of human BDNF in the ALS model wobbler mutant mice slowed the rate of grip strength decrease and improved muscle force (Sobuś, 2016). However, clinical trials based on BDNF injections in ALS patients did not show any relevant improvement of their clinical condition (Henriques, Pitzer and Schneider, 2010). When muscle progenitor cells (MPCs) overexpressing a combination of BDNF, GDNF, and insulin-like growth factor (IGF-1) were injected into the hind limbs of *SOD1G93A* mice a significant delay of disease onset and prolonged lifespan was observed, as well as decreased neuromuscular junction degeneration and increased axonal survival (Henriques, Pitzer and Schneider, 2010). Therefore, exploiting neurotrophins as a potential treatment for ALS may represent a relevant neuroprotective strategy, but their pharmacokinetic constraints such as: poor blood-brain barrier (BBB) penetration, limited bioavailability, limited diffusion from the site of injection and short half-life, limited their therapeutical use (Sobuś, 2016). Consequently, new approaches for neurotrophin delivery are worthy of investigation.

1.8.1 Direct infusion of Neurotrophic Factors and Neurotrophins as treatment for neurodegenerative disorders

The first attempts to verify the efficacy of neurotrophic factors (NTFs) in ALS was a series of trials employing subcutaneous (SC) injections of recombinant human ciliary neurotrophic

factor CNTF (rhCNTF) to obtain a systemic exposure (Bartus and Johnson 2017a). The study conducted on hundreds of ALS patients as multi-dose, double-blind, randomized, showed no benefit, and highlighted important dose-limiting side effects including anorexia (Bartus and Johnson 2017a). The last SC approach for ALS used insulin-like growth factor (IGF-1) in 3 separate studies which showed conflicting results (Borasio et al, 1998; Sorenson et al, 2008). All studies did not reveal serious adverse effects, but only one (Lai et al, 1997) reported beneficial effects for the patients. The issues with dose-related side effects and the lack of therapeutic efficacy via SC injection required a change of approach, therefore the following trials attempted the delivery of NTFs in ALS patients through intrathecal injection (IT). Initially, investigators tested IT injection of recombinant CNTF and BDNF (Penn et al. 1997). This approach did not show the side effects previously observed with SC delivery of rhCNTF. Lumbar and cervical taps also showed that injected rhCNTF and rhBDNF were well-diffused in the spinal cord. Nonetheless, IT administration of rhCNTF produced other side effects diverse from the ones observed with SC administration, including: headache and radicular pain. 3 more studies were conducted with IT injection of BDNF (Ochs et al, 2000; Kalra, Genge, and Arnold 2003) to assess whether IT was a better delivery system. These studies obtained similar results; BDNF was well-diffused in the spinal canal, but produced unique dose-related side effects, such as: sleep disturbance and lower limbs paraesthesia. These results implied the necessity of lowering the dosage when employing IT injection as a delivery approach, leading the investigators to adopt better delivery paradigms for future trials to safely provide NTFs as a therapy for ALS (Bartus and Johnson 2017b).

Trying to address issues related to NTFs delivery for treating neurodegenerative disorders, other studies delivered NTFs directly into the lateral ventricles through intracerebral ventricular injection (ICV) of patients affected from Alzheimer's disease (AD) or Parkinson's disease (PD), as a way to overcome the difficulty of crossing the BBB when delivering NTFs. 2 separated clinical trials (Olson et al, 1992; Seiger et al, 1993) injected rhNGF through ICV in AD patients. In the first study, this approach did not report side-effects and also resulted in slight memory improvements and revealed enhanced cerebral and cholinergic activity. Despite these promising results, the second study did not show any cognitive improvement on the treated patients and revealed several side-effects including back pain and weight loss.

Animal data in PD models (Gash et al, 2005; Granholm et al, 2000) demonstrated a recovery of degenerating nigrostriatal neurons after treatment with GDNF. Following these results, investigators tried to deliver rhGDNF to PD patients through ICV (Nutt et al, 2003). The results showed enhanced integrity of the nigrostriatal dopamine system in post-mortem brain tissues collected from the treated patients and improved bioavailability of GDNF in the CNS, but PD symptoms were not improved prior to death. Therefore, the clinical benefits of ICV injections of NTFs have been considered too limited for pursuing the use of this delivery system to treat neurodegenerative disorders.

Another NTFs delivery approach that has been tested was the direct injection into the target tissue. A small study in advanced standardized PD patients (Gill et al, 2003) tried intraparenchymal delivery of rhGDNF, which resulted in clinical improvements and enhanced dopamine uptake, without revealing any side-effects. 3 other publications (Love et al. 2005; Patel et al. 2005, 2013) from the same study provided some additional data; increased tyrosine hydroxylase and enhanced L-DOPA uptake were observed along the needle track in the infused hemisphere after collecting post-mortem brain tissues from the treated patients. Another open label study used intraparenchymal infusion, delivering rhGDNF unilaterally into the putamen of a small sample of advanced standardized PD patients (Slevin et al. 2005), resulting in a slight improvement of the clinical condition in some treated patients with no clear safety issues. Unfortunately, another study (Lang et al. 2006) adopting the same approach on a larger cohort of PD patients was unable to replicate the results observed in the previous study. The slow and limited diffusion of rhGDNF emerged as a serious limit of the intraparenchymal infusion (Salvatore et al. 2006; Sherer et al. 2006).

Collectively, all the information acquired from clinical trials delivering NTFs through different injection systems to treat neurodegenerative disorders induced the scientific community to move towards gene therapy delivery approaches.

1.8.2 Gene therapy approaches employing Neurotrophic Factors and Neurotrophins

Gene therapy is divided into two approaches: *ex vivo* and *in vivo*. *Ex vivo* gene therapy employs the use of cells, which can also be taken directly from patients, that are then modified to express the gene of interest and injected into the patient to allow the subsequent secretion of the therapeutic protein from the implanted cells.

In vivo gene therapy instead requires the delivery of therapeutic gene into the target endogenous cells of the patient, usually employing engineered viral vectors (Bartus and Johnson 2017a).

Gene therapy systems have been used for delivering NTFs in animal models of neurodegenerative disorders, including ALS. However, clinical trials reached advanced stages only for AD and PD patients (Bartus and Johnson 2017a).

The benefits obtained through gene therapy are the improvement of protein expression in the target tissues, the very low immunogenic potential due to the endogenous production of the protein, and the reduction of the complexities and disadvantages linked to chronic protein infusions and surgical procedures. Despite these advantages, since there are evidences related to the serious side effects occurring when NTFs are mis-targeted in the brain (Salvatore et al, 2006; Kordower et al, 2006), if these issues emerge after the gene therapy has been performed it will be impossible to prevent the transplanted cells from producing the transgene protein. Moreover, some NTFs might also play a role in tumorigenesis and metastasis (Krüttgen, Schneider, and Weis 2006).

Therefore, these aspects raised some concerns in relation to the delivery of NTFs through gene therapy approaches.

Ex vivo implantation of autologous fibroblasts genetically engineered for expressing NGF has been tested in a small open-label trial for AD patients. The cells were injected into the nucleus basalis of Meynert, and no serious side effects were observed in correlation with the expression of NGF. Implanted cells shown increased glucose consumption, and post-mortem analysis revealed cholinergic fibres responding to the NGF secreted by the transplanted cells (Tuszynski et al, 2005).

A different *ex vivo* trial involving NGF delivery was performed using genetically engineered cells obtained from a retinal pigment epithelial (RPE) cell line (Eriksdotter-Jönhagen et al, 2012). 6 AD patients were implanted with a removable device containing the NGF-secreting cells. No adverse side-effects were noticed, but only 2 patients showed minor improvements of their clinical conditions.

Another reported AD gene therapy Phase 1 trial employed instead the *in vivo* approach through the administration of the AAV2-NGF vector to the basal forebrain region (Rafii et al, 2014). This approach was reported to be well-tolerated from the treated patients. Brain

autopsies showed long-term NGF expression precisely targeting to the nucleus basalis of Meynert and inducing biological response. The following Phase 2 trial confirmed the feasibility and safety of this approach but failed to confirm the clinical improvements observed in the Phase 1 trial (Rafii 2015). Another gene therapy report provided further data obtained from autopsies of 10 AD patients that were enrolled in the previous trials. The report confirmed increase in cholinergic neurons activity and extension of neurites towards the NGF secreting cells, without pathological signs correlated with the viral vector or NGF itself (MH et al, 2015).

For PD patients, only in vivo gene therapy has been used in relation to NTFs delivery, with 4 trials testing AAV2-NRTN (Neuritin) and one trial testing AAV2-GDNF.

In the first Phase 1 trial employing AAV2-NRTN, the vector has been injected into the putamen of 12 PD patients. No safety issues were observed, while the treatment significantly improved cognitive and motor conditions in almost all treated patients (Marks et al. 2008). A following double-blind sham-surgery controlled trial in patients with advanced PD provided further efficacy data. After 12 months, the analysis of the primary endpoint motor component in off state of the Unified Parkinson's Disease Rating Scale (UPDRS) revealed a significant improvement in the treatment group compared to the sham surgery control group. Further analyses were also conducted on the following secondary endpoints: on-time without troublesome dyskinesia, off state mental subscale of the UPDRS, timed walking in the off state, and clinical global impression of improvements judged by the treating investigator and the patient. All these secondary endpoints showed significant improvement in the treated group (Marks et al, 2008; Bartus et al, 2013).

Autopsies of tissues obtained from 2 patients subjected to the previous trial showed that the secreted NRTN protein was precisely targeting putamen but was not detected in the substantia nigra (SN), where the degenerating dopamine cell bodies are found and where NRTN-signalling would provide the correct therapeutic response (Bartus et al. 2011).

Another AAV2-NRTN trial (Bartus et al, 2013) applied several protocol changes to increase the amount of NRTN expressed and its concentration at the neuronal terminals, aiming to enhance the clinical improvements in treated advanced PD patients. In this trial, AAV2-NRTN was also administered directly to the SN (Bartus and Johnson 2017b). This trial confirmed what has been observed previously, but despite the protocol changes aimed at

improving the therapy, the trial failed to achieve its primary endpoint and only few secondary endpoints showed significant improvements (Olanow et al. 2015).

1.9 Small neurotrophin mimetics

NTF mimetics are small organic molecules that mimic endogenous NTFs and therefore can bind the NTF receptors. Normally, NTFs mimetics are derived from specific domains of the endogenous NTFs and modified to improve bioavailability, BBB penetration and being less prone to proteolysis (Soto 2002). Some can also be designed for oral administration (Skaper 2011). Therefore, the potential of these molecules to overcome many of the endogenous NTFs limitation has attracted the interest of the scientific community in the last years (Price et al. 2007).

NTFs mimetics can also allow the precise activation of only one or few types of receptor, preventing potential side effects. For instance, direct activation of neurotrophin Trk receptors has been accomplished with xaliproden, an NGF potentiator and serotonin 5-HT_{1A} receptor agonist that improves neurite outgrowth in the presence of NGF (Liu et al., 2007), as well as the stimulation of endogenous growth factor receptors in motor neurons (Lacomblez et al., 2004). Xaliproden has been tested in a phase 3 trial of AD and ALS patients but failed to show clinical efficacy (Petrov et al. 2017).

7,8-dihydroxyflavone (7,8-DHF) can induce TrkB phosphorylation and promote neuroprotective activity (Kazim and Iqbal 2016; X. Liu et al. 2014). Studies testing 7,8-DHF in AD mouse models revealed beneficial effects on learning and memory after treatment (Castello et al. 2014). From the structure of 7,8-DHF, researchers also generated a prodrug called R7, which has improved potency and pharmacokinetics and emerged as a candidate for pre-clinical trials in AD patients (C. Liu, Chan, and Ye 2016).

The BDNF small mimetic compound called LM22A-4 can induce TrkB phosphorylation and prevent neuronal death in an *in vitro* model of AD (Massa et al., 2010).

The p75NTR binder LM11A-31 has been identified through *in silico* screening and was shown to block the A β -induced deleterious signalling (Yang et al., 2008) in AD transgenic mice (Simmons et al. 2014). LM11A-31 is currently in Phase II clinical trial for AD patients.

P6 is a small CNTF mimetic with longer half-life in the plasma, and better BBB penetration. P6 inhibits LIF signalling promoting neural precursor cell (NPCs) formation. Additionally, P6

increases the levels of BDNF mRNA, which can improve the survival and maturation of NPCs (Simmons et al, 2014; Bolognin et al, 2012). In a study on AD mice, the intraperitoneal administration of P6 for six weeks showed an improvement in spatial reference memory and short-term episodic memory by increasing neurogenesis and neuronal plasticity in the dentate gyrus (Kazim and Iqbal 2016). Previous preclinical studies on P6 have also shown neurogenic and neurotrophic effects in sporadic and familial AD animal models (Bolognin et al., 2012; Rockenstein et al., 2011).

The molecule P021 has been obtained by isolating and modifying P6 minimal biologically active region to enhance its BBB permeability (Kazim and Iqbal 2016). P021 increases the expression of synaptic markers and improves cognition in AD mice (B. Li et al, 2010). P021 treatment is also able to reduce tau pathology in AD mice, however it is only able to reduce the insoluble A β levels but not the A β plaques in the CA1 region of hippocampus (Kazim et al, 2014).

Despite the potential therapeutic benefits related to the NTFs mimetics, they have also shown limitations when employed for neurodegenerative disorders therapies, such as: insufficient receptor specificity, continuous dosing, and not brain region-specific effects (Longo and Massa 2013).

1.10 iNPCs in vitro models for ALS studies

Evidence from the last 20 years of research, highlighted the importance of the previously non-neuronal cellular types in the progression of the disorder and changed the concept of ALS to non-cell autonomous. Therefore, researchers began to investigate pathological mechanisms and test therapeutic strategies in non-neuronal cells (Haidet-Phillips et al., 2011).

To test interactions between astrocytes and MNs in the context of ALS, the system that has been adopted for the experiments presented in this thesis is a co-culture assay developed for screening therapeutics on astrocytes differentiated from induced neuronal progenitor cells (iNPCs) obtained from ALS patients (K Meyer et al., 2014). Direct conversion of NPCs from adult fibroblasts using reprogramming factors introduced by viral vectors, and subsequent stimulation with growth factors, allow to overcome the difficulties in isolating and expanding NPCs obtained from post-mortem tissues (K Meyer et al., 2014). Astrocytes

derived from iNPC adopting this reprogramming approach keep the detrimental properties leading to accelerated motorneuronal death that are normally observed with autopsy derived astrocytes (Haidet-Phillips et al., 2011).

Furthermore, it has been reported that the direct differentiation of iNPCs into iastrocytes exhibits age-related variations in genetic activity and characteristics (Gatto et al., 2021). These differences encompass aspects such as nuclear compartmentalization, reactions to oxidative stress, and responses to DNA damage. Additionally, following exposure to pro-inflammatory stimuli, iastrocytes obtained through iNPCs direct conversion show a distinct age-related neuronal supporting activity in co-culture. Lastly, this conversion protocol does not involve clonal expansion, which helps reducing the high variability associated with iPSCs direct conversion (Gatto et al., 2021).

1.11 Marine Extracts

The marine ecosystem contains a vast array of diverse organisms that experience distinct living conditions compared to those found in terrestrial environments. Numerous marine organisms are immobile, affixing themselves to various substances on the sea floor or forming symbiotic relationships with animals and plants. These complex connections between diverse groups of organisms are a notable feature of marine existence (Lindequist, 2016).

The unique challenges posed by the marine environment require organisms to develop specific adaptation mechanisms, often manifested through the creation of biologically active secondary compounds that serve a variety of functions. These functions include intra- and interspecific signalling, deterring herbivores and predators, thwarting neighbouring competitors, preventing bacterial and fungal intrusion, and offering defence against UV radiation (Lindequist, 2016). These secondary compounds hold significant promise for being developed into pharmaceuticals or medicinal products. While most drugs still originate from land-based sources, a substantial quantity of drug candidates and other bioactive compounds sourced from marine organisms have been discovered in recent times. These molecules are frequently distinguished by their unique structures, intricacy, and diversity (Kiuru et al., 2014; Hu et al., 2015).

Numerous research efforts have showcased that marine natural compounds often originate from microbes, predominantly bacteria or cyanobacteria. Nevertheless, these

microorganisms typically cannot be grown independently in a completely pure culture. Their growth is intricately linked to their host organisms. In instances where cultivating these microorganisms in isolation is feasible, only a subset of their genes is likely to be activated. Many genes tend to remain inactivated and are not manifested under laboratory conditions (Lindequist, 2016).

From a pharmacological perspective, the pursuit of new therapeutic marine compounds largely revolves around substances exhibiting cytostatic and cytotoxic properties. This can be rationalized by the ecological role of these compounds in defence mechanisms and the demand for novel antitumor medications (Mayer et al., 2010). Nonetheless, marine drugs can also provide diverse protective effects such as anti-oxidant, anti-inflammatory, and anti-apoptotic activity. In this respect, there have been some applications of marine-derived compounds for treating neurodegenerative disorders (Catanesi et al., 2021).

Fucoidan, a polysaccharide obtained from the brown algae *Saccharina japonica*, exhibited protective properties in the PD mice model using 1-methyl-4-phenyl-1,2,3,6-tetrahydropyridine (MPTP) C57BL/6. This application notably led to significant enhancements in motor function, mitigating impairments (Luo et al., 2009).

Astaxanthin, a carotenoid predominantly synthesized by the marine algae *Haematococcus pluvialis*, possesses notable anti-inflammatory and antioxidative properties. In vitro experiments involving Astaxanthin have shown cytoprotective effects able to prevent neuronal death following oxidative stress injury (Genç et al., 2020).

Fucoxanthin, another marine-derived carotenoid, has been found to be able to reduce A β -induced-oxidative stress in microglia, suggesting that it might be functional for AD treatment (Pangestuti et al., 2013). This outcome was linked to a decrease in the formation of ROS and the activation of antioxidative enzymes.

Marine extracts analysed in this thesis have been collected from the East-Mediterranean basin as sand, stones, or algae and sponge samples. When possible, the collected organisms have been taken into cultivation. Organisms able to grow in culture were subjected to stressful condition (i.e. high or low temperatures) before being expanded for extraction. This approach is not commonly used for marine extracts and follows the idea that if they can survive under those conditions, they might contain novel molecules giving them uncommon properties (Lindequist, 2016). This extra step should help the selection of peculiar

microorganisms producing unknown secondary metabolites that might be reflecting pro-survival properties when used as treatment *in vitro*. The following steps are the same as for terrestrial organisms and are explained in detail in the Chapter 2.

1.12 Overall Hypothesis, Aims and Objectives

Due to the current unavailability of a cure for ALS, the need for therapeutics able to slow or prevent the disease progression or treat the symptoms is essential. Neurotrophic factors have shown some promising results in past years, but always failed to translate into effective therapies at the clinical stages due to their limitations in BBB penetration, off-target effects, and excessively rapid clearance. Small neurotrophic mimetics have been studied as a possible way to overcome neurotrophic factors limitations while still being able to provide their therapeutic effects. Therefore, by investigating novel libraries of small molecule compounds and marine extracts we attempt to find new small neurotrophin mimetics able to provide a pro-survival therapeutic effect on MNs in co-culture with i-astrocytes derived from a panel of ALS patients carrying different ALS-related mutations. My hypothesis was that screening compound libraries and libraries of marine extracts in human cellular models of MND would allow identification of molecules mimicking the effect of neurotrophins and producing neuroprotective effects on motor neurons. These molecules may have the ability to translate into future therapies for at least specific subsets of ALS patients.

The overall aims of this project were to:

- 1. Perform a co-culture screening assay with murine MNs and i-astrocytes derived from a panel of ALS patients carrying different ALS-related mutations testing libraries of compounds or marine extracts.
- 2. Isolate and characterize the constituents of the top hit extracts and test their efficacy on the co-culture assay to identify which constituents or group of constituents is providing the therapeutic effect.
- 3. Perform molecular docking as *in silico* screening to predict which molecules obtained from the previous screenings and isolations might effectively bind to the neurotrophin receptors and therefore might be considered as potential small neurotrophin mimetics.

- 4. Understand the molecular and targeting aspects of the top hits and test their therapeutic efficacy in an ALS *C9ORF72* zebrafish model.

Chapter 2: Materials and Methods

All plastics for cell culture were purchased from Greiner Bio One, unless otherwise specified.

All cell culture reagents and chemicals were purchased as indicated in the methods.

2.1 Cell lines

iNPC cell lines (**Table 2.1**) were previously obtained through direct reprogramming of human skin fibroblasts collected from both ALS patients and healthy controls (Meyer *et al.*, 2014). All biopsy donors have provided informed consent prior to collection of biopsies. The biopsies collected at the University of Sheffield were collected under study number STH16573, research committee reference 12/YH/0330, the fibroblast samples from Ohio State University were collected under ethics number 04304AR; the fibroblasts provided by Cedar Sinai and the Coriell Institute are covered by material transfer agreement (MTA). Reprogramming was performed by Prof Laura Ferraiuolo and iNPC maintenance and housekeeping of iNPCs was kindly provided by Miss Lai Mei Wan, Miss Sarah M Granger, Miss Katie Roome and Dr Noemi Gatto.

Mouse embryonic stem cells Hb9-GFP were kindly gifted from Prof. Thomas Jessell.

Table 2. 1 iNPC Lines Clinical Information

iNPC Line	Diagnosis	ALS Genotype	Sex	Age at Biopsy (Years)	Source
C3050	Non-ALS	-	Male	55	University of Sheffield
C155v2	Non-ALS	-	Male	40	University of Sheffield
P183	ALS	C9ORF72	Male	50	University of Sheffield

P78	ALS	C9ORF72	Male	66	University of Sheffield
P201	ALS	C9ORF72	Female	66	University of Sheffield
ALS-52	ALS	C9ORF72	Male	49	Cedar Sinai
ALS-009	ALS	sporadic	Female	61	Ohio State University
ALS-12	ALS	sporadic	Male	29	Ohio State University
ALS-17	ALS	sporadic	Male	47	Ohio State University
P102	ALS	SOD1 (A4V)	Female	40	Ohio State University
ND29509	ALS	SOD1 (D90A)	Male	56	Coriell Biorepository

2.2 i-Astrocyte differentiation

iNPC lines were grown and maintained on fibronectin-coated 0.005% (v/v) (Merck Millipore, Burlington, Massachusetts, US) 10cm² plates (Fisher Scientific, Hampton, NH, USA) in iNPC medium (**Table 2.2**) until they reached 70-90% confluence. Then, iNPCs were differentiated into iAstrocytes as illustrated in (Meyer *et al.*, 2014) changing the medium to i-Astrocyte medium (**Table 2.3**) for 7 days. On the 5th day, cells were lifted with Accutase (Sigma Aldrich, St. Louis, Missouri, US) and plated onto a fibronectin-coated 384 well plate (**section 2.7**). The cells keep differentiating until the 7th day, where they start exhibiting an astrocyte-like morphology and express astrocytic markers.

Table 2. 2 iNPC Medium

DMEM/F12 (1:1) GlutaMax	(Gibco, Waltham, MA, USA)
N2 1% (v/v)	(Gibco, Waltham, MA, USA)
B27 2% (v/v)	(Gibco, Waltham, MA, USA)

FGF2 40 ng/ml	(Peprotech, Rocky Hill, NJ, USA)
---------------	----------------------------------

Table 2. 3 i-Astrocyte Medium

DMEM	(Fisher Scientific, Hampton, NH, USA)
FBS 10% (v/v)	(Life science production, Bedford, UK)
N2 0.2% (v/v)	(Gibco, Waltham, MA, USA)
Penicillin/Streptomycin 1% (v/v)	(Sigma, St. Louis, MO, USA)

2.3 Mouse embryonic stem cell (mESC) maintenance

mESCs were plated and maintained as colonies on a mitotically inactive primary mouse embryonic fibroblast (MEFs) (Merck, Burlington, MA, USA) feeder layer, that supports the growth of mESCs and is crucial for keeping them undifferentiated in a prolonged culture. The MEFs layer was plated and grown for 16h on a fibronectin-coated 0.005% (v/v) 10cm² plate containing i-Astrocyte medium (**Table 2.3**). i-Astrocyte medium was switched to 15mL of mESC medium enriched with 1.5µL (v/v) of Leukemia Inhibitory Factor (LIF) (Merk Millipore, Burlington, Massachusetts, US), and then mESCs were plated over the feeder layer. LIF signalling has long been known as one of the major pathways involved in maintaining the proliferation, pluripotency and facilitating the growth of mESCs (Nagy and Vintersten, 2006).

2.4 mESC split

After 3/4 days where mESCs were kept growing on the feeder layer, cells were lifted with trypsin (Sigma, St. Louis, MO, USA). Clumps of cells formed after the trypsinization were broken down into single cells, by applying mechanical pressure through aspirating and releasing the cells against the bottom of the plate with a 10ml strippette. Cells were then incubated for 30min to allow most of the MEFs to become suspended. Suspended mESCs were then collected and filtered through a 70 µm nylon mesh cell strainer, and finally plated onto new plates containing a new feeder layer and 15mL of mESC medium (Table 2.4) enriched with 2µL (v/v) of LIF.

Table 2. 4 mESC Medium

KnockOut DMEM	(Gibco, Waltham, MA, USA)
Embryonic stem-cell FBS 15% (v/v)	(Gibco, Waltham, MA, USA)
L-glutamine 2 mM	(Gibco, Waltham, MA, USA)
Nonessential amino acids 1% (v/v)	(Gibco, Waltham, MA, USA)
2-mercaptoethanol 0.00072% (v/v)	(Sigma, St. Louis, MO, USA)

2.5 Differentiation of motor neurons

At the end of the mESC split (**Table 2.4**), part of the filtered mESCs were plated into 10cm² dishes containing embryoid body (EB) medium (**Table 2.5**). These cells form EBs that then differentiate into Hb9-GFP⁺ motor neurons. The differentiation procedure requires 7 days (**Figure 2.1**). The medium was replaced each day by collecting all the cell-containing medium, transferring it into a 50mL tube, leaving the EBs to sediment for 5min, and then removing the old medium and replacing it with fresh medium. Starting from the 2nd day of differentiation, the fresh medium was replenished every day with 2 μ M retinoic acid (Sigma, St. Louis, MO, USA) and 1 μ M smoothed agonist (Sigma, St. Louis, MO, USA). These factors are essential to allow the differentiation into motor neurons (Faravelli *et al.*, 2014).

Table 2. 5 EB Medium

Knock Out DMEM (1:2)	(Gibco, Waltham, MA, USA)
F12 Medium Supplement (1:2)	(Gibco, Waltham, MA, USA)
Knockout serum replacement 10% (v/v)	(Gibco, Waltham, MA, USA)
N2 1%	(Gibco, Waltham, MA, USA)
L-glutamine 1mM	(Gibco, Waltham, MA, USA)

Glucose 0.5% (w/v)	(Sigma, St. Louis, MO, USA)
2-mercaptoethanol 0.0016% (v/v)	(Sigma, St. Louis, MO, USA)

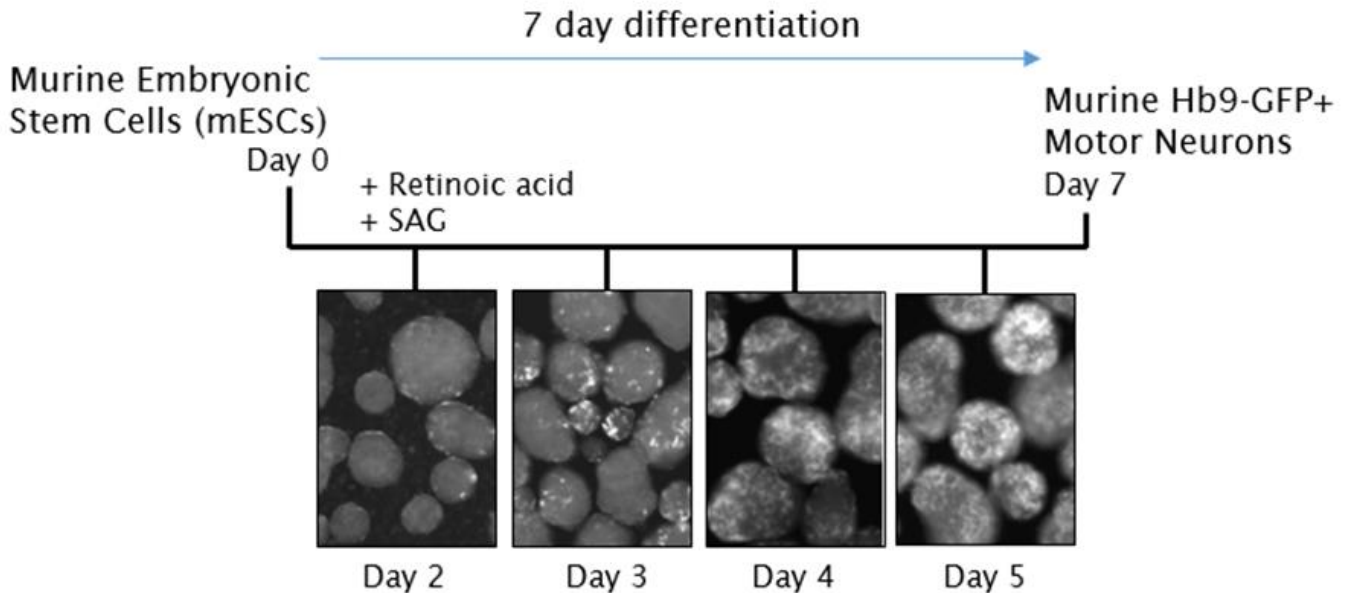


Figure 2. 1 Differentiation of mESCs into murine Hb9-GFP+ MNs over a 7-day differentiation period (images provided by Dr M. Stopford)

Media was supplemented with RA and SAG from Day 2 to drive the neuronal fate. MNs were visualised using the GFP expressed under the control of the Hb9 promoter region. This characteristic enabled us to evaluate the efficiency of the differentiation process and visualise the MNs live.

2.6 Dissociation of EBs with papain

To be able to plate and analyse the murine Hb9-GFP+ motor neurons, the EBs were dissociated into single cells. To achieve this, on the 7th day of differentiation EBs were collected, medium was removed, and the cells were resuspended into 2.75 mL of enzyme buffer (**Table 2.6**). 75 μ L of papain 200 U/mL (Sigma Aldrich, St. Louis, Missouri, US) were added to the enzyme buffer, and cells were incubated in the waterbath at 37°C for 5min. Papain is a cysteine protease enzyme present in papaya (*Carica papaya*) and mountain papaya (*Vasconcellea cundinamarcensis*) that allows the dissociation of the EBs into single cells (Konno *et al.*, 2004). After the incubation, 2 mL more of enzyme buffer and 50 μ L more of papain 200 U/mL were added to the mix. Cells were then incubated again for 5min within the waterbath at 37°C. After the second incubation, 50 μ L more of papain 200 U/mL was added to the mix and then cells were incubated for the third time in the waterbath at 37°C for 5min.

After resuspension, cells were incubated again in the waterbath at 37°C for 5min. Cells were then centrifuged for 5 min, 300 x g, at RT. Supernatant was removed and the following mix was used to resuspend the cells: 2.7mL enzyme buffer, 300 µL foetal bovine serum (FBS) and 150 µL of DNase 1mg/mL (Sigma Aldrich, St. Louis, Missouri, US). FBS was then slowly added to the mix to create a cushion that allowed for the filtering of the dissociated cells (heavier) from any debris (lighter), giving a much cleaner Hb9-GFP+ MN solution. Cells were centrifuged for 5 min, 300 x g, at RT, then the supernatant was removed, and cells were resuspended into MN medium (**Table 2.7**) and filtered through a 40 µm pore filter. Hb9-GFP+ MN were then plated on to a 384 well plate as explained in the next section (**section 2.7**).

Table 2. 6 Enzyme Buffer

NaCl	116 mM
KCl	5.4 mM
NaHCO ₃	26 mM
NaH ₂ PO ₄	1 mM
CaCl ₂	1.5 mM
MgSO ₄	1 mM
Glucose	25 mM
EDTA	0.5 mM
dH ₂ O	
Cysteine	1 mM

Table 2. 7 MN Medium

Knock Out DMEM (1:2)	(Gibco, Waltham, MA, USA)
F12 Medium Supplement (1:2)	(Gibco, Waltham, MA, USA)
Knockout serum replacement 10% (v/v)	(Gibco, Waltham, MA, USA)

N2 1%	(Gibco, Waltham, MA, USA)
L-glutamine 1mM	(Gibco, Waltham, MA, USA)
Glucose 0,5% (w/v)	(Sigma, St. Louis, MO, USA)
2-mercaptoethanol 0.0016% (v/v)	(Sigma, St. Louis, MO, USA)
BDNF 0,01% (v/v)	(Preprotech, London, UK)
GDNF 0,01% (v/v)	(Preprotech, London, UK)
CNTF 0,01% (v/v)	(Preprotech, London, UK)

2.7 High-throughput drug screening on human iastrocyte – murine Hb9-GFP+ motor neuron co-cultures

The following protocol (Stopford, Allen and Ferraiuolo, 2019) describes the generation of the co-culture system for drug screening. I-Astrocytes were differentiated from iNPC lines (**Section 2.2**) and plated onto a 384 well plate during the 5th day of differentiation (2000 cells/well). In parallel, motor neurons were differentiated from mESC (**Section 2.5**) and plated on the 7th day of differentiation (2500 cells/well) over the i-astrocytes to create the co-culture. During the 6th day of differentiation, the plates containing i-astrocytes were treated with the drugs of interest. The drugs were delivered using a Echo550 acoustic liquid handler (Labcyte, Norton Canes, Cannock, UK). This machine focuses ultrasonic acoustic energy at the meniscus of a fluid sample to eject small 40 nL droplets of liquid from wells containing the drugs to precisely deliver them to each well of the plate containing the cells.

The day after MN plating, 15µl MN medium without any drug was added to each well to feed the co-cultures. During the 8th day (after 24h of co-culture), and during the 10th day (after 72h of co-culture), Hb9-GFP+ motor neurons were imaged using an INCELL analyser 2000 (GE Healthcare), an automated cellular and subcellular imaging system for fixed and live cells. The Columbus analyser software (PerkinElmer, Waltham, Massachusetts, US) was used to assess the number of viable motor neurons present at both days of data acquisition. The number of viable motor neurons, defined as GFP+ motor neurons with at least one process, that survive after 72 hours in co-culture is calculated as a percentage of the number of viable motor neurons after 24 hours in co-culture.

2.8 Small-scale extracts of bacterial and fungal strains forming the Marine Extracts library utilized for the co-culture screening

The work performed towards the preparation of small-scale extracts of selected bacterial and fungal marine-derived strains, which were then assayed for their neuroprotective activity through the co-culture assay, has been performed by our partners at the National and Kapodistrian University of Athens (NKUA).

85 bacterial and 15 fungal strains of marine origin were cultivated in small scale to obtain extracts to be evaluated for their neuroprotective activity.

These have been selected by Prof Vassilos Roussis based on their chemical profile and availability among the bacterial and fungal strains (deposited at -80 °C in glycerol stocks) available at the strain collection/microbank belonging to the Department of Pharmacognosy and Chemistry of Natural Products, Faculty of Pharmacy (NKUA).

The strains have been isolated either from marine sediments of variable depth (0-250m) or as symbionts from marine macroorganisms, such as algae and sponges.

Selected bacterial strains were streaked from a glycerol stock onto a freshly prepared agar plate containing a seawater-based (A1BFe+C) medium (**Table 2.8**).

Table 2. 8 A1BFe+C medium

Ingredients	Amount (g/L)
Starch	10
Yeast Extract	4
Peptone	2
CaCO ₃	1
KBr	0.1
Fe ₂ (SO ₄) ₃ 5H ₂ O	0.04
Agar (only added for solid cultures)	17

The ingredients are added to 1 L of filtered seawater and subsequently the medium is sterilized by autoclaving at 121 °C for 20 min prior to use.

Selected fungal strains were streaked from a glycerol stock onto a freshly prepared agar plate containing a seawater-based (PD-S) medium (**Table 2.9**).

Table 2. 9 PD-S medium

Ingredients	Amount (g/L)
Potato (after boiling in distilled water for 30 min)	200
Dextrose	20
Agar (only added for solid cultures)	20

The ingredients are added to 1 L of filtered seawater and subsequently the medium is sterilized by autoclaving at 121 °C for 20 min prior to use.

After sufficient growth of the strains was observed, colonies or mycelia were picked from the agar plate and were inoculated into 250 mL flasks containing 100 mL of the same seawater-based medium that were incubated at appropriate temperatures (12-37 C) for an appropriate period (5-30 days). Bacterial strains were shaken at 100-160 rpm in an orbit shaker, whereas fungal strains were left standing.

At the conclusion of the fermentation process, Amberlite XAD-7HP resin was included in each flask to adsorb extracellular metabolites, with a concentration of 20 g/L. The flask contents and resin were agitated slowly overnight. The resin and cell mass were then separated by straining through cheesecloth, and washed with deionized water to eliminate salts. The resin, cell mass, and cheesecloth were later subjected to extraction using Me₂CO for 2 hours. The extract was then filtered, and the solvent was removed through vacuum distillation at 40°C to obtain the organic residues. In another approach, at the end of the fermentation period, the broth was partitioned with EtOAc and after separation of the aqueous and organic phases, the latter was evaporated under vacuum at 40 °C to yield the organic residues.

For the fungal strains instead, at the end of the fermentation period, the mycelia were separated from the broth via filtration under vacuum. Subsequently, mycelia were extracted with Me₂CO, while the broth was partitioned with EtOAc. The two organic extracts were pooled together, and the solvent was removed under vacuum to afford the organic residue.

The organic residues were profiled using ¹H NMR spectroscopy and liquid chromatography-mass spectroscopy (LC-MS).

2.9 Isolation and characterization of bacterial strain secondary metabolites

Based on the biological screening, to obtain pure compounds from the extracts, bacterial strains selected for further investigation were cultured on a large-scale in flasks containing a sea water-based medium and the resulting organic residue derived from the extraction was subjected to a multi-step fractionation process. The fractionation techniques involved to obtain the pure compounds were the following: Vacuum Liquid Chromatography (VLC) on silica gel, Thin Layer Chromatography (TLC) and High-Performance Liquid Chromatography (HPLC). All these techniques relied on dissolving the mixture in a fluid called the mobile phase that carries the material through a structure containing a different material called the stationary phase. The various constituents of the mixture travel at different speeds depending on their affinity, provided by their polarity, to the mobile and solid phases, causing them to separate. Nuclear magnetic resonance (NMR) has been used for the characterization of the molecular structure of metabolites (A.C. Dona et al, 2016). NMR perturbs the nuclei of atoms in a strong constant magnetic field using a weak oscillating magnetic field. Each nucleus responds by producing an electromagnetic signal with a frequency characteristic of the magnetic field at the nucleus.

2.10 In silico screening of UNICAEN 18000-membered compound library for candidate selection for co-culture screening

Synthetic molecules for the in vitro co-culture experiments that have been delayed and then stopped due to the COVID19 pandemic have been obtained from our partners at University of Caen through in silico studies on the crystal structure of the TrkB receptor to determine the most important interactions between TrkB and its natural ligand neurotrophin - 4/5 (NT-4/5). The results of in silico screening of the unique 18000-membered UNICAEN library of compounds were conducted by Dr Mirjana Antonijević (University of Caen) based on the pharmacophore hypothesis developed from interactions of TrkB and its synthetic ligands from the LM22A data set, because except for the LM22A data set of compounds, there is no other data set of small molecule agonists for the TrkB receptor.

For docking studies, we have used crystal structure of TrkB in a complex with neurotrophin-4/5 (NT-4/5), (PDB ID: 1HCF). Because the PDB structure was obtained by X-ray diffraction,

this method can only reveal heavy atoms, and thus PDB structures lack hydrogens, and because chemical bonds have false order, and they are always presented as simple bonds. Before using this protein for calculation, it has been submitted to preparation procedure in Maestro® 10.7 program using Protein Preparation Wizard software.

LM22A data set of 4 compounds was developed as BDNF loop II mimetics, but not BDNF secretagogues, with proven in vitro activity on the TrkB receptor. Each of these compounds exhibits a distinct chemotype: LM22A-1 as tripeptide which was the reason why this compound is excluded from further research; LM22A-2, LM22A-3 and LM22A-4 do not contain peptidic bonds.

Each of the remaining compounds was converted into its form at physiological pH= 7.4 and was optimized in the Maestro 10.7 program using LigPrep software.

Investigating the main interactions between TrkB receptor and its ligands required Glide docking study using domain 5 of the TrkB receptor (binding domain) and three compounds from the LM22A data set with proven in vitro activity. The coordinates of the carboxylate group of Asp298 were used for grid-centering. Each of these ligands has been docked using Maestro 10.7 program.

For obtaining a valid data set from the UNICAEN library, our partners conducted a similarity screening based on the structure of three different TrkB ligands – LM22A-2, LM22A-3, LM22A-4 in Pipeline Pilot Client 9.5 program. Besides the structure similarity, as the main filter for screening, hit compounds had to satisfy the Lipinski rule of five and drug-likeness to be selected from the library, which is a set of physical and chemical parameters observed through the analysis of a wide panel of drugs that are orally active in humans. Most orally administered drugs result being small and relatively lipophilic.

Maestro 11.7 also offers tools for creating a structure database that can be explored for matches to a pharmacophore hypothesis. The database must include 3D structures of all atoms that represent the experimental structures appropriately. The process of creating a database involves adding structures, cleaning the structures if required, generating conformers if required, and creating molecule subsets for searching the database as desired. Three data sets obtained after similarity screening were used for creating a new unified database. This final dataset has been used to test the Pharmacophore hypothesis, searching for geometric arrangements of pharmacophore sites that match the site types and inter-site

distances of the chosen hypothesis. The relevant conformers are retrieved and aligned with the hypothesis.

The final data set obtained included 169 compounds highlighted as potential TrkB ligands and considered suitable for co-culture screening.

2.11 Generation of DHEA derivatives substituted by five, six or three membered-17-spiro substituents for co-culture screening

Based on the promising anti-apoptotic and neuroprotective activity of BNN27, our partners at National Hellenic Research Foundation (NHRF) synthesized 22 Dehydroepiandrosterone (DHEA) analogues with modifications at position C17 of the steroid skeleton, replacing the potentially metabolically labile oxirane ring by a cyclopropane moiety to increase the stability and avoid potential epoxide ring opening in vivo which may result in loss of activity. Different substituents on the cyclopropyl ring were introduced through Wittig, Horner-Emmons and Suzuki coupling reactions.

2.12 SDS-polyacrylamide gel preparation

To prepare the desired acrylamide % (w/v) resolving gel, the reagents listed in **Table 2.10** were combined. The Mini-PROTEAN® Tetra Cell Casting Stand and clamps (Bio-Rad), along with spacer plates with 1.0 mm integrated spacers (Bio-Rad) and short plates (Bio-Rad) were assembled. The gel was then poured into glass plates, and a layer of isopropanol was added to the top of the gels to ensure the gel was leveled and to prevent dehydration. The gel was left for at least 30 mins to polymerize. 5% stacking gels were prepared by mixing reagents listed in **Table 2.10**, and then poured onto the set resolving gels in the glass plates after removing the isopropanol. 1.0 mm Mini-PROTEAN® Comb (Bio-Rad) was then inserted into the stacking gels and left for at least 30 mins to set.

Table 2. 10 Composition of 5% stacking gel and 12% resolving gel

Reagents	5% Stacking Gel	12% Resolving Gel
dH ₂ O	5.8mL	3.5mL
30 % (w/v) Acrylamide	1.7mL	4mL
Resolving buffer (1.5 M Trizma [®] , 13.9 mM SDS, pH 8.8, filtered)	-	2.5mL
Stacking buffer (0.5 M Trizma [®] , 13.9 mM SDS, pH 6.8, filtered)	2.5mL	-
10 % (w/v) APS	50uL	50uL
TEMED	20uL	20uL

2.13 Cell lysis for immunoblotting

Dishes containing the cells were placed on top of a box full of ice. Media was carefully removed from the dishes, and cells were then washed with PBS at 4°C. Cells were scraped into Ice cold IP lysis buffer (150 mM NaCl, 50 mM HEPES, 1 mM EDTA, 1 mM DTT, 0.5% (v/v) Triton™ X-100, PIC, pH 8.0) using a cell scraper, incubated for a 15 min on ice, and then centrifuged at 17,000 x g for 5 mins at 4°C. The lysate supernatant containing proteins was then kept for further experiments, while the pellet was discarded.

If it was not possible to proceed with the immunoblotting on the day where cells reached the optimal level of differentiation or treatment, cells were simply scraped in cold PBS, then centrifuged at 17,000 x g for 5 mins at 4°C and kept at -80°C until the day of the experiment. Once samples were taken out from the -80°C freezer, the PBS supernatant was removed, and IP lysis buffer was added to the samples for a 15min incubation on ice before following the protocol described above.

2.14 Bradford assay

To measure the protein concentration of cell lysates, Bradford assays were employed. Initially, the protein assay dye reagent concentrate was diluted in dH₂O at a ratio of 1:4 to create a working concentration of the Bradford reagent. Next, 1 µL of cell lysate was added to 1 mL of the Bradford reagent, mixed thoroughly, and loaded into a polystyrene cuvette

with a 1 cm path length. The shift in optical density at 595nm (OD_{595nm}) of the protein sample in relation to a blank control (IP lysis buffer only) was then measured using a WPA S1200 Diode Array Spectrophotometer (Biochrom®). The concentration of the protein lysate was then calculated and converted to µg/mL using the Beer-Lambert law (OD_{595nm} = εcl; where ε = 1/15, and l = 1cm).

2.15 SDS-polyacrylamide gel electrophoresis

The proteins from the cells were extracted and mixed with 4X Laemmli buffer (228mM Tris-HCl, 38% (v/v) glycerol, 277mM SDS, 0.038% (w/v) bromophenol blue, 5% (v/v) β-mercaptoethanol, pH 6.8). The denatured proteins were loaded onto 12% SDS-polyacrylamide gels and placed in a Mini-PROTEAN® Tetra Vertical Electrophoresis Cell (Bio-Rad), which was filled with running buffer (25 mM Tris, 3.5 mM SDS, 20 mM glycine). To perform immunoblotting, 25 µg of denatured protein was added to each well of SDS-polyacrylamide gels. In addition, a pre-stained protein ladder (2 µL) was loaded as a molecular weight marker in one well per gel. Gel electrophoresis was performed at 50V for 30 mins, then 150V for approximately 1.5h until the dye front had reached the bottom of the gel. Gels were then removed from the electrophoresis cell and assembled with transfer buffer-saturated nitrocellulose membranes in a semi-dry transfer apparatus. Electrophoretic transfer of the proteins from the gels to the membranes was performed at 0.15A / gel transferred for 1h. Membranes were then stained with Ponceau stain (0.1% (w/v) Ponceau S, 5% (v/v) acetic acid), and trimmed accordingly to the theoretical weight of the proteins of interest.

2.16 Immunoblotting

Membranes were blocked in 5% (w/v) milk/Tris Buffered Saline, with Tween® 20 (TBST) (20 mM Tris, 137 mM NaCl, 0.2% (v/v) Tween® 20, pH 7.6) for 1h at room temperature on a roller. Then membranes were incubated with primary antibody appropriately diluted in blocking buffer overnight at 4°C on a roller. The membranes were then washed 3 times in TBST for 15 mins at room temperature. The membranes were then incubated with secondary antibody conjugated to horseradish peroxidase (HRP) in 5% milk/TBST for 1h at room temperature on a roller. The membranes were then washed 3 times in TBST for 15 mins at room temperature. The membranes were then incubated with ECL for 1 min and imaged using a G-BOX (Syngene).

Table 2. 11 Antibodies for Immunoblotting

Target	Clone	Species	Supplier	Catalogue Number
Beta-Actin	AC-15	Mouse	Abcam	Ab6276
P75NTR	Polyclonal	Rabbit	Cell Signalling Technologies	#8238

2.17 Paraformaldehyde fixation

Once cells were fully differentiated in a 96w plate, wells were washed 3 times with PBS and incubated with 4% paraformaldehyde (PFA) in PBS for 10 min. After the incubation, wells were washed twice in PBS and then stored in a cold room until ready to stain. When a prolonged period in the cold room was required, 0.1% (v/v) sodium-azide 1 mM was added to the PBS to avoid contamination.

2.18 Immunocytochemistry

Cells were permeabilised and non-specific binding sites were blocked by incubating them in blocking solution (5% normal horse serum (NHS) in PBS) containing 0.5% Triton at RT for 30 minutes. Primary antibodies were then diluted at the required concentration in blocking solution and incubated O/N at 4°C.

Plates were then washed first in PBS containing 0.2% Tween to help with the removal of non-specifically bound antibodies, and then two more times with PBS alone. NFkB antibody at 1:500 and a Vimentin at 1:1000 were used (**Table 2.12**). Secondary antibodies were then diluted 1:1000 in blocking solution and incubated at RT for 30 minutes protected from light. Lastly, Hoechst 33342 was diluted 1:6000 in PBS and incubated for 5 minutes at RT protected from light, followed by two washes with PBS containing 0.2% Tween. Plates were imaged using the confocal analyser Opera Phenix (Molecular Devices) to observe differences in nuclear transportation of NF-kB.

Table 2. 12 Antibodies for Immunocytochemistry

Target	Clone	Species	Supplier	Catalogue Number
Vimentin	Polyclonal	Chicken	Millipore	Ab5733
Nf-kB P65	Polyclonal	Rabbit	Cell Signalling Technologies	#8242

2.19 Zebrafish C9ORF72 screening assay

For investigation of positive hits *in vivo*, I adopted as a suitable model a C9orf72 zebrafish line and experiments were conducted under the supervision of Dr David Burrows and Prof Tennore Ramesh. The model available at SITraN expressed interrupted C4G2 expansions and showed phenotypical and pathological features in line with features observed in human C9orf72-ALS. This model also presents pathological RNA foci and DPRs which allow it to be utilized for experiments based on the identification of poly(PR) DPRs (Shaw et al, 2018).

Adult and larvae zebrafish (*Danio rerio*) were maintained and bred by Dr David Burrows according to established procedures. The care and maintenance of animals were performed under a Home Office project license as per the Animals Scientific Procedures Act of 1981 (ASPA) (Act 1986 Amendment Regulations 2012 (SI 2012/3039) amend the Animals (Scientific Procedures) Act 1986 (ASPA) to transpose European Directive 2010/63/EU on the protection of animals used for scientific purposes). The Directive sets out revised measures for the protection of animals used for scientific purposes. This guidance is issued under the terms of section 21(1) of ASPA and provides information about the way in which the UK Secretary of State for the Home Office propose to exercise their powers under the Act. This guidance needs to be adopted by everyone involved with animals that are bred for, supplied for, or used in scientific procedures.

C9ORF72 anti-sense (C4G2) zebrafish were crossed with non-transgenic zebrafish. At 2 days post fertilization (dpf) embryos were treated at different dosages of compound exposure. Each embryo was kept individually in a 96 well plate (96 well, μ Clear, Greiner Bio-One) and chronically dosed by immersion in 250 μ l volume of drug solution in E3 embryo medium (**Table 2.13**) from 2dpf until 5 dpf at 28.5°C. At 5dpf, transgenic embryos were phenotypically identified by DsRed expression using the InCell Analyzer 2000 (DsRed, 583 nm).

Table 2. 13 E3 Embryo Medium 60x

Ingredients	Amount
NaCl	34.8g
KCl	1.6g
MgCl ₂ 6H ₂ O	9.78g
CaCl ₂ 2H ₂ O	5.8g
ddiH ₂ O	2L

To prepare 1x E3 embryo medium, 16.5 ml 60x stock were diluted in 1 L ddiH₂O and 100 µl 1% methylene blue was added.

2.20 Molecular docking

Molecular Docking experiments have been performed under the supervision of Prof Rebecca Wade (Molecular and Cellular Modelling Group (MCM) at the Heidelberg Institute for Theoretical Studies (HITS), Heidelberg, Germany), Mr Athanasios-Alexandros Tsengenes and Ms Christina Athanasiou.

Molecular structures from a library of natural products (NPs) isolated and characterized from the top hit marine compounds were prepared prior to docking using the Schrödinger-Maestro 2020r4[®] software resulting in the formation of a library of 100 compounds with all the possible stereoisomers.

After the ligand preparation, the library of prepared compounds was subjected to QuikProp and the QikProp properties were obtained for all compounds as an absorption, distribution, metabolism, and excretion (ADME) prediction program integrated in Schrödinger-Maestro 2020r4[®] to predict pharmaceutically relevant properties.

Following the QuikProp analysis, protein preparation was performed on the 3D structures of the neurotrophic receptors available on the Protein Data Bank (PDB).

- TrkA receptor in complex with nerve growth factor (NGF) (PDB: 1WWW).
- TrkB receptor bound to NT-4 neurotrophin (PDB: 1HCF).
- p75NTR receptor in complex with NGF (PDB: 1SG1).

Schrödinger-Maestro 2020r4[®] has also been adopted for finding the binding sites for the protein-ligands followed by molecular docking using the Maestro feature, Glide XP (extra Precision).

2.21 Statistical Analysis

One-way ANOVA with Dunnett's post hoc test (comparing each condition to DMSO-treated cells as negative control) was performed if using raw motor neuron counts and raw percentage survival, as well as two-way ANOVA with Dunnett's multiple comparisons using the intensity difference between treatment and control obtained through the Columbus Software. Statistical analysis has been performed through the software GraphPad Prism version 8.2.1 for Windows (GraphPad Software, La Jolla California USA).

Chapter 3: Screening of a library of marine extracts in a panel of ALS-derived iAstrocytes and motor neurons co-cultures

3.1 Introduction

High-throughput drug screening (HTDS) is a term that is used to describe different types of assays aimed at handling large numbers of samples using robotics, liquid handling, high-content imaging, and data analysis pipelines (McGown A et al., 2019). This approach can help researchers to find next generation therapeutics for treating ALS patients.

Cells are powerful models suitable for HTDS, they can undergo genetic manipulation and can be kept in culture to obtain large amounts. Phenotypic HTDS using ALS patient-derived is now a common procedure in many laboratories.

Patient-derived cells are commonly obtained through reprogramming patient somatic cells into human induced pluripotent stem cells (hiPSCs) able to be differentiated in the cell type of interest while keeping the genetic information from the donor, generating a powerful tool for the investigation of pathological mechanisms as well as an appropriate drug testing platform. HiPSCs can be cultured in either 2D or 3D systems. The latter model provides additional advantages but requires a better knowledge of cell-ECM (extracellular matrix) and cell-cell interactions to create reproducible standardized protocols for overcoming cell reprogramming variability between the clones, and to become cost-efficient and easy to work (McGown A et al., 2019).

Cell-based assays offer powerful tools for investigating a wide range of ALS-related mechanisms and potential therapeutic agents. For instance, multiple cell-based assays are used to identify compounds able to reduce SOD1 protein levels based on the data strongly supporting that mutant SOD1 protein has a toxic gain-of-toxic function (Woo et al., 2021). As explained in the introduction chapter, protein aggregation is a pathological hallmark of ALS, and therefore several HTDS assays have been developed and used to identify compounds able to reduce the aggregation of ALS related proteins such as SOD1, TDP-43, or FUS aggregation (Boyd et al., 2014). HTDS has also been applied to investigate the *C9ORF72* genetic subtype of ALS, detecting the most abundant toxic aggregates of dipeptide repeat proteins (DPRs) (poly-GA, poly-GP and poly-GR) generated via unconventional translation of sense and antisense repeat transcripts (Quaegebeur et al., 2020).

As reported in the introduction chapter, reprogrammed patient cells provide a powerful model for investigating phenotypical and molecular characteristics of ALS. One of the main issues encountered with reprogramming somatic cell into iPSCs is the embryonic nature of these cells and the variability from clone to clone (Shutova et al., 2016), which can lead to the loss ageing features that are known to play an important role in ALS.

Generating induced neuronal progenitor cells (iNPCs) from skin fibroblasts in a faster and efficient method to overcome these limitations and avoid long-term *in vitro* culture accumulation of chromosomal abnormalities observed in iPSCs. Moreover, other than the fact that direct generation of homogenous iNPCs is faster compared to the iPSCs counterpart, it also bypasses the induced pluripotency stage, therefore reducing the probability of generating carcinogenic iPSCs (Liu et al., 2020).

The majority of iNPCs obtained through reported reprogramming methods are expandable, and can provide the generation of many cells for subsequent differentiation or manipulation (Ottoboni et al. 2021), including astrocytes, neurons, and oligodendrocytes, which maintain the ageing features of the donor (Gatto et al., 2021).

Our assay shows that this method can be used to model neurodegenerative diseases such as amyotrophic lateral sclerosis. Indeed, induced astrocytes differentiated from ALS patients display toxic features against co-cultured motor neurons, as reported in similar co-culture assays obtained from post-mortem human tissues or mouse models (Haidet-Phillips et al., 2011). Because the origin of ALS is mainly sporadic (SALS) with unknown cause, methods to model the disease are very helpful to understand the mechanisms underlying subtypes of ALS and discover new therapeutic targets.

Our HTDS assay, being based on NPCs reprogrammed from different ALS patients and therefore carrying a different panel of mutations, might present sometimes issues with positive and negative controls. Drugs used as positive controls or DMSO used as a negative control might show different responses in terms of cell survival depending on the line in use. Especially treatments with drugs acting as positive controls, therefore enhancing MN survival, might show different efficacy levels in different subsets of lines. In this specific study, the drug chosen as the positive control shows, on average, a better response in lines of iAstrocytes carrying mutations in the *C9ORF72* gene. This aspect must be taken into consideration when performing experiments with lines from multiple subgroups of patients. NPCs are also delicate and stress-prone cells, especially during the phase of differentiation

into astrocytes, and show morphological and phenotypic changes over a certain number of passages or if they are left to grow too confluent. The most common aspect that can be observed once the cells reached the phase of decay due to their ageing, is a variability in their levels of toxicity, either an increase or decrease, or their supportive properties towards MNs. These characteristics have led us to establish stringent quality control parameters for cell maintenance and for our assay, such as cut-offs for passage numbers, time in culture and positive/negative controls. All cell lines used were able to grow at high density and provide a consistent effect between passage 14 and 20, with the exception of patient #201 which displayed a consistent toxicity level between passage 21 and 25.

Hence, an important aspect worth taking into consideration is that the handling of these cell lines requires consistent and precise work from the researcher in charge of their maintenance and usage, as this might affect the quality and reliability of the experimental results.

3.2 Screening marine extracts for neuroprotective effects in a motor neuron-astrocyte co-culture system

The initial aim of the project was to identify new potential neurotrophin mimetics able to rescue motor neuronal survival in an ALS patient-derived *in vitro* model through the screening of a library of 100 marine extracts derived from a collection of extracts of 1500 bacterial strains and 500 fungal strains from the East Mediterranean basin. Isolation of natural products from marine bacteria and/or fungi from the East Mediterranean basin that act as mimetics of neurotrophins using a bioassay-guided isolation protocol is a core part of the Euroneurotrophin consortium. The 100 extracts were pre-selected by our partners at the Kapodistrian University of Athens (NKUA) who analysed the chemical NMR profiles of small-scale fermentation of existing strains from the MicroBank available at NKUA. The analysis has been manually performed by Prof. Vassilios Roussis and Prof. Efstathia Ioannou from the NKUA Section of Pharmacognosy and Natural Product Chemistry. NMR profiles of full extracts have been compared with NMR profiles of neurotrophins to find similarities in the NMR peaks. Extracts containing peaks that are present in the neurotrophins spectra as well, might contain molecules having structural similarities with the neurotrophins themselves. This provides an indication that some molecules able to bind the neurotrophin receptors could be present within the extracts and helped to reduce the overall number of extracts for testing.

Moreover, fermentation of extracts can be a time-consuming procedure, therefore also availability was taken into consideration before comparing chemical profiles. Large-scale fermentation was performed only for the extracts that showed neuroprotective activity in the co-culture assay to obtain larger amounts for the following steps of fractionation.

A high-throughput iAstrocyte-murine Hb9-GFP+ motor neuron co-culture assay has been previously developed to identify compounds with potential neuroprotective effects in an ALS *in vitro* system (Stopford, Allen and Ferraiuolo, 2019). In this assay, human iAstrocytes derived from iNPCs (Meyer et al., 2014) were grown in co-culture with murine Hb9-GFP+ motor neurons (Wichterle et al., 2002). ALS patient-derived iAstrocytes are toxic toward the co-cultured motor neurons, exacerbating their death through both the release of toxic molecules, and the reduced production of neuroprotective molecules (Ciervo et al., 2021). The assay readout is motor neuron survival over 72h in co-culture. Here, iAstrocytes from one single donor (patient #183) carrying a C9orf72 mutation were used to perform the primary drug screen. This donor has been chosen for the primary assay based on the high level of astrocyte toxicity observed.

Previous studies carried out by the Ferraiuolo laboratory have observed a higher level of MN death in cocultures with iAstrocytes from patient #183. Compounds able to provide a significant therapeutic effect in this co-culture assay are predicted to be more likely to provide a higher or similar level of rescue when used as a treatment with other patient lines displaying a lesser degree of toxicity. This is particularly helpful during the first phases of compound screening because it helps to reduce the number of less effective hits before going ahead with further screening.

The normal pipeline that we adopt while screening for therapeutics in this assay is to test the library of compounds with a range of concentrations from 10 μ M to 0.001 μ M in a single iAstrocyte patient cell line. The hits identified in the primary screen are then investigated in a wider array of iAstrocyte lines, with some carrying mutations in the same gene as patient #183, others carrying mutations in the SOD1 gene, and other lines obtained from sALS patients. This provides information about the consistency of the therapeutic effect and helps to determine whether that effect is visible in few lines, or lines carrying mutations in the same gene or in a wider array of genotypes. Ideally, a good therapeutic agent should work in all

tested lines, but, even if it is effective only in a sub-population of patients, it still helps us narrow down which mechanisms might be involved in the therapeutic effect.

100 marine extracts (**Table 3.1**), derived from a collection of 1500 bacterial strains and 500 fungal strains from the East Mediterranean basin owned by the National and Kapodistrian University of Athens (NKUA), were screened in this co-culture assay at concentrations of 10µg/mL, 1µg/mL, 0.1µg/mL, 0.01µg/mL and 0.001µg/mL to generate a potential dose-response curve. DMSO was used as a negative control and iAstrocytes from a healthy donor (subject #3050) treated with DMSO, or C9orf72-ALS P183 iAstrocytes treated with an in-house neuroprotective compound were used as positive controls for increased motor neuron survival.

The positive control is a drug the Ferraiuolo laboratory has identified in collaboration with an industrial partner and is able to rescue MN survival in most of the lines available for the co-culture assay. Due to IP restrictions, it is not possible to provide further information relating to the structure and functional activity of this compound.

We introduced into our assay and screened 100 marine extracts using a working concentration range of 10µg/mL, 1µg/mL, 0.1µg/mL, 0.01µg/mL and 0.001µg/mL. Each plate contained 2 technical replicates of each concentration for each extract (**Figure 3.1**).

10 wells have been used as negative controls (healthy murine motor neurons plated with patient #183 *C9ORF72* iAstrocytes and treated with DMSO), 10 wells have been used as the first positive control (healthy murine motor neurons plated with patient #183 *C9ORF72* iAstrocytes and treated with our positive control drug), and 8 wells have been used as a second positive control (healthy murine motor neurons plated with healthy control derived iAstrocytes (sample #3050) and treated with DMSO). The aim was to repeat this experiment 3 times with different batches of astrocytes and MNs to obtain 3 biological replicates in order to allow statistical evaluation of which extracts were able to induce a pro-survival response.

	1	2	3	4	5	6	7	8	9	10	11	12	13	14	15	16	17	18	19	20	21	22	23	24
A	EMPTY	EMPTY	EMPTY	EMPTY	EMPTY	EMPTY	EMPTY	EMPTY	EMPTY	EMPTY	EMPTY	EMPTY	EMPTY	EMPTY	EMPTY	EMPTY	EMPTY	EMPTY	EMPTY	EMPTY	EMPTY	EMPTY	EMPTY	EMPTY
B	EMPTY	Extract 1										DMSO	DMSO	Extract 2										EMPTY
C	EMPTY	Extract 3										DMSO	DMSO	Extract 4										EMPTY
D	EMPTY	Extract 5										DMSO	DMSO	Extract 6										EMPTY
E	EMPTY	Extract 7										DMSO	DMSO	Extract 8										EMPTY
F	EMPTY	Extract 9										DMSO	DMSO	Extract 10										EMPTY
G	EMPTY	Extract 11										+ CTL	+ CTL	Extract 12										EMPTY
H	EMPTY	Extract 13										+ CTL	+ CTL	Extract 14										EMPTY
I	EMPTY	Extract 15										+ CTL	+ CTL	Extract 16										EMPTY
J	EMPTY	Extract 17										+ CTL	+ CTL	Extract 18										EMPTY
K	EMPTY	Extract 19										+ CTL	+ CTL	Extract 20										EMPTY
L	EMPTY	Extract 21										H CTL	H CTL	Extract 22										EMPTY
M	EMPTY	Extract 23										H CTL	H CTL	Extract 24										EMPTY
N	EMPTY	Extract 25										H CTL	H CTL	Extract 26										EMPTY
O	EMPTY	Extract 27										H CTL	H CTL	Extract 28										EMPTY
P	EMPTY	EMPTY	EMPTY	EMPTY	EMPTY	EMPTY	EMPTY	EMPTY	EMPTY	EMPTY	EMPTY	EMPTY	EMPTY	EMPTY	EMPTY	EMPTY	EMPTY	EMPTY	EMPTY	EMPTY	EMPTY	EMPTY	EMPTY	EMPTY

Figure 3. 1 384w template layout

This figure shows an example of the layout used for the primary screen.

As a readout for the assay, we measured motor neuronal survival over 72h in co-culture. We took 2 measures, after 24h and after 72h in co-culture and compared the number of neurons alive showing at least one process after 24h with the number of neurons alive showing at least one process after 72h in co-culture in the same wells. The percentages of survival of treated samples at different concentrations of the marine extracts were compared with the percentage MN survival in the co-cultures exposed to the positive control drug and the negative control set-up. All extracts able to reach a percentage of survival close to or higher than the positive control drug were considered potential hits.

As a result of this screen, out of all tested samples (n=100) only 8 Marine Extracts showed a significant increase in motor neuronal survival (**Figure 3.2**). Only 8 extracts showed a percentage of survival comparable to the positive control drug, the other 92 extracts showed a percentage of survival comparable to the DMSO control +/- 5%, indicating a lack of therapeutic activity. The 3 extracts showing the highest percentage of survival have been taken forward for further analysis (BI0394, BI0788 and BI0987). It was not possible to carry forward all positive hits because the large-scale fermentation and the isolation times to isolate molecules from the marine extracts were not suitable for a 3 year long project. Therefore, we selected the 3 best extracts from this screen. Even though BI0681 was showing results comparable to the 3 selected top hits, we had to exclude it from the selection because

of its unavailability at the start of the secondary screening. This aspect will be discussed in greater detail in chapter 4.

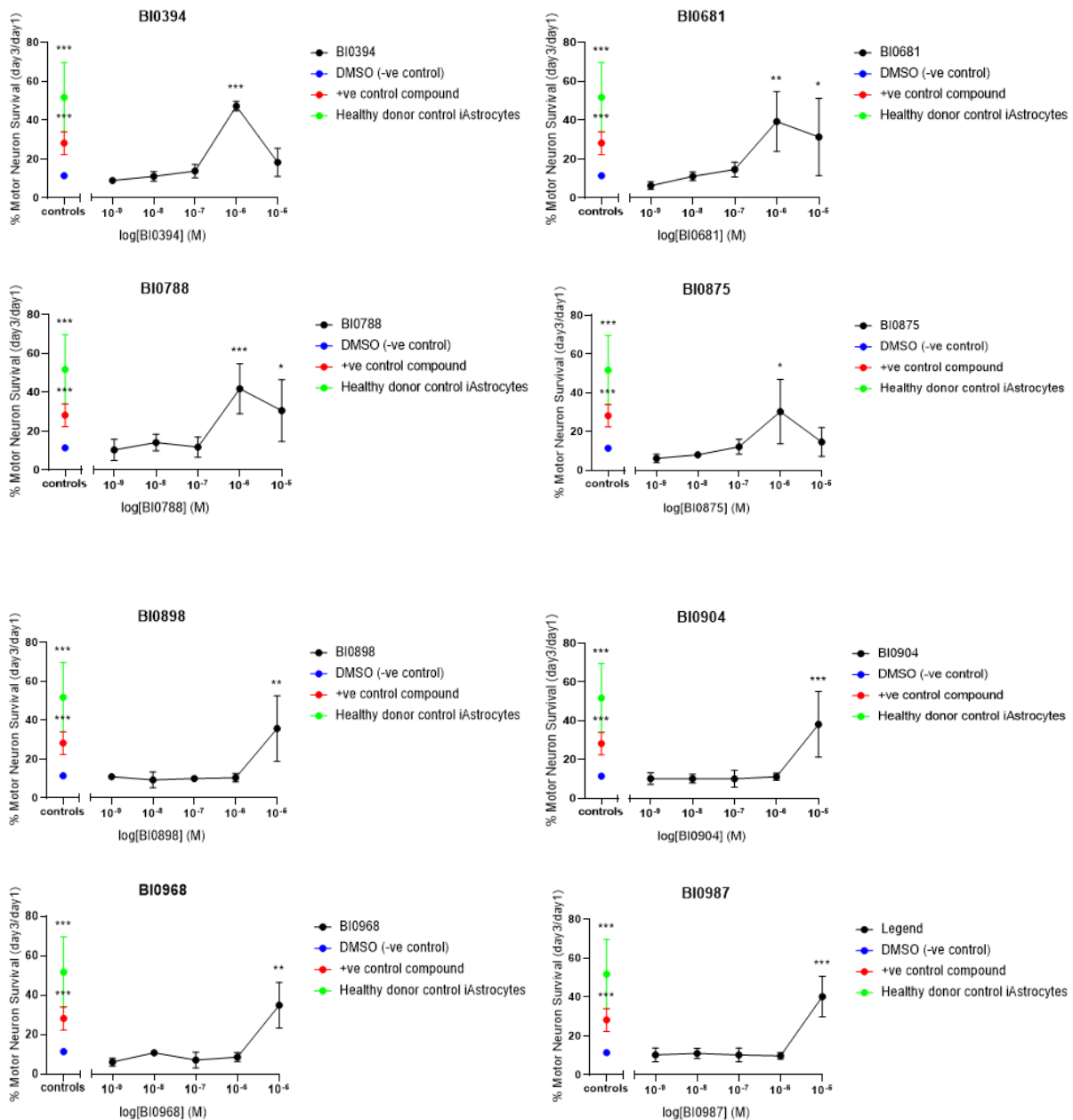


Figure 3. 2 Top hits from the marine extracts screen in C9orf72-ALS patient iAstrocyte and Hb9-GFP+ mouse motor neuron co-culture

Hb9-GFP+ motor neurons co-cultured with C9orf72-ALS patient #183 iAstrocytes displayed increased survival upon treatment with 8 different marine extracts at various concentrations (black line) over DMSO only treatment (blue dot). These 8 extracts yielded similar motor neuron rescue as our +ve control compound at a concentration of 100nM (red). Healthy donor control iAstrocytes treated with DMSO only (green) acted as positive control for the assay. Hb9-GFP+ mouse motor neurons were

seeded in co-culture at day 7 of the astrocyte cultures. GFP+ motor neurons were imaged at 24 and 72 hours of co-culture, and viable motor neurons were counted. Motor neuron survival at day 3 was calculated as a percentage of the number of motor neurons alive at day using the software Columbus, with a tailored algorithm for counting MNs in fluorescence exhibiting at least one neuronal process. Plates have been scanned using an Incell 2000 imaging system. 1. N = 3, data are mean ± SD. One-way ANOVA with Dunnett's multiple comparisons ($p^ < 0.05$, $p^{**} < 0.01$, $p^{***} < 0.001$).*

Compounds from these extracts were isolated and characterized to be tested again on this co-culture system to determine which molecules, precisely, are capable of inhibiting motor neuronal death. Marine extracts are complex mixtures of natural compounds, which can have different synergistic effects that can lead to the observed therapeutic effect. To understand which compounds, present within the extracts promote MN survival, it is necessary to isolate and test them separately or in combination. To do that, our partners at the National and Kapodistrian University of Athens adopted a range of different techniques aimed at purifying and isolating the compounds contained in the top hits' extracts that emerged from the co-culture assay. It is important to take into consideration that, despite all the progress made with extraction-separation procedures in recent years, the isolation of natural products from marine extracts, or other types of natural extracts, remains a challenging task (Zhang et al., 2009).

Most experiment pipelines deployed to isolate adequate amounts of pure isolated compounds employ the use of liquid chromatographic techniques such as Medium pressure liquid chromatography (MPLC), Vacuum liquid chromatography (VLC), and High-performance liquid chromatography (HPLC) (Koleva et al., 2002). The complex nature of extracts requires indeed the employment of different separation techniques for the extraction and purification of molecules with slight diameter and polarity differences. Solid-phase extraction is normally accepted as the first approach for rapid fractionation. The sub-fractions obtained in this first phase normally do not contain single purified compounds, but mixtures of compounds separated based on their charge or molecular weight depending on the specific resin or solvent utilized. Further HPLC separations and capillary NMR tests are required to identify and isolate pure compounds from the extract sub-fractions. This assay procedures relative to our experiments are described in more detail in Results, Chapter 4.

Table 3. 1 List of all extracts tested in the primary screening assay with the source and amount received.

Internal-Code	Source	Amount Recived (mg)
BI0181	bacterial extract	5mg
BI0182	bacterial extract	5mg
BI0211	bacterial extract	5mg
5BI0236	bacterial extract	5mg
BI0323	bacterial extract	5mg
BI0327	bacterial extract	5mg
BI0338	bacterial extract	5mg
BI0344	bacterial extract	5mg
BI0381	bacterial extract	5mg
BI0383	bacterial extract	5mg
BI0394	bacterial extract	5mg
BI0415	bacterial extract	5mg
BI0430	bacterial extract	5mg
BI0445	bacterial extract	5mg
BI0468	bacterial extract	5mg
BI0519	bacterial extract	5mg
BI0556	bacterial extract	5mg
BI0618	bacterial extract	5mg
BI0681	bacterial extract	5mg
BI0733	bacterial extract	5mg
BI0788	bacterial extract	5mg
BI0850	bacterial extract	5mg
BI0856	bacterial extract	5mg
BI0871	bacterial extract	5mg
BI0875	bacterial extract	5mg
BI0881	bacterial extract	5mg
BI0883	bacterial extract	5mg
BI0887	bacterial extract	5mg
BI0891	bacterial extract	5mg
BI0892	bacterial extract	5mg
BI0894	bacterial extract	5mg
BI0895	bacterial extract	5mg
BI0896	bacterial extract	5mg
BI0898	bacterial extract	5mg
BI0904	bacterial extract	5mg
BI0905	bacterial extract	5mg
BI0908	bacterial extract	5mg
BI0911	bacterial extract	5mg
BI0912	bacterial extract	5mg
BI0915	bacterial extract	5mg
BI0916	bacterial extract	5mg
BI0917	bacterial extract	5mg
BI0918	bacterial extract	5mg

BI0921	bacterial extract	5mg
BI0922	bacterial extract	5mg
BI0924	bacterial extract	5mg
BI0932	bacterial extract	5mg
BI0933	bacterial extract	5mg
BI0937	bacterial extract	5mg
BI0938	bacterial extract	5mg
BI0941	bacterial extract	5mg
BI0942	bacterial extract	5mg
BI0944	bacterial extract	5mg
BI0949	bacterial extract	5mg
BI0952	bacterial extract	5mg
BI0956	bacterial extract	5mg
BI0962	bacterial extract	5mg
BI0968	bacterial extract	5mg
BI0973	bacterial extract	5mg
BI0975	bacterial extract	5mg
BI0977	bacterial extract	5mg
BI0980	bacterial extract	5mg
BI0981	bacterial extract	5mg
BI0987	bacterial extract	5mg
BI0988	bacterial extract	5mg
BI0989	bacterial extract	5mg
BI0991	bacterial extract	5mg
BI0994	bacterial extract	5mg
BI0996	bacterial extract	5mg
BI1005	bacterial extract	5mg
BI1014	bacterial extract	5mg
BI1016	bacterial extract	5mg
BI1018	bacterial extract	5mg
BI1020	bacterial extract	5mg
BI1026	bacterial extract	5mg
BI1032	bacterial extract	5mg
BI1033	bacterial extract	5mg
BI1039	bacterial extract	5mg
BI1040	bacterial extract	5mg
BI1152	bacterial extract	5mg
BI1161	bacterial extract	5mg
BI1193	bacterial extract	5mg
BI1198	bacterial extract	5mg
BI1202	bacterial extract	5mg
BI1212	bacterial extract	5mg
FI0005	fungus extract	5mg
FI0009a	fungus extract	5mg
FI0009b	fungus extract	5mg
FI0010	fungus extract	5mg
FI0011a	fungus extract	5mg
FI0011b	fungus extract	5mg

FI0013	fungal extract	5mg
FI0019	fungal extract	5mg
FI0071	fungal extract	5mg
FI0074	fungal extract	5mg
FI0093	fungal extract	5mg
FI0107	fungal extract	5mg
FI0119	fungal extract	5mg
FI0120	fungal extract	5mg
FI0122	fungal extract	5mg

3.3 Multi-donor Screening in iAstrocyte co-cultures derived from ALS patients carrying different ALS-related genetic mutations.

The primary screen allowed the identification of 8 extracts exhibiting a level of motor neuron rescue comparable or higher than the positive control drug. Since the screening was carried out on a single ALS patient line, and ALS is by nature is a heterogeneous disorder with multiple associated genes, it is necessary to evaluate the efficacy of the top hits on a much wider panel of patients carrying different mutations. In this respect, the hexanucleotide GGGGCC repeat expansion mutations in the *C9ORF72* gene can be different among patients and can potentially influence the severity of the disorder (Suzuki et al., 2022). Different pathways can be affected in different ways by *C9ORF72* mutations; therefore, it is worth screening the top hit marine extracts in other available *C9ORF72* patient lines (patient #78, patient #ALS 52). Another common gene frequently found in patients with familial ALS is *SOD1*. Even though there is a common thread between all ALS forms, different pathways can contribute to different extents to the outcome of the disease. Thus, testing the extracts in the *SOD1* iAstrocyte lines available (patient #102 and patient #ND29505) can provide further information regarding their efficacy.

The most common form of ALS is sporadic (sALS); it occurs randomly with no known or clearly associated risk factors, and no recorded family history of the disease. Family members of people with sALS might have an increased risk of developing the disease, but the overall risk seems to be lower than family members of patients with fALS. Nonetheless, data highlighted that lack of information about the family pedigree might hide a fALS cases, and therefore a proportion of sALS patients could carry a pathogenic gene mutation (Shepherd et al., 2020). sALS patients might or might not have mutations in the above-mentioned genes and can display a wide array of mutations that still need to be recorded in databases.

Considering the availability of iNPC lines collected from sALS patients and reprogrammed from their fibroblasts, and the importance of sALS cases in the overall picture of the disease, we included 3 sporadic lines (patient #009, patient #012 and patient #017) into our multi-donor assay. Extracts which can provide a significant therapeutic effect in these lines as well could constitute an interesting pool for further investigation, due to their potential ability to interact with pathophysiological pathways commonly found in different ALS patients.

As explained before, due to time constraints dictated by the length of the isolation and purification protocols of natural extracts, we selected the top 3 hits out of the 8 neuroprotective extracts identified. To allow a better understanding of the results, the screen will be shown as each dose response curve biological triplicate for each extract in all the lines tested (**Figure 3.3-3.11**). Each extract will be shown separately to allow an easier understanding of the multi-donor screen (**Figure 3.3-3.11**). These results will be described in detail in Chapter 4.

We prepared the same plate layout for each extract to have consistent and comparable results. We introduced into the assay and screened the three marine extracts (BI0394, BI0788 and BI0987) using a working concentration range of 10 $\mu\text{g}/\text{mL}$, 1 $\mu\text{g}/\text{mL}$, 0.1 $\mu\text{g}/\text{mL}$, 0.01 $\mu\text{g}/\text{mL}$, and 0.001 $\mu\text{g}/\text{mL}$. Each plate contained 4 technical replicates of each concentration per each extract. 10 wells have been used as negative controls (healthy murine motor neurons plated with patient iAstrocytes and treated with DMSO); 10 wells have been used as the first positive control (healthy murine motor neurons plated with patient iAstrocytes and treated with a drug known to improve the survival of motor neurons *in vitro*), and 8 wells have been used as the second positive control (healthy murine motor neurons plated with a different control iAstrocyte line (sample #C155v2) and treated with DMSO). The assay was repeated 3 times with iAstrocytes and MNs obtained from 3 different batches of cells and differentiation rounds to reach 3 biological replicates to perform statistical evaluation of which extracts were able to induce a pro-survival response. The patient lines used are shown in **Table 3.2**.

Table 3. 2 List of all lines used for the top hit marine extracts multi-donor screening

Patient Line	Mutation
78	C9ORF72
ALS-52	C9ORF72
102	SOD1
ND29505	SOD1
009	sALS
012	sALS
017	sALS

The results observed in this assay showed that BI0788 was the most consistent extract resulting in motor neuron rescue in all the lines tested. BI0788 was able to provide its therapeutic effect in most of the lines used in this assay, including all 3 sALS lines, and showed a higher or at least comparable effect to the compound used as +/-ve control (Figure 3.6, 3.7 and 3.8). BI394 instead did not show any significant increase in the sALS lines, while it had mild neuroprotective effects in a subset of familial cases (Figure 3.3, 3.4 and 3.5), and BI0987 did not show any significant motor neuron rescue in general (Figure 3.9, 3.10 and 3.11). All extracts were not able to provide any significant rescue in co-culture with ND29505 (Figure 3.4, 3.7 and 3.10), this line is also extremely toxic and challenging to rescue in co-culture based on previous experience. Having identified BI0788 as the most promising extract from those tested in both the primary assay and the secondary multi-donor assay, it was selected for further experiments. Several fractions were purified and isolated from this extract. Experiments relative to BI0788 and its fractions will be discussed in detail in Chapter 4.

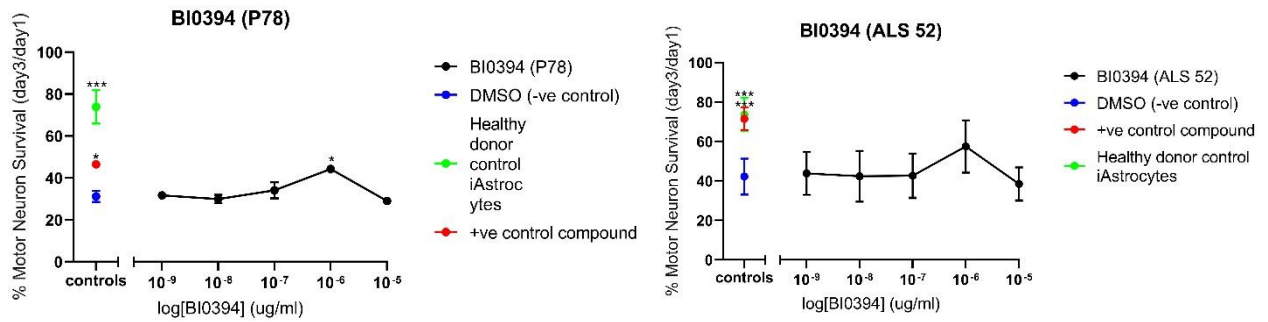


Figure 3. 3 Top hit BI0394 screen in C9orf72-ALS patient #78 and #ALS-52 iAstrocyte and Hb9-GFP+ mouse motor neuron co-culture

Hb9-GFP+ motor neurons co-cultured with C9orf72-ALS patient #78 and #ALS-52 iAstrocytes displayed increased survival in patient #78 upon treatment with the marine extract top hit BI0394 at 1mg/ml (black line) over DMSO only treatment (blue dot). This extract yielded similar motor neuron rescue as our +ve control compound at a concentration of 1 μ g/mL (red) in patient #78, while at the same concentration in patient #ALS-52 shows just a positive trend compared to the negative DMSO control (blue dot). Healthy donor control iAstrocytes treated with DMSO only (green dot) acted as positive control for the assay. Motor neuron survival at day 3 was calculated as a percentage of the number of motor neurons alive at day 1. N = 3, data are mean \pm SD. One-way ANOVA with Dunnett's multiple comparisons (* p <0.05).

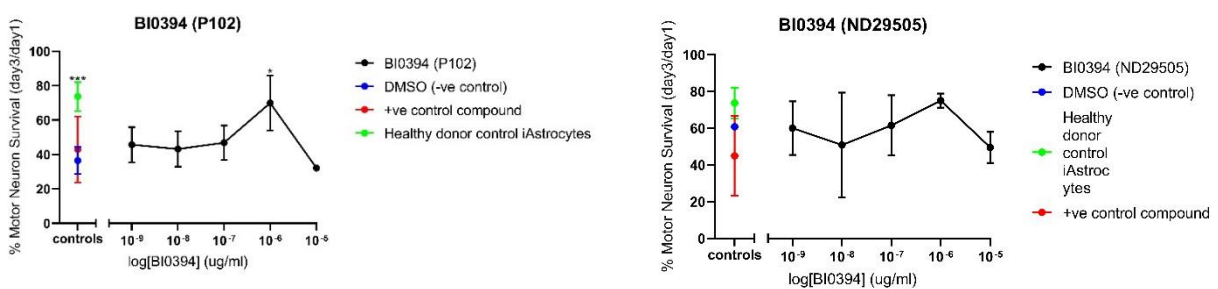


Figure 3. 4 Top hit BI0394 screen in SOD1-ALS patient #102 and #ND29505 iAstrocyte and Hb9-GFP+ mouse motor neuron co-culture

Hb9-GFP+ motor neurons co-cultured with SOD1-ALS patient #102 and #ND29505 iAstrocytes displayed increased survival in #P102 upon treatment with the marine extracts top hit BI0394 at various concentrations (black line) over DMSO only treatment (blue dot). This extract yielded significantly higher motor neuron rescue than our +ve control compound at a concentration of 1 μ g/mL (red) in patient #102, while it displayed variable results in patient #ND29505. Healthy donor control

*i*Astrocytes treated with DMSO only (green dot) acted as positive control for the assay. Motor neuron survival at day 3 was calculated as a percentage of the number of motor neurons alive at day 1. $N = 3$, data are mean \pm SD. One-way ANOVA with Dunnett's multiple comparisons ($***p < 0.001$, $*p < 0.05$).

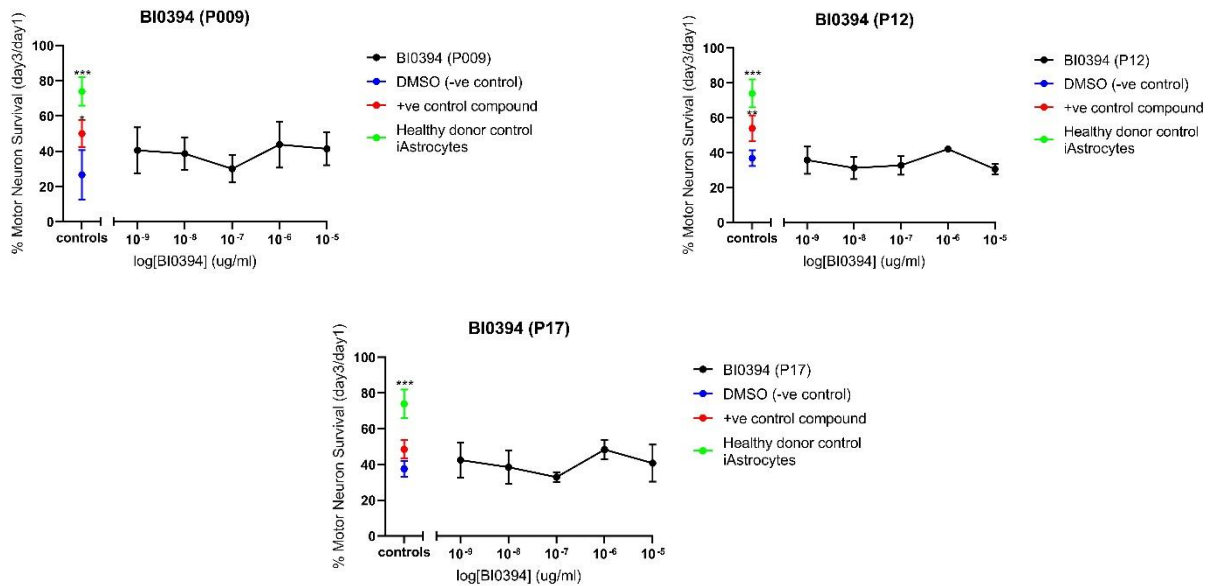


Figure 3. 5 Top hit BIO394 screening in sALS patient #009, #012 and #017 *i*Astrocyte and Hb9-GFP+ mouse motor neuron co-culture

Hb9-GFP+ motor neurons co-cultured with sALS patient #009, #012 and #017 *i*Astrocytes did not display any increased survival upon treatment with the marine extracts top hit BIO394 at various concentrations (black line) over DMSO only treatment (blue dot). Healthy donor control *i*Astrocytes treated with DMSO only (green dot) acted as positive control for the assay. Motor neuron survival at day 3 was calculated as a percentage of the number of motor neurons alive at day 1. $N = 3$, data are mean \pm SD. One-way ANOVA with Dunnett's multiple comparisons ($***p < 0.001$, $p^{**} < 0.01$).

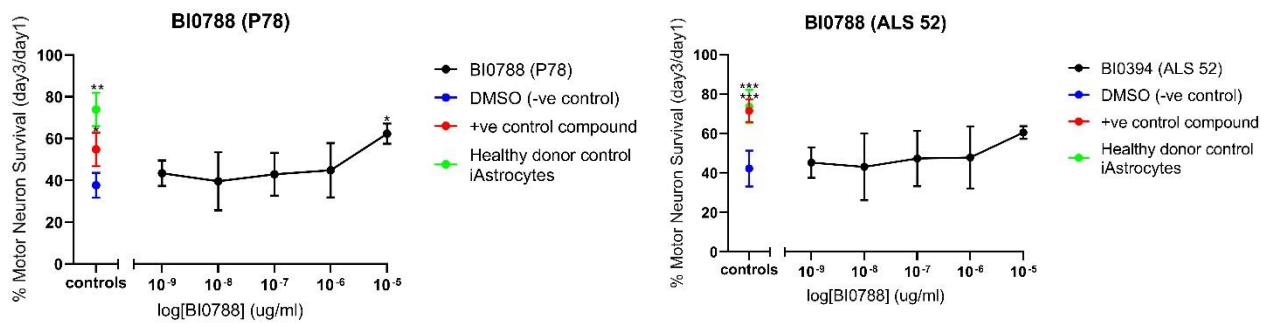


Figure 3. 6 Top hit BI0788 screen in C9orf72-ALS patient #78 and #ALS-52 iAstrocyte and Hb9-GFP+ mouse motor neuron co-culture

Hb9-GFP+ motor neurons co-cultured with C9orf72-ALS patient #78 and #ALS-52 iAstrocytes displayed increased survival in patient #78 upon treatment with the marine extracts top hit BI0788 at various concentrations (black line) over DMSO only treatment (blue dot). This extract yielded similar motor neuron rescue as our +ve control compound at a concentration of 10 $\mu\text{g}/\text{mL}$ (red) in patient #78, while at the same concentration in patient #ALS-52 shows just a positive trend compared to the negative DMSO control (blue dot). Healthy donor control iAstrocytes treated with DMSO only (green dot) acted as positive control for the assay. Motor neuron survival at day 3 was calculated as a percentage of the number of motor neurons alive at day 1. $N = 3$, data are mean \pm SD. One-way ANOVA with Dunnett's multiple comparisons ($***p < 0.001$, $p^* < 0.05$).

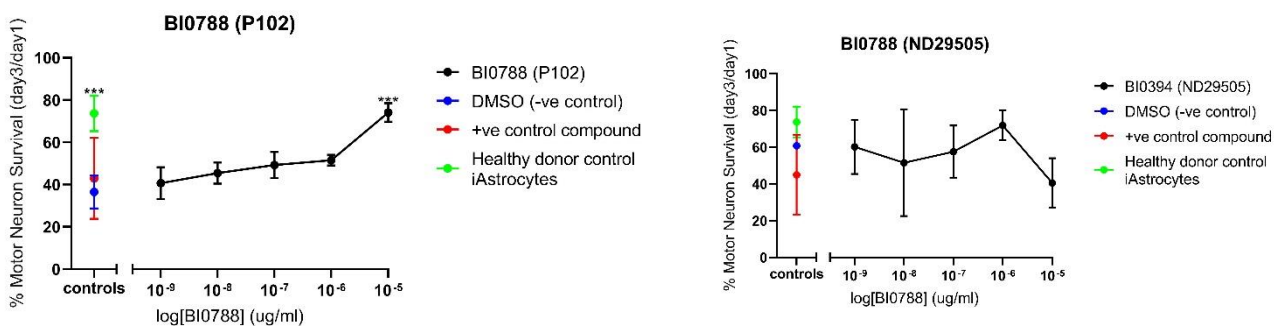


Figure 3. 7 Top hit BI0788 screen in SOD1-ALS patient #102 and #ND29505 iAstrocyte and Hb9-GFP+ mouse motor neuron co-culture

Hb9-GFP+ motor neurons co-cultured with SOD1-ALS patient #102 and #ND29505 iAstrocytes displayed increased survival in patient #102 upon treatment with the marine extracts top hit B788 at various concentrations (black line) over DMSO only treatment (blue dot). This extract yielded higher motor neuron rescue than our +ve control compound at a concentration of 10 $\mu\text{g}/\text{mL}$ (red) in patient #102, while it displayed variable results at various concentrations in patient #ND29505. Healthy donor

control *iAstrocytes* treated with DMSO only (green dot) acted as positive control for the assay. Motor neuron survival at day 3 was calculated as a percentage of the number of motor neurons alive at day 1. $N = 3$, data are mean \pm SD. One-way ANOVA with Dunnett's multiple comparisons ($***p < 0.001$).

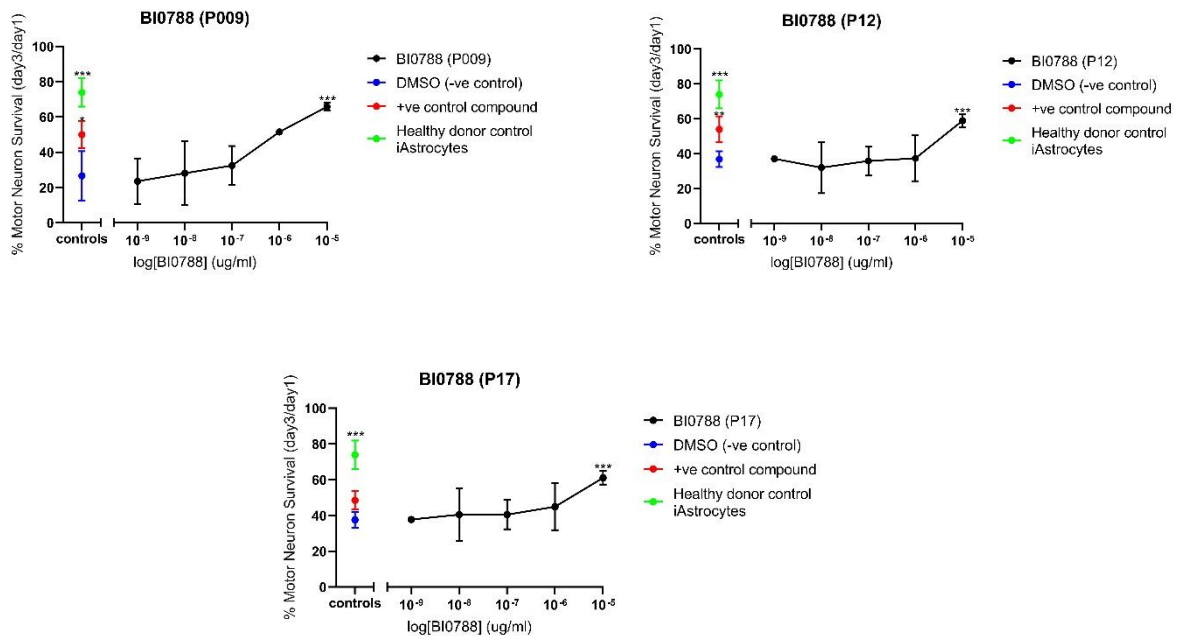


Figure 3. 8 Top hit BIO788 screen in sALS patient #009, #012 and #017 *iAstrocyte* and Hb9-GFP+ mouse motor neuron co-culture

Hb9-GFP+ motor neurons co-cultured with sALS patient #009, #012 and #017 *iAstrocytes* displayed increased survival upon treatment with the marine extracts top hit BIO788 at 10 μ g/mL (black line) over DMSO only treatment (blue dot) in all the lines tested. Healthy donor control *iAstrocytes* treated with DMSO only (green dot) acted as positive control for the assay. Motor neuron survival at day 3 was calculated as a percentage of the number of motor neurons alive at day 1. $N = 3$, data are mean \pm SD. One-way ANOVA with Dunnett's multiple comparisons ($***p < 0.001$, $p^{**} < 0.01$, $p^* < 0.05$).

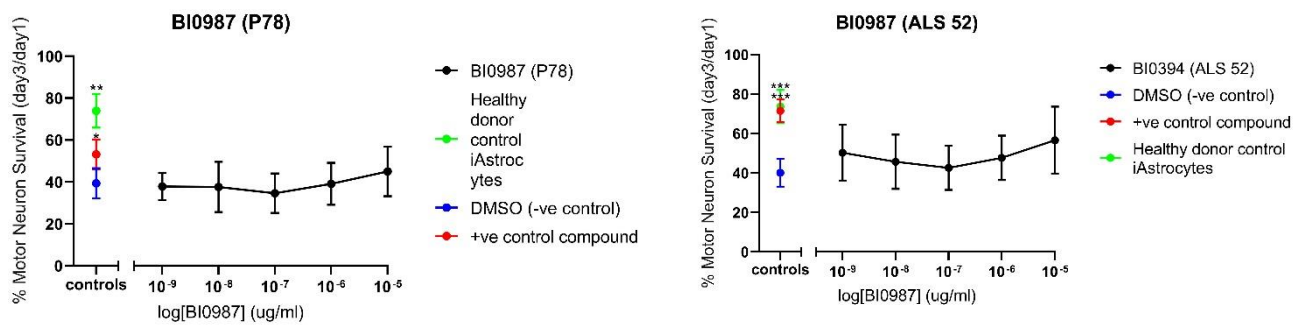


Figure 3. 9 Top hit BI0987 screen in C9orf72-ALS patient #78 and #ALS-52 iAstrocyte and Hb9-GFP+ mouse motor neuron co-culture

Hb9-GFP+ motor neurons co-cultured with C9orf72-ALS patient #78 and #ALS-52 iAstrocytes did not display increased survival in any of the patient lines upon treatment with the marine extracts top hit BI0987 at various concentrations (black line) over DMSO only treatment (blue dot). Healthy donor control iAstrocytes treated with DMSO only (green dot) acted as positive control for the assay. Motor neuron survival at day 3 was calculated as a percentage of the number of motor neurons alive at day 1. N = 3, data are mean ± SD. One-way ANOVA with Dunnett’s multiple comparisons (***p<0.001, p* < 0.05).

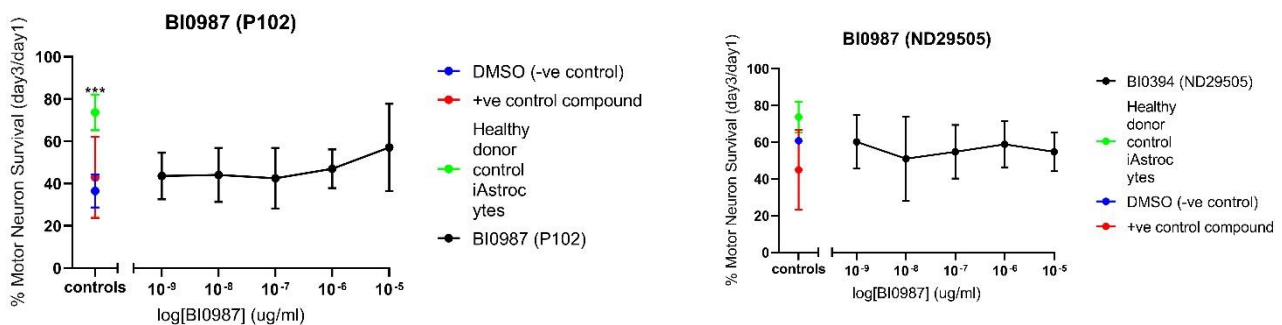


Figure 3. 10 Top hit BI0987 screening in SOD1-ALS patient #102 and #ND29505 iAstrocyte and Hb9-GFP+ mouse motor neuron co-culture

Hb9-GFP+ motor neurons co-cultured with SOD1-ALS patient #102 and #ND29505 iAstrocytes did not display any increased survival upon treatment with the marine extracts top hit B987 at various concentrations (black line) over DMSO only treatment (blue dot). Healthy donor control iAstrocytes treated with DMSO only (green dot) acted as positive control for the assay. Motor neuron survival at

day 3 was calculated as a percentage of the number of motor neurons alive at day 1. $N = 3$, data are mean \pm SD. One-way ANOVA with Dunnett's multiple comparisons ($***p < 0.001$).

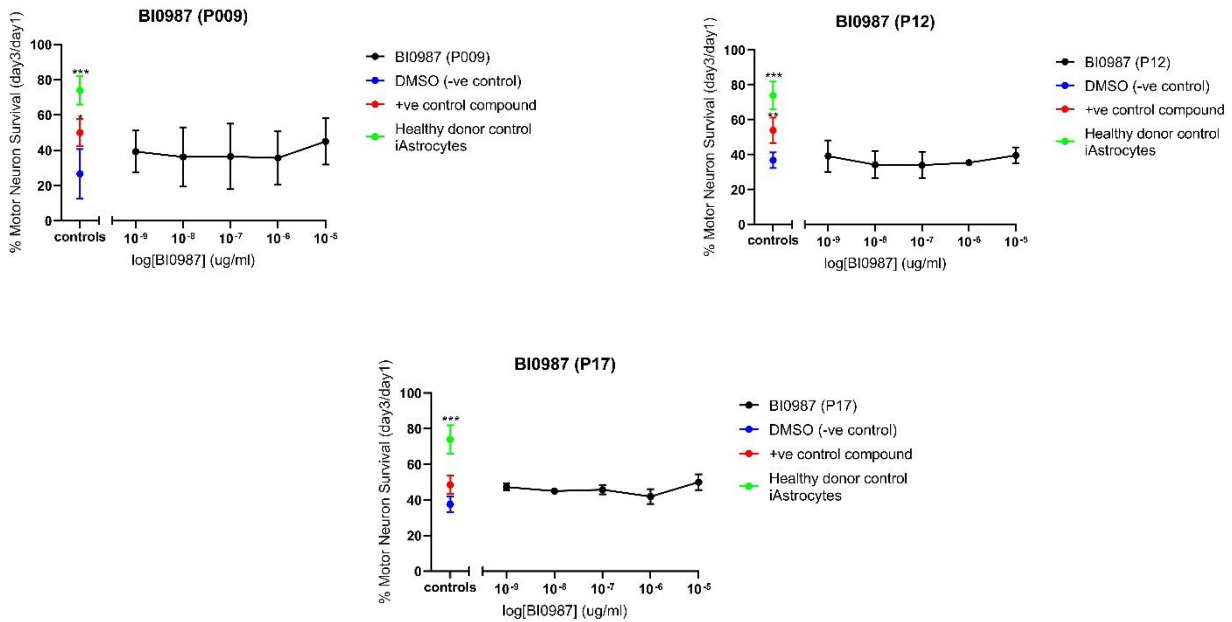


Figure 3. 11 Top hit BIO987 screening in sALS patient #009, #012 and #017 iAstrocyte and Hb9-GFP+ mouse motor neuron co-culture

Hb9-GFP+ motor neurons co-cultured with sALS patient #009, #012 and #017 iAstrocytes did not display any increased survival upon treatment with the marine extracts top hit B987 at various concentrations (black line) over DMSO only treatment (blue dot). Healthy donor control iAstrocytes treated with DMSO only (green dot) acted as positive control for the assay. Motor neuron survival at day 3 was calculated as a percentage of the number of motor neurons alive at day 1. $N = 3$, data are mean \pm SD. One-way ANOVA with Dunnett's multiple comparisons ($***p < 0.001$).

3.4 Screening of Dehydroepiandrosterone (DHEA) derivatives for neuroprotective effects in a motor neuron -astrocyte co-culture system.

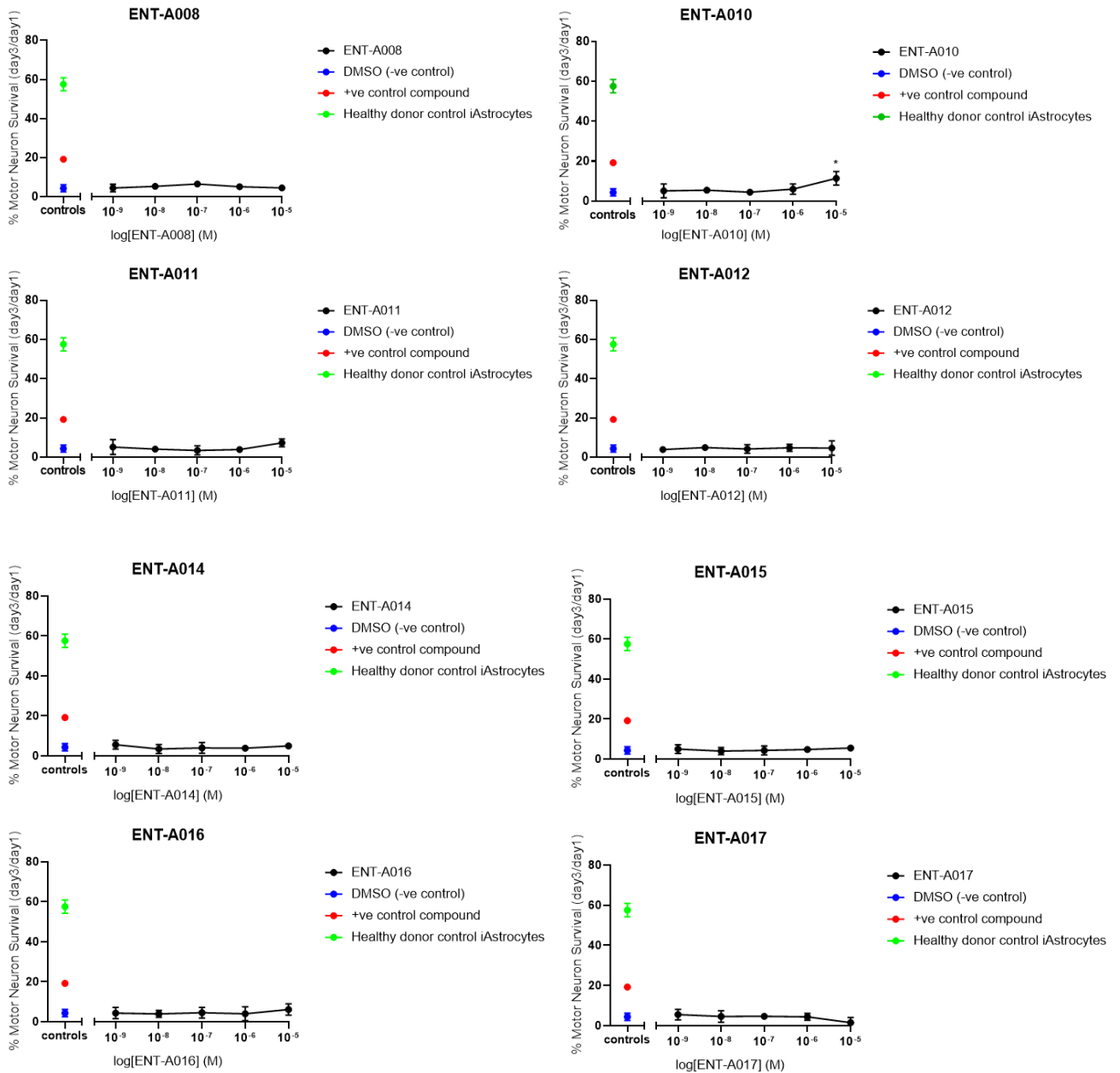
Within the Euroneurotrophin consortium, dehydroepiandrosterone (DHEA) derivatives were studied for their potential neurotrophic activity. Synthesis and characterisation of complex new steroidal compounds, to obtain structure-activity-relationships of 17C-spiroepoxy-DHEA derivatives agonists of neurotrophin receptors for optimum neuroprotective activity was undertaken by our partners at the National Hellenic Research Foundation. The same partner also worked on the synthesis, purification, and characterization of chiral 17C-spiroepoxy-DHEA derivatives bearing three-membered rings, which were further modified to introduce pharmacophore groups. These compounds were not initially included in the screening plan, but since some of them were found to be neuroprotective in other screenings and disease models adopted from our partners within the Euroneurotrophin consortium, we have asked to include them in our screening model to confirm their efficacy.

DHEA and dehydroepiandrosterone sulphate (DHEAS) are reported to be neurosteroids involved in cognition. BNN27 is a 17C-spiroepoxy-DHEA derivative that possesses neuroprotective effects (Pitsikas et al., 2021) and was recently shown to bind to the NGF high-affinity receptor, TrkA and p75NTR (Pediaditakis et al., 2016). Steroid compounds used in our consortium are all based on BNN27 as a scaffold, with the aim of finding a derivative with better functional activity in different neurological and neurodegenerative disorders. In this specific case, we tested the derivatives in our co-culture assay to find which compounds have a therapeutic effect in our ALS co-culture model.

We introduced into the assay and screened 16 steroid compounds using a working concentration range of 10 μ M, 1 μ M, 0.1 μ M, 0.01 μ M, and 0.001 μ M. Each plate contained 4 technical replicates of each concentration for each drug.

10 wells have been used as negative controls (healthy murine motor neurons plated with P183 C9ORF72 iAstrocytes and treated with DMSO), 10 wells have been used as the first positive control (healthy murine motor neurons plated with P183 C9ORF72 iAstrocytes and treated with our positive control drug), and 8 wells have been used as the second positive control (healthy murine motor neurons plated with control derived iAstrocytes 155v2 and treated with DMSO).

The results showed only ENT-A010 as having a slight effect in rescuing motor neuron survival (Figure 3.12). Experiments from other members of the consortium confirmed its efficacy in models of AD and microglia-mediated neuroinflammation, and this compound appears to have anti-inflammatory properties.



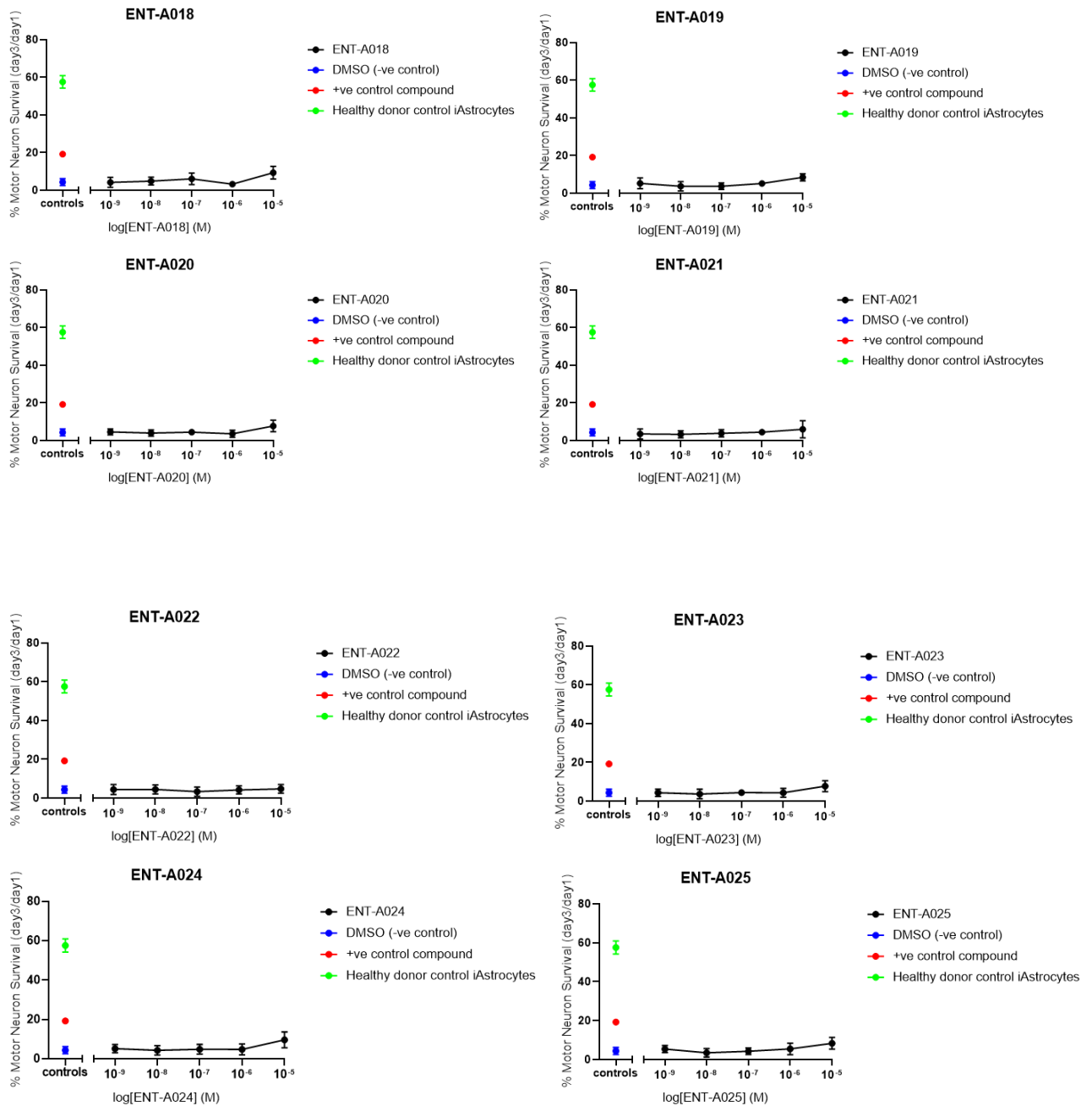


Figure 3. 12 Dose-Response curves obtained from the steroid compound screen in *C9orf72*-ALS patient *iAstrocyte-Hb9 GFP+* mouse motor neuron co-culture

C9orf72-ALS patient #183 *iAstrocytes* were treated with various concentrations of each steroid compound, +ve control compound or DMSO only at day 6. Healthy donor control *iAstrocytes* were also treated with DMSO only. The motor neuron survival at day 3 was calculated as a percentage of the number of motor neurons at day 1. $N = 3$, data are mean \pm SD. One-way ANOVA with Dunnett's multiple comparisons.

3.5 Discussion

The mutations in *C9ORF72* that cause ALS are nucleotide repeat expansion mutations (DeJesus-Hernandez et al., 2011) of a hexanucleotide (G4C2) sequence located in the first intron between two transcription initiation sites. Repeats of up to 30 seem to have no negative effect on gene function, but the minimum repeat length linked to disease is not yet established (Rohrer et al., 2015). *C9ORF72* repeat expansion is the most common gene variant associated with fALS and sALS, therefore finding pharmaceuticals able to improve the clinical conditions of patients affected by *C9ORF72*-ALS would be extremely beneficial. The *C9ORF72* iAstrocyte line (patient #183) chosen for the primary screening has been selected for its very high toxicity towards motor neurons. Based on previous drug screening data collected in the Ferraiuolo team, compounds able to rescue motor neurons in co-culture with this iAstrocyte line show a consistent improvement also in the other patient lines carrying *C9ORF72* mutations. Therefore, it represents a good benchmark to determine the neuroprotective efficacy of drugs within a tested library.

Natural products have been an important source of new pharmaceuticals in the last fifty years (Dias, Urban and Roessner, 2012). Marine natural products exhibit extended structural diversity and a multitude of biological effects derived from the high biodiversity of marine organisms and the intense competition for survival and growth in the marine environment. A number of marine natural products are already commercial drugs, e.g. the pain reliever Prialt® and the anti-tumour drug Yondelis®, while more than 15 compounds are in advanced clinical trials for the treatment of various diseases (Martins et al., 2014). Research efforts in the last years have been aimed at identifying marine natural products with neuroprotective activity for AD, PD and ischaemic stroke (Martins et al., 2014). Therefore, screening marine natural products represents an important route to the discovery of novel therapeutics for neurodegenerative disorders.

Among the 100 marine extracts tested on the co-culture system based on human iAstrocytes derived from a *C9ORF72* ALS patient (patient #183) and murine Hb9-GFP+ motor neurons, 8 extracts showed a significant improvement in motor neuronal survival. The 3 best top hits BI0394, BI0788 and BI0987 were screened in wider set of lines: 2 x *C9ORF72* lines (patient #78, #ALS-52), 2 x *SOD1* lines (patient #102, #ND29505) and 3 x sALS lines (patient #009, #012, #017) to test if their therapeutic effect is exerted in multiple subtypes of ALS. Extracts or even molecules found to be active on a certain patient line might not have the same degrees of

efficacy on other patient lines. Similarly, molecules that did not yield a significant improvement of motor neuronal survival when tested in a co-culture based on a *C9ORF72* patient, could show a pro-survival activity on system based on a different patient iAstrocyte line.

Extracts able to deliver a therapeutic effect in lines affected by a variety of mutations in different genes, other than increasing the chances of being potentially interesting from a medical perspective, might also mean that they act on a pathway or group of pathways common to most ALS patients. If they are not able to show any therapeutic effect in lines with mutations in different genes, if they are still consistent in the same sub-population of patients, this can help in narrowing down in which pathway they operate and can still be considered worth testing for personalised medicine approaches.

Following the results of the multi-donor assay we observed that, amongst the 3 extracts chosen for this screening, BI0788 was the one able to improve motor neuron survival in most lines tested, including sALS lines. This indicates that the pathway(s) targeted by BI0788 might be common to ALS patients carrying different mutations.

Given that the extracts contain unknown mixtures of different compounds, it is impossible to determine which molecules are providing the therapeutic effect from this first screen. Therefore, the top hit BI0788 was subjected to fractionation to then obtain the single pure molecules to test again in the co-culture system. This approach will shed light on the compound, or the mixture of synergistic compounds which provide the neuroprotective effect. These results will be discussed in detail in Chapter 4.

Another important aspect that must be taken into consideration is that this screening approach can provide only phenotypical information, and not functional information about the activity of the extracts towards motor neurons or astrocytes.

Consequently, once the compounds driving the pro-survival effect have been identified, it will be important to perform downstream assays to determine the source of the therapeutic activity of those molecules. Moreover, even though these extracts have been pre-selected for putatively containing neurotrophin mimetics, there is no certainty that the neuroprotective effect stems from a compound with neurotrophic properties. Further analyses are required to understand if these mimetics are present in BI0788 and if these constituents can promote motor neuron rescue in ALS conditions.

To obtain single purified molecules, the extracts must be subjected to several steps of fractionation through several chromatography techniques as described in the materials and methods (**Chapter 2**). All fractions contain a different number of compounds with similar polarity, which can be separated using HPLC with the appropriate solid and liquid phases, that vary depending on the polarity of the single fraction.

There is also a chance that the pro-survival effect encountered in the first phases of screening could be lost after isolating and purifying the compounds in BI0788. There are several potential explanations for this outcome: First, it must be considered that the extract represents a complex system where multiple molecules might interact with each other producing synergistic effects. Natural extracts might contain hundreds of individual constituents at different concentrations (Caesar and Cech, 2019). Detecting the compound(s) responsible for a certain biological effect represents a significant challenge. Often, it is proposed that the biological effect provided by a mixture is exerted by just a few constituents (Caesar and Cech, 2019). However, evidence from reports has shown that activity of natural extracts can result from mixtures of molecules with synergistic, additive, or antagonistic activities (Wagner and Ulrich-Merzenich, 2009). In this respect, the isolation process of natural extracts can lead to the loss of therapeutic activity (Wagner and Ulrich-Merzenich, 2009). Among the possible explanations for this failure there are the irreversible adsorption of metabolites on to the columns during the fractionation and purification processes (Manadas et al., 2010), and the loss of the synergistic activity of multiple constituents responsible for the therapeutic effect. Despite these issues, given the complexity of natural extracts the research methodology often takes a reductionist approach, focusing on just a minority of fractions or isolated compounds, or ignoring the biological effects of complex mixtures (Caesar and Cech, 2019). Since validating the therapeutic effect of an extract is such a challenging process, companies do not tend to take extracts forward for therapeutic approaches but rather focus on single molecules. These are normally easier to validate following the rules for releasing a new therapeutic agent into the market.

One more point that could create complications while proceeding with the BI0788 testing is that it mostly shows efficacy at 10 µg/mL. Therefore, therapeutic effects might be achieved only at high concentrations. If none of the individual compounds can achieve the rescue observed in the extract, it will be hard, or even impossible, to deliver the necessary dose in

the clinic considering the challenge of drug delivery to the CNS.

The work on DHEA compounds has not been taken forward due to time constraints, it was not part of the original screening plan and since we had several disruption factors throughout the PhD period we were not able to include anything unrelated to the extracts for further studies. Therefore, in agreement with the other Euroneurotrophin partners we decided to keep focusing only on the extract library.

Chapter 4: Isolation and characterization of BI788 constituents and *in silico* analysis for potential neurotrophin receptor binding

4.1 Introduction

Discovery of therapeutic products from natural extracts requires a methodological approach to achieve a complete purification and characterization of the constituents. Therefore, it is necessary to develop a pipeline, which either be achieved through ethnopharmacological knowledge or by screening a libraries of extracts for bioactivity (Atamasov et al., 2015). After discovering that a natural extract contains bioactive molecules, a bioassay-guided fractionation is usually performed following these steps: fractionation of the extract by chromatography, bioassay screening of each relevant fraction, isolation of the molecules contained inside the fractions, characterization of the isolated constituents and evaluation of their biological activity (Atamasov et al., 2015).

As reported in chapter 4, loss of activity or failure in isolating the compounds during the fractionation is very common, and can be due to: degradation of the therapeutic compounds during the purification process, insufficient amount of the therapeutic compounds allowing an efficient isolation, and loss of synergistic effects between multiple compounds.

It is therefore important to detect therapeutic candidate molecules as early as possible during the fractionation pipeline to rationalize the isolation procedure towards the most relevant fractions (Nothias et al, 2018).

After the primary screening described in chapter 3, we therefore performed, directly or through our collaborators at the National and Kapodistrian University of Athens (NKUA), chromatography experiments to isolate fractions and purified compounds from the top 3 extracts detected through the co-culture assays. Among the 8 extracts that showed potential therapeutic activity, BI0394, BI0788 and BI0987 as the most active extracts were selected for isolation. Chromatographic experiments have been firstly performed on BI0987, rather than our most promising candidate BI0788, due to its immediate availability and amount. The first phase of isolation has been conducted during a fellowship-related secondment at the NKUA (Athens) in collaboration with Mr Paolo Giaccio, a PhD student

working in the same network, Prof Vassilios Roussis and Prof Efstathia Ioannou. The aim of this secondment was to familiarize myself and better understand the techniques involved in the above-mentioned process of extract isolation while continuing with the analysis of data obtained through the primary screening.

After the purification and quantification of extract fractions, we also employed Nuclear Magnetic Resonance (NMR) for the identification of small molecule structures.

After the recognition of a clear pool of molecules from the NMR analysis, we also performed molecular docking to understand their similarity in structure to neurotrophin receptor binders.

Over the past few decades, molecular docking has emerged as a crucial tool in the field of drug discovery. The development of modern high-throughput protein purification, crystallography, and NMR spectroscopy techniques has allowed for the elucidation of structural details of proteins and receptor-ligand complexes (Stark et al, 2012). These advances have enabled the creation of computational strategies to aid in the drug discovery process.

Molecular docking is the most widely used method for structure-based drug design and analysis, employing programs based on various algorithms (Sliwosky 2013). The molecular docking approach models the atomic-level interaction between a small molecule and a protein, thereby enabling the characterization of the behaviour of small molecules within the binding site of target proteins. The docking process involves predicting the ligand conformation, as well as its position and orientation within these sites, and assessing the binding affinity (Meng et al., 2011).

Being able to know the location of the binding site beforehand significantly increases the efficiency of the docking process. In several cases, information about the binding site can be obtained by comparing the target protein with proteins that share a similar function or with proteins co-crystallized with other ligands. If knowledge about the binding sites is unavailable, cavity detection software or online servers can be utilized to identify potential active sites within proteins (Morris 2008). Modern docking algorithms are developed using the "induced-fit" principle, which considers that the active site of the protein is continually reshaped by interactions with the ligand, allowing for a more accurate analysis of ligand-receptor interaction (Meng et al., 2011).

We performed molecular docking on a library of molecules isolated from the top hit extracts BI0394, BI0788 and BI0987. Since our co-culture assay provides just phenotypical information, it is impossible to tell from the results which extracts contain molecules able to interact with the neurotrophin receptors, or if the pro-survival response comes from an interaction with those receptors or other binding sites. Therefore, once the constituents were isolated, we have been able to employ molecular docking to gather information about which compounds were potential binders of the neurotrophin receptors. These results can guide us through some of the future experimental steps. If the molecules providing the therapeutic effect also bind to the neurotrophin receptors, we can aim to perform experiments associated with the neurotrophin pathways to better understand what their molecular function is in relation to ALS and what pathways are involved in their mechanism of action.

4.2 Isolation and Characterization of Secondary Metabolites from BI0987

Based on the primary co-culture screening shown in chapter 3, the top 3 out of the 8 marine extracts showing pro-survival activity in our ALS *C9ORF72* model were selected for further chemical investigation. This experimental procedure was carried out during a 2-month long secondment at the NKUA. BI0987 was prioritized over the other top hit extracts (BI0394 and BI0788) due to its immediate availability at the time of the secondment, while BI0788 and BI0394 were deprioritised due to lack of immediate availability. The latter fractions have been entirely used to produce the first batch that was sent to SITraN for investigation. Considering that the secondment was just 2 months long, we had to start with the only top hit already available, BI0987. The other two top hits have just been put into large-scale fermentation to allow their isolation after the end of the secondment, by our partners at NKUA.

The bacterial strain was cultured on a large-scale in flasks containing a sea water-based medium and the resulting organic residue derived from its extraction was subjected to a multi-step fractionation scheme, which led to the isolation of seven secondary metabolites.

Purification of individual compounds began from extract BI0987 by fractionation.

Specifically, the crude extract of strain BI0987 was subjected to vacuum liquid chromatography on silica gel with solvent mixtures of increasing polarity as eluent (**Table 4.1**), to yield nine fractions (A-I).

Table 4. 1 Eluents employed for the first phase of BI0987 chromatography

Eluants (%)		Volume (mL)	Fractions
cHex 100	EtOAc 0	100	A
cHex 80	EtOAc 20	100	
cHex 60	EtOAc 40	100	B
cHex 40	EtOAc 60	100	C
cHex 20	EtOAc 80	100	D
cHex 0	EtOAc 100	100	E
MeOH 5	EtOAc 95	100	F
MeOH 10	EtOAc 90	100	G
MeOH 20	EtOAc 80	100	H
MeOH 50	EtOAc 50	100	I
MeOH 100	EtOAc 0	100	

This table describes the ratios of the eluents employed for the first phase of BI0987 chromatography, which resulted in 9 different sub-fractions (A-I).

The following eluents have been used in different ratios to allow the elution of all constituents within BI0987. Constituents can have different polarities, weights, and ability to remain attached at the resins within the chromatographic columns. Therefore, not knowing exactly what eluents are necessary to obtain each single fraction, we had to try different combinations until the last fractions presented only eluents.

cHex = Cyclohexane

MeOH = Methanol

EtOAc = Ethyl Acetate

After the analysis of the ¹H-NMR spectra of the fractions obtained, the fractions F, G, H and I were prioritized and purified by vacuum and/or gravity liquid chromatography (**Table 4.2**) because they contained the highest number of different peaks and therefore more constituents that needed to be separated. Fractions F and G were combined and further purified by gravity column chromatography on silica gel because they came out with similar eluent ratios and presented similar peaks. Ten fractions (F1-F10) were generated after purification with solvent mixtures of increasing polarity.

Moreover, fraction H was subject to vacuum liquid chromatography on silica gel, using as eluant, solvent systems of increasing polarity to yield six fractions (H1-H6). Reverse-phase vacuum liquid chromatography was performed on fraction I and generated ten further fractions (I1-I10).

Table 4. 2 Eluents employed for the second phase of BI0987 chromatography

Eluants %		Volume (mL)	Fractions	
cHex:Me ₂ CO	70:30	100	1	F1
			2-3	F2
			4-5	F3
			6-7	F4
			8	F5
cHex:Me ₂ CO	67:33	50	9-10	F6
			11-13	F7
cHex:Me ₂ CO	65:35	50	14-15	F8
cHex:Me ₂ CO	60:40	50	16-18	F9
cHex:Me ₂ CO	55:45	50	19-35	F10
cHex:Me ₂ CO	45:55	50		
cHex:Me ₂ CO	35:65	20		
Me ₂ CO	100	20		
Me ₂ CO:MeOH	50:50	20		
MeOH	100	50		

Eluants %	Volume (mL)	Fractions	
H ₂ O:MeOH	80:20	50	I1
H ₂ O:MeOH	60:40	50	I2
H ₂ O:MeOH	40:60	50	I3
H ₂ O:MeOH	20:80	50	I4
MeOH	100	100	I5
			I6
EtOAc:MeOH	10:90	50	I7
EtOAc:MeOH	50:50	50	I8
EtOAc	100	50	I9
CH ₂ Cl ₂	100	50	I10

Eluants %	Volume (mL)	Fractions		
cHex:Me ₂ CO	70:30	50	1	
cHex:Me ₂ CO	65:35	50		
cHex:Me ₂ CO	60:40	50		
cHex:Me ₂ CO	55:45	50	4	H2
cHex:Me ₂ CO	30:70	50	5	H3
cHex:Me ₂ CO	10:90	50	6	H4
Me ₂ CO	100	50	7	H5
Me ₂ CO:MeOH	20:80	50	8	H6

These tables describe the ratios of the eluents employed for the second phase of BI0987 chromatography, which implies the fractionation of the sub-fractions F, H and I selected after looking at the NMR spectra for potentially interesting molecules, based on the spectra analysed from our collaborators showing peaks indicating the presence of chemical groups commonly found in biologically active molecules.

Subsequently, fractions F2, F3, F4, F5/F6, F7-10, H1 and H3 were purified by normal phase HPLC on a silica gel column using mixtures of cHex/Me₂CO in diverse ratios, in order to obtain seven compounds in pure form (BI0987-01, BI0987-02, BI0987-03, BI0987-04, BI0987-05, BI0987-06 and BI0987-07) (**Figure 4.1**).

Isolation of additional compounds from the extract of strain BI0987 was taken forward with fraction I by vacuum liquid chromatography on reversed phase silica gel, with solvent mixtures of decreasing polarity (from H₂O/MeOH 9:1 to CH₂Cl₂ 100%) as the mobile phase,

to generate ten fractions (I1-I10). Afterwards, fractions I4, I6 and I7 were purified by reverse phase HPLC on a C18 column using mixtures of MeCN/H₂O in different ratios.

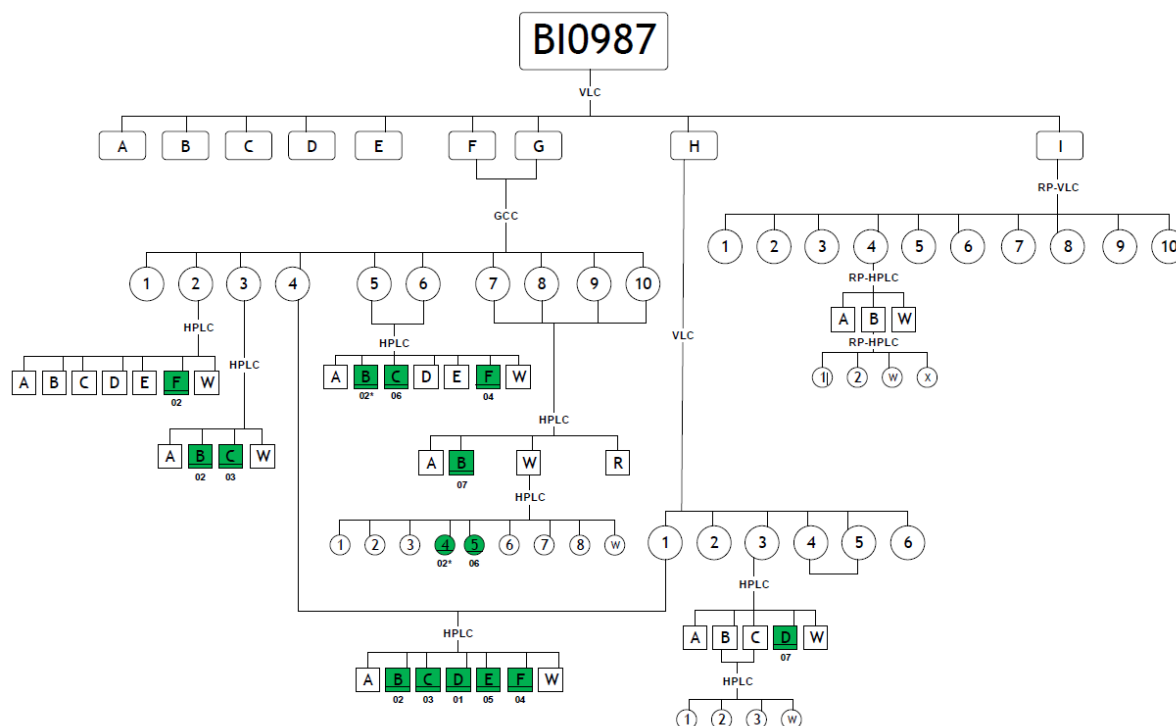


Figure 4. 1 Isolation of secondary metabolites from BI0987

BI0987 was fractionated into fractions A-H. Fractions F and G were then combined due to their similar profile shown by Thin Layer Chromatography (TLC), and further purified through gravity column chromatography (GCC) into purer fractions. These fractions were then purified through several HPLC steps. Fraction H received a further step of fractionation through Vacuum Liquid Chromatography (VLC), then its fraction 3 has been purified through HPLC. Green boxes indicate the 7 pure compounds that have been isolated from BI0987 during this process and have been named from BI0987-01 to BI0987-07 following the numerical order described in the flow diagram. Fractions containing the same compound have been merged in order to achieve a higher amount. The * reported in some fractions containing only the compound BI0987-02 indicates the presence of some impurities identified through ¹H-NMR.

Compounds BI0987-01, BI0987-02, BI0987-03, BI0987-04, BI0987-05 and BI0987-07 were identified as 2,5-diketopiperazines by comparison of their spectroscopic and physical characteristics with those reported in the literature (**Figure 4.2**). These compounds have been respectively re-named: ENTM110 (BI0987-01), ENT-M111 (BI0987-03), ENT-M112 (BI0987-04), ENT-M113 (BI0987-05), ENTM114 (BI0987-07). ENTM110 (BI0987-02) presented impurities at the time of this fractionation and purification, therefore, despite being able to understand its chemical structure, we could not use it in a pure form for experiments.

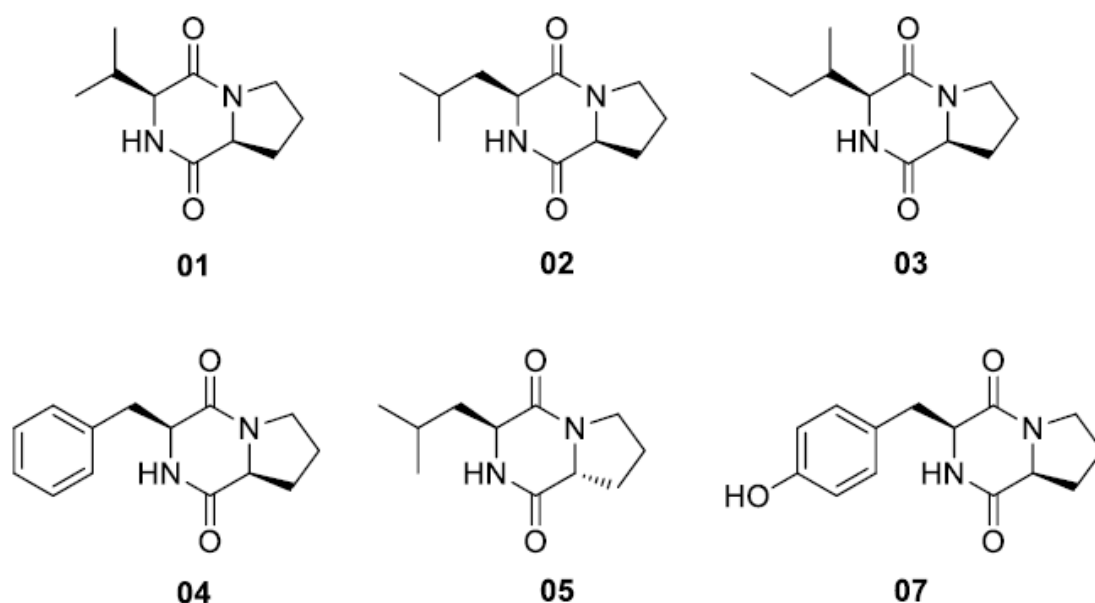


Figure 4. 2 2,5-diketopiperazines isolated from BI0987

The figure shows the molecular structures of compounds isolated from the top hit extract BI0987. Structures have been determined by comparison of $^1\text{H-NMR}$ spectra, obtained from fractions containing only the pure compounds, with $^1\text{H-NMR}$ spectra archives. Spectra showing the same peaks indicated the presence of the same molecule within the fraction. BI0987-06 was not yet characterized, since there were no spectra corresponding to the one obtained from fractions containing only BI0987 in the examined archives.

4.3 Screening 2,5-diketopiperazines Isolated from BI0987 for neuroprotective effects in a motor neuron and C9ORF72 iastrocyte co-culture assay

The 5 pure compounds, 2,5-diketopiperazines, isolated from BI0987 were then tested in the ALS Patient iAstrocyte-Murine Hb9-GFP+ Motor Neuron Co-Culture Assay. These compounds have been screened in the previously described co-culture system based on human iAstrocytes derived from a *C9ORF72* ALS patient #183 and murine Hb9-GFP+ motor neurons, to understand which compounds promote neuronal survival when cells are treated with the BI0987 marine extract.

Each compound has been tested at five different concentrations: 10 μ M, 1 μ M, 0.1 μ M, 0.01 μ M and 0.001 μ M. DMSO was used as a negative control. Healthy donor control #155 iAstrocytes treated with DMSO, or patient #183 iAstrocytes treated with an in-house neuroprotective compound were used as positive controls for increased motor neuron survival (**Figure 4.3**).

Unfortunately, none of the tested molecules gave any positive rescue in the assay. This often happens during the process of extract fractionation and purification. The extracts are complex mixtures of molecules, therefore it is not guaranteed that the individual constituents can provide the pro-survival effect alone, they might act in multiple groups or simply, since we have not had extracted all the constituents, the few we tested may not be the ones delivering the therapeutic effect.

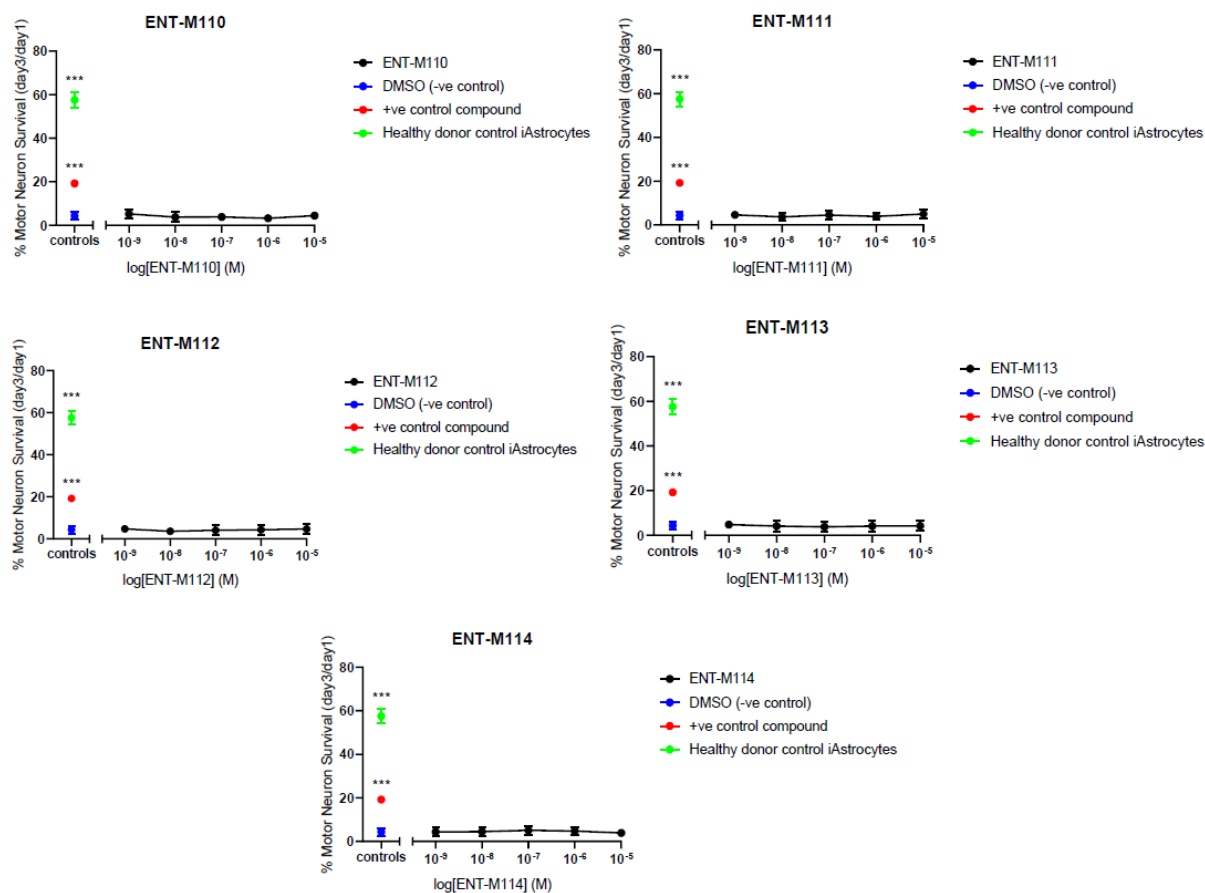


Figure 4. 3 2,5-diketopiperazines isolated from BI0987 did not improve motor neuron survival in the C9orf72-ALS patient iAstrocyte and Hb9-GFP+ mouse motor neuron co-culture

Hb9-GFP+ motor neurons co-cultured with C9ORF72-ALS patient #183 iAstrocytes did not display increased survival upon treatment with 5 different 2,5-diketopiperazines isolated from BI0987 at various concentrations (black line) over DMSO only treatment (blue squares). These 5 compounds did not yield motor neuron rescue compared to our +ve control compound at a concentration of 100nM (red circles). Healthy donor control iAstrocytes treated with DMSO only (green circles) acted as positive control for the assay. Hb9-GFP+ mouse motor neurons were seeded in co-culture at day 7. GFP+ motor neurons were imaged at 24 and 72 hours following co-culture, and viable motor neurons were counted. Motor neuron survival at day 3 was calculated as a percentage of the number of motor neurons alive at day 1. N = 3, data are mean \pm SD. One-way ANOVA with Dunnett's multiple comparisons (***) $p < 0.001$.

4.4 Screening 2,5-diketopiperazines Isolated from BI0987 for neuroprotective effects in a motor neuron -SOD1 astrocyte co-culture assay

The 5 compounds isolated and characterized from the top hit BI0987 were also screened in a co-culture system based on human iAstrocytes derived from a *SOD1* ALS patient #102 and murine Hb9-GFP+ motor neurons to investigate the effect of these compounds on a different ALS genotype. Since different ALS-related mutations create a diverse pathophysiological background, cells obtained from different patients possessing a diverse panel of mutations might respond in a different manner to the tested potential therapeutic agent. Therefore, it is always necessary to test the efficacy of the tested drugs on different co-culture systems based on diverse human iAstrocytes derived from ALS patients. Each compound was tested at five different concentrations: 10 μ M, 1 μ M, 0.1 μ M, 0.01 μ M and 0.001 μ M. DMSO was used as a negative control. Healthy donor control #155 iAstrocytes treated with DMSO, or patient #102 iAstrocytes treated with an in-house neuroprotective compound were used as positive controls for increased motor neuron survival (**Figure 4.4**). As expected from the previous results, none of the tested molecules gave any positive rescue in the assay. Since at the time of this screening on secondary metabolites we were still working on the multi-donor screening of the top hits extracts and we still lacked the full isolated compounds list, we did not take forward the isolated 2,5-diketopiperazines for further testing in other lines as we did for the full extracts aiming to do further testing later to optimize the time and the experimental pipeline.

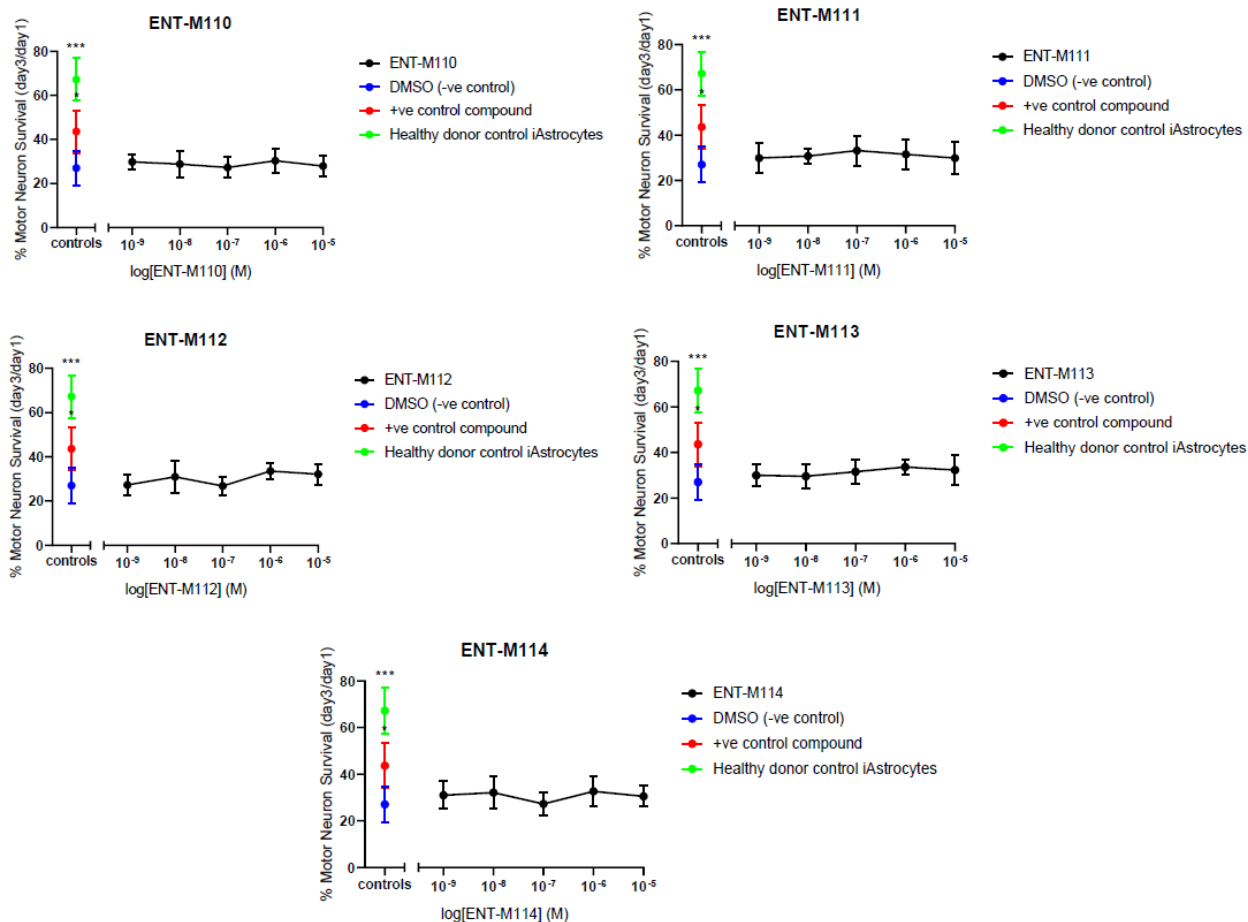


Figure 4. 4 2,5-diketopiperazines isolated from BI0987 did not improve motor neuron survival in the SOD1-ALS patient iAstrocyte and Hb9-GFP+ mouse motor neuron co-culture

Hb9-GFP+ motor neurons co-cultured with SOD1-ALS patient #102 iAstrocytes did not display increased survival upon treatment with 5 different 2,5-diketopiperazines isolated from BI0987 at various concentrations (black line) over DMSO only treatment (blue circles). These 5 compounds did not yield motor neuron rescue as our +ve control compound at a concentration of 100nM (red circles). Healthy donor control iAstrocytes treated with DMSO only (green circles) acted as positive control for the assay. Hb9-GFP+ mouse motor neurons were seeded in co-culture at day 7. GFP+ motor neurons were imaged at 24 and 72 hours following co-culture, and viable motor neurons were counted. Motor neuron survival at day 3 was calculated as a percentage of the number of motor neurons alive at day 1. N = 3, data are mean \pm SD. One-way ANOVA with Dunnett's multiple comparisons (***) $p < 0.001$.

4.5 BIO788 fractions multi-donor screening

As described in chapter 3, the primary screening allowed the identification of 8 extracts exhibiting a level of motor neuron rescue comparable or higher than the positive control drug. As explained previously, due to time constraints dictated by the length of the isolation and purification protocols of natural extracts, we selected the top 3 hits out of the 8 neuroprotective extracts identified, and those hits have been screened again on a multi-donor co-culture assay with patient i-astrocytes carrying a wider panel of different mutations to validate their therapeutic effect on a broader range of ALS astrocytes having different possible pathways impaired by the disease. Among them, BIO788 seemed to be the most neuroprotective on average in the different patient lines employed for the multi-donor screening due to its higher level of motor neuron rescue. That provides an indication that its constituents might have a good chance of providing the same therapeutic effect once isolated and characterized.

BIO788 was therefore selected as candidate for further analysis. The progression of the process of isolation and characterisation of natural extracts, as explained earlier in this chapter, requires an analysis of the fractions in the same biological assay used for the primary screening to help in defining which fractions can mimic the effect of the crude extract. If a subfraction can give a similar result, that could mean that the bioactive compounds are located within that fraction, limiting the time-consuming process of analysing every single compound contained within the extract. In this respect, we must always consider the limits of this procedure, including synergistic effects and loss of molecules throughout the steps of separation. Therefore, it is not guaranteed that once the extracts get split into different sub-fractions, that these can effectively provide the same effect. But overall, this extra step of analysis can provide important information regarding the content of the extract and its potential bioactive constituents.

To obtain an adequate amount of BIO788, our partners at the NKUA performed a series of small-scale fermentations of the bacterial strain BIO788. It is important to note that a large-scale fermentation does not often reproduce the same chemical profile of the small-scale fermentation of the same strain. Microorganisms may produce, upon large-scale fermentation, several derivatives, or even new compounds compared to those produced through small-scale fermentation, or alternatively they might not yield enough of the

bioactive products. Therefore, to address these problems based on preliminary tests, our collaborators decided to gather enough material for further testing and generation of metabolites through the collection of multiple batches of small-scale fermentations of the extract. Also, the production of different small-scale fermentations can lead to non-consistent batches containing different proportions of metabolites compared to the original extract tested during the primary screening. For this reason, the new batch of BI0788 was tested as well to check if the therapeutic effect was still present.

Chromatography on BI0788 led to the formation of 11 different sub-fractions (A-K) (**Figure 4.5a**). These fractions have been collected by submitting them to vacuum liquid chromatography on silica gel with solvent mixtures of increasing polarity (from cHex 100% to MeOH 100%). Fractions B/C/D were discovered to contain the same group of molecules, neoantimycins, therefore they have been combined into a single fraction, resulting in a total of 9 fractions (M217-M225) selected for the multi-donor assay.

We introduced into the co-culture assay and screened the 9 fractions (M217-M225) of BI0788 using a working concentration range of 10 µg/mL, 1 µg/mL, 0.1 µg/mL, 0.01 µg/mL, and 0.001 µg/mL. Each plate contained 4 technical replicates of each concentration per each extract. 10 wells have been used as negative controls (healthy murine motor neurons plated with patient iAstrocytes and treated with DMSO); 10 wells have been used as the first positive control (healthy murine motor neurons plated with patient iAstrocytes and treated with a drug known to improve the survival of motor neurons *in vitro*), and 8 wells have been used as the second positive control (healthy murine motor neurons plated with a different control iAstrocyte line (sample #155) and treated with DMSO). The assay was repeated 3 times with iAstrocytes and MNs obtained from 3 different batches of cells and differentiation rounds to reach 3 biological replicates to allow us to perform statistical evaluation of which extracts were able to induce a pro-survival response. The patient lines were selected as one per each type of ALS i-astrocytes available in the laboratory to perform a multi-donor screening.

The results observed in this assay showed that M219 was the only fraction able to achieve motor neuron rescue in all the lines tested (**Figure 4.5b**). M219 was able to provide a significant therapeutic effect in patients P17 and P201, with a higher or at least comparable neuroprotective effect compared to the +ve compound used as control. The SOD1 patient

P102 co-culture instead did not show any significant increase, even though there seems to be a positive trend at higher concentrations. This would require further replicates to confirm or refute this possibility, considering the variability across the biological replicates. Having only one fraction providing the therapeutic effect can help us to understand which bioactive compound is able to deliver the motor neuron rescue in the co-culture assay. The results of the other fractions are illustrated in the Chapter 7 (Appendix **Figure 7.1, 7.2 and 7.3**). As explained before in this chapter, there was a chance that part of the effect could have been lost throughout the fractionation steps, as did appear to happen in this case. Separation and loss of constituents during the chromatography processing of extracts can lead to a loss of activity. Also, it must be taken into consideration that working with extracts does not allow us to precisely treat the cells with proper defined concentrations, but we must rely on the molecular weight of the single fractions. Knowing which fraction contains the putative therapeutic molecules will allow us to recognize the ratio between the molecules belonging to M219 and their molecular weights. This would allow us to provide a more targeted treatment in future experiments.

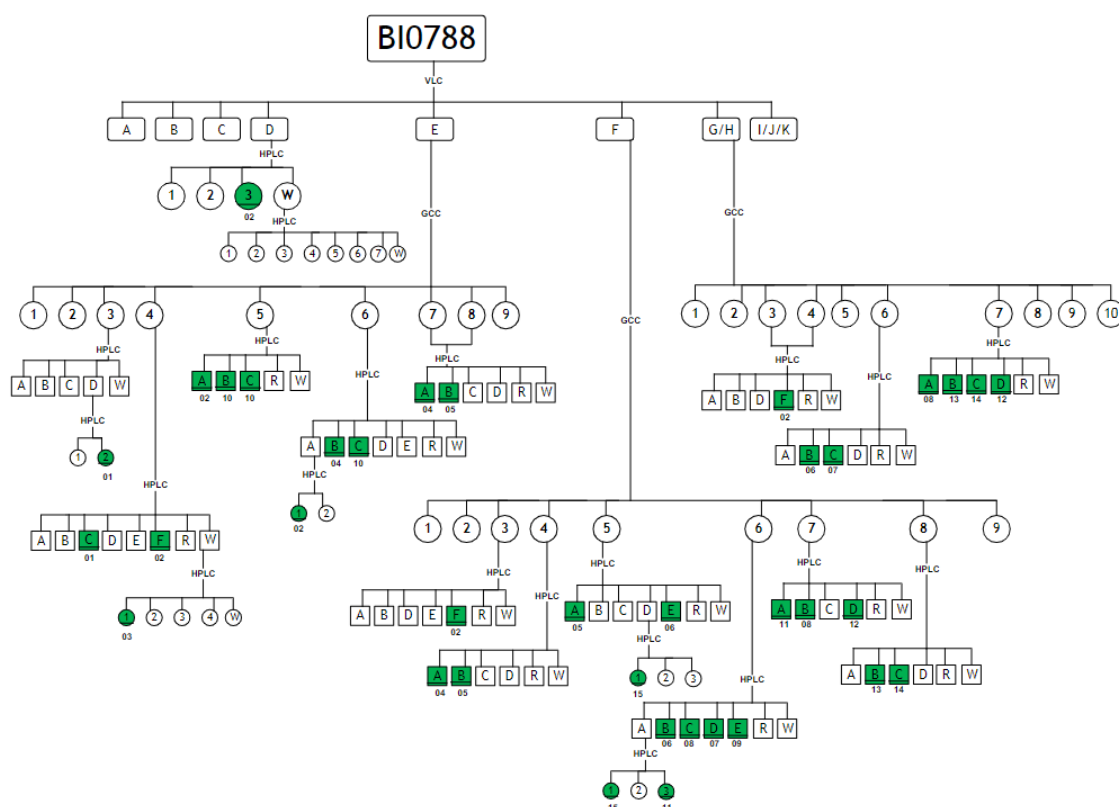


Figure 4. 5.a Isolation of sub-fractions and secondary metabolites from BIO788

Chromatography on BIO788 led to the formation of 11 different sub-fractions (A-K) collected by submitting them to vacuum liquid chromatography on silica gel with solvent mixtures of increasing polarity (from *c*Hex 100% to MeOH 100%) as eluant, to yield eleven fractions (A-K). Fractions G/H, F and E were purified by gravity column chromatography on silica gel (GCC), affording ten (G1-G10), nine (F1-F9) and nine (E1-E9) fractions, respectively.

Sequentially fractions E3-E8, F3-F8 and G3-G7 were purified by normal phase HPLC on a silica column using mixtures of *c*Hex/EtOAc and *c*Hex/Me₂CO in various ratios, to yield fifteen compounds in pure form (BIO788-01, BIO788-02, BIO788-03, BIO788-04, BIO788-05, BIO788-06, BIO788-07, BIO788-08, BIO788-09, BIO788-10, BIO788-11, BIO788-12, BIO788-13, BIO788-14, and BIO788-15). These pure compounds were not already available at the time when this screening had been performed and they do not constitute the entirety of molecules within BIO788). The additional fractions of this strain are currently under chemical investigation due to their interesting profile as observed by ¹H NMR spectroscopy.

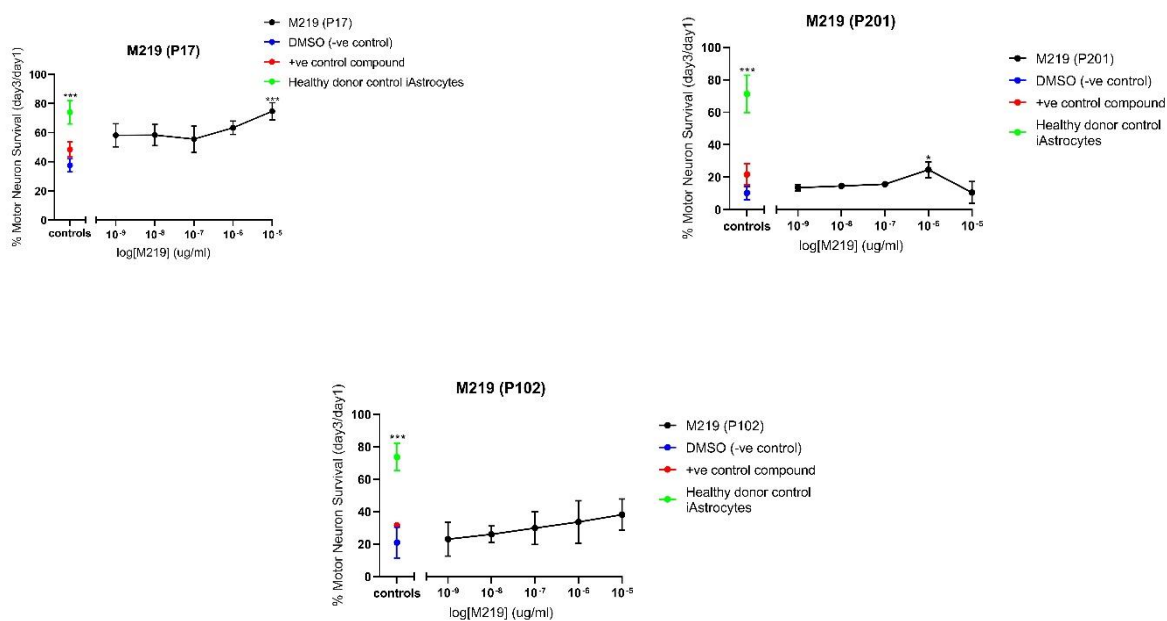


Figure 4. 5b M219 screen in sALS patient #17, C9orf72-ALS patient #201 and SOD1-ALS patient #102 iAstrocyte and Hb9-GFP+ mouse motor neuron co-culture

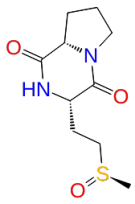
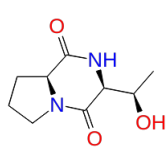
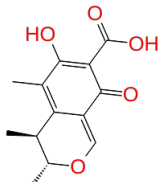
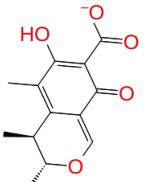
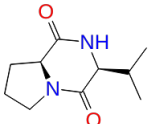
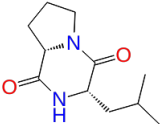
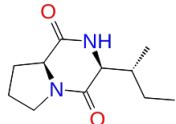
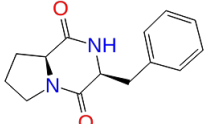
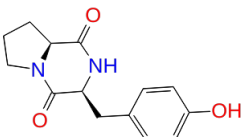
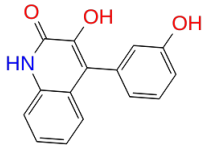
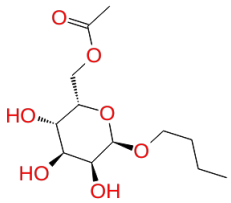
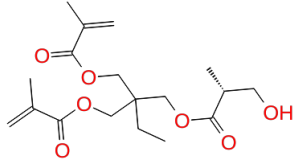
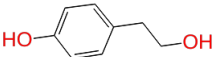
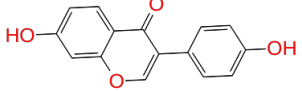
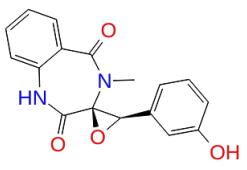
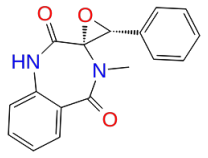
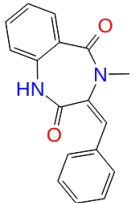
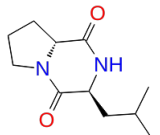
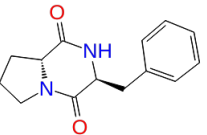
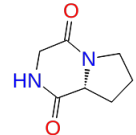
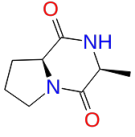

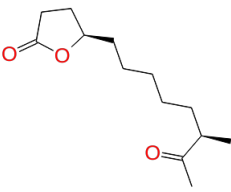
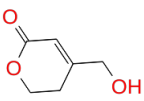
Hb9-GFP+ motor neurons co-cultured with C9orf72-ALS patient #201 and SOD1-ALS #102 iAstrocytes displayed increased survival upon treatment with the marine extract BI0788 top hit fraction M219 at 10mg/ml and 1mg/ml (black line) respectively over DMSO only treatment (blue circles). This extract yielded similar motor neuron rescue as our +ve control compound at a concentration of 10 μ g/mL (red circle) in patient #17, and in patient 201 at 1 μ g/mL, while in patient #102 shows just a positive trend compared to the negative DMSO control (blue dot). Healthy donor control iAstrocytes treated with DMSO only (green circles) acted as positive control for the assay. Motor neuron survival at day 3 was calculated as a percentage of the number of motor neurons alive at day 1. $N = 3$, data are mean \pm SD. One-way ANOVA with Dunnett's multiple comparisons ($*p < 0.001$, $*p < 0.05$).

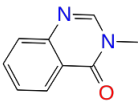
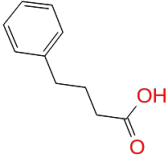
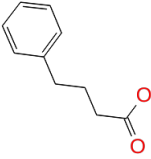
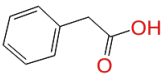
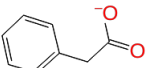
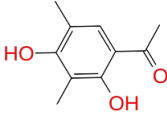
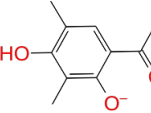
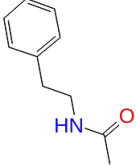
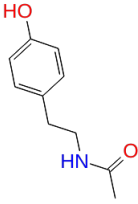
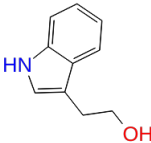
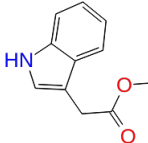
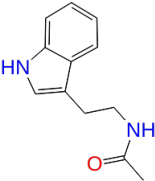
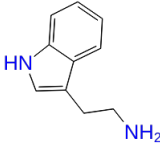
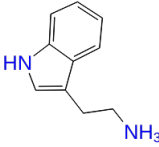
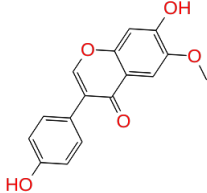
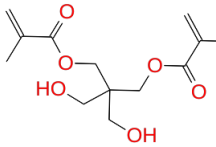
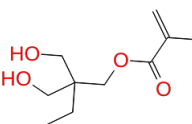
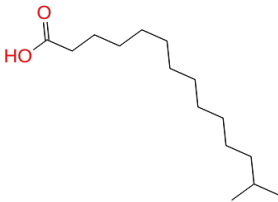
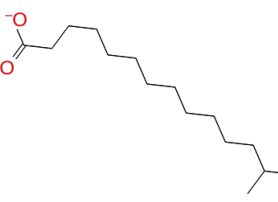
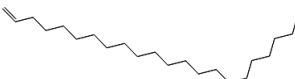
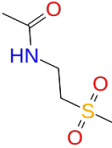
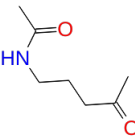
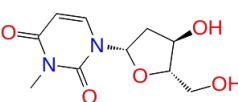
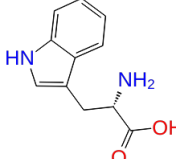
4.6 Loading, Preparing and Styling Ligands for Molecular Docking of Neurotrophin Receptors

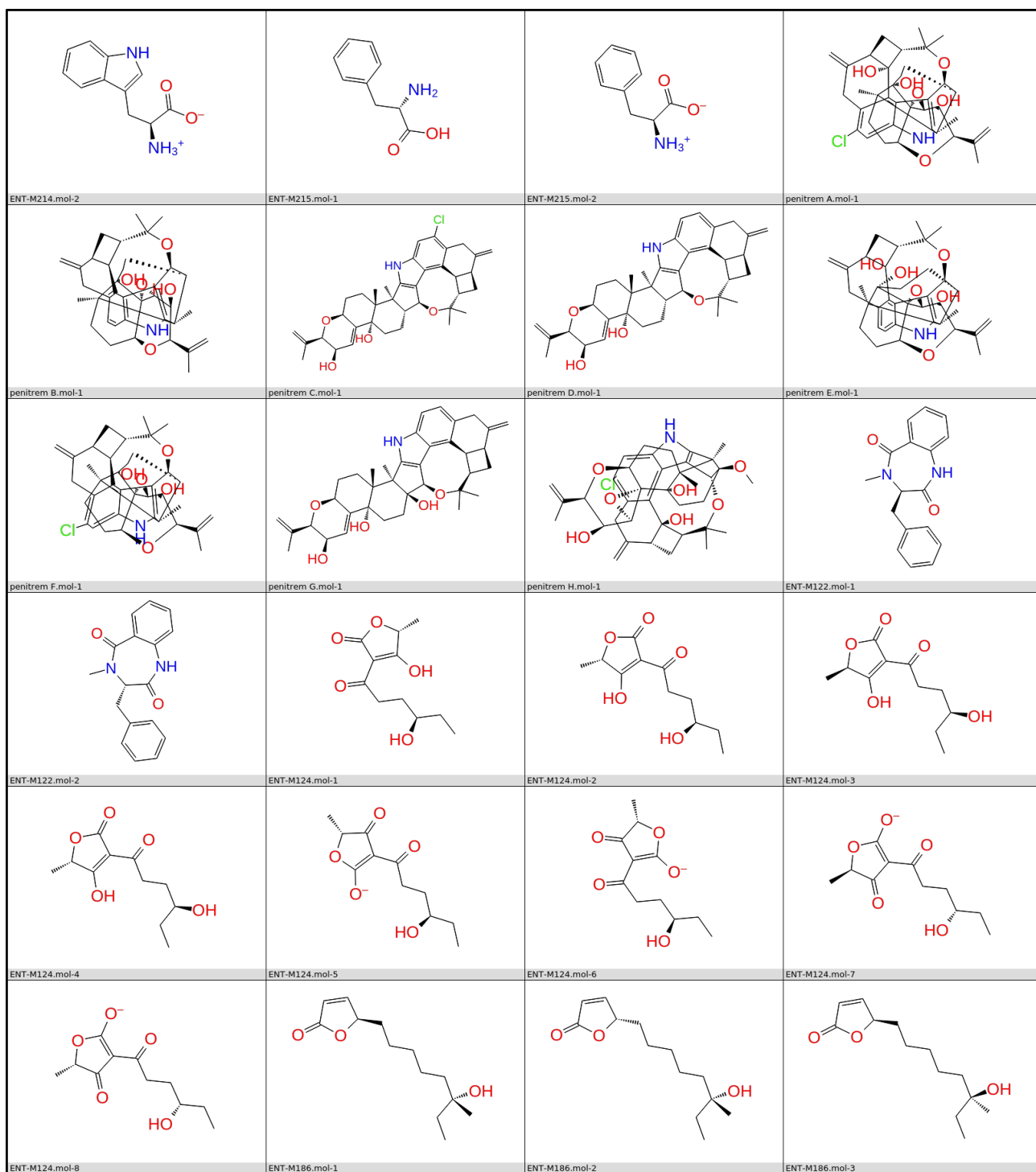
During the secondment at Heidelberg Institute for Theoretical Studies (HITS), under the supervision of Prof Rebecca Wade (Molecular and Cellular Modelling group (MCM) at the Heidelberg Institute for Theoretical Studies (HITS), Heidelberg, Germany), Mr Athanasios-Alexandros Tsengenes and Ms Christina Athanasiou, we performed molecular docking studies of a library of Natural Products (NPs) isolated and characterized from the top hit marine extracts: BI0987, BI0394 and BI0788. The aim was to select the most promising compounds as possible ligands for the neurotrophin receptors: TrkA, TrkB and p75. In

addition, we also designed possible chemical modifications of the NPs and their possible combinations with the modified neurosteroids synthesized at National Hellenic Research Foundation (NHRF) described in chapter 3.

The first step required for the docking analysis was to prepare a library of ligands based on the molecules isolated from: BI0394, BI0788, BI0987. Structure-based virtual screening is a valuable addition to other screening approaches in drug discovery. Prior to docking, molecular structures must be prepared by adding hydrogen atoms, optimizing hydrogen bonds, removing atomic clashes, and performing other operations that are not typically involved in the structure refinement process. Furthermore, ligands must be prepared to generate 3-dimensional geometries, assign appropriate bond orders, and create accessible tautomer and ionization states before virtual screening can take place. The Schrödinger-Maestro 2020r4 software has been used and a library of 100 compounds has been created (**Figure 4.6**). This library includes all the NPs isolated and identified so far from the aforementioned top hit extracts. For those compounds with undefined stereochemistry, all the possible stereoisomers were analysed (these compounds were distinguished with sequential increasing numbers at the end of the name: compound1.mol-1, compound1.mol-2, compound1.mol-3 ... etc).

			
dis-cyclo-(Pro-OMet).mol-1	cis-cyclo-(Pro-Thr).mol-1	citrinin.mol-1	citrinin.mol-2
			
ENT-M110.mol-1	ENT-M111.mol-1	ENT-M112.mol-1	ENT-M113.mol-1
			
ENT-M114.mol-1	ENT-M115.mol-1	ENT-M116.mol-1	ENT-M117.mol-1
			
ENT-M118.mol-1	ENT-M119.mol-1	ENT-M120.mol-1	ENT-M121.mol-1
			
ENT-M123.mol-1	ENT-M180.mol-1	ENT-M181.mol-1	ENT-M182.mol-1
			
ENT-M183.mol-1	ENT-M184.mol-1	ENT-M185.mol-1	ENT-M190.mol-1

			
ENT-M191.mol-1	ENT-M192.mol-1	ENT-M192.mol-2	ENT-M193.mol-1
			
ENT-M193.mol-2	ENT-M195.mol-1	ENT-M195.mol-2	ENT-M196.mol-1
			
ENT-M197.mol-1	ENT-M198.mol-1	ENT-M199.mol-1	ENT-M200.mol-1
			
ENT-M201.mol-1	ENT-M201.mol-2	ENT-M202.mol-1	ENT-M203.mol-1
			
ENT-M204.mol-1	ENT-M207.mol-1	ENT-M207.mol-2	ENT-M208.mol-1
			
ENT-M209.mol-1	ENT-M210.mol-1	ENT-M213.mol-1	ENT-M214.mol-1



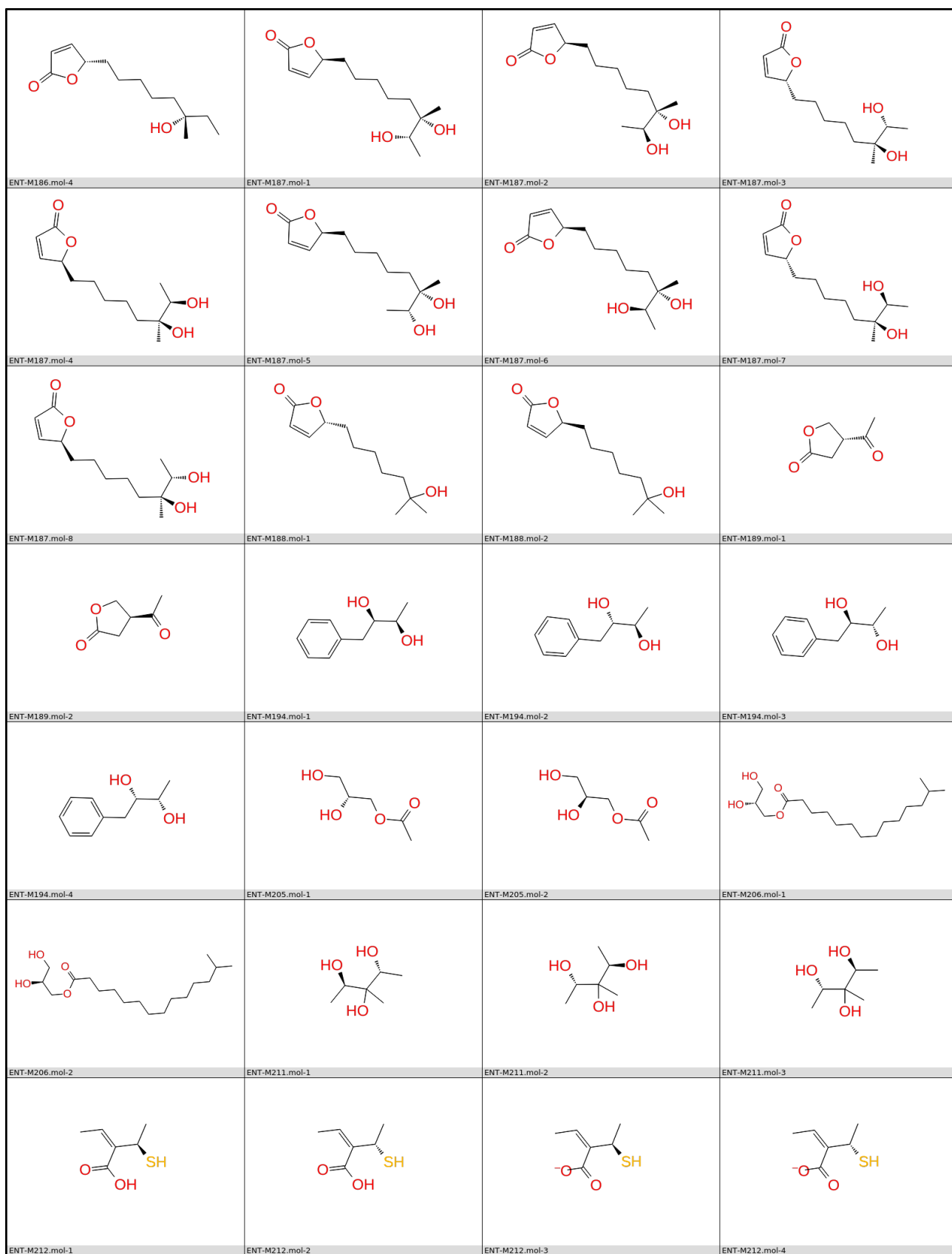


Figure 4. 6 Library of compounds from the top hit extracts after preparation for the docking process

4.7 Loading, Preparing and Styling Ligands for Molecular Docking of Neurotrophin Receptors

A significant proportion of drug candidates fail in clinical trials due to suboptimal ADME (absorption, distribution, metabolism, and excretion) properties, accounting for nearly 40% of failures. This phenomenon contributes considerably to the escalating cost of new drug development, particularly as these failures typically occur in the later stages of drug development. By detecting problematic drug candidates early, the amount of wasted time and resources can be reduced, and the overall therapeutic development process can be streamlined. The accurate prediction of ADME properties before conducting expensive experimental procedures can eliminate the need for testing compounds that are likely to fail. Furthermore, ADME prediction can be used to focus lead optimization efforts on enhancing the desired properties of a particular compound.

Therefore, after the ligand preparation, the library of prepared compounds was subjected to QuikProp and the QikProp properties were obtained for all compounds (**Table 4.3**).

QikProp is an ADME prediction program that is integrated in Schrödinger-Maestro 2020r4. It is fast, accurate, and easy-to-use and predicts physiologically relevant properties of organic molecules. The program can predict a variety of pharmaceutically important properties, including permeability, protein binding, and HERG K⁺-channel blockage. QikProp uses the full 3D molecular structure, making it equally effective for molecules with novel scaffolds and analogues of well-known drugs. It can screen compound libraries for hits, identifying molecules with properties outside the range of known drugs. During lead optimization, QikProp can analyse similarity within a class of compounds and identify compounds to avoid based on their predicted properties.

We used a colour scheme to allow better visualization of the parameters analysed through QikProp. Most of the NPs processed through this algorithm show good ADME properties within the ranges established by QikProp, that indicates a likelihood for being drug candidates in further testing.

The following table shows the values obtained by each molecule belonging to the library that has been subjected to QikProp. The range of acceptance is color-coded; all values displayed in green are considered positive, while the values displayed in yellow are considered acceptable but not ideal, and the values in red are out of range.

Ideally, a good drug candidate should satisfy all values tested with QuikProp, even though it

is not guaranteed that once taken forward for in vitro and in vivo experiments they will act as therapeutics. This is in fact just a preliminary screening helping to cut off unpromising candidates from large libraries of molecules.

Table 4. 3 Main QikProp properties analysed for the NPs

ENT-M compounds	#rtvFG	mol MW	donorHB	accptHB	QPlogPo/w	QPlogS	QPPCaco	QPPMDCK	QPlogBB	#metab	QPlogKhsa
cis-cyclo-(Pro-OMet).mol-1	0	244.308	1	9.5	-1.627	1.831	6.181	309.928	-0.779	3	-1.692
cis-cyclo-(Pro-Thr).mol-1	0	198.221	1	6.2	-1.156	0.457	150.128	216.556	-0.706	3	-1.335
citrinin.mol-1	0	250.251	0	4.45	1.587	-2.401	58.566	29.293	-0.955	3	-0.563
citrinin.mol-2	0	250.251	0	4.45	1.575	-2.444	55.8	27.8	-0.993	3	-0.563
ENT-M110.mol-1	0	196.249	1	5.5	-0.39	-0.208	343.583	561.176	-0.35	2	-1.099
ENT-M111.mol-1	0	210.275	1	5.5	-0.095	-0.493	327.897	512.077	-0.451	2	-1.013
ENT-M112.mol-1	0	210.275	1	5.5	-0.06	-0.488	343.686	564.205	-0.429	2	-1.013
ENT-M113.mol-1	0	244.293	1	5.5	0.549	-1.208	239.723	406.919	-0.623	3	-0.829
ENT-M114.mol-1	0	260.292	2	6.25	-0.125	-1.093	72.731	112.09	-1.216	4	-0.928
ENT-M115.mol-1	0	253.257	3	4	1.459	-3.011	212.26	92.635	-1.185	3	-0.182
ENT-M116.mol-1	2	278.302	3	10.5	-0.279	-1.876	223.255	97.832	-1.628	3	-0.956
ENT-M117.mol-1	3	356.415	0	6.7	3.231	-3.876	322.855	145.762	-1.739	4	-0.035
ENT-M118.mol-1	0	138.166	2	2.45	0.966	-0.97	868.487	424.777	-0.569	3	-0.576
ENT-M119.mol-1	0	254.242	2	4	1.782	-3.011	376.266	171.993	-0.93	2	-0.135
ENT-M120.mol-1	3	310.309	1.25	7.5	1.285	-3.27	321.134	144.923	-0.894	3	-0.285
ENT-M121.mol-1	3	294.309	0.25	6.75	1.813	-3.038	1070.545	532.537	-0.327	2	-0.329
ENT-M122.mol-1	0	280.326	1	5.5	2.455	-3.898	1198.193	601.49	-0.4	3	-0.015
ENT-M122.mol-2	0	280.326	1	5.5	2.461	-3.919	1198.897	601.872	-0.403	3	-0.014
ENT-M123.mol-1	1	278.31	1	5.5	2.465	-3.802	1240.547	624.503	-0.366	1	0.003
ENT-M124.mol-1	0	228.244	1	6.45	0.484	-1.513	320.373	144.552	-1.21	4	-0.721
ENT-M124.mol-2	0	228.244	1	6.45	0.488	-1.539	326.468	147.526	-1.211	4	-0.722
ENT-M124.mol-3	0	228.244	1	6.45	0.428	-1.594	249.924	110.523	-1.329	4	-0.715
ENT-M124.mol-4	0	228.244	1	6.45	0.429	-1.594	250.701	110.894	-1.327	4	-0.715
ENT-M124.mol-5	0	228.244	1	5.7	0.833	-1.749	389.561	178.571	-1.138	4	-0.595
ENT-M124.mol-6	0	228.244	1	5.7	0.834	-1.759	385.003	176.314	-1.145	4	-0.594
ENT-M124.mol-7	0	228.244	1	5.7	0.814	-1.918	304.755	136.95	-1.272	4	-0.577
ENT-M124.mol-8	0	228.244	1	5.7	0.813	-1.917	304.858	137	-1.272	4	-0.577
ENT-M180.mol-1	0	210.275	1	5.5	-0.147	-0.051	250.059	479.313	-0.469	2	-1.025
ENT-M181.mol-1	0	244.293	1	5.5	0.44	-0.425	268.271	513.404	-0.44	3	-0.88
ENT-M182.mol-1	0	154.168	1	5.5	-1.576	1.493	142.647	277.716	-0.423	2	-1.411
ENT-M183.mol-1	0	168.195	1	5.5	-1.139	0.73	237.491	411.524	-0.341	2	-1.301
ENT-M184.mol-1	1	224.299	0	5	1.835	-2.141	932.473	458.702	-0.836	2	-0.507
ENT-M185.mol-1	2	226.315	0	5	1.985	-2.562	1035.609	513.778	-0.829	2	-0.418
ENT-M186.mol-1	0	226.315	1	3.75	2.625	-3.173	1089.351	542.655	-0.852	2	-0.042
ENT-M186.mol-2	0	226.315	1	3.75	2.624	-3.162	1097.324	546.95	-0.847	2	-0.043
ENT-M186.mol-3	0	226.315	1	3.75	2.561	-3.073	959.64	473.164	-0.89	2	-0.051
ENT-M186.mol-4	0	226.315	1	3.75	2.596	-3.015	1211.07	608.48	-0.789	2	-0.065
ENT-M187.mol-1	0	242.314	2	5.45	1.638	-2.569	464.672	216.06	-1.275	3	-0.365
ENT-M187.mol-2	0	242.314	2	5.45	1.688	-2.682	471.171	219.328	-1.29	3	-0.352
ENT-M187.mol-3	0	242.314	2	5.45	1.691	-2.686	477.665	222.597	-1.285	3	-0.353
ENT-M187.mol-4	0	242.314	2	5.45	1.628	-2.607	411.889	189.659	-1.331	3	-0.357
ENT-M187.mol-5	0	242.314	2	5.45	1.641	-2.569	465.134	216.293	-1.274	3	-0.364
ENT-M187.mol-6	0	242.314	2	5.45	1.691	-2.677	480.058	223.803	-1.281	3	-0.354
ENT-M187.mol-7	0	242.314	2	5.45	1.689	-2.696	467.147	217.304	-1.296	3	-0.351
ENT-M187.mol-8	0	242.314	2	5.45	1.635	-2.609	423.463	195.426	-1.32	3	-0.358
ENT-M188.mol-1	0	212.288	1	3.75	2.206	-2.73	951.22	468.678	-0.807	2	-0.151
ENT-M188.mol-2	0	212.288	1	3.75	2.211	-2.731	948.312	467.129	-0.807	2	-0.148
ENT-M189.mol-1	2	128.127	0	5	-0.814	0.743	874.769	428.098	-0.305	2	-1.385
ENT-M189.mol-2	2	128.127	0	5	-0.814	0.742	874.79	428.11	-0.305	2	-1.385
ENT-M190.mol-1	1	128.127	1	4.7	-0.354	-0.349	712.84	343.125	-0.444	2	-0.884
ENT-M191.mol-1	0	160.175	0	4	1.069	-0.927	2194.51	1156.899	0.016	1	-0.784
ENT-M192.mol-1	0	164.204	1	2	2.112	-1.893	230.798	128.979	-0.606	2	-0.348
ENT-M192.mol-2	0	164.204	1	2	2.108	-1.875	239.169	134.042	-0.589	2	-0.355
ENT-M193.mol-1	0	136.15	1	2	2.159	-1.752	255.332	143.86	-0.38	1	-0.574
ENT-M193.mol-2	0	136.15	1	2	2.159	-1.74	275.433	156.139	-0.347	1	-0.582
ENT-M194.mol-1	0	166.219	2	3.4	1.55	-1.172	2083.986	1094.051	-0.332	3	-0.467
ENT-M194.mol-2	0	166.219	2	3.4	1.534	-1.169	2005.106	1049.361	-0.348	3	-0.469
ENT-M194.mol-3	0	166.219	2	3.4	1.534	-1.169	2005.159	1049.39	-0.348	3	-0.469
ENT-M194.mol-4	0	166.219	2	3.4	1.55	-1.172	2083.997	1094.057	-0.332	3	-0.467

ENT-M compounds	#rtvFG	mol MW	donorHB	accptHB	QLogPo/w	QLogS	QPPcaco	QPPMDCK	QLogBB	#metab	QLogKhsa
ENT-M195.mol-1	0	180.203	1	2.5	1.564	-2.34	795.272	386.206	-0.575	4	-0.204
ENT-M195.mol-2	0	180.203	1	2.5	1.562	-2.339	803.56	390.559	-0.572	4	-0.207
ENT-M196.mol-1	0	163.219	1	2.5	2.048	-1.96	1455.872	1413.476	-0.145	1	-0.496
ENT-M197.mol-1	0	179.218	2	3.25	0.829	-1.416	446.731	392.182	-0.69	2	-0.656
ENT-M198.mol-1	0	161.203	2	1.7	1.728	-1.832	1546.477	792.516	-0.3	2	-0.313
ENT-M199.mol-1	1	189.213	1	2	2.37	-2.762	1854.152	964.236	-0.184	1	-0.006
ENT-M200.mol-1	0	202.255	2	2.5	1.705	-2.091	930.512	802.576	-0.36	1	-0.374
ENT-M201.mol-1	0	160.218	3	1	1.159	-0.465	329.717	164.967	0.038	3	-0.369
ENT-M201.mol-2	0	160.218	3	1	1.17	-0.488	325.456	162.664	0.033	3	-0.363
ENT-M202.mol-1	0	284.268	2	4.75	1.939	-3.291	407.24	187.346	-0.996	3	-0.101
ENT-M203.mol-1	2	272.297	2	7.4	1.096	-2.453	219.188	95.907	-1.695	4	-0.545
ENT-M204.mol-1	1	202.25	2	5.4	0.967	-1.637	651.088	311.112	-0.988	3	-0.595
ENT-M205.mol-1	1	134.132	2	5.4	-0.626	-0.741	281.61	125.743	-1.134	2	-0.935
ENT-M205.mol-2	1	134.132	2	5.4	-0.626	-0.741	281.667	125.771	-1.134	2	-0.935
ENT-M206.mol-1	1	316.48	2	5.4	4.006	-5.31	409.082	188.262	-2.169	3	0.301
ENT-M206.mol-2	1	316.48	2	5.4	4.001	-5.283	410.32	188.878	-2.162	3	0.299
ENT-M207.mol-1	0	242.401	1	2	4.793	-5.023	227.544	127.014	-1.31	1	0.425
ENT-M207.mol-2	0	242.401	1	2	4.826	-5.085	239.015	133.949	-1.294	1	0.433
ENT-M208.mol-1	0	308.59	0	0	11.496	-12.673	9906.038	5899.293	1.768	1	1.955
ENT-M209.mol-1	0	165.207	0	5.5	-1.054	0.843	246.116	211.023	-0.825	0	-1.553
ENT-M210.mol-1	1	143.185	1	4.5	-0.112	-0.367	436.584	391.545	-0.67	1	-0.99
ENT-M211.mol-1	0	134.175	3	4.15	0.074	-0.567	1028.927	510.195	-0.524	3	-0.792
ENT-M211.mol-2	0	134.175	3	4.15	0.074	-0.538	1034.996	513.449	-0.513	3	-0.789
ENT-M211.mol-3	0	134.175	3	4.15	0.107	-0.524	1152.152	576.547	-0.473	3	-0.788
ENT-M212.mol-1	2	146.204	1	1.5	2.14	-1.848	376.814	499.09	-0.142	3	-0.509
ENT-M212.mol-2	2	146.204	1	1.5	2.14	-1.848	376.816	499.033	-0.142	3	-0.509
ENT-M212.mol-3	2	146.204	1	1.5	2.138	-1.857	371.909	480.299	-0.152	3	-0.504
ENT-M212.mol-4	2	146.204	1	1.5	2.138	-1.857	371.92	480.329	-0.152	3	-0.504
ENT-M213.mol-1	0	242.231	2	8.6	-0.474	-1.523	244.404	107.887	-0.995	3	-0.808
ENT-M214.mol-1	0	204.228	4	3	-1.06	-1.18	13.626	6.701	-0.747	4	-0.624
ENT-M214.mol-2	0	204.228	4	3	-1.06	-1.18	16.216	8.088	-0.663	4	-0.64
ENT-M215.mol-1	0	165.191	3	3	-1.154	-0.866	24.682	12.736	-0.489	4	-0.719
ENT-M215.mol-2	0	165.191	3	3	-1.151	-0.774	28.166	14.689	-0.419	4	-0.728
penitrem A.mol-1	1	634.211	4	7.65	5.982	-7.656	1385.406	1521.615	-0.386	10	1.389
penitrem B.mol-1	1	583.766	3	6.9	6.128	-7.534	2397.666	1273.083	-0.226	11	1.507
penitrem C.mol-1	0	602.212	3	4.9	7.574	-9.468	2495.429	2874.062	-0.114	12	2.025
penitrem D.mol-1	0	567.767	3	4.9	7.133	-8.843	2489.892	1326.094	-0.254	12	1.922
penitrem E.mol-1	1	599.766	4	7.65	5.558	-7.074	1376.388	698.735	-0.525	10	1.298
penitrem F.mol-1	1	618.211	3	6.9	6.564	-8.146	2402.677	2758.352	-0.087	11	1.605
penitrem G.mol-1	0	583.766	4	5.65	6.61	-8.011	2323.29	1230.452	-0.325	13	1.657
penitrem H.mol-1	1	664.237	4	8.4	6.159	-7.623	1681.258	1874.861	-0.363	10	1.385

Different colours meaning, accordingly the QikProp range values: green = in the range, yellow = acceptable values, red = out of the range. The ranges are dictated by the Lipinski rules of five and determined by QikProp. The parameters considered by the algorithm are the following:

- #rtvFG: Number of reactive functional groups can lead to false positives through in vitro assays (values between 0-2 are considered acceptable).
- mol MW: Molecular Weight (130.0 – 725.0).
- donorHB: Estimated number of hydrogen bonds that would be donated

by the solute to water molecules in an aqueous solution (0.0 – 6.0).

- *accptHB*: Estimated number of hydrogen bonds that would be accepted

by the solute from water molecules in an aqueous solution (2.0 – 20.0).

- *QPlogPo/w*: Predicted octanol/water partition coefficient (-2.0 – 6.5).

- *QPlogS*: Predicted aqueous solubility (-6.5 – 0.5).

- *QPPCaco*: Predicted apparent Caco-2 cell permeability in nm/sec (<25 poor, >500 great).

- *QPPMDCK*: Predicted apparent MDCK cell permeability in nm/sec (<25 poor, >500 great).

- *QPlogBB*: Predicted brain/blood partition coefficient (-3.0 – 1.2).

- *#metab*: Number of likely metabolic reactions (1 – 8).

- *QPlogKhsa*: Prediction of binding to human serum albumin (-1.5 – 1.5).

4.8 Protein Preparation and Site Map analysis

After the determination of the QikProp values, protein preparation was performed on the 3D structures of the neurotrophic receptors available on the Protein Data Bank (PDB).

Preparation has been performed in the same way as was undertaken for the ligand library.

Protein preparation was possible for all the neurotrophin receptors except TrkC. TrkC still lacks a reliable crystal structure with a resolution high enough to guarantee reliable results from docking analysis. A good crystal structure model for docking must have a resolution close to 2Å. The goal of obtaining a better crystal structure of Trice is part of

EuroNeurotrophin consortium and will allow the same experiments to be performed as for the other neurotrophin receptors, with the new TrkC structure, to gather more information about our ligand library. The receptor structure models that have been used include the following:

- TrkA receptor in complex with Nerve Growth Factor (NGF) (PDB: 1WWW). This model is the crystal structure of NGF in complex with the ligand-binding domain of the TrkA receptor with a resolution of 2.2Å and was expressed in *E. coli*.
- TrkB receptor bound to NT-4 neurotrophin (PDB: 1HCF). This model is the crystal structure of Trkb-D5 in complex with Neurotrophin-4/5 with a resolution of 2.7Å and

was expressed in *E. coli* BL21.

- p75^{NTR} receptor in complex with NGF (PDB: 1SG1). This model is the crystal structure of the Receptor-Ligand Complex between NGF and p75 with a resolution of 2.4Å and was expressed in *E. coli*.

The next step was finding the binding sites for the protein-ligands. Site Map calculation determined all the binding sites and their relative volumes (**Figure 4.7-10**). Five binding sites were found for TrkA: site 3 is the binding site TrkA-NGF, sites 4 and 5 are symmetrical (site 1b), site 2 and 1 are symmetrical as well (site 1a). Site 1b and site 1a were identified as the binding sites for the ligands, in agreement with the published literature (I. Pediaditakis et al, 2016).

Five binding sites were found for TrkB as well: site 3 is the binding site TrkA-NT-4 neurotrophin, sites 5 and 4 are symmetrical (site 1b), sites 2 and 1 are symmetrical as well (site 1a). Site 1b and site 1a were identified as the binding sites for the ligands, in agreement with the data available in literature (I. Pediaditakis et al, 2016). For TrkA and TrkB all the sites were explored, except the binding site receptor-neurotrophin.

Five binding sites were also found on p75^{NTR} but only the sites 3, 4 and 1 were analyzed, supported by published literature data (I. Pediaditakis et al, 2016).

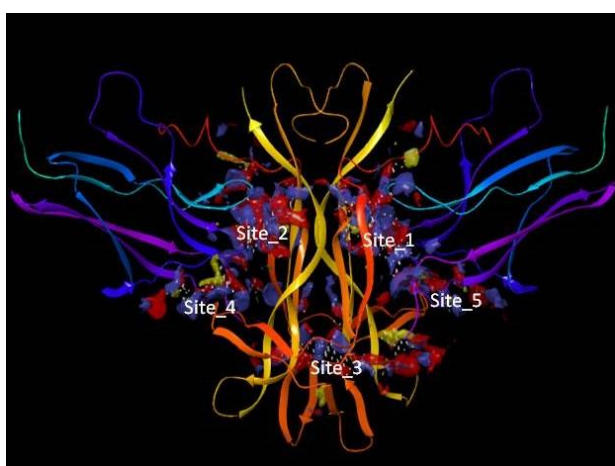


Figure 4. 7 Binding sites of the external domain of TrkA.

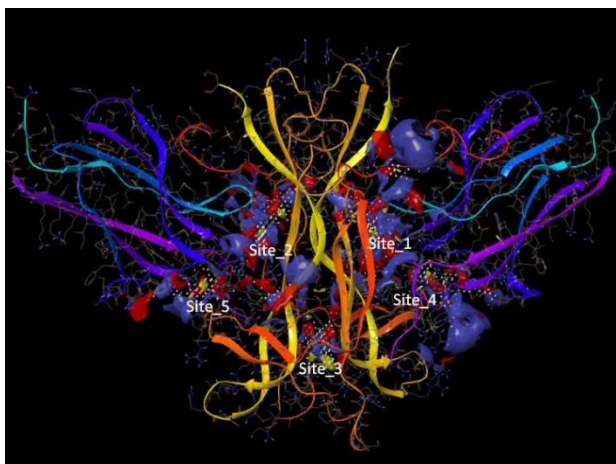


Figure 4. 8 Binding sites of the external domain of TrkB

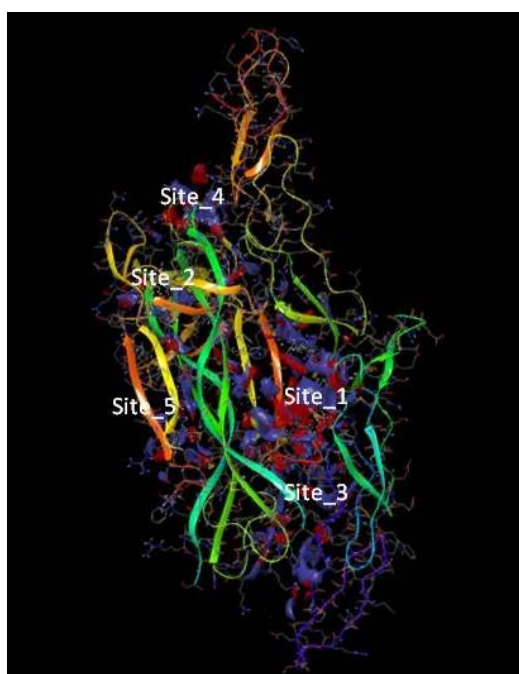


Figure 4. 9 Binding sites of the external domain of p75

	site		volume Å ³	
TrkA	1a	chain W	sitemap_1WWW_2_site_1	400.624
		chain V	sitemap_1WWW_2_site_2	389.648
	1b	chain Y	sitemap_1WWW_2_site_4	170.814
		chain X	sitemap_1WWW_2_site_5	161.896
TrkB	1a	chain A	sitemap_1HCF_2_site_1	468.195
		chain B	sitemap_1HCF_2_site_2	431.494
	1b	chain Y	sitemap_1HCF_2_site_4	222.607
		chain X	sitemap_1HCF_2_site_5	166.698
p75			sitemap_1SG1_2_site_1	785.813
		chain B	sitemap_1SG1_2_site_3	352.947
		chain A	sitemap_1SG1_2_site_4	175.959

Figure 4. 10 A. TrkA; B. TrkB and C. p75^{NTR} with the identified binding sites and their volumes

4.9 Molecular Docking

After the identification of the binding sites, molecular docking was performed using the Maestro feature, Glide. The first step was to generate a grid box highlighting the part of the protein where the ligand will bind. Afterwards, Glide uses this grid box and the chosen ligands as input for the calculation. This step is used for both SP (Standard Precision) and XP (Extra Precision) docking algorithms. XP docking does more extensive sampling than SP docking, and it also employs a more sophisticated scoring function with greater requirements for ligand-receptor shape complementarity. This removes false positives that SP lets through. For this reason, we decided to perform the molecular docking with the XP algorithm obtaining predictions of the binding pose of the ligands to the proteins, ligand-protein interactions, and relative scores.

Sites 1a and 1b were evaluated for both the symmetric sites of TrkA and a cut-off of -5.00 kcal/mol was chosen to select the best compounds (**Table 4.4**). Figure 8 also displays poses of the compounds with the highest XP docking scores in TrkA.

Sites 1a and 1b were evaluated for both the symmetric sites for TrkB as well, using the same criteria used for TrkA. The compounds with the best docking scores and their relative poses are shown in Table 4 and in Figure 9.

For both TrkA and TrkB, molecules seem to better fit into site 1b. This can be explained by the size of the site itself. Site 1b is larger than site 1a in both cases, which allows more flexible accommodation within the receptor. This also explains why more molecules had positive result for the XP algorithm in TrkB.

All compounds displayed in table below scored -5.00 or lower in at least one of the TrkA or TrkB symmetric sites, indicating that all of them could possibly bind at least one of the receptors or both. Ideally, compounds with lower scores in at least one of the sites should be more likely to bind the receptors in vivo. For TrkA, ENT-M116.mol-1 and ENT-M194.mol-1 scored below -8.00 in TrkA site 1a chain V and scored below -5.00 in 3 out of 4 chains, therefore they emerged as top hits in the in silico molecular docking. Despite these results, both ENT-M116.mol-1 and ENT-M194.mol-1 scored lower than -5.00 in most of the TrkB tested chains, indicating that they could not be specific for TrkA. Ideally, we are looking for molecules able to precisely target one receptor to avoid non-specific binding and effects.

In the case of TrkB, ENT-M213.mol-1, ENT-M202.mol-1, ENT-M187.mol-4, ENT-M187.mol-5,

ENT-M187.mol-7, ENT-M187.mol-8 and ENT-M115.mol-1 scored below -7.00 in at least one of the TrkB chains, but they also scored values below -5.00 in some of the TrkA chains.

Therefore, the problem of potential non-specific bindings applies also for the TrkB top hits.

Table 4. 4 Compounds with highest XP docking in TrkA and TrkB

TrkA	site 1a		site 1b		TrkB	site 1a		site 1b	
	1WWW	chain W	chain V	chain Y		chain X	1HCF	chain A	chain B
ENT-M115.mol-1	-6.461	-7.542	-4.714	-6.708	ENT-M213.mol-1	-7.254	-6.396	-5.939	-6.899
ENT-M116.mol-1	-6.396	-8.347	-5.414	-4.849	ENT-M202.mol-1	-7.401	-7.364	-5.916	-5.667
ENT-M194.mol-1	-6.276	-8.04	-4.792	-5.074	ENT-M187.mol-4	-7.484	-5.991	-6.516	-5.34
ENT-M194.mol-3	-5.546	-8.11	-4.652	-4.361	ENT-M187.mol-8	-7.186	-5.676	-6.51	-5.886
ENT-M211.mol-3	-5.324	-6.215	-5.266	-5.061	ENT-M115.mol-1	-7.11	-6.937	-5.109	-6.029
ENT-M213.mol-1	-6.862	-5.53	-4.455	-5.018	ENT-M187.mol-5	-7.542	-4.912	-6.314	-5.622
ENT-M194.mol-4	-6.803	-5.916	-4.562	-4.502	ENT-M187.mol-6	-6.773	-5.642	-6.422	-4.789
ENT-M117.mol-1	-5.44	-5.49	-5.73	-4.856	ENT-M187.mol-7	-7.234	-5.989	-5.161	-5.111
ENT-M205.mol-2	-5.498	-6.175	-5.425	-4.376	ENT-M181.mol-1	-5.482	-6.687	-6.791	-3.984
ENT-M194.mol-2	-5.872	-6.306	-3.955	-4.517	ENT-M124.mol-5	-6.05	-5.515	-5.052	-6.204
ENT-M187.mol-8	-6.026	-5.294	-4.934	-4.363	ENT-M124.mol-7	-6.12	-6.112	-5.049	-5.333
ENT-M187.mol-4	-5.865	-6.464	-4.403	-3.517	ENT-M211.mol-3	-5.766	-5.781	-5.805	-5.173
ENT-M195.mol-1	-5.532	-5.683	-4.25	-4.514	ENT-M187.mol-2	-6.327	-4.906	-6.874	-4.407
ENT-M201.mol-2	-5.586	-5.534	-4.121	-4.729	ENT-M194.mol-4	-5.527	-5.652	-5.351	-5.812
ENT-M205.mol-1	-4.897	-6.95	-3.845	-4.141	ENT-M187.mol-1	-6.536	-5.147	-6.071	-4.326
ENT-M211.mol-2	-4.607	-4.807	-4.902	-5.51	ENT-M194.mol-1	-5.298	-5.384	-5.273	-6.103
ENT-M124.mol-6	-6.118	-5.544	-4.344	-3.819	ENT-M211.mol-2	-5.274	-5.778	-5.291	-5.599
ENT-M124.mol-8	-6.253	-6.096	-4.441	-3.034	ENT-M124.mol-8	-5.538	-6.04	-5.367	-4.811
ENT-M187.mol-2	-3.965	-6.307	-3.988	-5.55	ENT-M206.mol-2	-4.694	-4.168	-6.686	-6.105
ENT-M211.mol-1	-5.704	-4.904	-4.513	-4.659	ENT-M214.mol-2	-5.445	-4.872	-5.214	-6.064
ENT-M187.mol-3	-5.697	-5.481	-4.289	-4.099	ENT-M211.mol-1	-5.041	-5.29	-5.624	-5.587
ENT-M202.mol-1	-4.553	-4.501	-5.46	-4.919	ENT-M116.mol-1	-5.504	-3.817	-6.593	-5.614
ENT-M190.mol-1	-4.664	-4.864	-5.789	-4.032	ENT-M180.mol-1	-6.259	-6.243	-4.142	-4.826
ENT-M187.mol-5	-6.262	-4.582	-4.745	-3.656	ENT-M194.mol-2	-5.287	-5.274	-5.225	-5.67
ENT-M187.mol-6	-4.282	-6.015	-4.429	-4.382	citrinin.mol-2	-3.64	-5.593	-5.146	-6.9
ENT-M187.mol-1	-4.295	-6.249	-3.589	-4.749	ENT-M117.mol-1	-5.388	-5.713	-5.574	-4.587
ENT-M187.mol-7	-5.747	-5.117	-3.553	-4.453	ENT-M187.mol-3	-6.965	-4.121	-4.898	-4.922
cis-cyclo-(Pro-Thr).mol-1	-4.97	-5.379	-4.534	-3.961	ENT-M194.mol-3	-5.147	-5.069	-4.961	-5.564
ENT-M203.mol-1	-5.394	-5.885	-3.709	-3.638	ENT-M184.mol-1	-6.282	-5.195	-5.098	-4.105
ENT-M200.mol-1	-5.062	-4.813	-3.923	-4.66	cis-cyclo-(Pro-Thr).mol-1	-6.61	-5.157	-4.725	-4.112
ENT-M198.mol-1	-5.116	-5.051	-4.322	-3.86	ENT-M186.mol-1	-6.453	-4.897	-5.227	-3.847
ENT-M186.mol-1	-4.925	-5.069	-4.002	-3.701	ENT-M205.mol-2	-4.968	-5.231	-5.008	-5.196
ENT-M124.mol-5	-4.296	-5.157	-4.172	-3.738	ENT-M124.mol-6	-5.874	-4.41	-4.538	-5.537
ENT-M188.mol-1	-4.367	-4.262	-5.286	-3.417	ENT-M206.mol-1	-4.938	-4.677	-4.854	-5.861
ENT-M214.mol-2	-4.813	-5.388	-3.834	-2.986	ENT-M205.mol-1	-4.67	-5.161	-5.157	-5.291
ENT-M119.mol-1	-3.638	-3.92	-5.038	-4.315	cis-cyclo-(Pro-OMet).mol-1	-6.952	-5.125	-3.86	-4.095
ENT-M206.mol-2	-3.728	0.36	-5.072	-5.221	ENT-M186.mol-2	-5.054	-5.473	-4.481	-4.872
ENT-M206.mol-1	-0.022	-0.735	-5.441	-4.791	ENT-M120.mol-1	-6.953	-3.492	-4.656	-4.653
ENT-M207.mol-2	2.599	2.699	-2.494	-5.753	ENT-M203.mol-1	-5.459	-5.234	-4.356	-4.434
					ENT-M188.mol-2	-5.567	-5.203	-4.076	-4.621
					ENT-M195.mol-1	-4.801	-4.62	-4.786	-5.169
					ENT-M185.mol-1	-5.649	-5.675	-4.058	-3.943
					ENT-M186.mol-3	-5.425	-5.834	-4.599	-3.382
					ENT-M200.mol-1	-5.308	-4.919	-4.544	-4.344
					ENT-M119.mol-1	-4.849	-5.174	-3.595	-5.462
					ENT-M190.mol-1	-5.421	-4.617	-3.992	-4.959
					ENT-M198.mol-1	-5.88	-4.205	-4.228	-4.669
					ENT-M114.mol-1	-5.524	-3.341	-5.136	-4.9
					ENT-M186.mol-4	-4.925	-5.047	-4.202	-4.577
					ENT-M112.mol-1	-6.236	-4.721	-3.514	-3.963
					ENT-M111.mol-1	-6.063	-4.141	-3.804	-4.414
					ENT-M188.mol-1	-4.643	-5.491	-3.793	-4.128
					ENT-M113.mol-1	-5.19	-4.302	-3.98	-4.087
					ENT-M182.mol-1	-5.462	-4.239	-3.34	-3.649

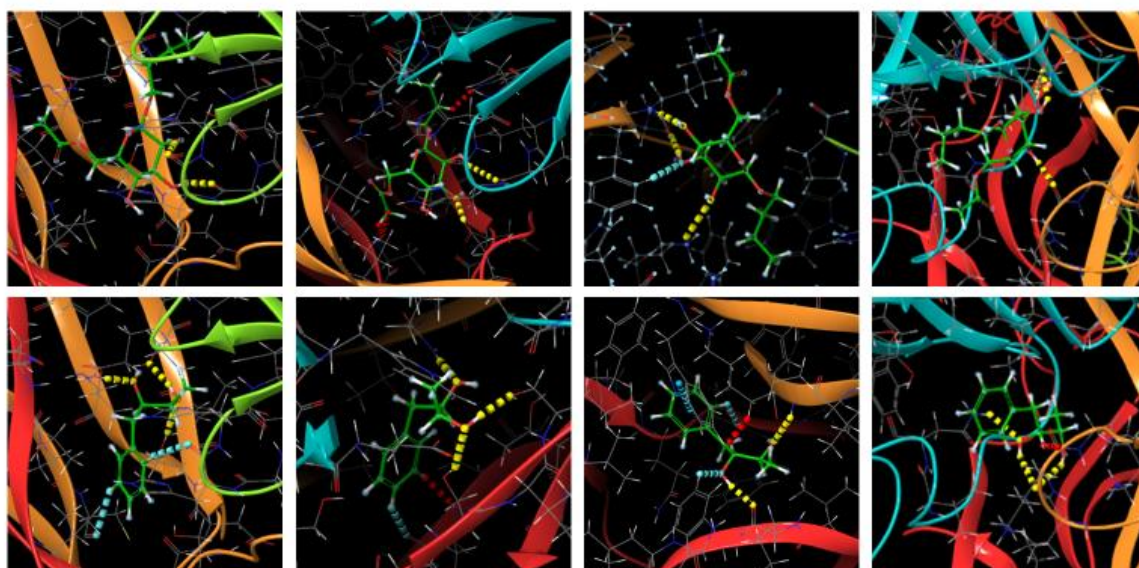


Figure 4. 11 Poses of compounds with best XP docking scores in TrkA sites 1a and 1b

The first 4 images on top show the binding site 1a, while the 4 images at the bottom show the binding site 1b.

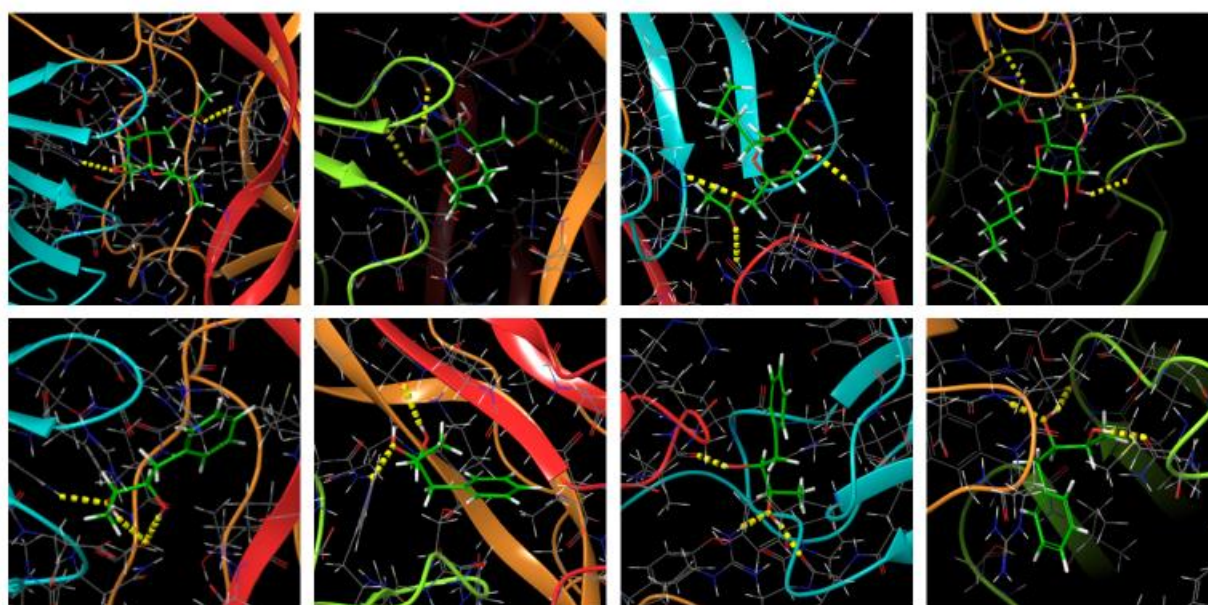


Figure 4. 12 Poses of compounds with best XP docking scores in TrkB sites 1a and 1b

The first 4 images on top show the binding site 1a, while the 4 images at the bottom show the binding site 1b.

An overview of the structures of the compounds with the best docking scores is shown in **Figure 4.13**, their different colours are related to the possible selectivity (Δ XPscores ≥ 1) for TrkA (red), TrkB (green) or their possibility to bind both receptors with comparable docking score values (blue).

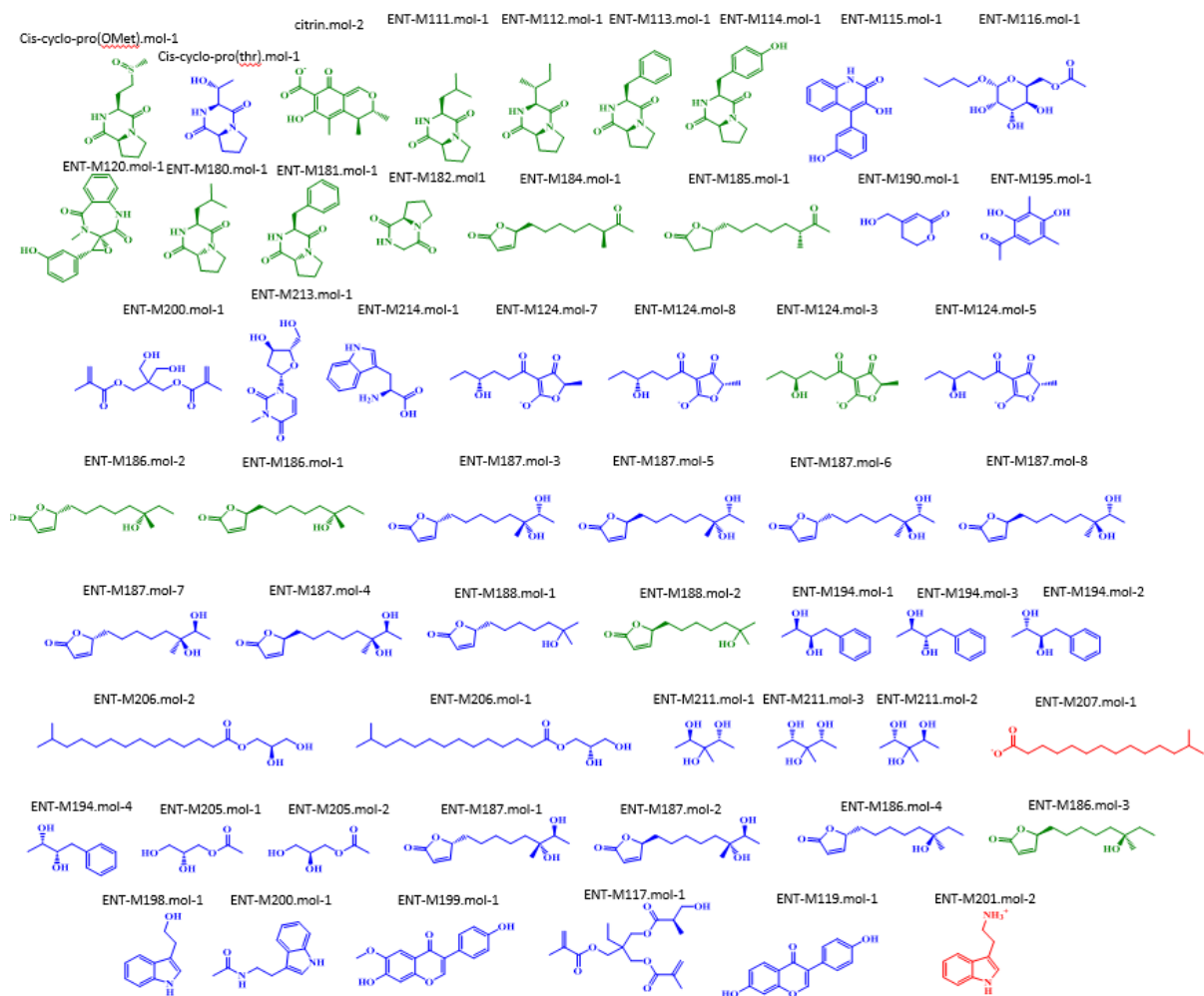


Figure 4. 13 Structures of the best positive docking score hits for TrkA and TrkB receptors

Sites 3, 4 and 1 were explored in p75^{NTR} and XP docking was performed for all the three sites, applying the same cut-off used for TrkA and B receptors. According to the studies reported by Peditakis et al (2016), site 3 and site 4 have been identified as the most prone to form stable interactions with ligands. The best p75 ligands are reported below in **Table 4.5**. As explained for the previous receptors XP docking, Site 1 being larger than the other 2 sites, can accommodate a broader range of molecules. In this case, only ENT-M202.mol-1 and ENT-M213.mol-1 scored lower than -5.00 in all 3 docked sites of p75. Considering that the average scores of all the positive hits are not much lower than -5.00, those two compounds can be considered the best candidates for further analysis, due to their likelihood for binding p75 site1, site4 and site5.

Table 4. 5 XP docking scores and structures of the best positive hits for the p75^{NTR} receptor

15G1 - p75	site1	site4	site5
ENT-M114.mol-1	-5.526	-3.01	-3.014
ENT-M115.mol-1	-6.168	-3.865	-5.024
ENT-M116.mol-1	-6.768	-4.951	-5.561
ENT-M119.mol-1	-6.237	-4.664	-4.08
ENT-M120.mol-1	-5.64	-4.354	-4.445
ENT-M124.mol-5	-5.703	-3.9	-4.212
ENT-M124.mol-7	-5.539	-3.728	-4.233
ENT-M186.mol-4	-5.132	-3.705	-2.824
ENT-M187.mol-1	-5.009	-4.202	-3.145
ENT-M187.mol-3	-5.274	-3.932	-3.245
ENT-M187.mol-4	-5.937	-4.175	-3.759
ENT-M187.mol-5	-6.173	-4.541	-4.223
ENT-M187.mol-6	-5.681	-4.189	-3.687
ENT-M187.mol-7	-5.126	-3.689	-5.099
ENT-M187.mol-8	-5.946	-3.805	-4.472
ENT-M189.mol-2	-5.122	-3.551	-3.242
ENT-M194.mol-1	-5.582	-3.999	-3.919
ENT-M194.mol-2	-5.552	-3.274	-4.078
ENT-M194.mol-3	-5.564	-3.681	-3.093
ENT-M194.mol-4	-5.299	-4.173	-4.901
ENT-M195.mol-1	-5.342	-3.428	-3.99
ENT-M198.mol-1	-5.055	-3.447	-3.872
ENT-M201.mol-2	-5.917	-5.552	-4.799
ENT-M202.mol-1	-5.595	-5.182	-5.13
ENT-M203.mol-1	-5.333	-2.605	-4.182
ENT-M204.mol-1	-5.074	-3.497	-4.063
ENT-M211.mol-2	-5.154	-3.56	-4.238
ENT-M211.mol-3	-5.352	-3.184	-4.349
ENT-M213.mol-1	-6.473	-5.566	-6.86
ENT-M214.mol-2	-6.547	-4.813	-4.524
ENT-M215.mol-2	-5.308	-3.585	-3.124
penitrem A.mol-1	-5.115	-3.462	-3.641
penitrem F.mol-1	-5.071	-2.993	-3.655

4.10 Discussion:

For many years, natural product samples have been used in drug screening programs both in industry and academia. However, as assay systems improved and became more target-oriented and high-throughput, the use of crude natural product extracts became less useful. As a result, purification techniques for natural product libraries have become more popular in screening programs (Wilson et al., 2020).

After a first round of screening on the marine extracts' library provided from the NKUA collaborators, we selected the 3 top hits (BI0394, BI0788 and BI0987) for further investigation. The aims were to gather further and more precise information about the content of the extracts and to discover which molecules were able to provide the motor neuron rescue in both the primary and multi-donor screenings discussed in chapter 3.

Once the process of fractionation started, BI0987 was prioritized over the other top hit extracts (BI0384 and BI0788) due to its immediate availability at the time of the secondment. The bacterial strain was cultured in large-scale in flasks containing a sea water-based medium and the resulting organic residue derived from its extraction was subjected to a multi-step fractionation scheme that had, up to the time of this first round of isolation and purification, led to the isolation of seven secondary metabolites.

Two out of seven metabolites were not completely purified or recognized when the extraction took place, the remaining 5 belonged to the class of 2,5-diketopiperazines. These molecules are cyclic dipeptides containing a 2,5-diketopiperazine backbone. The scaffold is made up of a six-membered ring that may or may not have different groups attached to it, arranged in a specific manner. This structure offers a three-dimensional shape, greater stability, chirality, the ability to control stereochemistry of substituents, and the promotion of intermolecular hydrogen bonding interactions with biological targets via corresponding donor and acceptor sites of the scaffold. Additionally, it can stimulate the pharmacophoric peptide groups (Borthwick et al., 2012). It is worth mentioning that 2,5-diketopiperazines are extremely common in nature, but very little applicability as neuroprotective agents have been shown so far (Cornacchia et al, 2012). In this respect, all 5 constituents extracted from BI0987 were tested again in the same assay used for the primary screening and another assay including *SOD1* ALS i-astrocytes. None of the assays highlighted any positive rescue at

any of the tested concentrations. This is often found when extracts are isolated and can occur for various reasons: loss of components throughout the fractionation steps; loss of synergies; or simply failure to isolate the effective molecules. As explained above, 2,5-diketopiperazine compounds do not seem to have a relevant impact as therapeutic agents for neurodegenerative disorders, but there are indications that they could be active as neuroprotective agents in some circumstances. For example, according to Prakash et al. (2002), 2,5-diketopiperazines prevented neuronal death in an in vitro model of traumatic injury. The study found that the compound effectively prevented cell death through two mechanisms: directly blocking the induction of free radicals and inhibiting calcium mobilization caused by an agent that leads to rapid, necrotic death. Additionally, the protective effect of 2,5-diketopiperazines was observed in a dose-dependent manner.

The following steps of extraction and fractionation were performed by our partners at NKUA, while we proceeded to screen the fractions obtained from BIO788.

BIO788 showed neuroprotective properties in a wider range of lines during the multi-donor assay, compared to the other 2 top hits BIO394 and BI987. Therefore, once we obtained 9 fractions (M217-M225), we introduced them into the co-culture assay and screened them using a working concentration range of 10 µg/mL, 1 µg/mL, 0.1 µg/mL, 0.01 µg/mL, and 0.001 µg/mL.

M219 was the only fraction able to show motor neuron rescue in two out of three patients, i.e., sporadic ALS P17 and C9orf72 P201, while we did not reproduce the neuroprotective effect observed with the full extract in SOD1 P102. As explained before, there is a possibility that part of the neuroprotective effect could have been lost throughout the fractionation steps. In addition, knowing that inside this fraction there might be the molecules that generated the rescue during the previous assay will help us to find the constituents of interest. BIO394 has not been investigated further due to its inconsistencies in promoting neuronal survival during the multi-donor screening, and its ability to show activity only at 1µg/mL, the highest concentration used in the co-culture assay.

Considering the high number of compounds isolated by our partners while fractionating BIO788, BIO394 and BIO987, we decided to perform molecular docking on the library of compounds we obtained. Prediction of ADME properties could allow us to narrow down the number of molecules that can be related to the neurotrophin receptor ligands and that are

more likely to exhibit satisfactory performance during clinical trials.

The results highlighted several molecules that could act as neurotrophin receptor binders, and which would need to be explored in further experiments. None of them has been tested yet to confirm their affinity for those binding sites. Also, it was not possible to test them for docking in TrkC due to the lack of a reliable crystal structure of this receptor. Therefore, there is still a chance that they might activate the downstream cascade from TrkC as well. Also, it must be taken into consideration that all molecules were small, therefore their ability to fit inside a receptor binding site is higher, despite the charges, making these results less reliable compared to a physiological context. Indeed, the major limitation of molecular docking is due to the lack of confidence in the ability of scoring functions to provide accurate binding energies, and this stems from the fact that some intermolecular interactions are hard to predict accurately, such as solvation effect and entropy changes. Some intermolecular interactions which have been proven to be of significance are rarely considered in scoring functions, such as halogen bonds contributing to protein-ligand binding affinity and guanidine-arginine interactions (Pinzi and Rastelli, 2019). Overall, molecular docking is a useful tool for predicting protein-ligand interactions, but its limitations must be carefully considered and addressed to improve the accuracy of the predictions.

So far, the experiments focused only on trying to understand the content and the activity of the extracts, but without retrieving any information about the molecular activity.

Therefore, it is still necessary to perform molecular assays to confirm or refute their ability to bind neurotrophin receptors. To clarify the molecular aspects of the activity of the extracts, the next chapter will focus on the molecular assays we managed to perform within the time available for this project. It is still unclear, which molecule or group of molecules can increase motor neuron rescue, therefore further isolation and screening experiments will be required in future work.

Chapter 5: Molecular Analysis of BI788 and In Vivo Testing on Zebrafish ALS models.

5.1 Introduction

In this study I have used a mixed approach to identify neuroprotective compounds i.e. I have tested compounds that had been designed and synthesised to mimic neurotrophins, as well as I have screened natural compounds, which have unknown targets. Although our *in-silico* data indicate that some of the molecules found inside BI0788 can activate the neurotrophin receptors: TrkA, TrkB and P75. Those molecules are ENT-M110, ENT-M111, ENT-M112, ENT-M113, ENT-M184, ENT-M185 and ENT-M186. As reported on the previous chapter, those molecules belonging to BI0788 were able to fit the binding site of TrkA, TrkB and P75. No in-vitro screening has yet been performed to confirm what has been obtained through the molecular docking and no information on the mechanisms of action of BI0788 are currently available.

Indeed, phenotypical screening platforms, such as the one used in this study, can be highly effective in discovering compounds that have neuroprotective properties for complex diseases. In situations where the mechanisms of toxicity and their actual impact on neuronal death are not yet fully understood, these screening platforms can provide valuable insights. Once a neuroprotective compound is identified, further investigation into its mechanism of action can begin.

In this chapter I focussed on our main hit, BI0788, based on the information previously gathered on the neuroprotective effect of marine compounds, the plan was to focus on the potential activation of neurotrophin receptors and the inflammatory response.

Neurotrophins play a role in regulating astrocytic responses to injury. Following injuries to the central nervous system or in cases of neurodegenerative disorders, growth factors, such as those belonging to the neurotrophin family, are expressed by neuronal and glial cells. Astrocytes can express functional TrkB receptors during their reactive state after experiencing chronic insult (McKeon et al, 1991). In our context of research, it is then important to evaluate if our ALS-derived astrocyte model can express TrkB and other neurotrophin receptors. The same applies for motorneurons, which are as well known to express neurotrophin receptors that are necessary to respond to the neurotrophins released from the glial cells compartment to cope with injuries or throughout their development stages. As stated in Chapter I, neurotrophins are indeed known to have important roles in motor neuronal survival, development, and homeostasis.

Not being able to assess any information regarding neurotrophin and neurotrophin receptors throughout the previous assays, we had to start addressing some of these questions to validate the hypothesis that our extracts could contain small neurotrophin mimetics able to act in a neuroprotective manner when introduced in an ALS co-culture system. Therefore, investigating if neurotrophin receptors are present and in which relative amount in both neurones and astrocytes is a mandatory step.

We adopted western-blot as our initial screening assay. We screened part of the relevant lines based on their availability and amount to assess the presence of p75 receptor in our ALS-astrocyte and motor neurone lines. This will be used as starting point for future experiments to assess whether our top-hit has an impact on the neurotrophin cascade.

I also decided to interrogate the effect of BI0788 on the localisation of the nuclear factor-kappa B (NF- κ B), which has a dual function, activator of inflammation (Liu et al., 2017), but also a major regulator of the growth and elaboration of neural processes (Liu et al., 2017).

The NF- κ B signalling pathway is involved in regulating several developmental processes, including axon initiation, elongation, guidance, and branching, as well as dendrite size and complexity. Its activity can be influenced by a variety of extracellular signals, including neurotrophins, which can either promote or inhibit growth depending on the phosphorylation status of the p65 subunit (Liu et al., 2017). Recent evidence also suggests that NF- κ B plays a role in regulating neurogenesis in both the embryonic and adult nervous systems, which has important implications for learning and memory.

However, NF- κ B is also a key mediator of inflammatory responses and is involved in regulating the expression of pro-inflammatory genes, such as cytokines and chemokines. This means that deregulated NF- κ B activation can contribute to the pathogenesis of various inflammatory disorders. Therefore, the impact of NF- κ B activation in neurodegenerative disorders is still a subject of debate, as it could either activate pro-inflammatory or pro-survival mechanisms. Its complex interaction with the inflammatory network makes it difficult to investigate and regulate to achieve only the desired effects (Liu et al., 2017).

Having available an assay for measuring the relative amount of NF- κ B within the cells and being aware of his correlation with the neurotrophin signalling, we also tried to analyse the impact of BI0788 treatment to gather more information about its putative correlation with neurotrophins.

As part of our initial planning, we have also taken forward BI0788 testing into zebrafish model of ALS. Given the onsite availability of zebrafish lines expressing *C9ORF72*.

This model mimics the motor deficits, cognitive impairment, muscle atrophy, motor neuron loss, and early mortality observed in human *C9ORF72*-ALS/FTD patients. The use of ALS-Zebrafish larvae allows for convenient and high-throughput in-vivo screening to estimate the potential therapeutic effects in humans. Zebrafish are small, low-cost, easy to breed, and transparent, making them an ideal model for testing drugs. Furthermore, they share similarities with other higher order vertebrates in terms of molecular signalling processes, neurodevelopment, genetic composition, and tissue/organ structures (D'Amora et al., 2018). To test the effects of BI0788 and its fractions, we used a zebrafish model that expresses DsRed under the control of a heat shock promoter and accumulates RNA foci and DPRs while activating the heat shock response. We tested different concentrations of BI0788 and its fractions to determine if they increase the survival of zebrafish embryos after treatment and if there is a decrease in RNA foci, DPRs, or heatshock response (HSR).

5.2 P75 receptor expression in a panel of i-astrocytes and motor neuron lines

Because the screening assay used to identify neuroprotective drugs focuses on astrocytes toxicity and p75 is known to be expressed mainly on glial cells in the adult brain, I first tried to assess the presence of p75 in some of the lines tested during the multi-donor assay through western-blot. Initially, we only tested untreated lines to understand what concentration of antibody was ideal to detect the presence the p75 receptor. We included in the assay 6 different iastrocyte lines: P201 and P78 as *C9ORF72* lines, P009 as sALS line, CS14 and C155 as control lines. We also tested Hb9-MNs, as they are part of the co-culture assay and are also exposed to the drugs, iPSC-derived MNs, to interrogate whether in vitro human MNs would behave like the mouse MN, and TDP-43 murine brain tissue as a positive control. The iPSC-derived MNs have been introduced with the idea of carrying on the drug screening on a co-culture assay made only by human derived cell lines, to address the issue of having a human/murine mixed co-culture model.

As result of the first western-blot experiment (**Figure 5.1**), we managed to identify presence of p75 in the Hb9-MNs, P201, P78, P009, TDP-43 and C155. IPSC-derived MNs, P102 and CS14 did not show any band at the weight of p75. Because of the first COVID lockdown I did not manage to complete triplicate experiments, hence I could not confirm the absence of p75 in the above-mentioned lines, as well as I could not confirm consistent expression of this receptor in the other

cell lines tested. However, in the initial experiment Hb9-MNs and P009 show a stronger band compared to the other tested lines.

Moreover, I have not managed to verify if TrkA, TrkB and TrkC are expressed in our cell lines. Consequently, it will be necessary to perform western-blot for those receptors as well, other than completing the biological triplicate for p75. I was also unable to assess whether BI0788 has any effect on the expression of these receptors, thus indicating if any of them is a direct or indirect target.

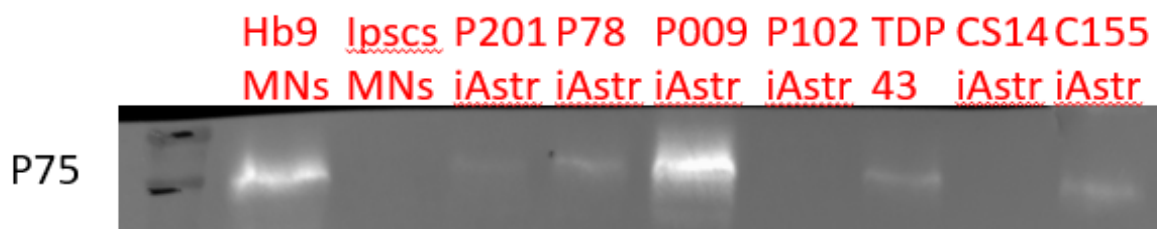


Figure 5. 1 P75 western-blot on a panel of i-astrocytes, mns and murine lines/tissues

The figure shows the first attempt at assessing the presence of the p75 receptor in the chosen array of cellular samples. Hb9 MNs and P009 show the brightest bands among the tested samples, indicating the probability of a higher concentration of the receptor. Ipsc-derived MNs, P102 and CS14 did not show any band at the level of p75 molecular weight. This experiment has been performed only once. Therefore, different concentrations of the antibody and a higher number of replicates are still necessary to prove the presence or absence of the receptor. Other lines tested previously must be included in the assay in order to provide a complete picture of p75 in all lines associated with the multidonor screening.

5.3 NF- κ B screening in BI0788 treated and untreated cells.

Neurotrophins such as NGF and BDNF have been shown to induce the translocation of NF- κ B from the cytoplasm to the nucleus, thus activating its transcriptional response (A.M. Marini et al, 2004), as well as other cellular responses. We therefore decided to assess whether nuclear NF- κ B was activated by the treatment with BI0788 through ICC staining. We compared the co-localization of DAPI with an antibody staining for pan-NF- κ B. The software Columbus has been adopted for the qualitative analysis of nuclear NF- κ B after acquiring the data with an Opera-Phenix High-Content Screening system. For this initial exploratory phase, the astrocyte lines have been chosen based on the multi-donor screening assay, i.e., the patient lines that showed the most robust response, and on previous preliminary data obtained within the Ferraiuolo laboratory indicating that some patient lines exhibit higher baseline levels of NF- κ B and are, therefore, easier to assess in assays using less sensitive methods such as immunostaining. A control, and one line per each ALS-associated mutation have been selected for this assay (**Figure 5.2**). All lines, except P17, i.e. the only sporadic patient tested, showed a significant increase in nuclear translocation of NF- κ B upon treatment. The discordant response of the sporadic patient might be indicative of underlying pathobiological differences between genetic and sporadic cases, or it could be related to differential expression of BI0788 target.

Although interesting, further tests are required to assess the consistency of these results in different panels of astrocyte lines and especially the downstream consequences of this pathway activation. Also, it seems opportune to introduce MNs into the assay and verify if its effect is extended to other cellular types relevant to ALS.

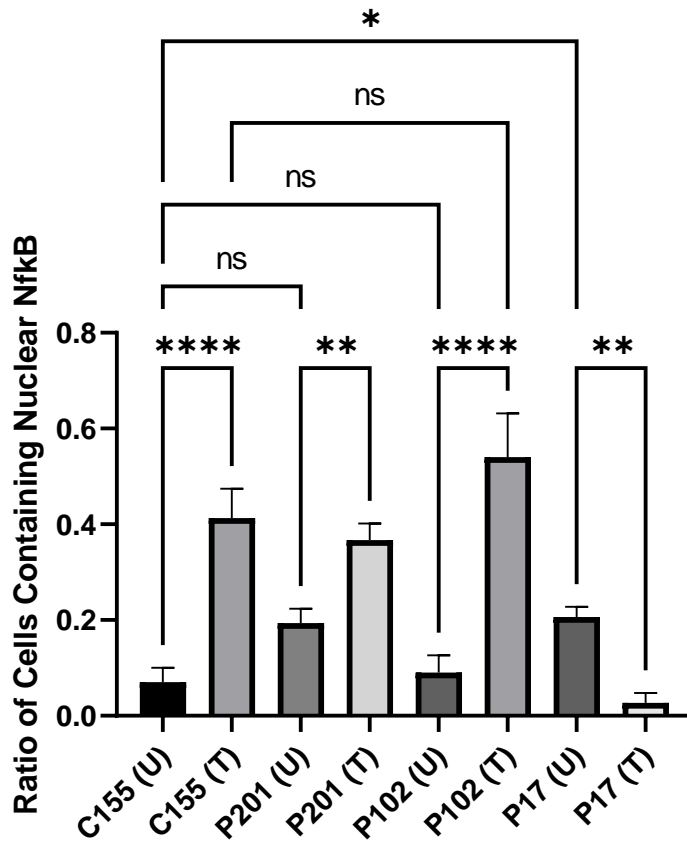


Figure 5. 2 NF-κB screening in ALS-i-astrocyte lines with different ALS-associated mutations upon BI0788 treatment

Cells have been treated for 24h with BI0788 at 10ug/ml, the concentration that showed a therapeutic effect in most-lines during the multi-donor screening. C155, P201 and P102 showed a significant increase in NF-κB translocation. P17 instead showed a reduction in NF-κB nuclear translocation. It also showed a significantly higher amount of cytoplasmic NF-κB before treatment compared to the control line C155. This might indicate an impairment in the nuclear transport of NF-κB in this specific line, but more experimental repeats are required to confirm or deny this hypothesis, including also other iastrocyte control lines. N = 3, data are mean ± SD. Two-way ANOVA with Dunnett's multiple comparisons (****p<0.0001, ***p<0.001, **p<0.01, *p<0.05).

5.4 C9orf72 Zebrafish lines treatment with BI0788

Following the positive results obtained from the multi-donor screening, we proceeded investigating the effect of BI0788 and its fractions. Investigation of positive hits in *in vivo* should have been a key part of the research project, but due to issues and delays encountered through the PhD period and time constraints we managed to start these experiments only during the last months. Therefore, this is still a preliminary screening of the BI0788 and its fractions on the *C9ORF72* zebrafish line (**Figure 5.3**). These tests have been carried on at the same time of the multi-donor screening of the BI0788 fractions, therefore we were not aware of ENT-M219 being the only active BI0788 fraction. For these experiments, we employed the ALS-C9ORF72 zebrafish models available at the University of Sheffield. These models involve the stable expression of interrupted C4G2 expansions, resulting in RNA foci and DPR pathology. The zebrafish models closely mirror the behavioural, cognitive, and motor defects, as well as reduced survival, that are associated with C9ORF72-ALS/FTD. Using these zebrafish models, Shaw et al. (2018) were able to identify that poly(PR) DPRs form higher molecular weight species. Adult and larvae zebrafish (*Danio rerio*) were maintained and bred by Dr David J Burrows according to established procedures. The care and maintenance of animals were performed under the Home Office project licence as per the animals (scientific procedures) act of 1981 (ASPA). *C9ORF72* anti-sense (C4G2) zebrafish were crossed with AB non-transgenic zebrafish. At 2 days post fertilisation (dpf) embryos were treated with BI0788 and its fractions, firstly with different doses resembling the co-culture assay (10 µg/mL, 1 µg/mL, 0.1 µg/mL, 0.01 µg/mL, and 0,001 µg/mL), and on a second round of experiment with lower dosage (0.03 µg/mL, 0.01 µg/mL, 0.003 µg/mL, 0.001µg/mL, and 0.0003). Each embryo was kept individually in a 96 well plate (96 well, µClear, Greiner Bio-One) and chronically dosed by immersion in 250 µl volume of drug solution from 2dpf until 5 dpf at 28.5°C. At 5dpf, transgenic embryos were phenotypically identified by DsRed expression using the InCell Analyzer 2000 (DsRed, 583 nm) (**Figure 5.4**).

Unfortunately, all tested concentrations resulted in toxicity for all embryos treated in each experiment. None of the embryos managed to survive more than 48h after being treated with either BI0788 or any of its fractions. We are still lacking information about BI788 and its fractions toxicity towards cells, therefore we cannot exclude a toxic effect towards all or just selective populations of cells at high concentrations. It will be necessaire to reduce the dosage and try again the treatment with lower concentrations to understand the cut off at which we can observe an effect of a lack of toxicity the treatment. Furthermore, as explained for the previous experiments

not having yet found which molecules are promoting the pro-survival effect and not knowing the relative molecular weight makes treatments way less precise to perform. Being aware of what molecule or molecules can provide the therapeutic effect will improve the efficacy and reliability of *in vivo* treatments.

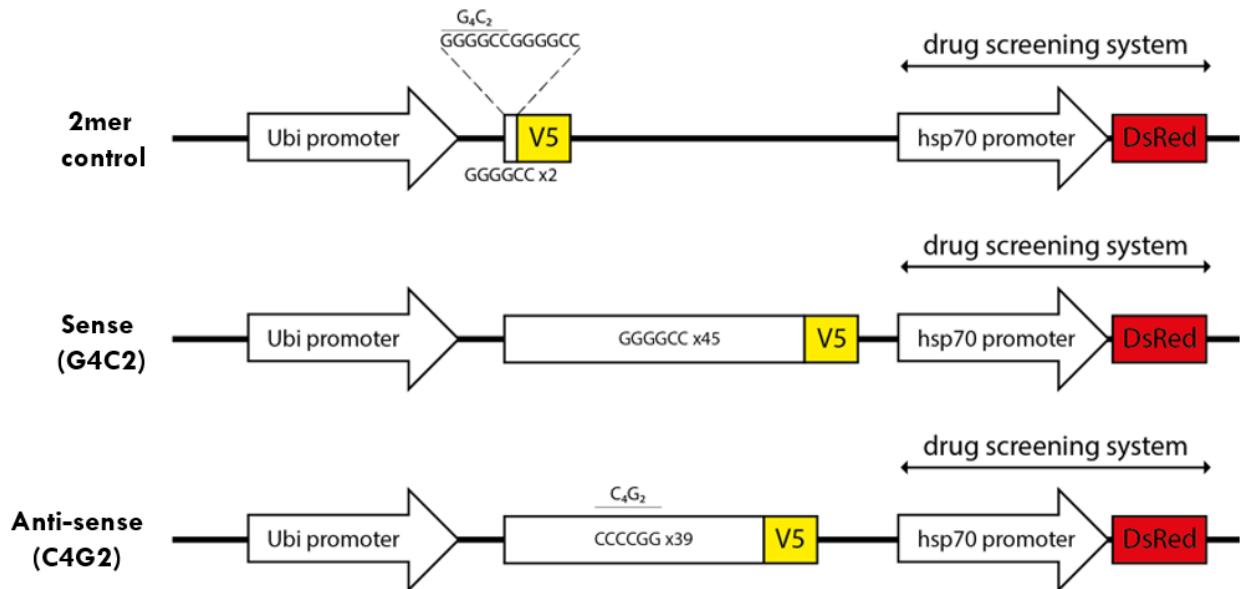


Figure 5. 3 Schematic of transgene used to create pure repeat RAN transgenic zebrafish lines

The pure repeats were cloned into an identical vector that was used to create our stable ATG-driven DPR transgenic zebrafish lines, as previously described¹. Embryos were injected with a DNA construct containing either 45 repeats of the C9orf72 sense hexanucleotide GGGGCC (G4C2), 39 repeats of the hexanucleotide CCCCCG (C4G2) or 2 repeats of the sense hexanucleotide repeat (2mer control). An hsp70 promoter then drives DsRed production. A V5 epitope tag was also included following the repeat, so that RAN translation can be tracked in all three frames. This picture has been kindly provided by Dr David J Burrows.

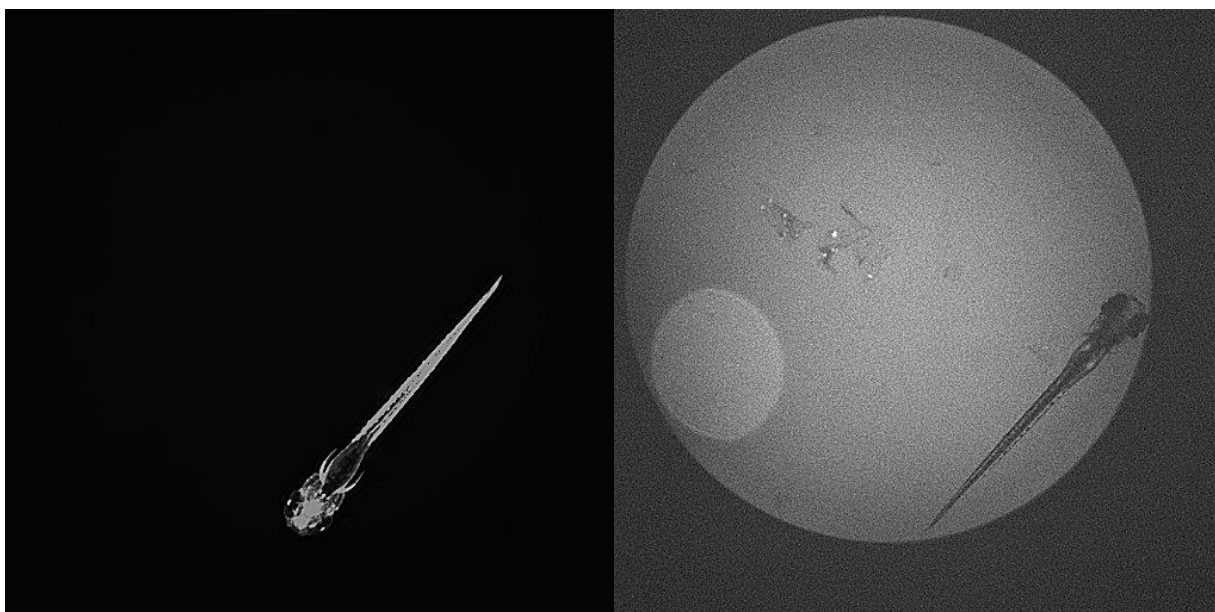


Figure 5. 4 *DsRed expression images obtained in control lines through InCell Analyzer 2000*

Images taken at 5 days post-fertilization (dpf) using the InCell Analyzer 2000 - 2X objective with DsRed – 583 nm wavelength on a control embryo. The Scale bar is 1 mm. Anti-sense (C4G2) line was used for compound fraction screening, all fractions were toxic at any concentration following 72h treatment (2 – 5 dpf), therefore no images of the treated embryos are available.

5.5 Discussion

Because of the phenotypic nature of our screening assay and the unknown properties of the marine compounds, in this chapter we started interrogating various potential neuroprotective pathways. Considering that the focus of this project is the assessment of neuroprotection via neurotrophin mimics, we started by assessing the expression of the main neurotrophin receptors, after the molecular docking results provided us with the possibility of having a binding with some of the BI0788 constituents: ENT-M110, ENT-M111, ENT-M112, ENT-M113, ENT-M184, ENT-M185 and ENT-M186. With a first preliminary screening of p75 on a panel of different iastrocyte lines, neurons, and ALS-murine tissue via western-blot. Despite obtaining some results in relation to the specificity of the chosen antibody for this type of screening, we have not observed the presence of p75 in all tested lines. Having managed to complete only one experiment, it will be necessary to test different concentration of p75 antibody, including more lines from the multi-donor screening. Moreover, so far, we have not completed a biological triplicate to prove if p75 is present in all lines, and if there is a difference in the relative expression among the lines. It seems from this preliminary data, that HB9-GFP MNs and P009 have the highest amount of p75. The high expression levels displayed by HB9-GFP MNs are not surprising considering their embryonic nature of these cells. It

is, in fact, known that MNs express high levels of p75 during development, but these decrease in adulthood. Indeed, re-expression of p75 in adult MNs has been linked to neurodegeneration. Since neurotrophin actions through P75 may also participate in the functional differentiation of non-neuronal cells, confirming alterations of P75 in iastrocytes might explain phenomena of de-regulation of supportive or deleterious actions of these cells in the injured nervous system other than a lack of correct responsiveness due to alterations of P75 on the motorneurons themselves.

It is also worth mentioning, that western-blotting does not provide any information about the cellular localization of p75, so it will be important to perform other assay, i.e. ICCs, to assess if p75 is actually present in the cellular membrane and able to interact with the other Trk receptors to modulate a response. Further analysis must be done also on the Trk receptor family. Western-blotting should be performed on those receptors as well, and the effective implication of p75 in their signalling must be assessed to have complete view of the effective presence in our iastrocytes and motor neuron lines, with particular focus on those lines that have been adopted for the co-culture screening. Also, variations of these receptors relative amount upon BI0788 treatment must be assessed, to see if it is affecting positively or negatively their expression.

We have also evaluated the effect of BI0788 treatment on NF- κ B nuclear translocation, finding a consistent pattern in multiple lines. BI0788, in fact, seems to promote the translocation of NF- κ B in C9orf72 and SOD1 iastrocyte lines compare to the control line used. In the patient line P17 it appears to have the opposite effect, reducing the amount of nuclear NF- κ B. This could be due to a defect intrinsic of the P17 lines caused by one or more disease-associated mutations present in this specific line. Therefore, it will be necessary to test multiple lines per each ALS-related genotype to confirm or deny the data observed so far. NF- κ B nuclear translocation upon BI0788 treatment provides little information about its correlation with neurotrophin activated pathway/cascades. Therefore, further analysis of the downstream pathways correlated with neurotrophin treatment must be analysed in the future to prove its ability to activate the neurotrophin receptors. The NF- κ B pathway must be activated to recruit the NF- κ B proteins in functional complexes and induce transcription. Those proteins are: p50, p52, p65/RelA, c-Rel, and RelB. There are two primary pathways for NF- κ B activation: the canonical and the non-canonical pathways. The canonical pathway is activated by several different immune receptors and mainly leads to the activation of NF- κ B proteins such as p65/RelA, p50, and c-Rel. In contrast, the non-canonical pathway is primarily triggered by specific receptors within the tumour necrosis factor receptor (TNFR) superfamily,

which results in the induction of p52 and RelB (Källsting et al., 2021).

All the above-mentioned molecules and pathways could be analysed in the future to assess the impact of NF- κ B pre and post BI0788 treatment in our cell lines.

The NF- κ B pathway is overactive in the spinal cord of ALS patients, and its activity in neurons may contribute to the disease in various ways (Källsting et al., 2021). For example, Inhibition of the NF- κ B pathway through neuron-specific expression of a super-repressor form of I κ B α has been shown to improve motor and cognitive functions and reduce motor neuron loss in both TDP-43A315T and TDP-43G348C transgenic mice (Dutta et al., 2020). Similarly, in *SOD1G93A* mice, inhibiting the NF- κ B pathway increased lifespan and reduced misfolded SOD1 accumulation.

While the normal function of NF- κ B signalling in healthy astrocytes is not well understood, it has been linked to inducing a pro-inflammatory astrocyte phenotype and impairing astrocytic neuroprotective properties such as promoting neuronal survival and synaptogenesis (Källsting et al., 2021). When pro-inflammatory astrocytes are co-cultured with spinal motor neurons, it results in significantly reduced neuronal viability, possibly due to the release of a yet-to-be-identified neurotoxin (Bouvier et al., 2022).

Regarding the ALS-*C9ORF72* zebrafish treatment, we have not managed to yet to find an appropriate concentration of BI788. The zebrafish model described here accurately reproduces important aspects of the behavioural, cognitive, and motor defects as well as reduced survival that are linked to C9-ALS/FTD. These zebrafish lines have been instrumental in discovering that poly(PR) DPRs can form higher molecular weight species (Shaw et al., 2018), but since all tested concentrations of BI0788 and its constituents resulted in death of the embryos, we have not managed to assess either DPRs levels or eventual defects in adult fish. This is a common issue while moving from cellular testing to actual animal models of the disease of interest. The inability to accurately predict the effectiveness of small molecules in vivo is due to several factors. In particular, the discrepancy between the potency of small molecules measured in vitro and their efficacy in vivo can be attributed to the fact that in vitro potency parameters such as K_d, K_i, IC₅₀, and EC₅₀ are measured in a closed system, which is vastly different from the open system encountered in vivo. In the in vivo environment, a drug interacts with various proteins, refractory pools, metabolism, and excretion, in addition to its intended target, leading to a more complex and unpredictable scenario (King Sing et al., 2019). Further decrease of the BI0788 concentration is required to see if it provides any effect related to the reduction of RNA Foci, DPRs or HSR in this line. Once the appropriate

concentration for testing will be found, we will also be able to test it in the available ALS-SOD1 Zebrafish to assert its activity on a wider range of ALS models. Dosing mixtures of compounds constitute a challenge in both in vitro and in vivo models, especially considering that we don't precisely know yet what molecules belong to each sub-fractions or to the entire extract. Not being able to precisely measure the concentration and amount of each constituent does not allow us to provide a precise treatment on the embryos. Explaining the loss of activity on fractionation by invoking synergism is difficult to experimentally support. It is usually attributed to either compound instability or irreversible binding to chromatography media, both of which can impact the effectiveness of sub-fractions for treatment. (Ulbricht, 2010).

Another point that needs to be assessed and might also affect the efficacy of the treatment, is the possibility that BI0788 constituents might have a toxic effect specific for the Zebrafish models. Zebrafish is increasingly becoming a popular animal model for toxicology due to its efficiency in assessing the toxicity of many compounds. This capability allows for the pre-screening of entire libraries of compounds to identify those with evident toxicity, which can be eliminated before proceeding to HTS. Alternatively, preliminary HTS hits can all be tested for toxicity to prioritize compounds for further development. Additionally, toxicological studies in zebrafish require only microgram or milligram quantities of a compound, whereas mammalian assays often require several grams to several hundred grams of the same compound (Zon et al., 2005).

The zebrafish is not as well established as a model for drug toxicology, and questions remain about how relevant fish toxicity is to humans since compounds can have specific toxicity towards the zebrafish. In this specific case, we don't know yet if BI0788 and its fractions can have a direct toxic effect on Zebrafish which would not appear in other animal models. Furthermore, not having been able yet to completely isolate and test all molecules contained in BI0788, this proposes the same issue of not being able to perform a treatment with a known and precise molecular concentration. Completing the screening and isolation of BI788 will allow us to perform more precise experiments in the future and obtain clearer information about its activity.

Chapter 6: Final Discussion

We interrogated a library of 100 marine extracts in a co-culture assay based on ALS-derived iastrocytes and MNs, with the aim of identifying molecules with neuroprotective properties. The first round of screening highlighted 8 potential candidates able to improve motor neuronal survival in a *C9ORF72* ALS derived iastrocyte line (#P183) and murine healthy motor neurons. The remaining extracts did not show any positive trend in improving survival. Among the 8 most promising hits, we selected the 3 candidates yielding the highest level of neuroprotection and proceeded with a multi-donor screening. ALS is a complex disorder caused by a wide variety of different genes and shows heterogeneity in terms of molecular pathogenicity, therefore finding a positive hit in a single *C9ORF72* model does not mean that the active compound will be effective in multiple lines derived from a larger number of patients with different genetic backgrounds (Hao et al., 2020).

The same concept of heterogeneity applies even for patients known to have mutations in the same gene, as for instance patients carrying mutations in *C9ORF72*. In fact, it is unknown if different repeat lengths may lead to different molecular outcomes, and an array of inherited and acquired risk factors are likely to contribute differently to the development of the disease (Gijssels et al, 2018). Therefore, we performed screening in a further 2 *C9ORF72* lines, 2 *SOD1* lines and 3 sALS lines to determine the activity of the extracts in different ALS models containing several different disease-causing mutations as well as sporadic ALS cases without an identified genetic cause.

Among the three extracts that underwent the multi-donor screening, the BI0788 extract stood out for consistency among the lines that have been included in the assay and became the top candidate to take forward for further analysis.

While performing this series of assays, we faced several challenges due to the intrinsic nature of marine extracts. As they are mixtures of unknown compounds, we did not have any information about their potential involvement with neurotrophins or neurotrophin-activated pathways. Furthermore, the assay we used for screening is phenotypical in nature and does not give any information about the molecular interactions of the extracts with either i-astrocytes or MNs. To answer the question about the nature of the neuroprotective molecule within the extracts, our partners at the NKUA initiated the process of

fractionation, isolation and characterization of the 3 top hits, i.e. BI0394, BI0788 and BI0987. This is a common procedure when dealing with natural extracts (Zhang et al., 2018). These are, in fact, often composed of a variety of molecules, which might have agonistic, antagonistic, or inert properties. Most molecules normally found inside natural extracts are known small molecules, but they also might contain novel molecules never discovered before (Zhang et al., 2018). Therefore, analysing natural extracts provides the possibility to find novel active molecules with potential beneficial effects in different disorders. Unfortunately, being normally complex mixtures, understanding what is inside the extract and which are the potential interactions within the components it is time consuming, and it is normally more suited for industrial rather than academic facilities (Abdelmohsen et al., 2022).

Another important aspect that must be taken into consideration is the fact that the concentrations of the various components were unknown at the time of the co-culture screening. This, therefore, did not allow us to work with precise concentrations calculated through molecular weights, but with dilutions of the weighted powders obtained from the dried extracts, thus reducing the overall reproducibility of the assay. This also raises some questions regarding the active concentrations of the top hits. All of them, showed significant activity only at the highest tested concentrations, 10ug/ml and 1 ug/ml. This of course is not ideal for a therapeutic agent; however, the hypothetical therapeutic compound or mixture of compounds might be present in very low concentrations within the hit extract. Hence, knowing which components are present within the extracts is a mandatory step to better understand what is providing the neuroprotective activity of interest. Those molecules might, in fact, be already active at a very low concentration. To address this limitation, other partners within the Euroneurotrophin consortium have undertaken the compound purification steps to allow us to perform further screening in order to confirm which molecules are active and at what concentrations.

To simplify this characterization procedure, we took 9 fractions obtained from BI0788 and screened them in smaller multi-donor assay. Knowing which fractions preserve their activity provides a clue for speeding up the process of isolation. In our case, only fraction ENT-M219 showed therapeutic activity, leading us to propose that this fraction might contain the

molecule or mixture of molecules of interest.

Even though this fraction showed a significant increase in MN survival, the level of rescue was not comparable to the full extract rescue. This might be explained by the fact that the fractions came from a different batch of BI0788. Culturing marine extracts, in fact, does not necessarily give the same yield of constituents, or even the same proportions of constituents, between different cultures. This in fact is a considerable drawback of producing biological components from bacterial extracts.

Therefore, a potential follow-up task, once we have identified which compounds are improving MN survival, would be to involve other partners within the EuroNeurotrophin network to synthesise the molecule of interest without depending on bacterial cultures, therefore overcoming the limits of the extractions.

Another explanation for the loss of activity could be the process of fractionation. This procedure, especially if not fully optimized, might produce some depletion of products which remain stuck to the resins despite the activity of the eluents. In this respect, it could be possible that some material has been lost through the procedure, thus reducing the final amount of therapeutic agent(s) present within the fractions.

As explained before, a good portion of BI394, BI0788 and BI0987 has already been isolated and characterized. These molecules have been docked to understand their potential binding with TrkA, TrkB and P75. Most of them conformed to the Lipinski set of rules for potential therapeutic effectiveness and were able to bind all the tested receptors. Despite being a promising result, this is still not enough to confirm their ability to act as neurotrophin mimetics.

In fact, the molecules isolated are all small molecules, thus making it more challenging to exclude non-specific binding through *in silico* models (Rodrigues, 2022). Algorithms are, in fact, likely to predict non-specific binding to large catalytic sites like the one present within P75 (Meng et al., 2011). Moreover, the algorithms used in this study modelled docking of the molecules considering the external domain of the neurotrophin receptors rather than the full protein. To overcome this limitation, our EuroNeurotrophin partners at the University of Siena are trying to obtain a full crystal structure of the neurotrophin receptors

as well as a structure of the receptor with a bound ligand. Once their structures are fully obtained, we will perform again the same analysis using more reliable models.

Another aspect that has not been possible to verify even *in silico* is the interaction of the molecules with TrkC, due to the unavailability of a good crystal structure on every database we investigated at the time of the analysis. This could provide further information about which receptors our extract constituents can bind.

Taking these considerations into account, it would have been ideal to treat cells with the molecules identified and confirm through either Western-Blot, ELISA or ICC whether or not the compounds can actually modulate the activity of the neurotrophin receptors.

Due to laboratory access restrictions imposed by the COVID pandemic, I did not have the time to complete these experiments, but I started optimizing the western-blot assay for P75. As result of the first western-blot experiment, we managed to identify the presence of the receptor protein in the Hb9-MNs, and various i-Astrocyte control and patient lines, while iPSC derived MNs, did not show any band at the molecular weight of P75. This was just a single experiment, so, ultimately, it is not conclusive, but it indicates that the cells used for the screening express the p75 receptor. Although I have not conducted the experiments myself, other lab members have produced data indicating that the i-Astrocytes and mouse motor neurons also express TrkA and TrkB, and in ALS the values of these receptors are dysregulated (Dehghani et al., 2022).

In addition to confirming these preliminary data via western blotting, it will also be opportune to investigate through ICC the presence of those receptors at the level of the cellular surface. In fact, for these receptors to be functional they need to be correctly positioned at the cell surface (Griffiths and Lucocq, 2014).

A number of marine extracts have been found to have anti-inflammatory or anti-oxidant properties (Vasarri and Degl'Innocenti, 2022) and neurotrophins such as NGF and BDNF have been shown to activate the NF- κ B response (Srinivasan and Lahiri, 2015). For this reason, we decided to assess whether treatment of i-Astrocytes with the hit extract BI0788 had an effect on NF- κ B translocation from the cytoplasm to the nucleus. All the tested lines except one sporadic patient showed a consistent increase of NF- κ B nuclear translocation

upon treatment, thus indicating that BI0788 is likely to act, at least in part, through NF- κ B driven pro-survival pathways (Srinivasan and Lahiri, 2015).

It is interesting that one sporadic patient, which responded to the treatment *in vitro*, displayed a different behaviour compared to the other samples. This would have to be investigated further, but it might indicate the importance of other genetic components in drug response and activation of neuroprotective pathways (Harry and Kraft, 2009). Hence, further testing is required to assess the mechanism of action of BI0788 on a wider panel of i-astrocyte lines. Also it will be required to introduce MNs into the assay.

We finally tried to test BI0788 and its fractions in a *C9ORF72* zebrafish ALS model. A reporter construct has been utilized in this model that expresses DsRed under the control of a heat shock promoter to screen for potential therapeutic compounds. This particular zebrafish line typically exhibits the accumulation of RNA foci and DPR, as well as motor deficits, cognitive impairment, muscle atrophy, motor neuron loss, and early adulthood mortality - all of which are characteristic of human *C9ORF72*-ALS/FTD patients (Shaw et al., 2018). Although I tested a wide range of concentrations, unfortunately, these all proved to be toxic for the zebrafish embryos. Translating from *in vitro* to *in vivo* experiments can often be challenging due to issues with the concentrations tested *in vitro*. Lowering the concentrations to the point where they do not result in toxicity to the zebrafish embryos and allow us to complete the full experiment will be a priority. Due to time constraints, this has not been possible within the time of the PhD. It is also possible that toxicity was observed at the concentrations tested because I performed the tests in embryos instead of adult fish. This is also a hypothesis worth testing in the future.

Not being able to get results out of the embryos treatment also prevented us from proceeding towards testing the compounds on adult fish and observe the potential effects on the phenotype, or follow the effects of early treatment on ALS-Zebrafish embryos throughout their development.

Due to time constraints, we could not investigate different *C9ORF72* zebrafish ALS model. Effects of the treatment could vary among different *C9ORF72* mutations, since they could affect a number pathways and we do not know yet which ones are targeted by the treatment. This is going to be an important aspect to evaluate in the future.

Furthermore, as explained before, treating with full extracts or fraction is not ideal, since they are too complex and might have different interactions depending on their constituents and synergies. This complicates validating the results and the effectiveness of the treatment, and it is difficult to take forward for other *in vivo* studies. This aspect further exacerbates the need of identifying and testing BI0788 constituents to be able obtain a clear profile of the treatment, and narrow down which constituents contribute to the effect.

If the therapeutic effect is observed in this model, we will also extend it to a *SOD1* zebrafish ALS model available in our facility at SITraN.

Regarding the DHEA derivatives screening, despite finding ENT-A010 as a positive hit, since this library was not part of the original screening plan, but it was added to complement other findings in the Euroneurotrophin network, we had to stop investigating ENT-A010 and just focus on the Marine Extracts library. In the future, given that ENT-A010 seems to be providing positive results in multiple assays carried on from our partners within the network, it would be worth investigating it further on a wider array of patient lines and *in vivo* models.

Another aspect that needs to be evaluated in the future, is the target engagement of our positive hits. We have not yet confirmed through which receptors our positive hits are able to provide the therapeutic effect. Our *in silico* analysis and the experiments we have done so far are not able to confirm their binding to any of neurotrophin receptors. It is not guaranteed that any of our hits can trigger a response through any of the neurotrophin receptors. As far we know from our data, they could be providing the therapeutic effect from receptors uncorrelated with neurotrophins. This aspect needs to be elucidated in the future to be able to adequately investigate the mechanism of action of our positive hits, and it requires a clear understanding of the extract constituents.

In conclusion I have identified new 3 marine extracts able to improve motor neuron survival in different ALS-astrocytes and healthy motor neurons co-culture assays. ALS-astrocytes have been taken from a panel of: *C9ORF72*, *SOD1* and sALS patient lines available in the laboratory. One of them, BI0788, showed consistent pro-survival results in multiple ALS lines and has been taken forward for multiple screening. It has been fractionated into 9 different sub-fractions which have undergone the multi-donor screening. One of them, ENT-M2019

has shown similar results to BI0788 and will be further screened in the future. All fractions and BI0788 have been screened in a *C9ORF72* Zebrafish model but did not give any positive result yet. Further evaluation of BI0788 and ENT-M2019 will be needed to assess their biological activity and therapeutic effect in ALS.

Chapter 7: Appendix

7.1 Patient #17 Screening of BI0788 sub-fractions (ENT-M217-M225)

All fractions aside ENT-M219 did not show any statistically significant motor neuron rescue in Patient #17 after treatment in our co-culture assay.

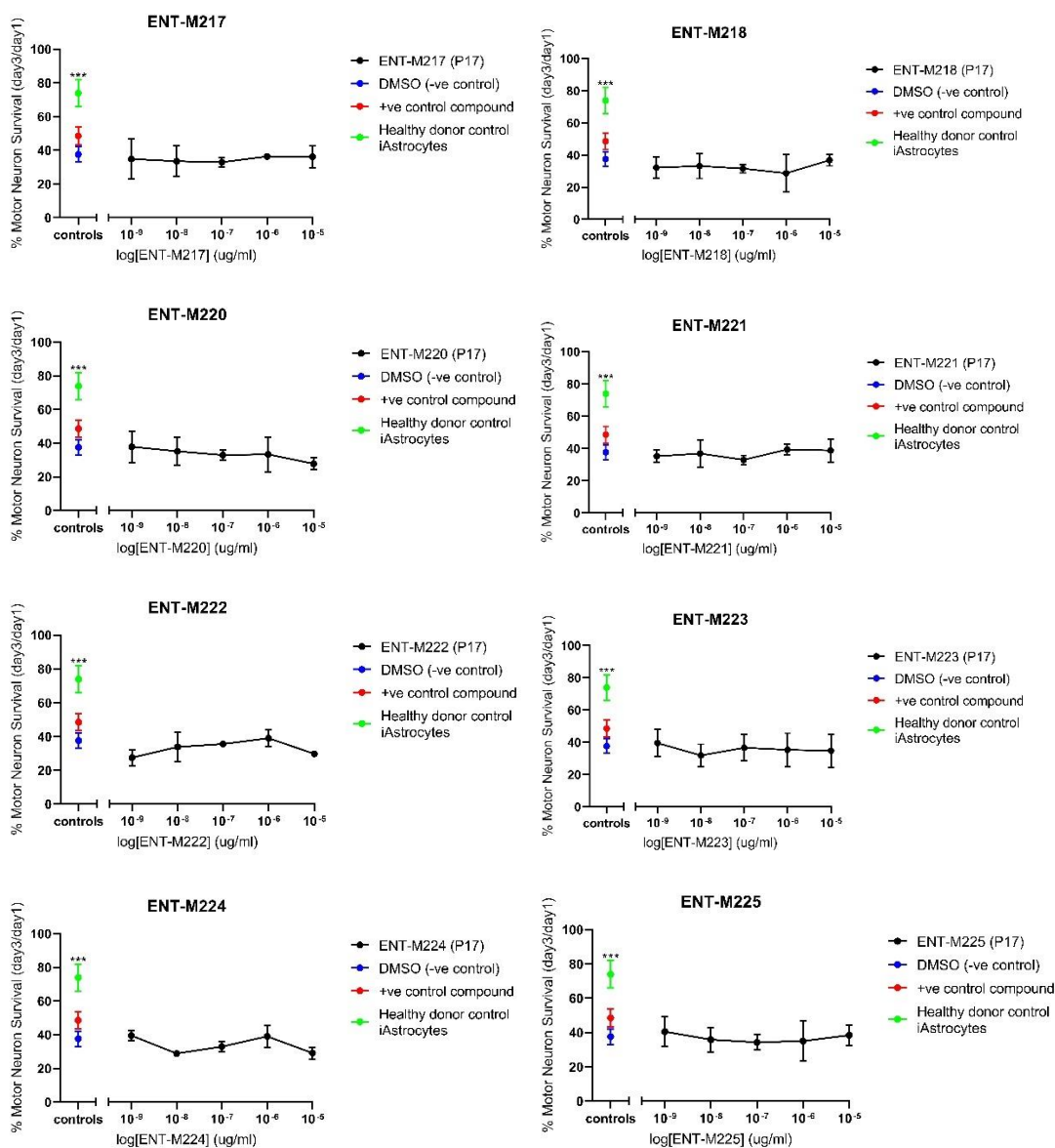


Figure 7. 1 ENT-M217-M225 screen in *sALS* patient #17 and Hb9-GFP+ mouse motor neuron co-culture.

7.2 Patient #102 Screening of BI0788 sub-fractions (ENT-M217-M225)

All fractions aside ENT-M219 did not show any statistically significant motor neuron rescue in P #102 after treatment in our co-culture assay.

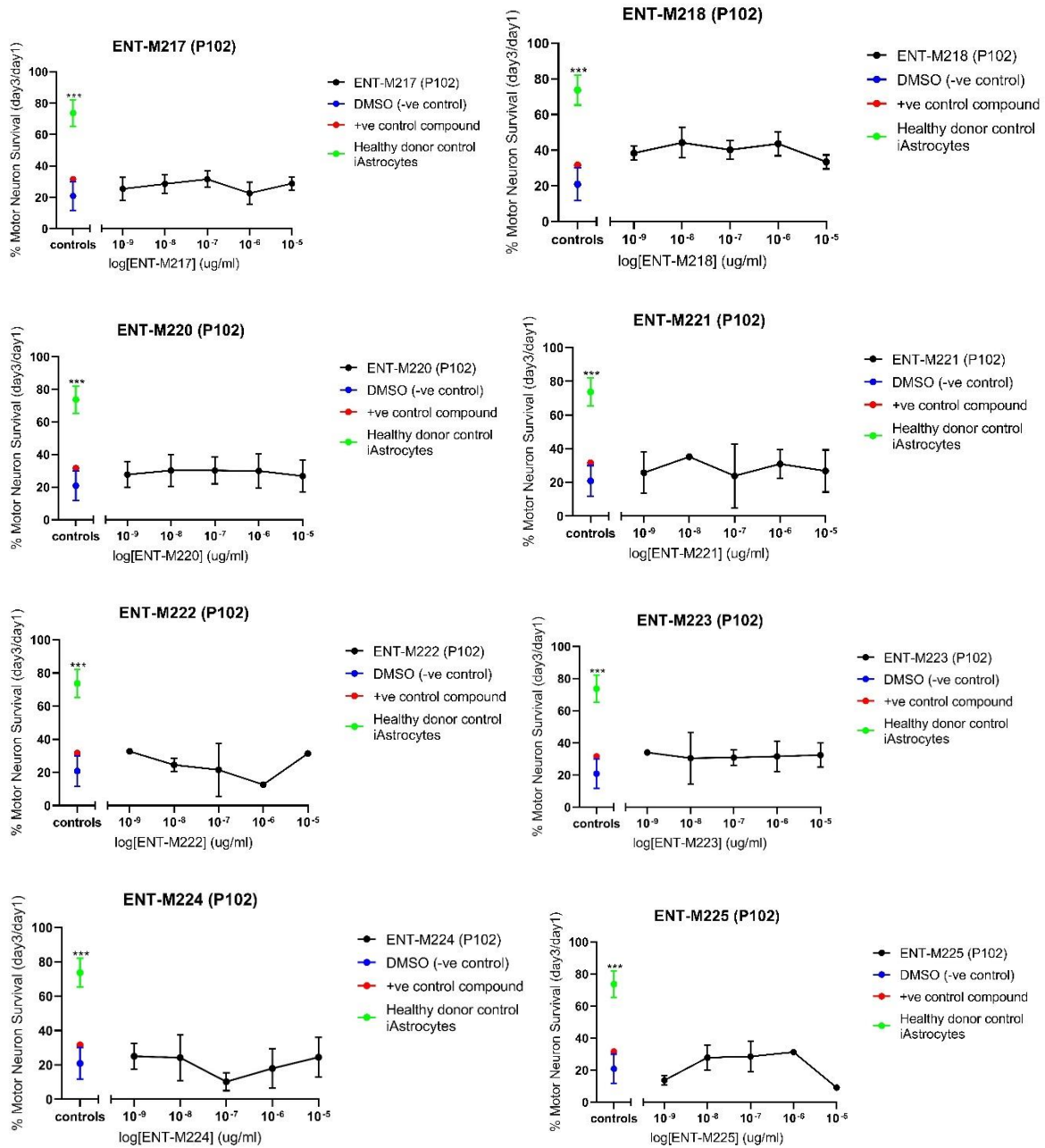


Figure 7. 2 ENT-M217-M225 screen in sALS patient #102 and Hb9-GFP+ mouse motor neuron co-culture.

7.3 Patient #201 Screening of BI0788 sub-fractions (ENT-M217-M225)

All fractions aside ENT-M219 did not show any statistically significant motor neuron rescue in P #201 after treatment in our co-culture assay.

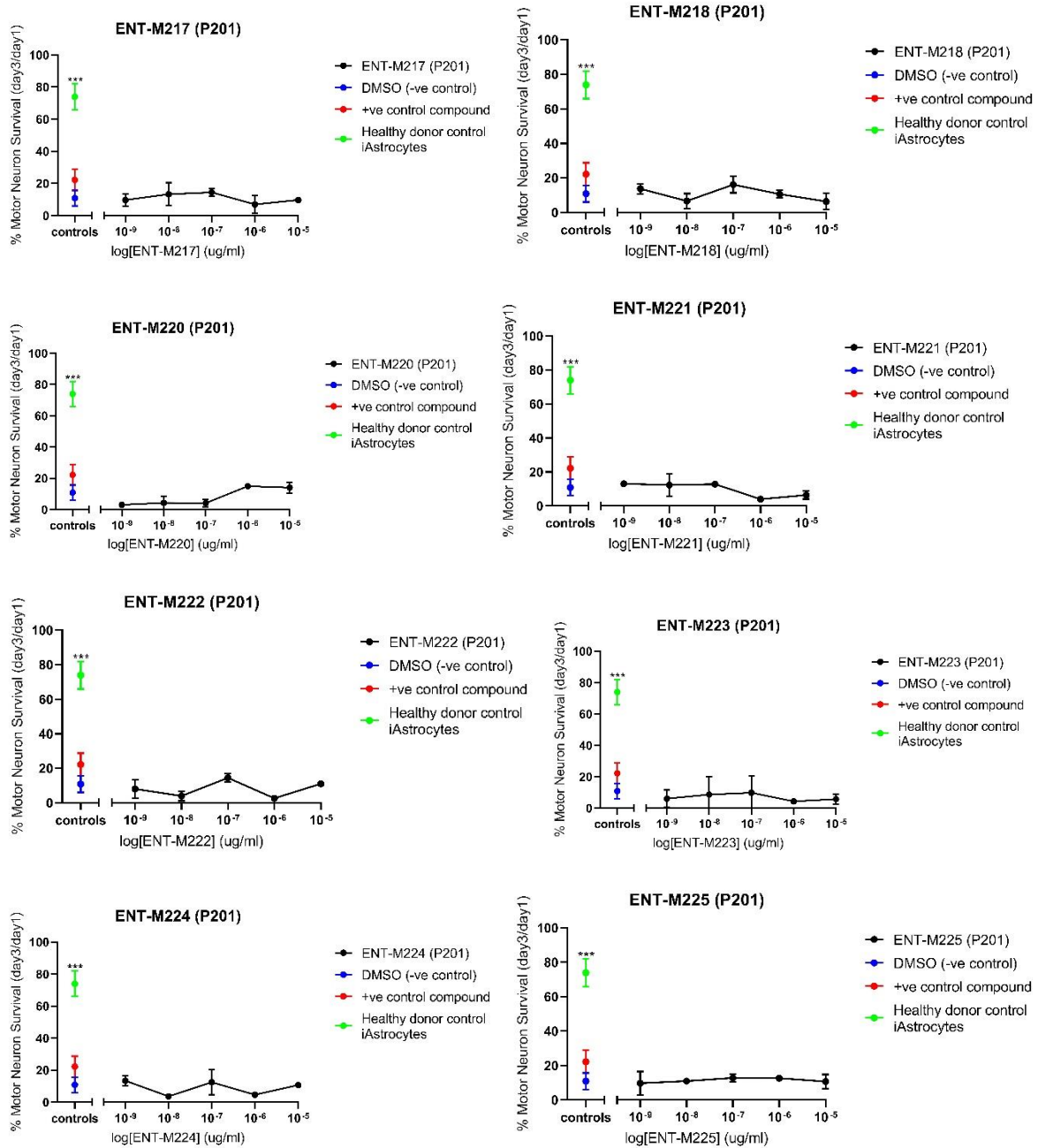


Figure 7. 3 ENT-M217-M225 screen in sALS patient #201 and Hb9-GFP+ mouse motor neuron co-culture.

Bibliography

Aebischer, J. et al. (2011) 'IFN γ Triggers a Light-Dependent Selective Death of Motoneurons Contributing to the Non-Cell-Autonomous Effects of Mutant SOD1', *Cell Death & Differentiation*, 18(5), pp. 754–768. doi: 10.1038/cdd.2010.143.

Abdelmohsen Usama Ramadan, Sayed Ahmed M., Elmaidomy Abeer H. Natural Products' Extraction and Isolation-Between Conventional and Modern Techniques. *Frontiers in Natural Products Volume 1 2022*. DOI=10.3389/fntpr.2022.873808.

Ahmed, S. B. M. and Prigent, S. A. (2017) 'Insights into the Shc Family of Adaptor Proteins', *Journal of molecular signaling. Ubiquity Press*, 12, p. 2. doi: 10.5334/1750-2187-12-2.

Ajrourd-Driss, S. and Siddique, T. (2015) 'Sporadic and Hereditary Amyotrophic Lateral Sclerosis (ALS)', *Biochimica et Biophysica Acta (BBA) - Molecular Basis of Disease*, 1852(4), pp. 679–684. doi: <https://doi.org/10.1016/j.bbadis.2014.08.010>.

Al-Chalabi, A. et al. (2010) 'An Estimate of Amyotrophic Lateral Sclerosis Heritability Using Twin Data', *Journal of Neurology, Neurosurgery & Psychiatry*, 81(12), p. 1324 LP-1326. doi: 10.1136/jnnp.2010.207464.

Al-Chalabi, A. et al. (2014) 'Analysis of Amyotrophic Lateral Sclerosis as a Multistep Process: a Population-Based Modelling Study', *The Lancet Neurology*, 13(11), pp. 1108–1113. doi: [https://doi.org/10.1016/S1474-4422\(14\)70219-4](https://doi.org/10.1016/S1474-4422(14)70219-4).

Al-Chalabi, A., van den Berg, L. H. and Veldink, J. (2016) 'Gene Discovery in Amyotrophic Lateral Sclerosis: Implications for Clinical Management', *Nature Reviews Neurology*. Nature Publishing Group, a division of Macmillan Publishers Limited. All Rights Reserved., 13, p. 96. Available at: <https://doi.org/10.1038/nrneurol.2016.182>.

Allen, S. J., Watson, J. J. and Dawbarn, D. (2011) 'The Neurotrophins and their Role in Alzheimer's Disease', *Current Neuropharmacology*. Bentham Science Publishers, 9(4), pp. 559–573. doi: 10.2174/157015911798376190.

Amick, J. and Ferguson, S. M. (2017) 'C9orf72: At the Intersection of Lysosome Cell Biology and Neurodegenerative Disease', *Traffic (Copenhagen, Denmark)*. 2017/03/23, 18(5), pp. 267–276. doi: 10.1111/tra.12477.

Andersen, P. M. and Al-Chalabi, A. (2011) 'Clinical Genetics of Amyotrophic Lateral Sclerosis: What do we Really Know?', *Nature Reviews Neurology*, 7(11), pp. 603–615. doi: 10.1038/nrneurol.2011.150.

Atanas G. Atanasov, Birgit Waltenberger, Eva-Maria Pferschy-Wenzig, Thomas Linder, Christoph Wawrosch, Pavel Uhrin, Veronika Temml, Limei Wang, Stefan Schwaiger, Elke H. Heiss, Judith M. Rollinger, Daniela Schuster, Johannes M. Breuss, Valery Bochkov, Marko D. Mihovilovic, Brigitte Kopp, Rudolf Bauer, Verena M. Dirsch, Hermann Stuppner, *Discovery and Resupply of Pharmacologically Active Plant-Derived Natural Products: a Review*, *Biotechnology Advances*, Volume 33, Issue 8, 2015, Pages 1582-1614, ISSN 0734-9750, <https://doi.org/10.1016/j.biotechadv.2015.08.001>.

Ash PE, Zhang YJ, Roberts CM, et al. Neurotoxic Effects of TDP-43 Overexpression in *C. elegans*. *Hum Mol Genet.* 2010;19:3206–3218.

Babić Leko, M. et al. (2019) 'Molecular Mechanisms of Neurodegeneration Related to C9orf72 Hexanucleotide Repeat Expansion', *Behavioural neurology*. Hindawi, 2019, p. 2909168. doi: 10.1155/2019/2909168.

Bartus, R. T. et al. (2011) 'Bioactivity of AAV2-Neurturin Gene Therapy (CERE-120): Differences Between Parkinson's Disease and Nonhuman Primate Brains', *Movement Disorders*. John Wiley & Sons, Ltd, 26(1), pp. 27–36. doi: 10.1002/mds.23442.

Bartus, R. T. et al. (2013) 'Advancing Neurotrophic Factors as Treatments for Age-Related Neurodegenerative Diseases: Developing And Demonstrating "Clinical Proof-Of-Concept" for AAV-Neurturin (CERE-120) in Parkinson's Disease', *Neurobiology of Aging*, 34(1), pp. 35–61. doi: <https://doi.org/10.1016/j.neurobiolaging.2012.07.018>.

Bartus, R. T. and Johnson, E. M. (2017a) 'Clinical Tests of Neurotrophic Factors for Human Neurodegenerative Diseases, Part 1: Where have we Been and What have we Learned?', *Neurobiology of Disease*, 97, pp. 156–168. doi: <https://doi.org/10.1016/j.nbd.2016.03.027>.

Bartus, R. T. and Johnson, E. M. (2017b) 'Clinical Tests of Neurotrophic Factors for Human Neurodegenerative Diseases, Part 2: Where do we Stand and where Must we Go Next?', *Neurobiology of Disease*, 97, pp. 169–178. doi: <https://doi.org/10.1016/j.nbd.2016.03.026>.

Bendotti, C. et al. (2012) 'Dysfunction of Constitutive and Inducible Ubiquitin-Proteasome System in Amyotrophic Lateral Sclerosis: Implication for Protein Aggregation and Immune Response', *Progress in Neurobiology*, 97(2), pp. 101–126. doi: <https://doi.org/10.1016/j.pneurobio.2011.10.001>.

Bergami, M. et al. (2008) 'Uptake and Recycling of Pro-BDNF for Transmitter-Induced Secretion by Cortical Astrocytes', *The Journal of Cell Biology*, 183(2), p. 213 LP-221. doi: [10.1083/jcb.200806137](https://doi.org/10.1083/jcb.200806137).

Blondy, S. et al. (2019) 'Neurotrophins and their Involvement in Digestive Cancers', *Cell Death & Disease*, 10(2), p. 123. doi: [10.1038/s41419-019-1385-8](https://doi.org/10.1038/s41419-019-1385-8).

Boillée, S. et al. (2006) 'Onset and Progression in Inherited ALS Determined by Motor Neurons and Microglia', *Science*, 312(5778), p. 1389 LP-1392. doi: [10.1126/science.1123511](https://doi.org/10.1126/science.1123511).

Bolognani, F. and Perrone-Bizzozero, N. I. (2008) 'RNA-Protein Interactions and Control Of mRNA Stability in Neurons', *Journal of Neuroscience Research*. John Wiley & Sons, Ltd, 86(3), pp. 481–489. doi: [10.1002/jnr.21473](https://doi.org/10.1002/jnr.21473).

Bolognin, S. et al. (2012) 'An Experimental Rat Model of Sporadic Alzheimer's Disease and Rescue of Cognitive Impairment With a Neurotrophic Peptide', *Acta Neuropathologica*. 2011/11/15, 123(1), pp. 133–151. doi: [10.1007/s00401-011-0908-x](https://doi.org/10.1007/s00401-011-0908-x).

Van Den Bosch, L. et al. (2004) 'Effects of Vascular Endothelial Growth Factor (Vegf) on Motor Neuron Degeneration', *Neurobiology of Disease*, 17(1), pp. 21–28. doi: <https://doi.org/10.1016/j.nbd.2004.06.004>.

Van Den Bosch, L. et al. (2006) 'The Role of Excitotoxicity in The Pathogenesis of Amyotrophic Lateral Sclerosis', *Biochimica et Biophysica Acta (BBA) - Molecular Basis of Disease*, 1762(11), pp. 1068–1082. doi: <https://doi.org/10.1016/j.bbadis.2006.05.002>.

Van Den Bosch, L. and Robberecht, W. (2008) 'Crosstalk Between Astrocytes and Motor Neurons: What is the Message?', *Experimental Neurology*, 211(1), pp. 1–6. doi: <https://doi.org/10.1016/j.expneurol.2008.01.008>.

- Borasio, G. D. et al. (1998) 'A Placebo-Controlled Trial of Insulin-Like Growth Factor-I in Amyotrophic Lateral Sclerosis', *Neurology*, 51(2), p. 583 LP-586. doi: 10.1212/WNL.51.2.583.
- Borthwick, A.D. 2,5-Diketopiperazines: Synthesis, Reactions, Medicinal Chemistry, and Bioactive Natural Products. *Chem. Rev.* 2012, 112, 3641–3716.
- Bothwell, M. (2016) 'Recent Advances in Understanding Neurotrophin Signaling', *F1000Research*. *F1000Research*, 5, p. F1000 Faculty Rev-1885. doi: 10.12688/f1000research.8434.1.
- Boutilier, J. et al. (2008) 'Proneurotrophins Require Endocytosis and Intracellular Proteolysis to Induce TrkA Activation', *The Journal of Biological Chemistry*. 2008/02/25. American Society for Biochemistry and Molecular Biology, 283(19), pp. 12709–12716. doi: 10.1074/jbc.M710018200.
- Bouvier DS, Fixemer S, Heurtaux T, Jeannelle F, Frauenknecht KBM, Mittelbronn M. The Multifaceted Neurotoxicity of Astrocytes in Ageing and Age-Related Neurodegenerative Diseases: A Translational Perspective. *Front Physiol.* 2022 Mar 17;13:814889. doi: 10.3389/fphys.2022.814889. PMID: 35370777; PMCID: PMC8969602.
- Boyd JD, Lee P, Feiler MS, Zaur N, Liu M, Concannon J, et al. A High-Content Screen Identifies Novel Compounds that Inhibit Stress-Induced TDP-43 Cellular Aggregation and Associated Cytotoxicity. *J Biomol Screen* 2014 Jan;19(1):44-56.
- Boylan, K. (2015) 'Familial Amyotrophic Lateral Sclerosis', *Neurologic Clinics*, 33(4), pp. 807–830. doi: <https://doi.org/10.1016/j.ncl.2015.07.001>.
- Brites, D. and Vaz, A. R. (2014) 'Microglia Centered Pathogenesis in Als: Insights in Cell Interconnectivity', *Frontiers in Cellular Neuroscience*, 8, p. 117. doi: 10.3389/fncel.2014.00117.
- Bruijn, L. I. et al. (1997) 'ALS-Linked SOD1 Mutant G85R Mediates Damage to Astrocytes and Promotes Rapidly Progressive Disease with SOD1-Containing Inclusions', *Neuron*. Elsevier, 18(2), pp. 327–338. doi: 10.1016/S0896-6273(00)80272-X.

- Bruijn, L. I. et al. (1998) 'Aggregation and Motor Neuron Toxicity of an ALS-Linked SOD1 Mutant Independent from Wild-Type SOD1', *Science*, 281(5384), p. 1851 LP-1854. doi: 10.1126/science.281.5384.1851.
- Bruno, V. et al. (1998) 'Neuroprotection by Glial Metabotropic Glutamate Receptors Is Mediated by Transforming Growth Factor- β ', *The Journal of Neuroscience*, 18(23), p. 9594 LP-9600. doi: 10.1523/JNEUROSCI.18-23-09594.1998.
- Burk, K. and Pasterkamp, R. J. (2019) 'Disrupted Neuronal Trafficking in Amyotrophic Lateral Sclerosis', *Acta Neuropathologica*. 2019/02/05. Springer Berlin Heidelberg, 137(6), pp. 859–877. doi: 10.1007/s00401-019-01964-7.
- Byrne, S. et al. (2013) 'Aggregation of Neurologic And Neuropsychiatric Disease in Amyotrophic Lateral Sclerosis Kindreds: A Population-Based Case–Control Cohort Study of Familial and Sporadic Amyotrophic Lateral Sclerosis', *Annals of Neurology*. John Wiley & Sons, Ltd, 74(5), pp. 699–708. doi: 10.1002/ana.23969.
- Caesar, L. K. and Cech, N. B. (2019) 'Synergy and Antagonism in Natural Product Extracts: When 1 + 1 does not Equal 2', *Natural Product Reports*. The Royal Society of Chemistry, 36(6), pp. 869–888. doi: 10.1039/C9NP00011A.
- Caporali, A. and Emanuelli, C. (2009) 'Cardiovascular Actions of Neurotrophins', *Physiological reviews*, 89(1), pp. 279–308. doi: 10.1152/physrev.00007.2008.
- Castello, N. A. et al. (2014) '7,8-Dihydroxyflavone, a Small Molecule TrkB Agonist, Improves Spatial Memory and Increases Thin Spine Density in a Mouse Model of Alzheimer Disease-Like Neuronal Loss', *PloS one*. Public Library of Science, 9(3), pp. e91453–e91453. doi: 10.1371/journal.pone.0091453.
- Catanesi M, Caioni G, Castelli V, Benedetti E, d'Angelo M, Cimini A. Benefits under the Sea: The Role of Marine Compounds in Neurodegenerative Disorders. *Mar Drugs*. 2021 Jan 8;19(1):24. doi: 10.3390/md19010024. PMID: 33430021; PMCID: PMC7827849.
- Chao, M. V (2003) 'Neurotrophins and their Receptors: A Convergence Point for Many Signalling Pathways', *Nature Reviews Neuroscience*. Nature Publishing Group, 4, p. 299. Available at: <https://doi.org/10.1038/nrn1078>.

Cheng, W. et al. (2018) 'C9ORF72 GGGGCC Repeat-Associated non-AUG Translation is Upregulated by Stress Through eIF2 α Phosphorylation', *Nature communications*. Nature Publishing Group UK, 9(1), p. 51. doi: 10.1038/s41467-017-02495-z.

Chia, R., Chiò, A. and Traynor, B. J. (2018) 'Novel Genes Associated with Amyotrophic Lateral Sclerosis: Diagnostic and Clinical Implications', *The Lancet Neurology*. Elsevier, 17(1), pp. 94–102. doi: 10.1016/S1474-4422(17)30401-5.

Ciervo Y, Gatto N, Allen C, Grierson A, Ferraiuolo L, Mead RJ, Shaw PJ. Adipose-Derived Stem Cells Protect Motor Neurons and Reduce Glial Activation in Both in Vitro And in Vivo Models of ALS. *Mol Ther Methods Clin Dev*. 2021 Mar 27;21:413-433. doi: 10.1016/j.omtm.2021.03.017. PMID: 33869658; PMCID: PMC8044387.

Clement, A. M. et al. (2003) 'Wild-Type Nonneuronal Cells Extend Survival of SOD1 Mutant Motor Neurons in ALS Mice', *Science*, 302(5642), p. 113 LP-117. doi: 10.1126/science.1086071.

Corcia, P. et al. (2013) 'Molecular Imaging of Microglial Activation in Amyotrophic Lateral Sclerosis', *PLOS ONE*. Public Library of Science, 7(12), p. e52941. Available at: <https://doi.org/10.1371/journal.pone.0052941>.

Corcia, P. et al. (2017) 'Genetics of Amyotrophic Lateral Sclerosis', *Revue Neurologique*, 5204(5), p. 243 YP-360. doi: <http://dx.doi.org/10.1016/j.neurol.2017.03.030>.

Cornacchia, C. et al. (2012) '2,5-Diketopiperazines as Neuroprotective Agents', *Mini-Reviews in Medicinal Chemistry*, pp. 2–12. doi: <http://dx.doi.org/10.2174/138955712798868959>.

Coskun, O. (2016) 'Separation Techniques: Chromatography', *Northern clinics of Istanbul*. Kare Publishing, 3(2), pp. 156–160. doi: 10.14744/nci.2016.32757.

d'Amora M, Giordani S. The Utility of Zebrafish as a Model for Screening Developmental Neurotoxicity. *Front Neurosci*. 2018 Dec 18;12:976. doi: 10.3389/fnins.2018.00976. PMID: 30618594; PMCID: PMC6305331.

DeJesus-Hernandez, M. et al. (2011) 'Expanded GGGGCC Hexanucleotide Repeat in Noncoding Region of C9ORF72 Causes Chromosome 9p-Linked FTD and ALS', *Neuron*. Elsevier, 72(2), pp. 245–256. doi: 10.1016/j.neuron.2011.09.011.

Dekkers, M. P. J., Nikolettou, V. and Barde, Y.-A. (2013) 'Cell Biology in Neuroscience: Death of Developing Neurons: New Insights and Implications for Connectivity', *The Journal of Cell Biology*. The Rockefeller University Press, 203(3), pp. 385–393. doi: 10.1083/jcb.201306136.

Deng, P. et al. (2016) 'Engineered BDNF Producing Cells as a Potential Treatment for Neurologic Disease', *Expert Opinion on Biological Therapy*. 2016/05/21, 16(8), pp. 1025–1033. doi: 10.1080/14712598.2016.1183641.

Dewil, M. et al. (2007) 'Vascular Endothelial Growth Factor Counteracts the Loss Of Phospho-Akt Preceding Motor Neurone Degeneration in Amyotrophic Lateral Sclerosis', *Neuropathology and Applied Neurobiology*. John Wiley & Sons, Ltd (10.1111), 33(5), pp. 499–509. doi: 10.1111/j.1365-2990.2007.00850.x.

Dehghani, F., Abdollahi, S., Shidfar, F., Cain, C. T., Clark & Sepideh Soltani (2022) Probiotics Supplementation and Brain-Derived Neurotrophic Factor (BDNF): a Systematic Review and Meta-Analysis of Randomized Controlled Trials, *Nutritional Neuroscience*, DOI: 10.1080/1028415X.2022.2110664.

Di Giorgio, F. P. et al. (2008) 'Human Embryonic Stem Cell-Derived Motor Neurons Are Sensitive to the Toxic Effect of Glial Cells Carrying an ALS-Causing Mutation', *Cell Stem Cell*. Elsevier, 3(6), pp. 637–648. doi: 10.1016/j.stem.2008.09.017.

Dias, D. A., Urban, S. and Roessner, U. (2012) 'A Historical Overview of Natural Products in Drug Discovery', *Metabolites*. MDPI, 2(2), pp. 303–336. doi: 10.3390/metabo2020303.

Dormann, D. and Haass, C. (2011) 'TDP-43 and FUS: a Nuclear Affair', *Trends in Neurosciences*. Elsevier, 34(7), pp. 339–348. doi: 10.1016/j.tins.2011.05.002.

Dovas, A. and Couchman, J. R. (2005) 'RhoGDI: Multiple Functions in The Regulation of Rho Family GTPase Activities', *The Biochemical Journal*. Portland Press Ltd., 390(Pt 1), pp. 1–9. doi: 10.1042/BJ20050104.

Dutta K, Thammisetty SS, Boutej H, Bareil C, Julien JP. Mitigation of ALS Pathology by Neuron-Specific Inhibition of Nuclear Factor Kappa B Signaling. *J Neurosci*. 2020 Jun 24;40(26):5137-5154. doi: 10.1523/JNEUROSCI.0536-20.2020. Epub 2020 May 26. PMID: 32457070; PMCID: PMC7314413.

- Ekester, E. (2004) 'Neurotrophic Factors and Amyotrophic Lateral Sclerosis', *Neurodegenerative Diseases*, 1(2–3), pp. 88–100. doi: 10.1159/000080049.
- Endo, F. et al. (2015) 'Astrocyte-Derived TGF- β 1 Accelerates Disease Progression in ALS Mice by Interfering with the Neuroprotective Functions of Microglia and T Cells', *Cell Reports*, 11(4), pp. 592–604. doi: <https://doi.org/10.1016/j.celrep.2015.03.053>.
- Eriksdotter-Jönhagen, M. et al. (2012) 'Encapsulated Cell Biodelivery of Nerve Growth Factor to the Basal Forebrain in Patients with Alzheimer's Disease', *Dementia and Geriatric Cognitive Disorders*, 33(1), pp. 18–28. doi: 10.1159/000336051.
- Evans, M. C. et al. (2013) 'Inflammation and Neurovascular Changes in Amyotrophic Lateral Sclerosis', *Molecular and Cellular Neuroscience*, 53, pp. 34–41. doi: <https://doi.org/10.1016/j.mcn.2012.10.008>.
- Faravelli, I. et al. (2014) 'Motor Neuron Derivation from Human Embryonic and Induced Pluripotent Stem Cells: Experimental Approaches and Clinical Perspectives', *Stem Cell Research & Therapy*. BioMed Central, 5(4), p. 87. doi: 10.1186/scrt476.
- Ferraiuolo, L., Higginbottom, A., et al. (2011) 'Dysregulation of Astrocyte–Motoneuron Cross-Talk in Mutant Superoxide Dismutase 1-Related Amyotrophic Lateral Sclerosis', *Brain*, 134(9), pp. 2627–2641. doi: 10.1093/brain/awr193.
- Ferraiuolo, L., Kirby, J., et al. (2011) 'Molecular Pathways of Motor Neuron Injury in Amyotrophic Lateral Sclerosis', *Nature Reviews Neurology*. Nature Publishing Group, a division of Macmillan Publishers Limited. All Rights Reserved., 7, p. 616. Available at: <https://doi.org/10.1038/nrneurol.2011.152>.
- Ferrari, R. et al. (2011) 'FTD and ALS: a Tale of Two Diseases', *Current Alzheimer research*, 8(3), pp. 273–294. Available at: <https://www.ncbi.nlm.nih.gov/pubmed/21222600>.
- Fu, H., Hardy, J. and Duff, K. E. (2018) 'Selective Vulnerability in Neurodegenerative Diseases', *Nature Neuroscience*. 2018/09/24, 21(10), pp. 1350–1358. doi: 10.1038/s41593-018-0221-2.

- Fujita, T., Tozaki-Saitoh, H. and Inoue, K. (2009) 'P2Y1 Receptor Signaling Enhances Neuroprotection by Astrocytes Against Oxidative Stress Via IL-6 release in Hippocampal Cultures', *Glia*. John Wiley & Sons, Ltd, 57(3), pp. 244–257. doi: 10.1002/glia.20749.
- Fünfschilling, U. et al. (2012) 'Glycolytic Oligodendrocytes Maintain Myelin and Long-Term Axonal Integrity', *Nature*, 485(7399), pp. 517–521. doi: 10.1038/nature11007.
- Furukawa, Y. and O'Halloran, T. V (2006) 'Posttranslational Modifications in Cu,Zn-Superoxide Dismutase and Mutations Associated with Amyotrophic Lateral Sclerosis', *Antioxidants & Redox Signaling*, 8(5–6), pp. 847–867. doi: 10.1089/ars.2006.8.847.
- Gash, D. M. et al. (2005) 'Trophic Factor Distribution Predicts Functional Recovery in Parkinsonian Monkeys', *Annals of Neurology*. John Wiley & Sons, Ltd, 58(2), pp. 224–233. doi: 10.1002/ana.20549.
- Gatto N, Dos Santos Souza C, Shaw AC, Bell SM, Myszczyńska MA, Powers S, Meyer K, Castelli LM, Karyka E, Mortiboys H, Azzouz M, Hautbergue GM, Márkus NM, Shaw PJ, Ferraiuolo L. Directly Converted Astrocytes Retain the Ageing Features of the Donor Fibroblasts and Elucidate The Astrocytic Contribution to Human CNS Health and Disease. *Aging Cell*. 2021 Jan;20(1):e13281. doi: 10.1111/accel.13281. Epub 2020 Dec 13. PMID: 33314575; PMCID: PMC7811849.
- Genç Y., Bardakci H., Yücel Ç., Karatoprak G.Ş., Küpeli Akkol E., Hakan Barak T., Sobarzo-Sánchez E. Oxidative Stress and Marine Carotenoids: Application by Using Nanoformulations. *Mar. Drugs*. 2020;18:423. doi: 10.3390/md18080423.
- Giannini, F. et al. (2010) 'D90A-SOD1 Mutation in ALS: The First Report Of Heterozygous Italian Patients and Unusual Findings', *Amyotrophic Lateral Sclerosis*. Taylor & Francis, 11(1–2), pp. 216–219. doi: 10.3109/17482960902721642.
- Gijssels I, Cruts M, Van Broeckhoven C. The Genetics of C9orf72 Expansions. *Cold Spring Harb Perspect Med*. 2018 Apr 2;8(4):a026757. doi: 10.1101/cshperspect.a026757. PMID: 28130313; PMCID: PMC5880162.
- Gill, S. S. et al. (2003) 'Direct Brain Infusion of Glial Cell Line–Derived Neurotrophic Factor in Parkinson Disease', *Nature Medicine*. Nature Publishing Group, 9, p. 589. Available at: <https://doi.org/10.1038/nm850>.

Goldstein, L. H. and Abrahams, S. (2013) 'Changes in Cognition and Behaviour in Amyotrophic Lateral Sclerosis: Nature of Impairment and Implications for Assessment', *The Lancet Neurology*. Elsevier, 12(4), pp. 368–380. doi: 10.1016/S1474-4422(13)70026-7.

Gómez-Gonzalo, M. et al. (2010) 'An Excitatory Loop with Astrocytes Contributes to Drive Neurons to Seizure Threshold', *PLOS Biology*. Public Library of Science, 8(4), p. e1000352. Available at: <https://doi.org/10.1371/journal.pbio.1000352>.

Grad L. I., Yerbury J. J., Turner B. J., Guest W. C., Pokrishevsky E., O'Neill M. A., et al. (2014). Intercellular Propagated Misfolding of Wild-Type Cu/Zn Superoxide Dismutase Occurs Via Exosome-Dependent and -Independent Mechanisms. *Proc. Natl. Acad. Sci. U S A* 111, 3620–3625. 10.1073/pnas.1312245111

Granhölm, A.-C. et al. (2000) 'Glial Cell Line-Derived Neurotrophic Factor Is Essential for Postnatal Survival of Midbrain Dopamine Neurons', *The Journal of Neuroscience*, 20(9), p. 3182 LP-3190. doi: 10.1523/JNEUROSCI.20-09-03182.2000.

Griffiths G, Lucocq JM. Antibodies for Immunolabeling by Light and Electron Microscopy: Not for The Faint Hearted. *Histochem Cell Biol*. 2014 Oct;142(4):347-60. doi: 10.1007/s00418-014-1263-5. Epub 2014 Aug 24. PMID: 25151300; PMCID: PMC4160575.

Grosskreutz, J., Van Den Bosch, L. and Keller, B. U. (2010) 'Calcium Dysregulation in Amyotrophic Lateral Sclerosis', *Cell Calcium*, 47(2), pp. 165–174. doi: <https://doi.org/10.1016/j.ceca.2009.12.002>.

Haidet-Phillips, AM, et al., Astrocytes from Familial and Sporadic ALS Patients are Toxic To Motor Neurons. *Nat Biotechnol* 29, 824–828 (2011).

Hao Z, Wang R, Ren H, Wang G. Role of the C9ORF72 Gene in the Pathogenesis of Amyotrophic Lateral Sclerosis and Frontotemporal Dementia. *Neurosci Bull*. 2020 Sep;36(9):1057-1070. doi: 10.1007/s12264-020-00567-7. Epub 2020 Aug 29. PMID: 32860626; PMCID: PMC7475143.

Hardiman, O. et al. (2017) 'Amyotrophic lateral sclerosis', *Nature Reviews Disease Primers*. Macmillan Publishers Limited, 3, p. 17071. Available at: <https://doi.org/10.1038/nrdp.2017.71>.

Hayden, M. S. and Ghosh, S. (2014) 'Regulation of NF- κ B by TNF Family Cytokines', *Seminars in Immunology*. 2014/06/21, 26(3), pp. 253–266. doi: 10.1016/j.smim.2014.05.004.

Harry GJ, Kraft AD. Neuroinflammation and Microglia: Considerations and Approaches for Neurotoxicity Assessment. *Expert Opin Drug Metab Toxicol*. 2008 Oct;4(10):1265-77. doi: 10.1517/17425255.4.10.1265. PMID: 18798697; PMCID: PMC2658618.

Henriques, A., Pitzer, C. and Schneider, A. (2010) 'Neurotrophic Growth Factors for the Treatment of Amyotrophic Lateral Sclerosis: where do we Stand?', *Frontiers in Neuroscience*. Frontiers Research Foundation, 4, p. 32. doi: 10.3389/fnins.2010.00032.

Holmes B. B., DeVos S. L., Kfoury N., Li M., Jacks R., Yanamandra K., et al.. (2013). Heparan Sulfate Proteoglycans Mediate Internalization and Propagation of Specific Proteopathic Seeds. *Proc. Natl. Acad. Sci. U S A* 110, E3138–E3147. 10.1073/pnas.1301440110.

Hu Y, Chen J, Hu G, Yu J, Zhu X, Lin Y, Chen S, Yuan J. Statistical research on the bioactivity of new marine natural products discovered during the 28 years from 1985 to 2012. *Mar. Drugs*. 2015;13:202–221. doi: 10.3390/md13010202.

Huang, E. J. and Reichardt, L. F. (2001) 'Neurotrophins: Roles in Neuronal Development and Function', *Annual Review of Neuroscience*, 24, pp. 677–736. doi: 10.1146/annurev.neuro.24.1.677.

Hyman, A. A., Weber, C. A. and Jülicher, F. (2014) 'Liquid-Liquid Phase Separation in Biology', *Annual Review of Cell and Developmental Biology*. *Annual Reviews*, 30(1), pp. 39–58. doi: 10.1146/annurev-cellbio-100913-013325.

Iacoangeli, A. et al. (2019) 'C9orf72 Intermediate Expansions Of 24–30 Repeats are Associated with ALS', *Acta Neuropathologica Communications*, 7(1), p. 115. doi: 10.1186/s40478-019-0724-4.

Ighodaro, O. M. and Akinloye, O. A. (2018) 'First Line Defence Antioxidants-Superoxide Dismutase (SOD), Catalase (CAT) and Glutathione Peroxidase (GPX): Their Fundamental Role in the Entire Antioxidant Defence Grid', *Alexandria Journal of Medicine*, 54(4), pp. 287–293. doi: <https://doi.org/10.1016/j.ajme.2017.09.001>.

- Jia, J. et al. (2009) 'Mechanisms of Drug Combinations: Interaction and Network Perspectives', *Nature Reviews Drug Discovery*, 8(2), pp. 111–128. doi: 10.1038/nrd2683.
- Johnson, J. O. et al. (2014) 'Mutations in the Matrin 3 Gene Cause Familial Amyotrophic Lateral Sclerosis', *Nature Neuroscience*. Nature Publishing Group, a division of Macmillan Publishers Limited. All Rights Reserved., 17, p. 664. Available at: <https://doi.org/10.1038/nn.3688>.
- Källstig E, McCabe BD, Schneider BL. (2021) The Links between ALS and NF-κB. *Int J Mol Sci*. 2021 Apr 8;22(8):3875. doi: 10.3390/ijms22083875. PMID: 33918092; PMCID: PMC8070122.
- Kalra, S., Genge, A. and Arnold, D. L. (2003) 'A Prospective, Randomized, Placebo-Controlled Evaluation of Corticoneuronal Response to Intrathecal BDNF Therapy in ALS Using Magnetic Resonance Spectroscopy: Feasibility and Results', *Amyotrophic Lateral Sclerosis and Other Motor Neuron Disorders*. Taylor & Francis, 4(1), pp. 22–26. doi: 10.1080/14660820310006689.
- Kazim, S. F. et al. (2014) 'Disease Modifying Effect of Chronic Oral Treatment with a Neurotrophic Peptidergic Compound in a Triple Transgenic Mouse Model of Alzheimer's Disease', *Neurobiology of Disease*, 71, pp. 110–130. doi: <https://doi.org/10.1016/j.nbd.2014.07.001>.
- Kazim, S. F. and Iqbal, K. (2016) 'Neurotrophic Factor Small-Molecule Mimetics Mediated Neuroregeneration and Synaptic Repair: Emerging Therapeutic Modality for Alzheimer's Disease', *Molecular Neurodegeneration*. BioMed Central, 11(1), p. 50. doi: 10.1186/s13024-016-0119-y.
- Kenna, K. P. et al. (2013) 'Delineating the Genetic Heterogeneity of ALS Using Targeted High-Throughput Sequencing', *Journal of Medical Genetics*, 50(11), p. 776 LP-783. doi: 10.1136/jmedgenet-2013-101795.
- Kin Sing Stephen Lee, Jun Yang, Jun Niu, Connie J. Ng, Karen M. Wagner, Hua Dong, Sean D. Kodani, Debin Wan, Christophe Morisseau, and Bruce D. (2019) *Hammock ACS Central Science* 2019 5 (9), 1614-1624 DOI: 10.1021/acscentsci.9b00770.

Kiuru P, D'Auria MV, Muller CD, Tammela P, Vuorela H, Yli-Kauhaluoma J. Exploring marine resources for bioactive compounds. *Planta Med.* 2014;80:1234–1246. doi: 10.1055/s-0034-1383001.

Koleva II, van Beek TA, Linssen JP, de Groot A, Evstatieva LN. (2002) Screening of Plant Extracts for Antioxidant Activity: a Comparative Study on Three Testing Methods. *Phytochem Anal.* 2002 Jan-Feb;13(1):8-17. doi: 10.1002/pca.611. PMID: 11899609.

Konno, K. et al. (2004) 'Papain Protects Papaya Trees from Herbivorous Insects: Role of Cysteine Proteases In Latex', *The Plant Journal*. John Wiley & Sons, Ltd (10.1111), 37(3), pp. 370–378. doi: 10.1046/j.1365-313X.2003.01968.x.

Kordower, J. H. et al. (2006) 'Delivery of Neurturin by AAV2 (CERE-120)-Mediated Gene Transfer Provides Structural and Functional Neuroprotection and Neurorestoration in MPTP-Treated Monkeys', *Annals of Neurology*. John Wiley & Sons, Ltd, 60(6), pp. 706–715. doi: 10.1002/ana.21032.

Kordower, J. H. and Bjorklund, A. (2013) 'Trophic Factor Gene Therapy for Parkinson's Disease', *Movement Disorders*. John Wiley & Sons, Ltd, 28(1), pp. 96–109. doi: 10.1002/mds.25344.

Kraemer, B. R. et al. (2014) 'A Role for the p75 Neurotrophin Receptor in Axonal Degeneration and Apoptosis Induced by Oxidative Stress', *The Journal of Biological Chemistry*. 2014/06/17. American Society for Biochemistry and Molecular Biology, 289(31), pp. 21205–21216. doi: 10.1074/jbc.M114.563403.

Krüttgen, A., Schneider, I. and Weis, J. (2006) 'The Dark Side of the NGF Family: Neurotrophins in Neoplasias', *Brain Pathology*. John Wiley & Sons, Ltd (10.1111), 16(4), pp. 304–310. doi: 10.1111/j.1750-3639.2006.00037.x.

Kwong LK, Neumann M, Sampathu DM, Lee VM, Trojanowski JQ. TDP-43 Proteinopathy: the Neuropathology Underlying Major Forms of Sporadic and Familial Frontotemporal Lobar Degeneration and Motor Neuron Disease. *Acta Neuropathol.* 2007;114:63–70.

Lacomblez, L. et al. (2004) 'Xaliproden in Amyotrophic Lateral Sclerosis: Early Clinical Trials', *Amyotrophic Lateral Sclerosis and Other Motor Neuron Disorders*. Taylor & Francis, 5(2), pp. 99–106. doi: 10.1080/14660820410018973.

Lagier-Tourenne, C. et al. (2012) 'Divergent Roles of ALS-Linked Proteins FUS/TLS and TDP-43 Intersect in Processing Long pre-mRNAs', *Nature Neuroscience*. Nature Publishing Group, a division of Macmillan Publishers Limited. All Rights Reserved., 15, p. 1488. Available at: <https://doi.org/10.1038/nn.3230>.

Lai EC, Felice KJ, Festoff BW, Gawel MJ, Gelinus DF, Kratz R, Murphy MF, Natter HM, Norris FH, Rudnicki SA. (1997) Effect of Recombinant Human Insulin-Like Growth Factor-I on Progression of ALS. A placebo-controlled study. The North America ALS/IGF-I Study Group. *Neurology*. 1997;49:1621–1630.

Lambrechts, D. et al. (2003) 'VEGF is a Modifier of Amyotrophic Lateral Sclerosis in Mice and Humans and Protects Motoneurons Against Ischemic Death', *Nature Genetics*, 34(4), pp. 383–394. doi: 10.1038/ng1211.

Lapidus, K. A., Soleimani, L. and Murrough, J. W. (2013) 'Novel Glutamatergic Drugs for the Treatment of Mood Disorders', *Neuropsychiatric Disease and Treatment*. 2013/08/07. Dove Medical Press, 9, pp. 1101–1112. doi: 10.2147/NDT.S36689.

Leblond, C. S. et al. (2014) 'Dissection of Genetic Factors Associated with Amyotrophic Lateral Sclerosis', *Experimental Neurology*, 262, pp. 91–101. doi: <https://doi.org/10.1016/j.expneurol.2014.04.013>.

Leloup, N., Chataigner, L. M. P. and Janssen, B. J. C. (2018) 'Structural Insights into SorCS2-Nerve Growth Factor Complex Formation', *Nature Communications*. Nature Publishing Group UK, 9(1), p. 2979. doi: 10.1038/s41467-018-05405-z.

Levine, T. P. et al. (2013) 'The Product of C9orf72, a Gene Strongly Implicated in Neurodegeneration, is Structurally Related to DENN Rab-GEFs', *Bioinformatics*, 29(4), pp. 499–503. doi: 10.1093/bioinformatics/bts725.

Li, H.-F. and Wu, Z.-Y. (2016) 'Genotype-Phenotype Correlations of Amyotrophic Lateral Sclerosis', *Translational Neurodegeneration*. BioMed Central, 5, p. 3. doi: 10.1186/s40035-016-0050-8.

Liang, X. et al. (2008) 'The Prostaglandin E2 EP2 Receptor Accelerates Disease Progression and Inflammation in a Model of Amyotrophic Lateral Sclerosis', *Annals of Neurology*. John Wiley & Sons, Ltd, 64(3), pp. 304–314. doi: 10.1002/ana.21437.

Lillo, P. and Hodges, J. R. (2009) 'Frontotemporal Dementia and Motor Neurone Disease: Overlapping Clinic-Pathological Disorders', *Journal of Clinical Neuroscience*. Elsevier, 16(9), pp. 1131–1135. doi: 10.1016/j.jocn.2009.03.005.

Lin, Z. et al. (2015) 'Structural Basis of Death Domain Signaling in The P75 Neurotrophin Receptor', *eLife*. eLife Sciences Publications, Ltd, 4, pp. e11692–e11692. doi: 10.7554/eLife.11692.

Lindequist U. Marine-Derived Pharmaceuticals - Challenges and Opportunities. *Biomol Ther* (Seoul). 2016 Nov 1;24(6):561-571. doi: 10.4062/biomolther.2016.181. PMID: 27795450; PMCID: PMC5098534.

Ling SC, Polymenidou M, Cleveland DW. (2013) Converging Mechanisms in ALS and FTD: Disrupted RNA and Protein Homeostasis. *Neuron*. 2013;79:416–438.

Liu, J. et al. (2007) 'Nerve Growth Factor-Mediated Neurite Outgrowth Via Regulation of Rab5', *Molecular Biology of the Cell*. The American Society for Cell Biology, 18(4), pp. 1375–1384. doi: 10.1091/mbc.e06-08-0725.

Liu, C., Chan, C. B. and Ye, K. (2016) '7,8-dihydroxyflavone, a Small Molecular TrkB agonist, is Useful for Treating Various BDNF-Implicated Human Disorders', *Translational Neurodegeneration*. BioMed Central, 5, p. 2. doi: 10.1186/s40035-015-0048-7.

Liu, X. et al. (2014) 'Biochemical and Biophysical Investigation of The Brain-Derived Neurotrophic Factor Mimetic 7,8-Dihydroxyflavone in the Binding and Activation of the TrkB Receptor', *The Journal of Biological Chemistry*. 2014/08/20. American Society for Biochemistry and Molecular Biology, 289(40), pp. 27571–27584. doi: 10.1074/jbc.M114.562561.

Liu G, David BT, Trawczynski M, Fessler RG. (2020) Advances in Pluripotent Stem Cells: History, Mechanisms, Technologies, and Applications. *Stem Cell Rev Rep*. 2020 Feb;16(1):3-32. doi: 10.1007/s12015-019-09935-x. PMID: 31760627; PMCID: PMC6987053.

Liu T, Zhang L, Joo D, Sun SC. (2017) NF- κ B Signaling in Inflammation. *Signal Transduct Target Ther*. 2017;2:17023–. doi: 10.1038/sigtrans.2017.23. Epub 2017 Jul 14. PMID: 29158945; PMCID: PMC5661633.

Longo, F. M. and Massa, S. M. (2013) 'Small-Molecule Modulation of Neurotrophin Receptors: A Strategy for the Treatment of Neurological Disease', *Nature Reviews Drug Discovery*. Nature Publishing Group, a division of Macmillan Publishers Limited. All Rights Reserved., 12, p. 507. Available at: <https://doi.org/10.1038/nrd4024>.

Louis-Félix Nothias, Mélissa Nothias-Esposito, Ricardo da Silva, Mingxun Wang, Ivan Protsyuk, Zheng Zhang, Abi Sarvepalli, Pieter Leyssen, David Touboul, Jean Costa, Julien Paolini, Theodore Alexandrov, Marc Litaudon, and Pieter C. Dorrestein. (2018) *Journal of Natural Products* 2018 81 (4), 758-767 DOI: 10.1021/acs.jnatprod.7b00737.

Love, S. et al. (2005) 'Glial Cell Line–Derived Neurotrophic Factor Induces Neuronal Sprouting in Human Brain', *Nature Medicine*. Nature Publishing Group, 11, p. 703. Available at: <https://doi.org/10.1038/nm0705-703>.

Lu, H. et al. (2016) 'Current Therapy of Drugs in Amyotrophic Lateral Sclerosis', *Current Neuropharmacology*. Bentham Science Publishers, 14(4), pp. 314–321. doi: 10.2174/1570159X14666160120152423.

Luo D., Zhang Q., Wang H., Cui Y., Sun Z., Yang J., Zheng Y., Jia J., Yu F., Wang X., et al. Fucoidan Protects against Dopaminergic Neuron Death In Vivo and In Vitro. *Eur. J. Pharmacol.* 2009;617:33–40. doi: 10.1016/j.ejphar.2009.06.015.

Luther, J. A. and Birren, S. J. (2009) 'p75 and TrkA Signaling Regulates Sympathetic Neuronal Firing Patterns Via Differential Modulation of Voltage-Gated Currents', *The Journal of Neuroscience : the official journal of the Society for Neuroscience*. Society for Neuroscience, 29(17), pp. 5411–5424. doi: 10.1523/JNEUROSCI.3503-08.2009.

Madji Hounoum, B. et al. (2017) 'Wildtype Motoneurons, ALS-Linked SOD1 Mutation and Glutamate Profoundly Modify Astrocyte Metabolism and Lactate Shuttling', *Glia*. John Wiley & Sons, Ltd, 65(4), pp. 592–605. doi: 10.1002/glia.23114.

Magrané, J. et al. (2009) 'Mutant SOD1 in Neuronal Mitochondria Causes Toxicity and Mitochondrial Dynamics Abnormalities', *Human Molecular Genetics*. 2009/09/24. Oxford University Press, 18(23), pp. 4552–4564. doi: 10.1093/hmg/ddp421.

Mahmoud, S. et al. (2019) 'Astrocytes Maintain Glutamate Homeostasis in the CNS by Controlling the Balance between Glutamate Uptake and Release', *Cells*. MDPI, 8(2), p. 184. doi: 10.3390/cells8020184.

Majounie, E. et al. (2012) 'Frequency of the C9orf72 Hexanucleotide Repeat Expansion in Patients with Amyotrophic Lateral Sclerosis and Frontotemporal Dementia: A Cross-Sectional Study', *The Lancet Neurology*. Elsevier, 11(4), pp. 323–330. doi: 10.1016/S1474-4422(12)70043-1.

Manadas, B. et al. (2010) 'Peptide Fractionation in Proteomics Approaches', *Expert Review of Proteomics*. Taylor & Francis, 7(5), pp. 655–663. doi: 10.1586/epr.10.46.

Mao, K. et al. (2017) 'Anticonvulsant Effect of Piperine Ameliorates Memory Impairment, Inflammation and Oxidative Stress in a Rat Model of Pilocarpine-Induced Epilepsy', *Experimental and Therapeutic Medicine*. 2016/12/27. D.A. Spandidos, 13(2), pp. 695–700. doi: 10.3892/etm.2016.4001.

Marion, D. (2013) 'An Introduction to Biological NMR Spectroscopy', *Molecular & Cellular Proteomics : MCP*. 2013/07/06. The American Society for Biochemistry and Molecular Biology, 12(11), pp. 3006–3025. doi: 10.1074/mcp.O113.030239.

Marks, W. J. et al. (2008) 'Safety and Tolerability of Intraputaminial Delivery of Cere-120 (Adeno-Associated Virus Serotype 2–Neurturin) to Patients with Idiopathic Parkinson's Disease: An Open-Label, Phase I Trial', *The Lancet Neurology*, 7(5), pp. 400–408. doi: [https://doi.org/10.1016/S1474-4422\(08\)70065-6](https://doi.org/10.1016/S1474-4422(08)70065-6).

Martins, A. et al. (2014) 'Marketed Marine Natural Products in The Pharmaceutical And Cosmeceutical Industries: Tips for Success', *Marine Drugs*. MDPI, 12(2), pp. 1066–1101. doi: 10.3390/md12021066.

Massa, S. M. et al. (2010) 'Small Molecule BDNF Mimetics Activate TrkB Signaling and Prevent Neuronal Degeneration in Rodents', *The Journal of Clinical Investigation*. 2010/04/19. American Society for Clinical Investigation, 120(5), pp. 1774–1785. doi: 10.1172/JCI41356.

Mauch, D. H. et al. (2001) 'CNS Synaptogenesis Promoted by Glia-Derived Cholesterol', *Science*, 294(5545), p. 1354 LP-1357. doi: 10.1126/science.294.5545.1354.

Mayer AM, Glaser KB, Cuevas C, Jacobs RS, Kem W, Little RD, McIntosh JM, Newman DJ, Potts BC, Shuster DE. The odyssey of marine pharmaceuticals: a current pipeline perspective. *Trends Pharmacol Sci.* 2010;31:255–265. doi: 10.1016/j.tips.2010.02.005.

McAlary L, Plotkin SS, Yerbury JJ, Cashman NR. (2019) Prion-Like Propagation of Protein Misfolding and Aggregation in Amyotrophic Lateral Sclerosis. *Front Mol Neurosci.* 2019 Nov 1;12:262. doi: 10.3389/fnmol.2019.00262. Erratum in: *Front Mol Neurosci.* 2020 Jan 21;12:311. PMID: 31736708; PMCID: PMC6838634.

McGown A, Stopford MJ. (2018) High-Throughput Drug Screens for Amyotrophic Lateral Sclerosis Drug Discovery. *Expert Opin Drug Discov.* 2018 Nov;13(11):1015-1025. doi: 10.1080/17460441.2018.1533953. Epub 2018 Oct 13. PMID: 30317895.

McKeon RJ, Schreiber RC, Rudge JS, Silver J. (1991) Reduction of Neurite Outgrowth in a Model of Glial Scarring Following CNS Injury is Correlated with the Expression of Inhibitory Molecules on Reactive Astrocytes. *J. Neurosci. Off. J. Soc. Neurosci.* 1991;11:3398–3411.

Mead, R.J., Shan, N., Reiser, H.J. et al. (2023) Amyotrophic Lateral Sclerosis: a Neurodegenerative Disorder Poised for Successful Therapeutic Translation. *Nat Rev Drug Discov* 22, 185–212 (2023). <https://doi.org/10.1038/s41573-022-00612-2>

Meeker, R. and Williams, K. (2014) 'Dynamic Nature of the p75 Neurotrophin Receptor in Response to Injury and Disease', *Journal of Neuroimmune Pharmacology : the official journal of the Society on NeuroImmune Pharmacology.* 2014/09/20, 9(5), pp. 615–628. doi: 10.1007/s11481-014-9566-9.

Meng XY, Zhang HX, Mezei M, Cui M. (2011) Molecular Docking: a Powerful Approach for Structure-Based Drug Discovery. *Curr Comput Aided Drug Des.* 2011 Jun;7(2):146-57. doi: 10.2174/157340911795677602. PMID: 21534921; PMCID: PMC3151162.

Meyer, K. et al. (2014) 'Direct Conversion of Patient Fibroblasts Demonstrates Non-Cell Autonomous Toxicity of Astrocytes to Motor Neurons in Familial and Sporadic ALS', *Proceedings of the National Academy of Sciences*, 111(2), p. 829 LP-832. doi: 10.1073/pnas.1314085111.

MH, T. et al. (2015) 'Nerve Growth Factor Gene Therapy: Activation of Neuronal Responses in Alzheimer Disease', *JAMA Neurology*, 72(10), pp. 1139–1147. Available at: <http://dx.doi.org/10.1001/jamaneurol.2015.1807>.

Mitre, M., Mariga, A. and Chao, M. V (2017) 'Neurotrophin Signalling: Novel Insights into Mechanisms and Pathophysiology', *Clinical Science (London, England : 1979)*, 131(1), pp. 13–23. doi: 10.1042/CS20160044.

Mitsumoto, H. et al. (2008) 'Oxidative Stress Biomarkers in Sporadic ALS', *Amyotrophic Lateral Sclerosis. Taylor & Francis*, 9(3), pp. 177–183. doi: 10.1080/17482960801933942.

Morris GM, Lim-Wilby M. (2008) Molecular docking. *Methods Mol Biol.* 2008;443:365-82. doi: 10.1007/978-1-59745-177-2_19. PMID: 18446297.

Münch C., Bertolotti A. (2010). Exposure of Hydrophobic Surfaces Initiates Aggregation of Diverse ALS-Causing Superoxide Dismutase-1 Mutants. *J. Mol. Biol.* 399, 512–525. 10.1016/j.jmb.2010.04.019

Muyderman, H. and Chen, T. (2014) 'Mitochondrial Dysfunction in Amyotrophic Lateral Sclerosis - A Valid Pharmacological Target?', *British Journal of Pharmacology. Blackwell Publishing Ltd*, 171(8), pp. 2191–2205. doi: 10.1111/bph.12476.

Nagy, A. and Vintersten, K. B. T.-M. in E. (2006) 'Murine Embryonic Stem Cells', in *Embryonic Stem Cells. Academic Press*, pp. 3–21. doi: [https://doi.org/10.1016/S0076-6879\(06\)18001-5](https://doi.org/10.1016/S0076-6879(06)18001-5).

Neary, D., Snowden, J. and Mann, D. (2005) 'Frontotemporal dementia', *The Lancet Neurology. Elsevier*, 4(11), pp. 771–780. doi: 10.1016/S1474-4422(05)70223-4.

Nedelsky, N. B. and Taylor, J. P. (2019) 'Bridging Biophysics and Neurology: Aberrant Phase Transitions in Neurodegenerative Disease', *Nature Reviews Neurology*, 15(5), pp. 272–286. doi: 10.1038/s41582-019-0157-5.

Neumann M, Sampathu DM, Kwong LK, et al. (2006) Ubiquitinated TDP-43 in Frontotemporal Lobar Degeneration and Amyotrophic Lateral Sclerosis. *Science.* 2006;314:130–133.

Nijssen, J., Comley, L. H. and Hedlund, E. (2017) 'Motor Neuron Vulnerability and Resistance in Amyotrophic Lateral Sclerosis', *Acta Neuropathologica*, 133(6), pp. 863–885. doi: 10.1007/s00401-017-1708-8.

Nita, M. and Grzybowski, A. (2016) 'The Role of the Reactive Oxygen Species and Oxidative Stress in the Pathomechanism of the Age-Related Ocular Diseases and Other Pathologies of the Anterior and Posterior Eye Segments in Adults', *Oxidative Medicine and Cellular Longevity*. 2016/01/10. Hindawi Publishing Corporation, 2016, p. 3164734. doi: 10.1155/2016/3164734.

Nutt, J. G. et al. (2003) 'Randomized, Double-Blind Trial of Glial Cell Line-Derived Neurotrophic Factor (GDNF) in PD', *Neurology*, 60(1), p. 69 LP-73. doi: 10.1212/WNL.60.1.69.

Ochs, G. et al. (2000) 'A Phase I/II Trial of Recombinant Methionyl Human Brain Derived Neurotrophic Factor Administered by Intrathecal Infusion to Patients with Amyotrophic Lateral Sclerosis', *Amyotrophic Lateral Sclerosis and Other Motor Neuron Disorders*. Taylor & Francis, 1(3), pp. 201–206. doi: 10.1080/14660820050515197.

Olanow, C. W. et al. (2015) 'Trophic Factors for Parkinson's Disease: To Live or Let Die', *Movement Disorders*. John Wiley & Sons, Ltd, 30(13), pp. 1715–1724. doi: 10.1002/mds.26426.

Olson, L. et al. (1992) 'Nerve Growth Factor Affects 11C-Nicotine Binding, Blood Flow, EEG, and Verbal Episodic Memory in An Alzheimer Patient (Case Report)', *Journal of Neural Transmission - Parkinson's Disease and Dementia Section*, 4(1), pp. 79–95. doi: 10.1007/BF02257624.

Ottoboni L, von Wunster B, Martino G. (2020) Therapeutic Plasticity of Neural Stem Cells. *Front Neurol*. 2020 Mar 20;11:148. doi: 10.3389/fneur.2020.00148. PMID: 32265815; PMCID: PMC7100551.

Pangestuti R., Vo T.-S., Ngo D.-H., Kim S.-K. Fucoxanthin Ameliorates Inflammation and Oxidative Responses in Microglia. *J. Agric. Food Chem*. 2013;61:3876–3883. doi: 10.1021/jf400015k.

Parone, P. A. et al. (2013) 'Enhancing Mitochondrial Calcium Buffering Capacity Reduces Aggregation of Misfolded SOD1 and Motor Neuron Cell Death without Extending Survival in Mouse Models of Inherited Amyotrophic Lateral Sclerosis', *The Journal of Neuroscience*, 33(11), p. 4657 LP-4671. doi: 10.1523/JNEUROSCI.1119-12.2013.

Patel, N. K. et al. (2005) 'Intrapataminal Infusion of Glial Cell Line-Derived Neurotrophic Factor in PD: A Two-Year Outcome Study', *Annals of Neurology*. John Wiley & Sons, Ltd, 57(2), pp. 298–302. doi: 10.1002/ana.20374.

Patel, N. K. et al. (2013) 'Benefits of Putaminal GDNF Infusion in Parkinson Disease are Maintained after GDNF Cessation', *Neurology*, 81(13), p. 1176 LP-1178. doi: 10.1212/WNL.0b013e3182a55ea5.

Pediaditakis I, Efstathopoulos P, Prousis KC, Zervou M, Arévalo JC, Alexaki VI, Nikolettou V, Karagianni E, Potamitis C, Tavernarakis N, Chavakis T, Margioris AN, Venihaki M, Calogeropoulou T, Charalampopoulos I, Gravanis A. (2016) Selective and Differential Interactions of BNN27, a Novel C17-Spiroepoxy Steroid Derivative, with TrkA Receptors, Regulating Neuronal Survival and Differentiation. *Neuropharmacology*. 2016 Dec;111:266-282. doi: 10.1016/j.neuropharm.2016.09.007. Epub 2016 Sep 9. PMID: 27618740.

Pehar, M., Harlan, B. A. and Vargas, K. M. K. and M. R. (2017) 'Role and Therapeutic Potential of Astrocytes in Amyotrophic Lateral Sclerosis', *Current Pharmaceutical Design*, pp. 5010–5021. doi: <http://dx.doi.org/10.2174/1381612823666170622095802>.

Penn, R. D. et al. (1997) 'Intrathecal Ciliary Neurotrophic Factor Delivery for Treatment of Amyotrophic Lateral Sclerosis (Phase I Trial)', *Neurosurgery*, 40(1), pp. 94–100. doi: 10.1097/00006123-199701000-00021.

Petrov, D. et al. (2017) 'ALS Clinical Trials Review: 20 Years of Failure. Are We Any Closer to Registering a New Treatment?', *Frontiers in Aging Neuroscience*. Frontiers Media S.A., 9, p. 68. doi: 10.3389/fnagi.2017.00068.

Philips, T. and Rothstein, J. D. (2014) 'Glial Cells in Amyotrophic Lateral Sclerosis', *Experimental Neurology*, 262, pp. 111–120. doi: <https://doi.org/10.1016/j.expneurol.2014.05.015>.

Phukan, J., Pender, N. P. and Hardiman, O. (2007) 'Cognitive Impairment in Amyotrophic Lateral Sclerosis', *The Lancet Neurology*. Elsevier, 6(11), pp. 994–1003. doi: 10.1016/S1474-4422(07)70265-X.

Pinzi L, Rastelli G. (2019) Molecular Docking: Shifting Paradigms in Drug Discovery. *Int J Mol Sci*. 2019 Sep 4;20(18):4331. doi: 10.3390/ijms20184331. PMID: 31487867; PMCID: PMC6769923.

Pitsikas N, Zoupa E, Gravanis A. (2021) The Novel Dehydroepiandrosterone (DHEA) Derivative BNN27 Counteracts Cognitive Deficits Induced by the D1/D2 Dopaminergic Receptor Agonist Apomorphine in Rats. *Psychopharmacology (Berl)*. 2021 Jan;238(1):227-237. doi: 10.1007/s00213-020-05672-z. Epub 2020 Oct 2. PMID: 33005973.

Polymenidou, M. et al. (2011) 'Long pre-mRNA Depletion and RNA Missplicing Contribute to Neuronal Vulnerability from Loss of TDP-43', *Nature Neuroscience*, 14(4), pp. 459–468. doi: 10.1038/nn.2779.

Prada, I. et al. (2011) 'REST/NRSF governs the Expression of Dense-Core Vesicle Gliosecretion in Astrocytes', *The Journal of Cell Biology*, 193(3), p. 537 LP-549. doi: 10.1083/jcb.201010126.

Pradhan, J., Noakes, P. G. and Bellingham, M. C. (2019) 'The Role of Altered BDNF/TrkB Signaling in Amyotrophic Lateral Sclerosis', *Frontiers in Cellular Neuroscience*. Frontiers Media S.A., 13, p. 368. doi: 10.3389/fncel.2019.00368.

Prakash, K.R.C., Tang, Y., Kozikowski, A., Filippen-Anderson, J.L. (2002) ChemInform Abstract: Synthesis and Biological Activity of Novel Neuroprotective Diketopiperazines. October 2002 *Bioorganic & Medicinal Chemistry* 10(9):3043-8 DOI:10.1016/S0968-0896(02)00132-3.

Prasad, A. et al. (2019) 'Molecular Mechanisms of TDP-43 Misfolding and Pathology in Amyotrophic Lateral Sclerosis', *Frontiers in Molecular Neuroscience*. Frontiers Media S.A., 12, p. 25. doi: 10.3389/fnmol.2019.00025.

Price, R. D. et al. (2007) 'Advances in Small Molecules Promoting Neurotrophic Function', *Pharmacology & Therapeutics*, 115(2), pp. 292–306. doi: <https://doi.org/10.1016/j.pharmthera.2007.03.005>.

- Purice, M. D. and Taylor, J. P. (2018) 'Linking hnRNP Function to ALS and FTD Pathology', *Frontiers in Neuroscience*. Frontiers Media S.A., 12, p. 326. doi: 10.3389/fnins.2018.00326.
- Quaegebeur A, Glaria I, Lashley T, Isaacs AM. (2020) Soluble and Insoluble Dipeptide Repeat Protein Measurements in C9orf72-Frontotemporal Dementia Brains Show Regional Differential Solubility and Correlation of Poly-GR with Clinical Severity. *Acta Neuropathol Commun*. 2020 Nov 9;8(1):184. doi: 10.1186/s40478-020-01036-y. PMID: 33168090; PMCID: PMC7650212.
- Rafii, M. S. et al. (2014) 'A Phase I Study of Stereotactic Gene Delivery of AAV2-NGF for Alzheimer's Disease', *Alzheimer's & Dementia*, 10(5), pp. 571–581. doi: <https://doi.org/10.1016/j.jalz.2013.09.004>.
- Rafii, M. S. (2015) 'A Phase II Trial of AAV2-NGF in Mild to Moderate Alzheimer's Disease', *J. Prev. Alzheimers Dis.*, 2(4), pp. 274–275.
- Redler, R. L. and Dokholyan, N. V (2012) 'The Complex Molecular Biology of Amyotrophic Lateral Sclerosis (ALS)'. *Progress in Molecular Biology and Translational Science*, 107, pp. 215–262. doi: 10.1016/B978-0-12-385883-2.00002-3.
- Renton, A. E. et al. (2011) 'A Hexanucleotide Repeat Expansion in C9ORF72 Is the Cause of Chromosome 9p21-Linked ALS-FTD', *Neuron*. Elsevier, 72(2), pp. 257–268. doi: 10.1016/j.neuron.2011.09.010.
- Renton, A. E., Chiò, A. and Traynor, B. J. (2013) 'State of Play In Amyotrophic Lateral Sclerosis Genetics', *Nature Neuroscience*. Nature Publishing Group, a division of Macmillan Publishers Limited. All Rights Reserved., 17, p. 17. Available at: <https://doi.org/10.1038/nn.3584>.
- Robberecht, W. and Philips, T. (2013) 'The Changing Scene of Amyotrophic Lateral Sclerosis', *Nature Reviews Neuroscience*, 14(4), pp. 248–264. doi: 10.1038/nrn3430.
- Rockenstein, E. et al. (2011) 'Regional Comparison of the Neurogenic Effects of CNTF-Derived Peptides and Cerebrolysin in A β PP Transgenic Mice', *Journal of Alzheimer's Disease* : JAD, 27(4), pp. 743–752. doi: 10.3233/JAD-2011-110914.

Rodrigues, T., Nuisance Small Molecules Under a Machine-Learning Lens. *Digit Discov*, 1 (2022), pp. 209-215.

Rohrer, J. D. et al. (2015) 'C9orf72 Expansions in Frontotemporal Dementia and Amyotrophic Lateral Sclerosis', *The Lancet Neurology*. Elsevier, 14(3), pp. 291–301. doi: 10.1016/S1474-4422(14)70233-9.

Rosen, D. R. et al. (1993) 'Mutations in Cu/Zn Superoxide Dismutase Gene are Associated with Familial Amyotrophic Lateral Sclerosis', *Nature*, 362(6415), pp. 59–62. doi: 10.1038/362059a0.

Scotter EL, Chen HJ, Shaw CE. (2015) TDP-43 Proteinopathy and ALS: Insights into Disease Mechanisms and Therapeutic Targets. *Neurotherapeutics*. 2015 Apr;12(2):352-63. doi: 10.1007/s13311-015-0338-x. Erratum in: *Neurotherapeutics*. 2015 Apr;12(2):515-8. PMID: 25652699; PMCID: PMC4404432.

Salvatore, M. F. et al. (2006) 'Point Source Concentration of GDNF May Explain Failure of Phase II Clinical Trial', *Experimental Neurology*, 202(2), pp. 497–505. doi: <https://doi.org/10.1016/j.expneurol.2006.07.015>.

Seiger, Å. et al. (1993) 'Intracranial Infusion of Purified Nerve Growth Factor to an Alzheimer Patient: The First Attempt of a Possible Future Treatment Strategy', *Behavioural Brain Research*, 57(2), pp. 255–261. doi: [https://doi.org/10.1016/0166-4328\(93\)90141-C](https://doi.org/10.1016/0166-4328(93)90141-C).

Shaw MP, Higginbottom A, McGown A, Castelli LM, James E, Hautbergue GM, Shaw PJ, Ramesh TM. (2018) Stable Transgenic C9orf72 Zebrafish Model Key Aspects of the ALS/FTD Phenotype and Reveal Novel Pathological Features. *Acta Neuropathol Commun*. 2018 Nov 19;6(1):125. doi: 10.1186/s40478-018-0629-7. PMID: 30454072; PMCID: PMC6240957.

Sherer, T. B. et al. (2006) 'Crossroads in GDNF Therapy for Parkinson's Disease', *Movement Disorders*. John Wiley & Sons, Ltd, 21(2), pp. 136–141. doi: 10.1002/mds.20861.

Shepherd SR, Parker MD, Cooper-Knock J, Verber NS, Tuddenham L, Heath P, Beauchamp N, Place E, Sollars ESA, Turner MR, Malaspina A, Fratta P, Hewamadduma C, Jenkins TM, McDermott CJ, Wang D, Kirby J, Shaw PJ; Project MINE Consortium; Project MinE. (2021) Value of Systematic Genetic Screening of Patients With Amyotrophic Lateral Sclerosis. *J*

Neurol Neurosurg Psychiatry. 2021 May;92(5):510-518. doi: 10.1136/jnnp-2020-325014. Epub 2021 Feb 14. PMID: 33589474; PMCID: PMC8053339.

Shutova MV, Surdina AV, Ischenko DS, Naumov VA, Bogomazova AN, Vassina EM, Alekseev DG, Lagarkova MA, Kiselev SL. (2016) An Integrative Analysis of Reprogramming in Human Isogenic System Identified a Clone Selection Criterion. *Cell Cycle*. 2016;15(7):986-97. doi: 10.1080/15384101.2016.1152425. PMID: 26919644; PMCID: PMC4889246.

Sliwoski G, Kothiwale S, Meiler J, Lowe EW Jr. (2013) Computational Methods in Drug Discovery. *Pharmacol Rev*. 2013 Dec 31;66(1):334-95. doi: 10.1124/pr.112.007336. PMID: 24381236; PMCID: PMC3880464.

Silverman J. M., Christy D., Shyu C. C., Moon K. M., Fernando S., Gidden Z., et al. (2019). CNS-Derived Extracellular Vesicles From Superoxide Dismutase 1 (SOD1)(G93A) ALS Mice Originate from Astrocytes and Neurons and Carry Misfolded SOD1. *J. Biol. Chem*. 294, 3744–3759. 10.1074/jbc.ra118.004825.

Simmons, D. A. et al. (2014) 'A Small Molecule p75^{NTR} Ligand, LM11A-31, Reverses Cholinergic Neurite Dystrophy in Alzheimer's Disease Mouse Models with Mid- To Late-Stage Disease Progression', *PLoS One*. Public Library of Science, 9(8), pp. e102136–e102136. doi: 10.1371/journal.pone.0102136.

Skaper, S. D. (2008) 'The Biology of Neurotrophins, Signalling Pathways, and Functional Peptide Mimetics of Neurotrophins and their Receptors', *CNS & Neurological Disorders - Drug Targets*, pp. 46–62. doi: <http://dx.doi.org/10.2174/187152708783885174>.

Skaper, S. D. (2011) 'Peptide Mimetics of Neurotrophins and their Receptors', *Current Pharmaceutical Design*, pp. 2704–2718. doi: <http://dx.doi.org/10.2174/138161211797415995>.

Slevin, J. T. et al. (2005) 'Improvement of Bilateral Motor Functions in Patients With Parkinson Disease Through the Unilateral Intraputaminial Infusion of Glial Cell Line—Derived Neurotrophic Factor', *Journal of Neurosurgery*, 102(2), pp. 216–222. doi: 10.3171/jns.2005.102.2.0216.

Sobuś, A. (2016) 'Trophic Factors in the Therapeutic Challenge Against ALS: Current Research Directions', in Valdés, B. M. E.-H. F. S. E.-L. de F. I. (ed.). Rijeka: IntechOpen, p. Ch. 11. doi: 10.5772/63428.

Sofroniew, M. V (2015) 'Astrocyte Barriers to Neurotoxic Inflammation', *Nature Reviews Neuroscience*, 16(5), pp. 249–263. doi: 10.1038/nrn3898.

Sorenson, E. J. et al. (2008) 'Subcutaneous IGF-1 is Not Beneficial in 2-year ALS Trial', *Neurology*, 71(22), p. 1770 LP-1775. doi: 10.1212/01.wnl.0000335970.78664.36.

Soto, C. A. and C. (2002) 'Converting a Peptide into a Drug: Strategies to Improve Stability and Bioavailability', *Current Medicinal Chemistry*, pp. 963–978. doi: <http://dx.doi.org/10.2174/0929867024606731>.

Srinivasan M, Lahiri DK. (2015) Significance of NF- κ B as a Pivotal Therapeutic Target in the Neurodegenerative Pathologies of Alzheimer's Disease and Multiple Sclerosis. *Expert Opin Ther Targets*. 2015 Apr;19(4):471-87. doi: 10.1517/14728222.2014.989834. Epub 2015 Feb 4. PMID: 25652642; PMCID: PMC5873291.

Stark, J.L., Powers, R. (2011). Application of NMR and Molecular Docking in Structure-Based Drug Discovery. In: Zhu, G. (eds) *NMR of Proteins and Small Biomolecules*. Topics in Current Chemistry, vol 326. Springer, Berlin, Heidelberg. https://doi.org/10.1007/128_2011_213

Stieber, A., Gonatas, J. O. and Gonatas, N. K. (2000) 'Aggregation of Ubiquitin and a Mutant ALS-linked SOD1 Protein Correlate with Disease Progression And Fragmentation Of The Golgi Apparatus', *Journal of the Neurological Sciences*. Elsevier, 173(1), pp. 53–62. doi: 10.1016/S0022-510X(99)00300-7.

Stopford, M. J., Allen, S. P. and Ferraiuolo, L. (2019) 'A High-throughput and Pathophysiologically Relevant Astrocyte-motor Neuron Co-culture Assay for Amyotrophic Lateral Sclerosis Therapeutic Discovery', *Bio-protocol*. Bio-protocol LLC., 9(17), p. e3353. doi: 10.21769/BioProtoc.3353.

Strong, M. J. (2010) 'The Evidence for Altered RNA Metabolism in Amyotrophic Lateral Sclerosis (ALS)', *Journal of the Neurological Sciences*. Elsevier, 288(1), pp. 1–12. doi: 10.1016/j.jns.2009.09.029.

Suzuki, N., Nishiyama, A., Warita, H. et al. (2023) Genetics of Amyotrophic Lateral Sclerosis: Seeking Therapeutic Targets in The Era Of Gene Therapy. *J Hum Genet* 68, 131–152 (2023). <https://doi.org/10.1038/s10038-022-01055-8>

Swinnen, B. and Robberecht, W. (2014) 'The Phenotypic Variability of Amyotrophic Lateral Sclerosis', *Nature Reviews Neurology*. Nature Publishing Group, a division of Macmillan Publishers Limited. All Rights Reserved., 10, p. 661. Available at: <https://doi.org/10.1038/nrneurol.2014.184>.

Tanaka, K. et al. (2016) 'Death Domain Signaling by Disulfide-Linked Dimers of the p75 Neurotrophin Receptor Mediates Neuronal Death in the CNS', *The Journal of Neuroscience*, 36(20), p. 5587 LP-5595. doi: 10.1523/JNEUROSCI.4536-15.2016.

Taylor, J. P., Brown Jr, R. H. and Cleveland, D. W. (2016) 'Decoding ALS: From Genes to Mechanism', *Nature*, 539(7628), pp. 197–206. doi: 10.1038/nature20413.

Teng, K. K. et al. (2010) 'Understanding Proneurotrophin Actions: Recent Advances and Challenges', *Developmental Neurobiology*, 70(5), pp. 350–359. doi: 10.1002/dneu.20768.

Tortelli, R. et al. (2013) 'Amyotrophic Lateral Sclerosis: a New Missense Mutation in the SOD1 Gene', *Neurobiology of Aging*, 34(6), p. 1709.e3-1709.e5. doi: <https://doi.org/10.1016/j.neurobiolaging.2012.10.027>.

Turner, M. R. et al. (2017) 'Genetic Screening in Sporadic ALS and FTD', *Journal of Neurology, Neurosurgery & Psychiatry*, 88(12), p. 1042 LP-1044. doi: 10.1136/jnnp-2017-315995.

Tuszynski, M. H. et al. (2005) 'A Phase I clinical Trial of Nerve Growth Factor Gene Therapy for Alzheimer Disease', *Nat. Med.*, pp. 1–5.

Ulbricht C, Tracee Rae Abrams, Ashley Brigham, James Ceurvels, Jessica Clubb, Whitney Curtiss, Catherine DeFranco Kirkwood, Nicole Giese, Kevin Hoehn, Ramon Iovin, Richard Isaac, Erica Rusie, Jill M. Grimes Serrano, Minney Varghese, Wendy Weissner & Regina C. Windsor (2010) An Evidence-Based Systematic Review of Rosemary (*Rosmarinus officinalis*) by the Natural Standard Research Collaboration, *Journal of Dietary Supplements*, 7:4, 351-413, DOI: 10.3109/19390211.2010.525049

- Uren, R. T. and Turnley, A. M. (2014) 'Regulation of Neurotrophin Receptor (Trk) signaling: Suppressor of Cytokine Signaling 2 (SOCS2) is a New Player', *Frontiers in Molecular Neuroscience*. Frontiers Media S.A., 7, p. 39. doi: 10.3389/fnmol.2014.00039.
- Valbuena, G. N. et al. (2017) 'Altered Metabolic Profiles Associate with Toxicity in SOD1G93A Astrocyte-Neuron Co-Cultures', *Scientific Reports*, 7(1), p. 50. doi: 10.1038/s41598-017-00072-4.
- Van Cutsem, P. et al. (2005) 'Excitotoxicity and Amyotrophic Lateral Sclerosis', *Neurodegenerative Diseases*, 2(3–4), pp. 147–159. doi: 10.1159/000089620.
- Vande Velde, C. et al. (2008) 'Selective Association of Misfolded Als-Linked Mutant SOD1 with the Cytoplasmic Face of Mitochondria', *Proceedings of the National Academy of Sciences*, 105(10), p. 4022 LP-4027. doi: 10.1073/pnas.0712209105.
- Vasarri M, Degl'Innocenti D. (2022) Antioxidant and Anti-Inflammatory Agents from the Sea: A Molecular Treasure for New Potential Drugs. *Mar Drugs*. 2022 Feb 10;20(2):132. doi: 10.3390/md20020132. PMID: 35200661; PMCID: PMC8876305.
- Wagner, H. and Ulrich-Merzenich, G. (2009) 'Synergy research: Approaching a New Generation of Phytopharmaceuticals', *Phytomedicine*, 16(2), pp. 97–110. doi: <https://doi.org/10.1016/j.phymed.2008.12.018>.
- Walsh, M. C., Lee, J. and Choi, Y. (2015) 'Tumor Necrosis Factor Receptor- Associated Factor 6 (TRAF6) Regulation of Development, Function, and Homeostasis of The Immune System', *Immunological Reviews*, 266(1), pp. 72–92. doi: 10.1111/imr.12302.
- Wang, D. B. et al. (2011) 'Genetic Strategies to Study TDP-43 in Rodents and to Develop Preclinical Therapeutics for Amyotrophic Lateral Sclerosis', *The European Journal of Neuroscience*. 2011/07/21, 34(8), pp. 1179–1188. doi: 10.1111/j.1460-9568.2011.07803.x.
- Wang, H. et al. (2018) 'cAMP Response Element-Binding Protein (CREB): A Possible Signaling Molecule Link in the Pathophysiology of Schizophrenia', *Frontiers in Molecular Neuroscience*. Frontiers Media S.A., 11, p. 255. doi: 10.3389/fnmol.2018.00255.

- Wang, L. et al. (2009) 'The Effect of Mutant SOD1 Dismutase Activity on Non-Cell Autonomous Degeneration in Familial Amyotrophic Lateral Sclerosis', *Neurobiology of Disease*, 35(2), pp. 234–240. doi: <https://doi.org/10.1016/j.nbd.2009.05.002>.
- Webster CP, Smith EF, Bauer CS, Moller A, Hautbergue GM, Ferraiuolo L, Myszczyńska MA, Higginbottom A, Walsh MJ, Whitworth AJ, Kaspar BK, Meyer K, Shaw PJ, Grierson AJ, De Vos KJ. (2016) The C9orf72 Protein Interacts with Rab1a and the ULK1 Complex to Regulate Initiation of Autophagy. *EMBO J*. 2016 Aug 1;35(15):1656-76. doi: 10.15252/embj.201694401. Epub 2016 Jun 22. PMID: 27334615; PMCID: PMC4969571.
- Webster, C. P. et al. (2018) 'C9orf72 Plays a Central Role in Rab GTPase-Dependent Regulation of Autophagy', *Small GTPases*. Taylor & Francis, 9(5), pp. 399–408. doi: 10.1080/21541248.2016.1240495.
- Wichterle, H. et al. (2002) 'Directed Differentiation of Embryonic Stem Cells into Motor Neurons'. *Cell*, 110(3), pp. 385–397. doi: [https://doi.org/10.1016/S0092-8674\(02\)00835-8](https://doi.org/10.1016/S0092-8674(02)00835-8).
- Wijesekera, L. C. and Leigh, P. N. (2009) 'Amyotrophic Lateral Sclerosis', *Orphanet Journal of Rare Diseases*. BioMed Central, 4, p. 3. doi: 10.1186/1750-1172-4-3.
- Wilson, B.P.; Thornburg, C.C.; Henrich, C.J.; Grkovic, T.; O'Keefe, B.R. (2020) Creating and Screening Natural Product Libraries. *Nat. Prod. Rep.* 2020, 37, 863–1032.
- Wong, C.-O. and Venkatachalam, K. (2019) 'Motor Neurons from ALS Patients with Mutations in C9ORF72 and SOD1 Exhibit Distinct Transcriptional Landscapes', *Human Molecular Genetics*, 28(16), pp. 2799–2810. doi: 10.1093/hmg/ddz104.
- Woo TG, Yoon MH, Kang SM, Park S, Cho JH, Hwang YJ, Ahn J, Jang H, Shin YJ, Jung EM, Ha NC, Kim BH, Kwon Y, Park BJ. (2021) Novel Chemical Inhibitor Against SOD1 Misfolding and Aggregation Protects Neuron-Loss and Ameliorates Disease Symptoms in ALS Mouse Model. *Commun Biol*. 2021 Dec 15;4(1):1397. doi: 10.1038/s42003-021-02862-z. PMID: 34912047; PMCID: PMC8674338.
- Yamanaka, K. et al. (2008) 'Astrocytes as Determinants of Disease Progression in Inherited Amyotrophic Lateral Sclerosis', *Nature Neuroscience*, 11(3), pp. 251–253. doi: 10.1038/nn2047.

Yamashita, N. and Kuruvilla, R. (2016) 'Neurotrophin Signaling Endosomes: Biogenesis, Regulation, and Functions', *Current Opinion in Neurobiology*. 2016/06/18, 39, pp. 139–145. doi: 10.1016/j.conb.2016.06.004.

Yang, T. et al. (2008) 'Small Molecule, Non-Peptide p75 Ligands Inhibit A-Beta-Induced Neurodegeneration and Synaptic Impairment', *PLoS One*. Public Library of Science, 3(11), pp. e3604–e3604. doi: 10.1371/journal.pone.0003604.

Zeineddine R., Pundavela J. F., Corcoran L., Stewart E. M., Do-Ha D., Bax M., et al. (2015). SOD1 Protein Aggregates Stimulate Macropinocytosis in Neurons to Facilitate Their Propagation. *Mol. Neurodegener.* 10:57. 10.1186/s13024-015-0053-4

Zhang, N. and Ashizawa, T. (2017) 'RNA Toxicity and Foci Formation In Microsatellite Expansion Diseases', *Current Opinion in Genetics & Development*, 44, pp. 17–29. doi: <https://doi.org/10.1016/j.gde.2017.01.005>.

Zhang, QW., Lin, LG. & Ye, WC. (2018) Techniques for Extraction and Isolation Of Natural Products: a Comprehensive Review. *Chin Med* 13, 20 (2018). <https://doi.org/10.1186/s13020-018-0177-x>.

Zon, L., Peterson, R. (2005) In Vivo Drug Discovery in The Zebrafish. *Nat Rev Drug Discov* 4, 35–44 (2005). <https://doi.org/10.1038/nrd1606>.

Zufiría, M. et al. (2016) 'ALS: A Bucket of Genes, Environment, Metabolism and Unknown Ingredients', *Progress in Neurobiology*, 142, pp. 104–129. doi: <https://doi.org/10.1016/j.pneurobio.2016.05.004>.